Two-Dimensional Acousto-optic Deflection

With Particular Reference to Lead Molybdate

D. W. Reeves

Thesis presented for the degree of

Doctor of Philosophy

of The City University, London.,

in the Department of Electrical and Electronic Engineering

June 1978

Abstract

The work contained in this thesis is related to the study of a device which can deflect light and control its position in two co-ordinates by acousto-optic means within a single medium. The acousto-optic deflection is achieved by the interaction of light with two co-existent, mutually orthogonal, ultrasonic waves within the medium.

The acousto-optic interaction has been theoretically analyzed to a more thorough degree than that previously reported and considerations regarding deflection efficiency, device geometry, and transducer alignment are discussed.

The interaction has initially been demonstrated using water as the interaction medium.

Of the recently discovered materials to show favourable acousto-optic properties lead molybdate has become a notable choice and a novel device using this material has been realised. A device has been constructed which is capable of displaying about 90 × 90 just resolvable spot positions with an access time of 1 μs albeit at a low scattering efficiency.

The thesis includes a description of the behaviour of acoustic transducers for bulk wave excitation and the relevant parameters of the crystalline materials used in this work along with some practical considerations for device fabrication. The interaction bandwidth, with respect to transducer geometry has also been included.

The device has shown to be potentially promising for high speed applications requiring low to moderate capacity for reasonable power levels.

Contents

List of Principal Symbols

α_o	Acoustic attenuation
C_o	Static capacitance
c	Velocity of light
D	Electric flux density
E	Electric field
ε	permittivity
ρ	Density
f	Frequency
ϕ	Electric potential
G	Conductance
I	Intensity or Electric Current
K	Acoustic wave vector
k	Optical wave vector
n	Refractive index
n	Unit vector or integer
P	Power
p	Photo-elastic coefficient
V	Acoustic velocity
Y	Admittance
λ	Optical wavelength
Λ	Acoustic wavelength
ω	Angular frequency
Ω	Acoustic angular frequency
λ_o	Optical wavelength in free space

1. Introduction

Light deflection methods have received increased attention in recent years primarily due to the advent of the laser. Although methods for the deflection of light have been known for many years the favourable properties of laser light have permitted many new functions to be performed, and new deflection techniques to be employed which previously had not been possible. Applications requiring laser deflection have demanded deflectors capable of providing, ideally, high speed, high resolution, and high deflection efficiency.

It has become the preference in modern times for suitable devices to be solid state and non-mechanical. For bulk optical systems, discrete deflector elements have emerged that utilise either the electro-optical effect or the acousto-optical effect to provide inertialess deflection. The requirements of high speed and large resolution are, to a large extent, not compatable and acousto-optic devices have appeared to offer the most favourable compromise. To date, acousto-optic deflectors are available which are capable of providing a capacity in excess of 1000 resolvable spot positions which are randomly accessible with a time in the region of 5 - 10 μs.

There are applications which require the deflection of light in both x and y coordinates. An inertialess means of achieving this has thus become mandatory. Although this function may be achieved by cascading two deflectors present philosophy leans towards compactness and miniaturization. Thus, the development of a single device capable of performing simultaneously x and y deflection within a single medium offers its attractions. Such a device possessing a symmetrical optical aperture and deflection from a common origin offers additional attractions.

This present work has been concerned with the investigation of a single device two-dimensional X,Y acousto-optic deflector in which the

diffraction process is produced by two mutually orthogonal, overlapping, travelling ultrasonic waves and operated in the bragg regime. The device can deflect light simultaneously into various first orders in each coordinate and into a composite, or cross order. It is the cross order that can be suitably controlled in two dimensions. Such a device has been considered elsewhere by other workers and is discussed in section 2. The interaction has been merely demonstrated and its theoretical behaviour appears not to have been adequately considered in the literature. The deflector warrants further investigation, therefore, so as to realise the extent to which the device may be developed and to attempt to improve the performance over that reported, to date, in the literature by previously demonstrated devices. The interaction has yet to be demonstrated using a solid medium operating under normal bragg diffraction conditions and this has been one of the purposes of this present work along with an investigation into its theoretical behaviour.

The renewed interest in acousto-optic deflection in recent years has brought with it further investigations and advances in techniques and materials. One such suitable interaction material to be discovered has been lead molybdate; the previously reported devices have not, as yet, utilised this newly discovered material for the interaction medium. Also, the availability of suitable materials has confined the work to be concerned with normal bragg diffraction which can be readily accomplished in lead molybdate. This material has been used as the interaction material for the greater part of this work.

The subject of acousto-optics, or acoustics, has not previously been undertaken within the Department of Electrical and Electronic Engineering. Consequently, the work here has been involved not only in relation to the acousto-optic interaction but also in areas to which

the aforesaid subjects are related. The necessary technology required to satisfactorily fabricate devices was not available within the department at the commencement of this work and therefore the development of some groundwork has been necessary and only possible. Certain techniques have been arranged so as to perform the work within the bounds and limits which the department has permitted. The practical work has thus been confined to using certain methods and materials which would otherwise be considered unsatisfactory where well established facilities are available.

The thesis is organised in the following way. A review of methods pertaining to x,y optical deflection in section 2 is followed by an analysis of the interaction process in section 3. Also included here are the aspects relating to efficiency, resolution, and bandwidth. Section 4 is concerned with the aspects relating to bulk acoustic wave generation of which the relevant theoretical considerations are given. The crystalline materials used in this work are discussed in section 5 along with considerations relevant to all materials which may be considered suitable for the interaction medium and piezo-electric materials. Some practical aspects relating to device fabrication are reviewed and discussed in section 6 together with some general aspects relating to the work undertaken here. Sections 7 and 8 describe some of the practical work undertaken and include some of the experimental work necessary to establish the techniques and know-how to realise a final two-dimensional lead molybdate deflector within the framework of the environment in which the work was carried out. The interaction was initially demonstrated using water as the interaction medium and the associated performance and problems are discussed in section 7. Section 8 includes some investigations of the bonding methods available to the author as well as containing a description of the work involving

the lead molybdate deflectors. Two lead molybdate deflectors are described each using one of the bonding materials available and have been referred to as Deflector 1 and Deflector 2. Further qualification is given in section 8.

This work has achieved the realisation of a two-dimensional deflector, using lead molybdate, which is capable of demonstrating a resolution of about 90 × 90 just resolvable spot positions and has uncovered some of the potential problems associated with this type of device. Together with an increased investigation into some of the theoretical aspects relating to this device it is felt by the author that the work has made a contribution to the knowledge in this field.

2. Review - Relating to X,Y Acousto-optic Deflection

2.1. Introduction

The subject of acousto-optics has been studied by many researchers for over the past fifty years. The renewed interest has come about with the advent of the laser. In this section several papers regarding the subject are reviewed. Also a comparison between acousto-optic deflection and other methods is briefly made. The methods of obtaining X-Y laser deflection by cascaded arrangements are reviewed and an account of the work involving two-dimensional deflection devices prior to this work is also described.

2.2. Acousto-optic Diffraction

The interaction between light and sound was first predicted by Brillouin in 1921. Experimental verification of the interaction was first observed by Debye and Sears in 1931. Notable workers in the subject of acousto-optics have been Raman and Nath, Lucas and Biquard, and Bergmann during the 1930's. The subject of acousto-optics includes other forms of light-sound interactions besides optical deflection and a historical review together with the various types of interactions has been summarized by Quate (1965).

With reference to acousto-optical deflection, the process is produced by virtue of the refractive index of the interaction medium being disturbed by the presence of a mechanical force. When either a travelling or standing wave propagates through a suitable material perturbations of the materials' refractive index occur to form an optical phased grating. The grating diffracts the light and the angular displacement of the diffracted beam may be altered by varying the wavelength of the acoustic wave. With the advent of the laser renewed interest

in this technique has occurred and some acousto-optic devices pertaining to the deflection and modulation of laser light have been reviewed by Gordon (1966). Adler (1967) has also given a review of acousto-optic methods and devices which can perform optical amplitude and phase modulation, deflection and focusing, and the frequency shifting of light. Also given is a description of a variety of applications in which suitable devices may be employed. The diffraction may be produced in two different ways depending on the difference between the optical and acoustic wavelengths and the length of the interaction region. Diffraction within the Raman Nath regime occurs when low * acoustic frequencies or a short interaction length are employed. Here the optical beam is positioned at normal incidence to the sound column and the resulting diffraction pattern consists of many orders displaced at equal angular increments either side of the incident beam position. The intensity of the orders is dependent on the amplitude of the acoustic wave. Diffraction within the bragg regime occurs when high * acoustic frequencies or a long interaction length are used. In this case the incident light beam is displaced by an angle approximately $\lambda/2\Lambda$ from the sound column normal and the resulting diffraction causes the light to essentially fall into one first order only, deflected by an angle λ/Λ from the incident beam position. The interaction is degenerate for light deflected into the other orders. Bragg deflection is thus perferable in regard to practical optical deflectors allowing practically all of the incident light to be deflected into one order only. The size of the acoustic wavelengths and interaction length are dependent on the optical wavelength and interaction medium involved.

* The relationships between the acoustic frequency, interaction length, and optical wavelength for the interaction occurring in either the Raman Nath or bragg regime are discussed in section 3.8.1.

Damon et al (1970) have also reviewed acousto-optic diffraction techniques including bragg deflection. The basic concepts of the interaction have been discussed along with the relevant theoretical considerations. They have considered the interaction occurring in both isotropic and anisotropic media and some applications utilising the acousto-optical effect have been described. Another comprehensive review of methods and techniques has been given by Sittig (1972) which includes a discussion of some of the more recently discovered suitable materials and also improved transducer geometries. Some of these aspects are discussed in the preceeding sections of this thesis. Both these monographs contain extensive lists of references which give a comprehensive account of many aspects of acousto-optics.

More recently, special attention has been paid to those aspects relating to acousto-optic modulation and deflection which are the basic functions that the interaction performs. Uchida and Niizeki (1973) have provided a comprehensive review on the subject. The performance of any device is dependent upon the materials and fabrication techniques employed. They have provided an extensive list of materials suitable for acousto-optic devices and have given lists of the relevant parameters such as refractive index, acoustic attenuation, optical transmissivitty, and figures of merit for different device configurations and application criteria. Information for both isotropic (i.e. glasses) and crystalline materials is given. Besides giving an account of the theoretical aspects they have also discussed some methods of transducer bonding and heat sinking. The performances of two Paratellurite (TeO_2) deflectors are described and their efficiency, bandwidth, capacity (the number of resolvable spot positions), and thermal stability are discussed. The topic has also been reviewed by Chang (1976). The acousto-optic interaction theory for bulk devices has been reviewed and a summary of

the parameters and device design criteria for suitable materials has also been given. Here, also, was discussed the transducer technology and bonding and fabrication techniques, the state of which has considerably advanced in recent years. Also included in his review are methods of acousto-optic filtering besides modulation and deflection. Applications of the various devices have been discussed and some future predictions have also been included.

These references thus illustrate the progression and interest in the subject of acousto-optics over recent years and indicate the state-of-the-art which the subject has reached.

2.3. Comparison Between Acousto-optic Deflection and Other Methods

Light deflection can also be performed by mechanical, electro-mechanical, or electro-optic deflectors. The actual choice of device depends on the specific requirements of the application. The parameters of performance to be considered are, in general, speed and resolution. The comparison of acousto-optic deflection with alternative methods is thus to be made on the basis of these considerations.

The alternative methods will only briefly be mentioned to give an indication of their capabilities.

A review of some mechanical, piezo-electric and electro-optic deflection techniques has been given by Fowler and Schlafer (1966). The alternative methods have also been discussed by Baker (1968) and Bieser (1974). Various mechanical methods are available such as rotating polygons, servo-controlled mirror galvanometers and nutating mirrors. Piezo-electrically driven mirrors form the basis of the piezo-electric devices. The mechanical devices offer a considerable resolution (from 100 to 20,000 spots depending on the available aperture

and mechanical method employed). However, due to inertia their access time is comparatively slow (between 50μs and 2s). The piezo-electric devices, although also of high resolution still have a slower response than that which can be obtained from acousto-optic or electro-optic devices. High scanning speeds may be accomplished by operating the devices in a resonant mode but this allows only a very narrow bandwidth and such operating conditions have only a limited use. An example is where constant scanning rates are required.

Of the electro-optic devices, electrically controllable prisms and digital switches are available (Kulcke et al 1966, Fowler and Schlafer 1966). Although the deflection process is inertialess and potentially almost instantaneous the associated electronics to control the required high voltages may limit the achievable response. Cascaded digital switches may also be bulky and complex and may suffer from alignment problems and the resolution obtained from prism deflectors is, in general, comparatively small (less than 5 spots). There are notable exceptions (i.e. F.S. Chen et al (1966), Wright and Wilson (1973), Ninomiya (1973)) but the physical dimensions and the availability of suitable materials are also limiting factors.

Thus, acousto-optic devices suitable for deflector applications form a compromise between mechanical and electro-optical methods. They are capable of giving a moderate resolution (approximately up to 1000 spots for a single-dimensional deflector) and a reasonably fast random access time (in the region of 1 - 10 μs, the time taken for the sound to traverse the optical beam and deflect the light from one position to another). Thus, apart from applications where exceptionally high speed or high resolution are required, the performance of acousto-optic deflectors appears to satisfy the middle range of requirements.

2.4. Cascaded Acousto-optic Deflection Systems

It is inevitable that the requirement to continuously scan light in two co-ordinates by completely non-mechanical means should become mandatory. A method of achieving this is to use two acousto-optic deflectors in cascade. The deflectors are arranged so that their directions of deflection are orthogonal with respect to one another.

Korpel et al (1969) have used a cascaded deflection arrangement for producing a laser television display. In their system acousto-optic water cells were used operating over a 16 M Hz bandwidth with centre frequencies of 42 M Hz and 28 M Hz for the horizontal and vertical deflectors respectively. Each had an optical slit aperture width of 3.0 cm. A He-Ne laser was followed by a beam expander to produce a 3.0 diameter circular beam. A cylindrical lens then focused the light to a horizontal sheet which was positioned within the horizontal deflection cell. The cell was succeeded by a spherical lens, suitably positioned, to produce a vertical sheet of light to pass through the vertically deflecting cell. This was then succeeded by another cylindrical lens and a telescope to reconstruct a circular section beam and provide magnification of the final display. The two deflectors were appropriately adjusted with respect to the optical beam to optimise the X-Y deflection. The resolution obtained by this arrangement was about 300 × 300 just resolvable spot positions. For this application a low intensity optical source was used. When used with higher power laser sources the focusing of the light to a thin sheet may cause heating of, and possible damage to, the acousto-optic interaction media and thus detrimentally affect the shape and stability of the deflected beam. Also, the X,Y deflected beam may not appear to originate from

a common origin for this arrangement.

Cascaded deflection systems have been used for controlling laser light in holographic storage systems. For this application the spatial stability of the deflected spot is of primary importance. Anderson (1968) has demonstrated a cascaded deflection system for this application. The arrangement simply consists of two water cell deflectors each with a 7.5 mm circular optical aperture operating in the frequency range, 15 M Hz to 45 M Hz. The deflectors were preceded by a beam expander to bring the incident light beam to the required circular diameter. The cells were then succeeded by a collimating spherical lens to form the deflected pattern and a telescope to magnify the pattern to the required size. A 32 × 32 spot matrix was demonstrated.

Pinnow and Williamson (1969) have also reported the operation of a cascaded system pertaining to optical memory applications. Their system is essentially the same as that reported by Anderson (1968). For 633 nm He-Ne light an electrical input of 3 watts was required by each transducer to deflect 70% of the incident beam. With an access time of 5 μs, corresponding to an optical aperture of 7.5 mm, 100 × 100 resolvable spot positions were reported. The dimensions of the transducers and the bandwidths have not been given however.

LaMacchia (1970) has reported using two cascaded lead molybdate devices also for use in an optical data storage system. Using the same optical arrangement as described by Anderson (1968) but with the optical aperture reduced to 5.5 mm a capacity of 32 × 32 well resolved spot positions could be obtained with a reduced access time of 1.5 μs. The two devices operated between 85 M Hz and 170 M Hz and required a drive power of 1.4 watts for 70% first order deflection when used with 514.5 nm Argon-ion laser light. The previous devices using water were

more efficient (0.5 watts) but had a slower access time. The arrangement was capable of giving 64 × 64 just resolvable spot positions. Lead molybdate has been a relatively new material to be discovered and its favourable acousto-optic properties have made it suitable for this kind of operation (Pinnow 1969, Coquin et al 1970).

Two lead molybdate devices have also been used by Grodnenskii et al (1975) in a cascaded light deflection system. The two devices each used a 3 mm × 12 mm 36^{o} rotated Y-cut lithium niobate transducer whose centre frequency was 175 M Hz. The lead molybdate samples had dimensions 6 × 8 × 15 mm. The percentage first order deflection, with 1 watt electrical power applied to each transducer, was 20% using a He-Ne laser operating at 633 nm wavelength. A '40.5 × 40.5' spot resolution was reported when the devices were operated between the frequencies 55 M Hz to 210 M Hz. Although not mentioned it is assumed that a 1 mm optical aperture was used. A 'response' time of 1μs was reported however. The optical arrangement used was essentially the same as that described for the previous two cascaded arrangements.

An acousto-optic cascaded X-Y light deflector has been made commercially available by Soro Electro-optics (1974). The resolution that can be obtained with an incident optical beam diameter of 2 cm is 800 × 400 spot positions and the optical arrangement to achieve this resolution is assumed to be similar to that used by Korpel et al (1969). The two deflectors and the necessary optics are all housed in a common assembly and the complete unit is supplied together with the appropriate electronic drivers. The devices operate over a bandwidth of 150 M Hz centred at 225 M Hz and the random access time is quoted as being 5.5 μs. The light deflected into the X-Y controlled beam is given as being greater than 40%. Although the interaction medium of

the deflectors is not given the resolution and access time quoted suggest that lead molybdate has been employed here also.

2.5. Two-Dimensional Deflectors

The concept of a device capable of deflecting light in two dimensions in which the diffraction process in each co-ordinate occurs simultaneously within a single medium is an obvious and natural progression from the cascaded arrangement. The device has been referred to as a two-dimensional deflector. The demonstration of such an acousto-optic interaction has only briefly been reported in the literature.

Uchida and Iwasaki (1969) have demonstrated the interaction using water as the deflecting medium. Two ultrasonic beams, produced by two X-cut quartz transducers cemented on to a glass intermediate medium, were propagated perpendicular to each other in the water. Deflection of each first order beam, using 633 nm He-Ne laser light, over a 15 M Hz bandwidth centred at a bragg frequency of 55 M Hz was achieved. The 1 cm width of the transducers allowed a maximum 1 cm. sq. rectangular optical aperture. The transducer lengths were not given however and to achieve a percentage light deflection of only 0.01% into the composite order 'several watts' of electrical power was required by each transducer. An array of 11 × 11 spots was achieved with a low scanning time (7 secs / spot) and the photographic exposure time was thus 'long'. They have also reported that the resolution was reduced appreciably due to the turbulance and thermal effects caused by the fairly high acoustic power loss in the water.

The diffraction of light by two orthogonal ultrasonic travelling waves under bragg angle incidence has been described by Chu and Mauldin (1973). The device they described was particularly relevant

for use in laser doppler velocimeter systems. The two orthogonal sound columns were produced by two 2.92 cm diameter X-cut quartz transducers operating at their third harmonic frequencies of 15 M Hz and 25 M Hz. Water was the interaction medium used here also. Bandwidth was not of importance and the transducers were in direct contact with the water. With just over 1 watt of applied electrical power to each transducer 25% of the incident 1 mm diameter 633 nm He-Ne laser light could be deflected into the two first orders and the composite or cross order. Bragg deflection was satisfied by driving each transducer in turn and appropriately adjusting the cell for maximum deflection into each first order. Equations have been given to describe the intensity of each order with the cell adjusted to satisfy exact bragg angle deflection.

The above device has been applied for use in a laser doppler velocimeter system (Farmer and Hornkohl 1973). The two acoustic frequencies here were also 15 M Hz and 25 M Hz and the construction of the device was identical to the device described by Chu and Mauldin (1973). The advantages of this device in this application are that the cell can be used both as a beam splitter and frequency shifter. The optical beam in each first order is shifted either up or down in frequency by the frequency of the associated diffracting acoustic wave and the cross order is shifted up or down by an amount equal to the sum or difference of the two acoustic frequencies, depending on how the incident optical beam and cell are adjusted. Suitably monitoring the light reflected from the moving object indicates both its velocity and direction. The system is less complex than other arrangements used for doppler velocimeter systems and is easier to align since the deflection of each beam appears to originate from a common origin.

This type of device has become commercially available (Spectron 1976) specifically for use in doppler velocimeter systems. The two acoustic frequencies are 15 M Hz and 22.5 M Hz and liquids other than water can be used as the interaction medium. The device has a clear aperture of 32 mm and can be used with optical wavelengths dependent on the interaction medium. The electrical power required by each transducer is thus also dependent on the liquid interaction medium used. Acoustic standing wave capability may also be provided.

A two-dimensional deflector using a paratellurite (TeO_2) single crystal as the interaction medium has been demonstrated by Uchida and Ohmachi (1970). Two 163^{o} rotated Y-cut shear wave lithium niobate transducers were bonded to the crystal so that the sound propagated in mutually perpendicular directions along the crystals' (110) axis. Paratellurite is extremely efficient for the purposes of acousto-optic diffraction for shear (transverse) wave sound propagating along this direction. A rectangular optical aperture of 5 mm × 5 mm was available for light propagating near the (001) axis although no mention was made as to the length and width of the transducers. The transducers centre frequencies were both 24 M Hz and deflection of light into each first order could be accomplished over a 6.5 M Hz bandwidth. With 90 mW of 'acoustic' power 13% of the incident 633 nm He-Ne laser beam could be deflected into each first order. Operating their device over twice the reported bandwidth an array of 70 × 70 just resolvable spot positions was demonstrated by the composite order. By controlling the composite order using a pulse modulated acoustic frequency method (Uchida 1970) an alpha-numeric display was also demonstrated. The percentage of light deflected into the composite order was not mentioned however.

LaMacchia and Coquin (1971) have proposed the concept that X-Y

acousto-optic deflection may occur simultaneously within a single medium. Given the condition that the incident optical beam exactly satisfies the bragg condition for each orthogonal sound column they also have presented equations describing the variation of intensity of the various orders with the associated refractive index change. For this condition they have found that the intrinsic deflection efficiency for two-dimensional deflection is the same as that for a cascaded deflection system. They have stated, without qualification, that the deflection efficiencies in each dimension should be the same. It has been suggested that lead molybdate may be a suitable material for this type of device. They have also commented that the choice between a two-dimensional deflector and a cascaded system should perhaps be determined from practical considerations. Where adequate resolution and deflection efficiency can be obtained with reasonable power levels the two-dimensional deflector may be preferable, resulting in conserved interaction material and a more compact device. An adverse effect on yield may result due to the device requiring two transducers however and they have thus suggested that a cascaded system may still be preferable if device fabrication is a problem. Demonstration of a device was not undertaken here.

3. The Acousto-optic Interaction

3.1. Introduction

In this section the acousto-optic interaction between the light and the two-dimensional phase grating produced by two orthogonal sound columns is examined. The discussion is limited to operation which is well within the bragg regime and is first considered to occur in a material that is essentially isotropic. The interaction has initially been analyzed using the coupled wave equation method. The analysis of the interaction has also been considered in terms of the integral equation method where the incident light is in the form of a gaussian beam. The effects due to the misalignment of the two sound columns have been considered along with the resolution, scattering efficiency, and bandwidth associated with the composite order. The application of the two-dimensional deflection technique to materials which are optically birefringent and in which abnormal, or birefringent, diffraction takes place is discussed. First the principles of operation are outlined.

3.2. Principles of Operation

When a plane travelling longitudinal acoustic wave propagates through an optically transparent material the wave generates planes consisting of high and low pressure regions caused by compression and rarefaction. The refractive index of the medium is thus correspondingly increased and decreased and consequently a travelling phased grating is produced. The grating will cause scattering of light incident at the appropriate angle and the arrangement is analogous to that of bragg X-ray diffraction by lattice planes of crystals. Constructive interference occurs in the case of X-ray diffraction when

the incident radiation of wavelength λ satisfies the well known bragg relationship

$$\sin\theta = \frac{n\lambda}{2d}$$

In the acousto-optic case the lattice spacing d is replaced by the distance between the planes of maximum intensity of the acoustic wave which is equal to the acoustic wavelength. Since the pressure intensity variation is sinusiodal only scattering into the first order is predominant. The incident and deflected optical waves thus make an angle with the acoustic wave normal given by

$$\sin\theta = \frac{\lambda}{2\Lambda}$$

Also, because the phase grating is not stationary, the frequency of the deflected light is increased or decreased by an amount equal to the acoustic frequency depending upon whether the angle between the incident light and the acoustic wave is positive or negative. In practice, the optical and acoustic beams are of finite width. As a result, spreading of the acoustic energy occurs, allowing deflection to be achieved over a range of acoustic frequencies for a fixed direction of the incident optical beam. Steering of the acoustic beam can also be accomplished to allow efficient deflection over a range of acoustic frequencies. Although the phase grating is physically three dimensional the interaction is referred to here as one-dimensional since the deflected light beam is scattered in one dimension only.

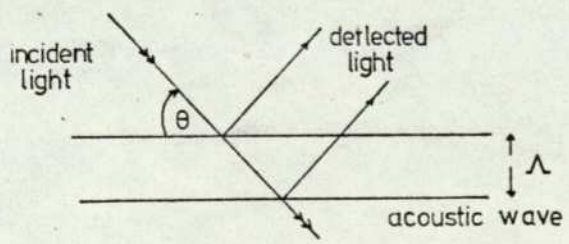

Fig. 3.2.1. One-dimensional acousto-optic bragg deflection.

The objective in introducing an orthogonal acoustic wave is to achieve a composite beam which is capable of being deflected and scanned in two co-ordinates. Light from the incident beam is deflected by each acoustic wave into two first orders which are orthogonal to each other. The orthogonal acoustic wave with respect to each diffracted first order beam will rescatter light from them into a cross order and it is this order that is capable of being deflected in two co-ordinates. Because this order can be deflected in two of its dimensions the interaction is referred to here as two-dimensional although the acoustic phase grating is again physically three dimensional.

3.3. Coupled Wave Equations

The interaction between light and sound can be analyzed using a coupled wave equation method. This has been done by Cohen and Gordon (1965) for a single-dimensional deflector operating within the bragg regime at low scattering efficiencies. Klein and Cook (1967) have considered the same arrangement for high scattering efficiencies. Mahajan (1975) has analyzed this arrangement for sound waves of an arbitary standing wave ratio. This method of approach has been followed here for the two-dimensional case.

The geometry of the interaction is shown in Fig. 3.3.1. The optical beam propagates through the interaction medium in a direction inclined at a small angle with respect to the z axis and the plane, $y = 0$. The two-dimensional optical phase grating is produced by two travelling sound waves, one propagating in the x direction and the other propagating in the y direction. The resulting change in the interaction mediums' optical permittivity, via the elasto-optic effect (see Appendix A), can be described as,

$$\Delta\varepsilon(x,y,t) = \frac{1}{2}\Delta\varepsilon_1 \exp j(\Omega_1 t - K_1 x) + \frac{1}{2}\Delta\varepsilon_2 \exp j(\Omega_2 t - K_2 y) + \text{complex conjugate} \qquad \text{Eq. 3.3.1.}$$

In the interaction medium the incident optical wave mixes with the acoustic waves to generate a number of scattered waves. If the incident optical beam has an angular frequency of ω_o and a wave vector of $\bar{k}_o$ the scattered light consists of waves having an angular frequency and wave vector given by

$$\omega = \omega_o + m\Omega_1 + n\Omega_2$$

$$\bar{k} = \bar{k}_o + m\bar{K}_1 + n\bar{K}_2 \qquad m,n = \pm 1, \pm 2 \text{ etc.}$$

The amplitude of the electric field of both the incident and diffracted optical waves can thus be represented as

$$E(x,y,z,t) = \sum_{m=0}^{\infty}\sum_{n=0}^{\infty} E_{mn}(z) \exp j\left((\omega_o + m\Omega_1 + n\Omega_2)t - (k\cos\beta\sin\alpha + mK_1)x - (k\sin\beta + nK_2)y - (k\cos\alpha\cos\beta)z\right) \qquad \text{Eq. 3.3.2.}$$

It is assumed that the optical and acoustic waves are both plane waves. Within the interaction medium the incident and diffracted optical electric fields must satisfy the wave equation

$$\nabla^2 E - \mu\frac{\partial^2}{\partial t^2}(\varepsilon E) = 0$$

The permittivity is included in the time derivative since it is time dependent. The wave equation can be rewritten as

$$\nabla^2 E - \frac{1}{c^2}\frac{\partial^2}{\partial t^2}\left((1 + \frac{\Delta\varepsilon}{\varepsilon})E\right) = 0 \qquad \text{Eq. 3.3.3.}$$

Substituting Eq. 3.3.1. and Eq. 3.3.2. into Eq. 3.3.3. and performing the required algebra a set of equations for the amplitudes is obtained and is given by

$$\frac{\partial^2 E_{mn}}{\partial z^2} - 2jk\cos\alpha\cos\beta\frac{\partial E_{mn}}{\partial z} + 2k\cos\alpha\cos\beta\,\gamma_{mn}E_{mn} = -\frac{1}{2}k^2\left(\frac{\Delta\varepsilon}{\varepsilon}_1 E_{m+1,n} + \frac{\Delta\varepsilon}{\varepsilon}_1^* E_{m-1,n} + \frac{\Delta\varepsilon}{\varepsilon}_2 E_{m,n+1} + \frac{\Delta\varepsilon}{\varepsilon}_2^* E_{m,n-1}\right) \qquad \text{Eq. 3.3.4.}$$

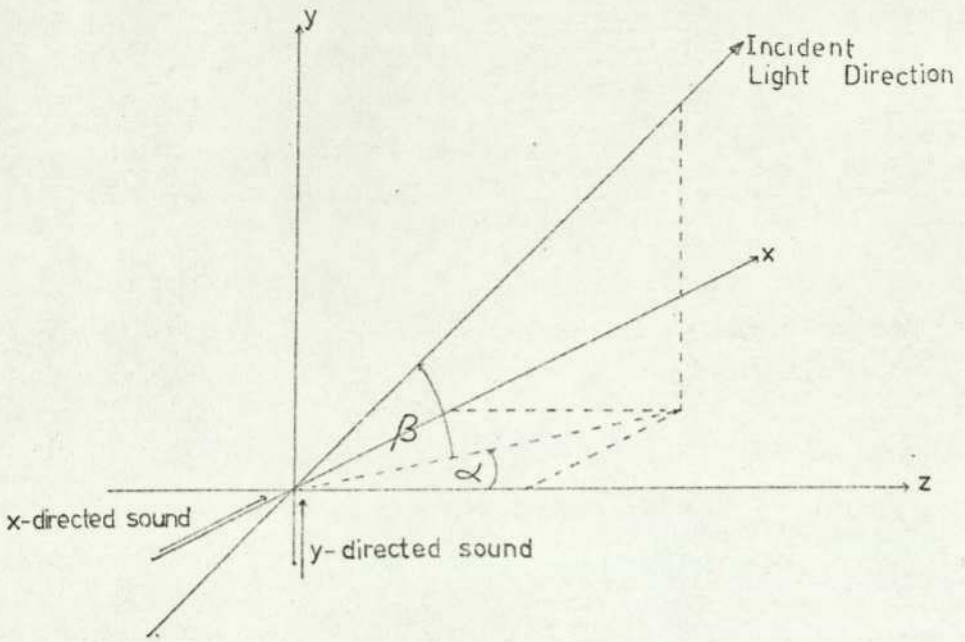

Fig. 3.3.1. Geometry of acousto-optic interaction.

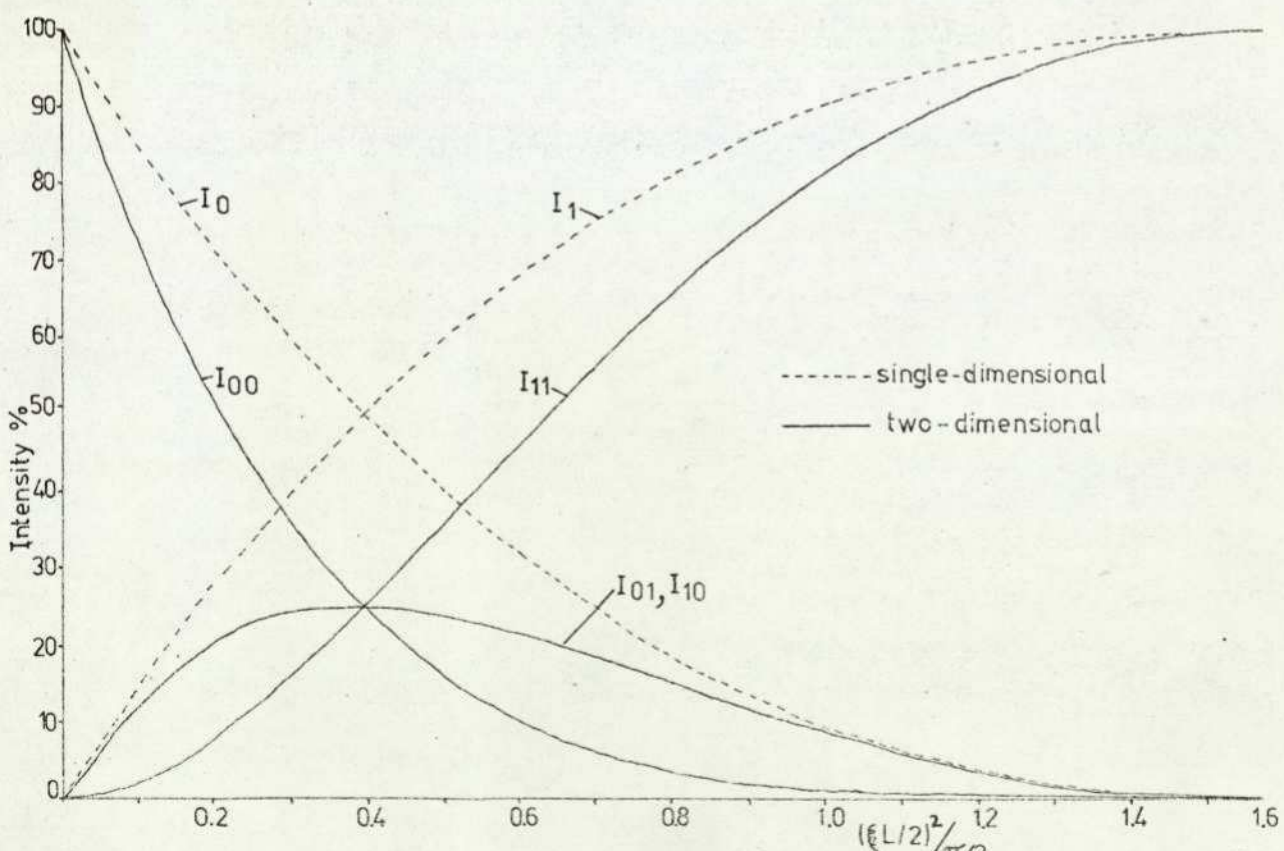

Fig. 3.4.1. The variation of intensity of the incident and deflected orders with acoustic power for both single-dimensional and two-dimensional deflection at the bragg angle, i.e. $\gamma_{mn}=0$.

where $\gamma_{mn} = \left(2mkK_1(\frac{v_1}{c} - \cos\beta\sin\alpha) - m^2K_1^2(1 - \frac{v_1^2}{c^2}) \right.$ Eq. 3.3.5.

$\left. + 2nkK_2(\frac{v_2}{c} - \sin\beta) - n^2K_2^2(1 - \frac{v_2^2}{c^2}) + 2\frac{v_1 v_2}{c^2}mnK_1K_2 \right) \Big/ 2k\cos\alpha\cos\beta$

The second order term is negligible compared to the other terms in Eq. 3.3.4. Since the acoustic frequency is negligible when compared to the optical frequency the following definition can be made.

$$\xi_i = -\frac{k}{2\cos\alpha\cos\beta}\frac{\Delta\varepsilon}{\varepsilon}i \,, \quad i = 1 \text{ or } 2 \qquad \text{Eq. 3.3.6.}$$

Thus Eq. 3.3.4. can be rewritten as

$$E'_{mn} + j\gamma_{mn}E_{mn} = \frac{1}{2}j\left(\xi_1 E_{m+1,n} + \xi_1^* E_{m-1,n} + \xi_2 E_{m,n+1} + \xi_2^* E_{m,n-1}\right) \qquad \text{Eq. 3.3.7.}$$

Since one desires to be able to deflect all of the incident light into the composite order the interaction is assumed to be well within the bragg regime and consequently the subscripts take on values of 0 or 1 only. Eq. 3.3.7. yields the following difference-differencial equations.

$$\begin{aligned}
E'_{00} &= \tfrac{1}{2}j\left(\xi_1 E_{10} + \xi_2 E_{01}\right) \\
E'_{01} + j\gamma_{01}E_{01} &= \tfrac{1}{2}j\left(\xi_1 E_{11} + \xi_2^* E_{00}\right) \\
E'_{10} + j\gamma_{10}E_{10} &= \tfrac{1}{2}j\left(\xi_1^* E_{00} + \xi_2 E_{11}\right) \\
E'_{11} + j(\gamma_{10} + \gamma_{01})E_{11} &= \tfrac{1}{2}j\left(\xi_1^* E_{01} + \xi_2^* E_{10}\right)
\end{aligned} \qquad \text{Eq. 3.3.8.}$$

where γ_{11} is replaced by $\gamma_{10} + \gamma_{01}$ assuming the last term in Eq. 3.3.5. to be negligible , and the prime denotes differentiation.

If we first consider the case where the arrangement is symmetrical in both x and y we may put $\gamma_{10} = \gamma_{01} = \gamma$, $\xi_{10} = \xi_{01} = \xi$, and $E_{10} = E_{01}$. Thus the difference equations reduce to

$$\begin{aligned}
D\,E_{00} &= j\,\xi\,E_{10} \\
(D + j\gamma)E_{10} &= \tfrac{1}{2}j\left(\xi\,E_{11} + \xi\,E_{00}\right) \\
(D + j2\gamma)E_{11} &= j\,\xi\,E_{10} \qquad \text{where } D = \frac{\partial}{\partial z}
\end{aligned} \qquad \text{Eq. 3.3.9.}$$

Solving for E_{mn} we obtain the differential equation,

$$\left(D^3 + 3j\gamma D^2 + (\xi^2 - 2\gamma^2)D + j\gamma\xi^2\right)E_{mn} = 0 \qquad \text{Eq. 3.3.10.}$$

The appropriate boundary conditions are,

at $z = 0$ $\quad E_{mn} = \hat{E}_o \quad m,n = 0$

$= 0 \quad m,n \neq 0$

Solving Eq. 3.3.10. subject to the given boundary conditions yields the following expressions for E_{mn} ,

$$E_{00} = \exp(-j\gamma z)\left(A_{00} - (A_{00} - \hat{E}_o)\cos\Gamma z + B_{00}\sin\Gamma z\right)$$

$$E_{10} = \exp(-j\gamma z)\left(A_{10}(1-\cos\Gamma z) + B_{10}\sin\Gamma z\right) \qquad \text{Eq. 3.3.11.}$$

$$E_{11} = \exp(-j\gamma z)\left(A_{11}(1-\cos\Gamma z) + B_{11}\sin\Gamma z\right)$$

where $\Gamma = (\xi^2 + \gamma^2)^{\frac{1}{2}}$

Substituting the expressions of Eq. 3.3.1.. back into Eq. 3.3.9. the constants in Eq. 3.3.11. can be found and by performing the necessary algebra the solutions for the various orders are given by,

$$E_{00} = \exp(-j\gamma z)\,\hat{E}_o\left(\cos\tfrac{1}{2}\Gamma z + j\frac{\gamma}{\Gamma}\sin\tfrac{1}{2}\Gamma z\right)^2 \qquad \text{Eq. 3.3.12.}$$

$$E_{01} = E_{10} = \exp(-j\gamma z)\cdot j\frac{\xi\hat{E}_o}{2}\cdot\frac{\sin\frac{1}{2}\Gamma z}{\frac{1}{2}\Gamma z}\left(\cos\tfrac{1}{2}\Gamma z + j\frac{\gamma}{\Gamma}\sin\tfrac{1}{2}\Gamma z\right)$$

$$E_{11} = \exp(-j\gamma z)\cdot -\frac{\xi^2\hat{E}_o}{4}\cdot\left(\frac{\sin\frac{1}{2}\Gamma z}{\frac{1}{2}\Gamma z}\right)^2$$

When trying to solve the four first order difference-differential equations when $\gamma_{10} \neq \gamma_{01}$, $\xi_{10} \neq \xi_{10}$, and $E_{10} \neq E_{01}$, the resulting equations become complex and somewhat difficult to solve analytically. However, because a solution has been obtained for E_{mn} when the interaction is symmetrical a guess may be made for the general solution of E_{mn} for the assymmetric case. Trial solutions can be made and those which, upon substitution, satisfy the differential equations Eq. 3.3.8. have been found to be

$$E_{00} = \hat{E}_o\exp(-\tfrac{1}{2}j(\gamma_{10}+\gamma_{01})z)\cdot\left(\cos\tfrac{1}{2}\Gamma_1 z + j\frac{\gamma_1}{\Gamma_1}\sin\tfrac{1}{2}\Gamma_1 z\right)\cdot\left(\cos\tfrac{1}{2}\Gamma_2 z + j\frac{\gamma_2}{\Gamma_2}\sin\tfrac{1}{2}\Gamma_2 z\right)$$

$$E_{10} = \hat{E}_o\exp(-\tfrac{1}{2}j(\gamma_{10}+\gamma_{01})z)\cdot\tfrac{1}{2}j\,\xi_1^*\cdot\frac{\sin\frac{1}{2}\Gamma_1 z}{\frac{1}{2}\Gamma_1}\cdot\left(\cos\tfrac{1}{2}\Gamma_2 z + j\frac{\gamma_2}{\Gamma_2}\sin\tfrac{1}{2}\Gamma_2 z\right) \qquad \text{Eq. 3.3.13.}$$

$$E_{01} = \hat{E}_o\exp(-\tfrac{1}{2}j(\gamma_{10}+\gamma_{01})z)\cdot\tfrac{1}{2}j\,\xi_2\cdot\frac{\sin\frac{1}{2}\Gamma_2 z}{\frac{1}{2}\Gamma_2}\cdot\left(\cos\tfrac{1}{2}\Gamma_1 z + j\frac{\gamma_1}{\Gamma_1}\sin\tfrac{1}{2}\Gamma_1 z\right)$$

$$E_{11} = -\hat{E}_o\exp(-\tfrac{1}{2}j(\gamma_{10}+\gamma_{01})z)\cdot\frac{\xi_1^*\xi_2}{4}\cdot\frac{\sin\frac{1}{2}\Gamma_1 z}{\frac{1}{2}\Gamma_1}\cdot\frac{\sin\frac{1}{2}\Gamma_2 z}{\frac{1}{2}\Gamma_2}$$

Consequently, if the interaction length is L then the intensity of the various orders is given by,

$$I_{mn} = E_{mn} \cdot E^{*}_{mn}$$

or

$$I_{00} = \hat{I}_o \left(\cos^2 \tfrac{1}{2}\Gamma_1 L + \frac{\gamma_1^2}{\Gamma_1^2} \sin^2 \tfrac{1}{2}\Gamma_1 L\right)\left(\cos^2 \tfrac{1}{2}\Gamma_2 L + \frac{\gamma_2^2}{\Gamma_2^2} \sin^2 \tfrac{1}{2}\Gamma_2 L\right)$$

$$I_{10} = \hat{I}_o \frac{|\underline{s}_1|^2 L^2}{4} \left(\frac{\sin \frac{1}{2}\Gamma_1 L}{\frac{1}{2}\Gamma_1 L}\right)^2 \left(\cos^2 \tfrac{1}{2}\Gamma_2 L + \frac{\gamma_2^2}{\Gamma_2^2} \sin^2 \tfrac{1}{2}\Gamma_2 L\right) \qquad \text{Eq. 3.3.14.}$$

$$I_{01} = \hat{I}_o \frac{|\underline{s}_2|^2 L^2}{4} \left(\frac{\sin \frac{1}{2}\Gamma_2 L}{\frac{1}{2}\Gamma_2 L}\right)^2 \left(\cos^2 \tfrac{1}{2}\Gamma_1 L + \frac{\gamma_1^2}{\Gamma_1^2} \sin^2 \tfrac{1}{2}\Gamma_1 L\right)$$

and

$$I_{11} = \hat{I}_o \frac{|\underline{s}_1|^2 |\underline{s}_2|^2 L^4}{16} \left(\frac{\sin \frac{1}{2}\Gamma_1 L}{\frac{1}{2}\Gamma_1 L}\right)^2 \left(\frac{\sin \frac{1}{2}\Gamma_2 L}{\frac{1}{2}\Gamma_2 L}\right)^2$$

It is interesting to note that, irrespective of the values of the various parameters in Eq. 3.3.14., the intensities of the various orders can be related by,

$$I_{00} \cdot I_{11} = I_{10} \cdot I_{01} \qquad \text{Eq. 3.3.15.}$$

Also, it is obvious that the sum of the intensities of the orders must equal the intensity of the incident beam

$$I_{00} + I_{01} + I_{10} + I_{11} = \hat{I}_o$$

Thus, the examination of equations Eq. 3.3.14. shows that for the interaction geometry considered the net effect produced is essentially the product of two single-dimensional deflections.

3.4. Efficiency

The acoustic amplitude function, $\underline{s}$, is usually small compared to γ except at the bragg angle. If the incident beam satisfies the bragg angle with respect to each sound column then $\gamma_{10} = \gamma_{01} = 0$.

Consequently the intensities are given by (LaMacchia and Coquin 1971, Chu and Mauldin 1973),

$$
\begin{aligned}
I_{00} &= \hat{I}_o \cos^2 \tfrac{1}{2}|\xi_1|L \cdot \cos^2 \tfrac{1}{2}|\xi_2|L \\
I_{10} &= \hat{I}_o \sin^2 \tfrac{1}{2}|\xi_1|L \cdot \cos^2 \tfrac{1}{2}|\xi_2|L \\
I_{01} &= \hat{I}_o \sin^2 \tfrac{1}{2}|\xi_2|L \cdot \cos^2 \tfrac{1}{2}|\xi_1|L \\
I_{11} &= \hat{I}_o \sin^2 \tfrac{1}{2}|\xi_1|L \cdot \sin^2 \tfrac{1}{2}|\xi_2|L
\end{aligned}
\qquad \text{Eq. 3.4.1.}
$$

and the bragg angles are given by,

$$
\begin{aligned}
\sin \Phi_1 &= \frac{v_1}{c} - \frac{K_1}{2k}\left(1 - \frac{v_1^2}{c^2}\right) \simeq -\frac{\lambda}{2\Lambda_1} \\
\sin \Phi_2 &= \frac{v_2}{c} - \frac{K_2}{2k}\left(1 - \frac{v_2^2}{c^2}\right) \simeq -\frac{\lambda}{2\Lambda_2}
\end{aligned}
\qquad \text{Eq. 3.4.2.}
$$

where $\gamma_{10} = K_1 (\sin \Phi_1 - \cos\beta \sin\alpha) / \cos\alpha\cos\beta$

$\gamma_{01} = K_2 (\sin \Phi_2 - \sin\beta) / \cos\alpha.\cos\beta$

It can be seen that when $\frac{1}{2}|\xi_1|L$ and $\frac{1}{2}|\xi_2|L$ are equal to $\frac{\pi}{2}$ all of the incident light can be deflected into the composite order I_{11} and that the zero order and the two first orders are extinguished.

By reverting to the case where the interaction geometry is symmetrical, i.e., $\xi_1 = \xi_2$, the variation of intensity of the four orders with respect to the power of each acoustic wave is shown in Fig. 3.4.1. For comparison the variation is shown for a single-dimensional deflector. Because the composite order follows a $\sin^4 x$ relationship the amount of light scattered at weak efficiencies is quite small. When the acoustic power in each co-ordinate is equal to that which can deflect 50% of the light in a single-dimensional deflector the light scattered into each order in the two-dimensional deflector is 25%. Above this power level the majority of the light will be deflected into the composite order.

Here, the deflection efficiency in the first co-ordinate is related by

$$P_{a_1} = \delta_1 . \frac{1}{M_{2_1}} . \frac{H_1}{L} \qquad \text{Eq. 3.4.3.}$$

where $M_{2_1} = \dfrac{\Pi_1^6 \; p_1^2}{\rho \; v_1^3}$ is a figure of merit,

H is the transducer height and,

$$\delta_1 = \frac{2 \lambda_o^2}{\pi^2} \left(\sin^{-1} \sqrt{\frac{I_{10}}{\hat{I}_o}} \right)^2$$

A similar expression exists for deflection in the orthogonal direction.

Use has been made of the expression (Gordon 1966),

$$P_a = \frac{1}{2} \rho \, v^3 |S|^2 \, L \, H$$

where P_a and S are the acoustic Power and Strain respectively.

3.5. The Integral Equation

The acousto-optic interaction can be described in terms of an integral equation. The solution to the wave equation can be derived, by the use of Greens' functions (Morse and Feshback 1953, Born and Wolf 1959), to yield Kirchhoffs formula (Papoulis 1968). For the general case the wave equation can be expressed as,

$$\nabla^2 E + k^2 E = W$$

Kirchoffs' formula has the form.

$$E_e(X,Y,Z) = \int_{S_o} \left(E(x_o,y_o,z_o) . \frac{\partial G(r_o,R)}{\partial \bar{n}_o} - G(r_o,R) . \frac{\partial E(x_o,y_o,z_o)}{\partial \bar{n}_o} \right) ds_o + \int_{V_o} W \, G(r_o,R) \, dv_o \qquad \text{Eq. 3.5.1.}$$

where $G(r_o,R) = - \dfrac{\exp(-jk(r_o - R))}{4\pi(r_o - R)}$ is the greens function in an infinite volume and E_e is the effect in the co-ordinate space

(X,Y,Z) produced by the source E in the co-ordinate space (x_o, y_o, z_o).

The wave equation, as expressed in Eq. 3.3.3., can be written in the form.

$$\nabla^2 E_s + k_s^2 E_s = \frac{\partial^2}{\partial t^2}\left(\frac{\Delta\varepsilon}{\varepsilon} E_i\right) \qquad \text{Eq. 3.5.2.}$$

where E_s and k_s are the amplitude and wave vector of electric field of the scattered light and E_i is the electric field of the incident light.

This treatment assumes that the sound intensity is sufficiently weak so that only a small fraction of the incident light is deflected. Effects due to rescattering are assumed negligible. As previously stated the interaction between the light and the sound produces scattered light whose frequency is shifted by an amount equal to multiples of the acoustic frequency. The interaction volume may thus be considered as the source of the radiated bragg diffracted light signal. The volume integral in Eq. 3.5.1. therefore need only be considered. Combining Eq. 3.5.1. and Eq. 3.5.2. the electric field of the scattered light can be expressed as

$$E_s(X,Y,Z) = \int_{v_o} \frac{\partial^2}{\partial t^2}\left(\frac{\Delta\varepsilon}{\varepsilon}(x_o y_o z_o) \cdot E_i(x_o y_o z_o)\right) \cdot G(r_o R)\, dv_o \qquad \text{Eq. 3.5.3.}$$

This approach has been followed by Gordon (1966) for considerations concerning modulation and deflection between an optical beam and a single acoustic beam, both of finite dimensions. McMahon (1969) has shown by this approach that the interaction efficiency decreases as the bragg angle increases and as the diameter of the incident light beam decreases relative to the sound column thickness, and that the difference between using an incident beam of gaussian or rectangular cross-section is small. Also Maydan (1970) has used this approach to analyze the acousto-optic interaction for pulse modulation purposes.

In the two-dimensional case substitution of Eq. 3.3.1. for the fractional change in permittivity yields,

$$E_s(X,Y,Z) = k_s^2 \int_{V_o} \frac{\Delta\varepsilon}{\varepsilon}_1(x_o).E_i(x_o,y_o,z_o).G(r_o,R).dv_o + k_s^2 \int_{V_o} \frac{\Delta\varepsilon}{\varepsilon}_2(y_o).E_i(x_o,y_o,z_o).G(r_o,R).dv_o$$

This merely represents the light scattered into the two first orders, I_{10} and I_{01} only, and information concerning the composite order is not given here since rescattering effects have been assumed negligible. However, the composite beam can be expressed, in the limit of weak scattering, by using Eq. 3.3.15., as

$$I_{11} = \frac{I_{10} \cdot I_{01}}{\hat{I}_o}$$

Consequently, the amplitude of the electric field of the composite order can be expressed as,

$$E_{s_{11}}(X,Y,Z) \propto \int_{V_o} \frac{\Delta\varepsilon}{\varepsilon}_1(x_o).E_i(x_o,y_o,z_o).G(r_o,R).dv_o \cdot \int_{V_o} \frac{\Delta\varepsilon}{\varepsilon}_2(y_o).E_i(x_o,y_o,z_o).G(r_o,R).dv_o \qquad \text{Eq. 3.5.4.}$$

The interaction geometry is shown in Fig. 3.5.1. The incident beam considered here, which can be obtained from most laser sources, is of a gaussian cross-section and can be expressed as,

$$E_i(x_o,y_o,z_o) = \hat{E}_o.\exp\left(jk(\cos\emptyset_o\sin\theta_o x_o + \sin\emptyset_o y_o - \cos\emptyset_o\cos\theta_o z_o)\right)$$
$$.\exp\left(-\frac{1}{w_o^2}[(\cos\emptyset_o y_o + \sin\emptyset_o(\cos\theta_o z_o - \sin\theta_o x_o))^2 + (\cos\theta_o x_o + \sin\theta_o z_o)^2]\right)$$

where k is the wave vector and $2w_o$ is the diameter of the beam waist .

Consequently, Eq. 3.5.4. can be expressed as,

$$E_{s_{11}} \propto \int_{V_o} F.\left|\frac{\Delta\varepsilon}{\varepsilon}_1\right|.\exp(-jK_1x_o).dv_o \cdot \int_{V_o} F.\left|\frac{\Delta\varepsilon}{\varepsilon}_2\right|\exp(-jK_2y_o).dv_o \qquad \text{Eq. 3.5.5.}$$

where

$$F = E_i(x_o,y_o,z_o).\frac{\exp(-jk_sR)}{R}$$
$$.\exp\left(j\,k_s(\cos\emptyset_o\sin\theta_o.x_o + \sin\emptyset_o.y_o + \cos\emptyset_o.\cos\theta_o.z_o)\right)$$

and where $R \gg r_o$

and $R - r_o \simeq R - \frac{X}{R}x_o - \frac{Y}{R}y_o - \frac{Z}{R}z_o$

and $\frac{X}{R} = \cos\emptyset\sin\theta \quad \frac{Y}{R} = \sin\emptyset \quad \frac{Z}{R} = \cos\emptyset\cos\theta$

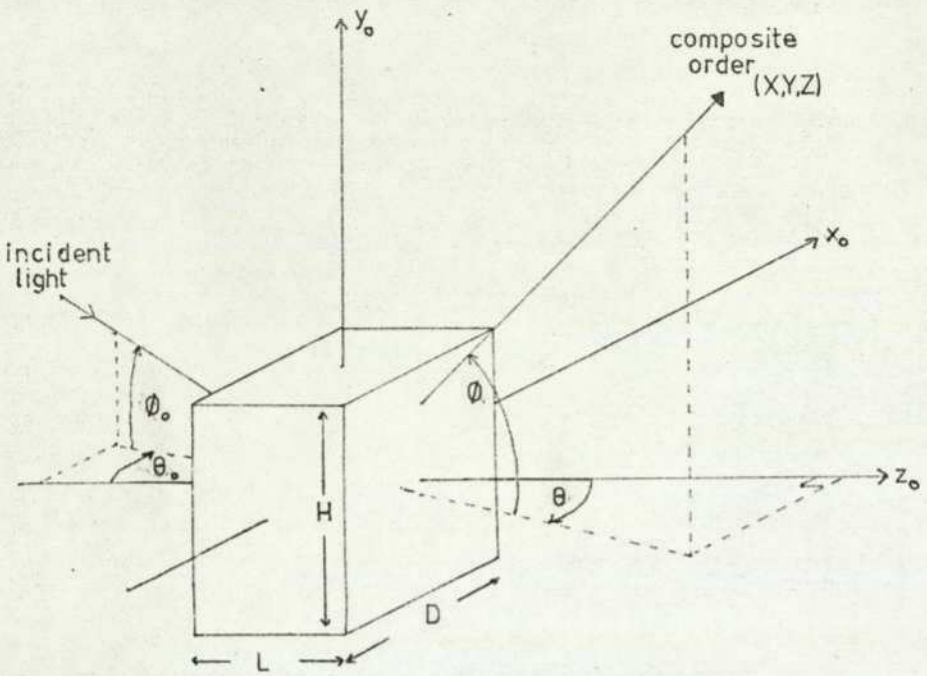

Fig. 3.5.1. Scattering geometry of the two-dimensional deflector. The acoustic wave normals are x- and y- directed.

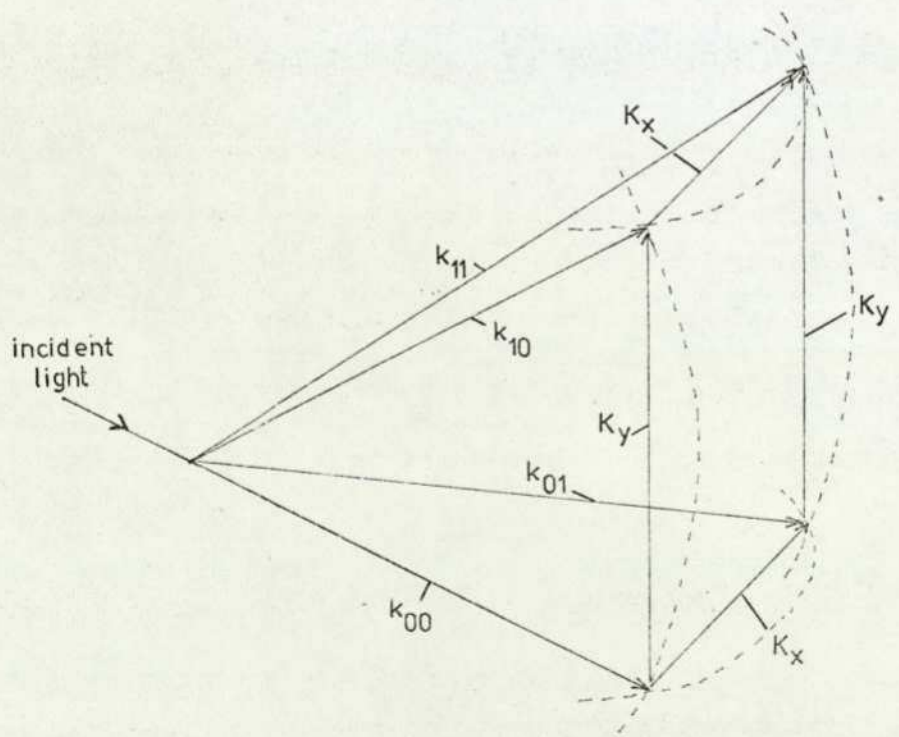

Fig. 3.5.2. Vector summation of the two-dimensional interaction under normal bragg conditions.

The solution to the integral equation in this case is quite lengthy. Solutions for the case where only a single acoustic beam is present have been admirably dealt with and given by both Gordon (1966) and Maydan (1970) and the extension of their results to the two-dimensional case is quite obvious. The equation for the light scattered into the composite order in the two-dimensional case given here is thus similar to their solutions apart from the fact that the incident light enters the interaction medium at an oblique angle with respect to both the x_0 and y_0 axes and that it is the product of two deflections instead of one. By assuming that essentially all the incident light is included within the interaction area the resulting distribution of the composite beam can be given approximately by,

$$|E_{s_{11}}| \propto \left(\hat{E}_o w_o\right) \cdot \left(\left|\frac{\Delta\varepsilon}{\bar{\varepsilon}}_1\right|^2 L H\right)^{\frac{1}{2}} \cdot \left[\frac{\operatorname{erf}^2\left(\frac{H\sqrt{a}}{2w_o}\right)}{\left(\frac{H\sqrt{a}}{2w_o}\right)}\right]^{\frac{1}{2}} \cdot \left[\frac{\operatorname{erf}^2\left(\frac{D\cos\phi_o\cos\theta_o}{2w_o\sqrt{a}}\right)}{\left(\frac{D\cos\phi_o\cos\theta_o}{2w_o\sqrt{a}}\right)}\right]^{\frac{1}{2}}$$

$$\cdot \left[\frac{LD\pi^2}{4\cos\phi_o\cos\theta_o}\right]^{\frac{1}{2}} \cdot \exp\left[-\frac{w_o^2}{4}\left(\frac{\gamma_1^2}{a} + \frac{\beta_1^2 a}{\cos^2\phi_o\cos^2\theta_o}\right)\right] \cdot \frac{\sin\left(\alpha_1 + \frac{\tan\phi_o}{\cos\theta_o}\beta_1\right)\frac{L}{2}}{\left(\alpha_1 + \frac{\tan\phi_o}{\cos\theta_o}\beta_1\right)\frac{L}{2}}$$

$$\times \quad \left(\hat{E}_o w_o\right) \cdot \left(\left|\frac{\Delta\varepsilon}{\bar{\varepsilon}}_2\right|^2 LD\right)^{\frac{1}{2}} \cdot \left[\frac{\operatorname{erf}^2\left(\frac{H\sqrt{a}}{2w_o}\right)}{\left(\frac{H\sqrt{a}}{2w_o}\right)}\right]^{\frac{1}{2}} \cdot \left[\frac{\operatorname{erf}^2\left(\frac{D\cos\phi_o\cos\theta_o}{2w_o\sqrt{a}}\right)}{\left(\frac{D\cos\phi_o\cos\theta_o}{2w_o\sqrt{a}}\right)}\right]^{-\frac{1}{2}} \qquad \text{Eq. 3.5.6.}$$

$$\cdot \left[\frac{LH\pi^2}{4\cos\phi_o\cos\theta_o}\right]^{\frac{1}{2}} \cdot \exp\left[-\frac{w_o^2}{4}\left(\frac{\gamma_2^2}{a} + \frac{\beta_2^2 a}{\cos^2\phi_o\cos^2\theta_o}\right)\right] \cdot \frac{\sin\left(\alpha_2 + \frac{\tan\phi_o}{\cos\theta_o}\beta_2\right)\frac{L}{2}}{\left(\alpha_2 + \frac{\tan\phi_o}{\cos\theta_o}\beta_2\right)\frac{L}{2}}$$

where $a = 1 - \sin^2\theta_o\cos^2\phi_o$

and $\gamma_1 = k\cos\phi_o\sin\theta_o + k_s\cos\phi\sin\theta - K_1$

$$\gamma_2 = \gamma_1 + K_1$$

$$\alpha_1 = \xi_1 + \gamma_1^2\frac{\sin 2\theta_o\cos^2\phi_o}{2a}$$

$$\alpha_2 = \xi_2 + \gamma_2^2\frac{\sin 2\theta_o\cos^2\phi_o}{2a}$$

$$\beta_1 = \eta_1 + \gamma_1^2\frac{\sin\theta_o\sin 2\phi_o}{2a}$$

$$\beta_2 = \eta_2 + \gamma_2^2\frac{\sin\theta_o\sin 2\phi_o}{2a}$$

where $\xi_1 = \xi_2 = k_s \cos\phi \cos\theta - k \cos\phi_o \cos\theta_o$

$\eta_1 = -(k \sin\phi_o + k_s \sin\phi)$ and $\eta_2 = \eta_1 + K_2$

The first term in each part corresponds to the amplitude of the optical beam. The second terms correspond to the amplitude of the acoustic waves. The error function terms indicate that there is an optimum acoustic beam height consistent with the diameter $2w_o$ of the incident optical beam. For a symmetric gaussian beam the optimum is given when $D = H \simeq 2w_o$. The final terms indicate that optimum scattering is achieved when $\bar{k}_s = \bar{k} + \bar{K}_1 + \bar{K}_2$. Since the scattering process is reactive, or parametric, the conservation of momentum applies and is illustrated in Fig. 3.5.2. If the bragg angle with respect to each sound column is not satisfied the vector sum of the wave vectors is no longer satisfied and consequently scattering of the incident beam into the composite order is no longer readily achieved.

3.6. Misalignment

So far we have considered the case where the interaction occurs when the two sound columns overlap, the two acoustic transducers are placed so that they are at right angles with respect to each other, and that the longitudinal axes of both transducers are parallel to the longitudinal axis of the interaction medium.

When the two sound columns only partially overlap or do not overlap at all no significant change to the interaction is produced. As previously mentioned the composite beam is essentially the product of two single deflections. Thus, if, say, the y propagating sound column is of length L_2 and is shifted along the z axis by a distance z'

with respect to the x propagating sound column then the expression for the composite beam in Eq. 3.3.14 merely takes the form,

$$I_{11} = \hat{I}_o \frac{|\xi_1|^2 |\xi_2|^2 L_1^2 L_2^2}{16} \left(\frac{\sin \frac{1}{2}\Gamma_1 L_1}{\frac{1}{2}\Gamma_1 L_1}\right)^2 \left(\frac{\sin \frac{1}{2}\Gamma_2 L_2}{\frac{1}{2}\Gamma_2 L_2}\right)^2 \qquad \text{Eq. 3.6.1.}$$

where L_1 is the length of the x propagating sound column.

The variation in the length z' then has no effect upon the interaction and misalignment of this type is thus of no consequence.

Misalignment can occur if the longitudinal axis of the transducers are not parallel to the longitudinal axis of the interaction medium. This means that the wavefronts of the sound columns are propagating in a direction which is at an angle with respect to the x or y axis. This can simply be corrected by readjusting the direction of the incident light so that the bragg angle is again satisfied with each sound column. This misalignment merely repositions the longitudinal axis of the interaction medium and is thus also of no real consequence.

The most significant type of misalignment is when the two sound columns are not orientated at right angles with respect to each other. When this occurs the wave vector summation is not satisfied and the deflection of light into the composite order will become increasingly difficult as the misalignment increases.

Consider the case where the change in optical permittivity is produced by an acoustic wave propagating along the x axis and by another propagating at an angle θ with respect to the x axis and lying in the plane $z = 0$. This is given by,

$$\Delta\varepsilon(x,y,t) = \tfrac{1}{2}\Delta\varepsilon_1 \exp j(\Omega_1 t - K_1 x) + \tfrac{1}{2}\Delta\varepsilon_2 \exp j(\Omega_2 t - K_2 \cos\theta . x - K_2 \sin\theta . y) + \text{complex conjugate} \qquad \text{Eq. 3.6.2.}$$

Following the coupled wave analysis the resulting equations

are the same as that in Eq. 3.3.8. except for the modifications,

$$\gamma_{11} = \gamma_{01} + \gamma_{10} + 2 K_1 K_2 \left(\frac{v_1 v_2}{c^2} - \cos\theta \right)$$

$$\gamma_{01} = 2 K_2 k \left(\frac{v_2}{c} \cdot - \sin\beta \sin\theta \right) - K_2^2 \left(1 - \frac{v_2^2}{c^2} \right) \qquad \text{Eq. 3.6.3.}$$

and γ_{10} is the same as that previously defined in Eq. 3.3.5.

The last term in the expression for γ_{11} is no longer negligible when the sound columns are not at right-angles with respect to each other. The inclusion of this term considerably complicates the analysis and an analytic solution for the different orders has not been found possible. By considering that the interaction medium is isotropic and that the light satisfies the bragg angle with respect to each sound column i.e. $\gamma_{01} = \gamma_{10} = 0$, the difference-differential equations have been solved numerically using Runge-Kutta techniques for the following conditions,

$$v = 10^3 \text{m/s} \ , \quad c = 10^8 \text{m/s} \ , \quad \lambda = 500 \text{ nm}$$

By assuming that when the two sound columns are at right angles to each other the acoustic power is such that all the light can be scattered into the composite order, i.e. $\xi_1 = \xi_2 = \pi$ for $L = 1\text{m}$, the difference equations can be simplified, for a symmetrical arrangement, to

$$\begin{aligned} E'_{00} &= j\pi E_{01} \\ E'_{10} = E'_{01} &= \tfrac{1}{2} j\pi (E_{00} + E_{11}) \\ E'_{11} + j\gamma_{11} E_{11} &= j\pi E_{01} \end{aligned} \qquad \text{Eq. 3.6.4.}$$

The variation of the intensity of the composite order I_{11} is shown in Fig. 3.6.1. as the angle θ varies $\pm 10^0$ about 90^0. Also shown is its variation for different values of the bragg frequency where,

$$\frac{\lambda}{\Lambda^2} = n'^2 \quad \text{or} \quad f_{(\text{bragg})} = n' f_{BM} \qquad \text{(see section 3.8.1.)}$$

The variation of intensity with angle θ of the other orders as

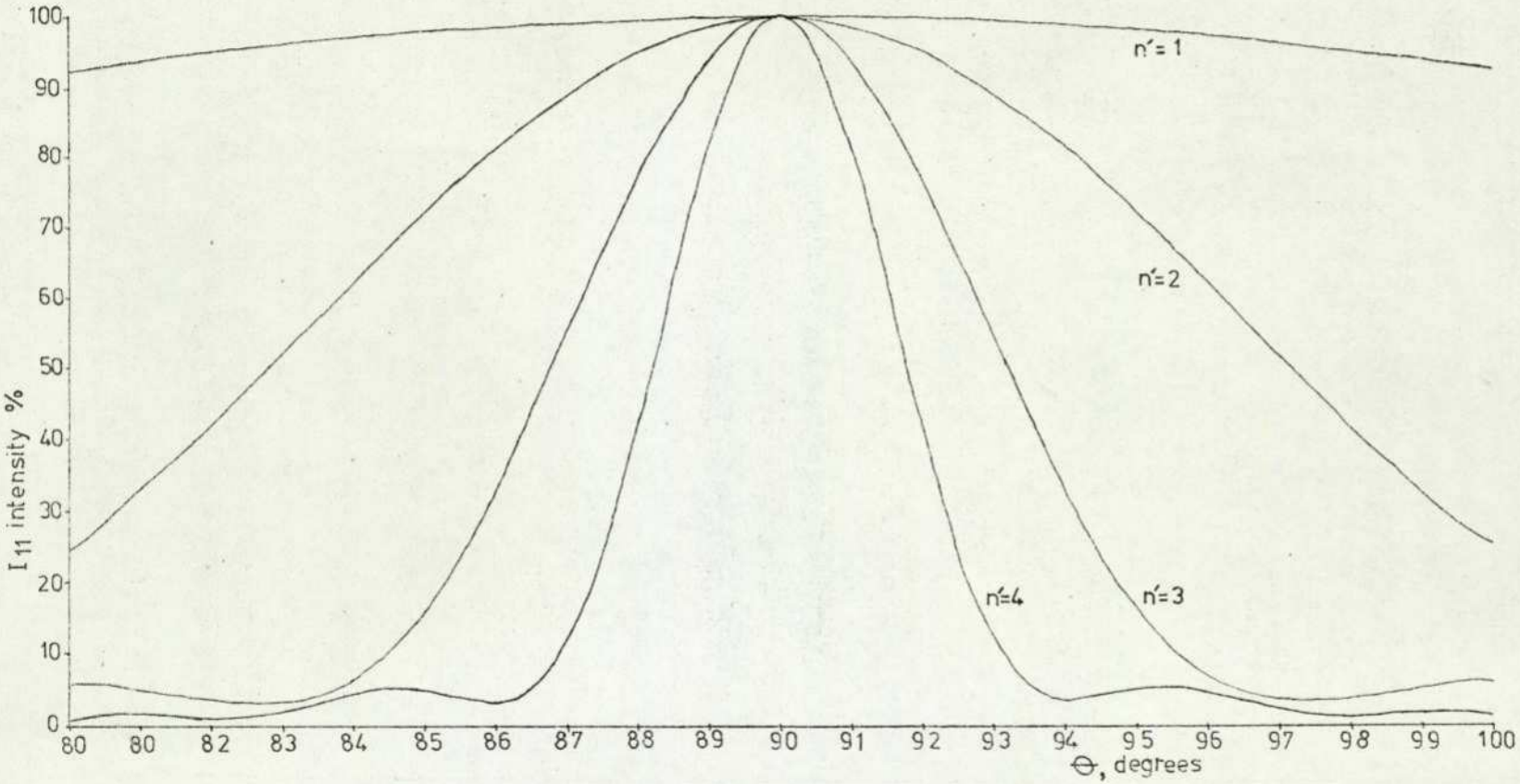

Fig. 3.6.1. Misalignment; Variation of intensity of composite order for various multiples of the minimum bragg frequency with respect to the angle between the two acoustic columns.

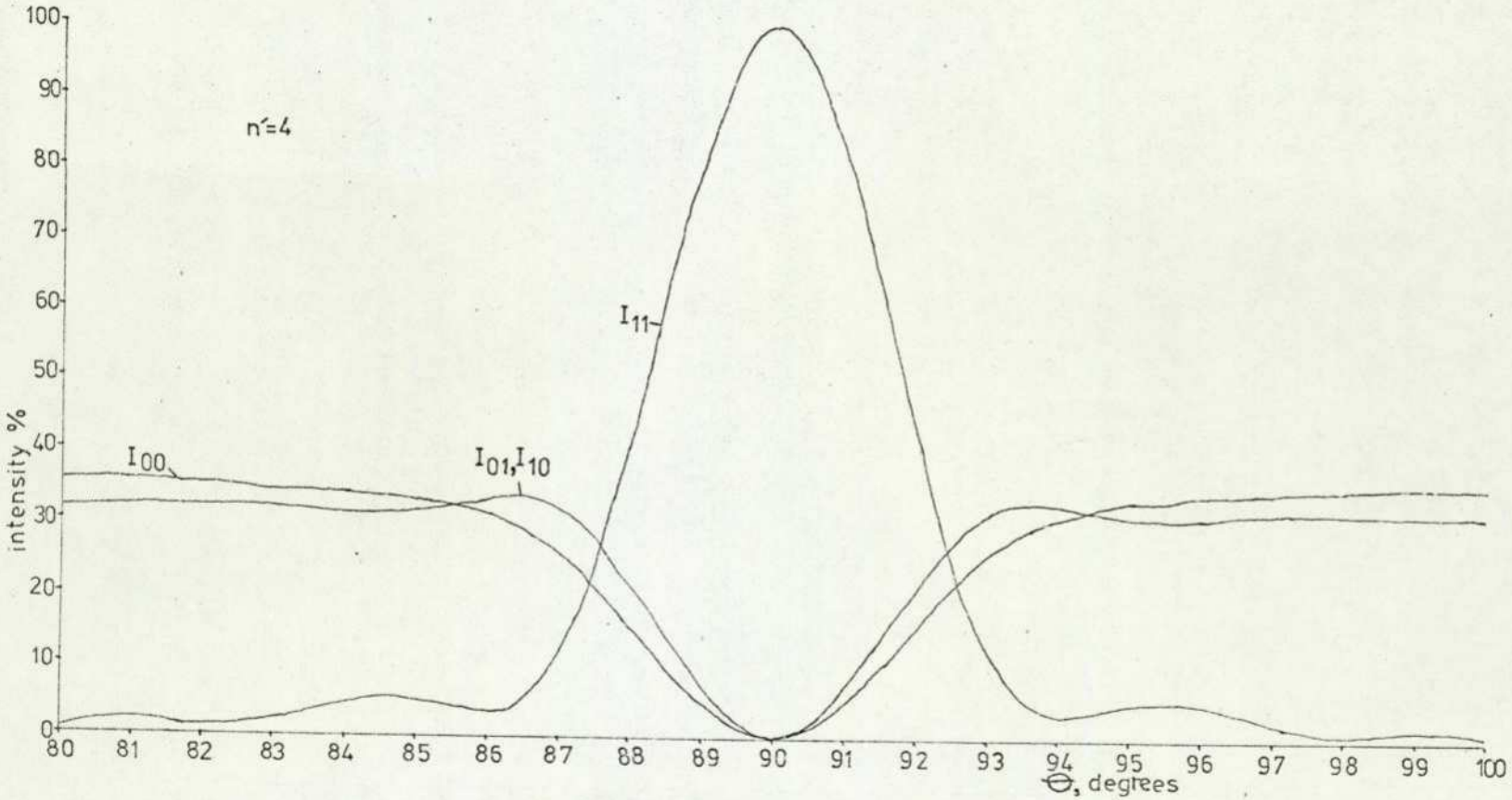

Fig. 3.6.2. Misalignment: Variation of intensity of the four orders for the highest bragg frequency considered with respect to the angle between the two acoustic columns.

well as the composite order is shown in Fig. 3.6.2. corresponding to the highest bragg frequency considered here.

It can be seen that the optimum setting for the conditions mentioned is when the sound columns are at right angles with respect to each other and for angles other than 90^{o} the efficiency of deflection of light into the composite beam decreases. The criticalness of alignment is dependent upon the bragg frequency. At low frequencies the tolerance is quite large but as the frequency increases the criticalness increases rapidly.

Although it is shown that all the light can be scattered into the composite order when properly aligned, in practice, at low frequencies, this is not strictly true. Light will be deflected into orders other than the four considered here and the maximum amount of light that can be deflected into the composite beam will be somewhat less than that in the incident beam. Low frequency scattering for single-dimensional deflectors has been considered by Klien and Cook (1967) for example. Thus the situation here is only reached when n' is very large and consequently the angle θ must be 90^{o} for efficient composite order deflection.

3.7. Resolution

It is well known that the resolution that can be obtained from a one-dimensional deflector is given by,

$$N = \frac{\Delta\theta}{\frac{1}{2}\delta\phi} \qquad \text{Eq. 3.7.1.}$$

where N is the number of resolvable spots, $\Delta\theta$ is the total angular range in which the incident optical beam can be deflected and $\delta\phi$ is the angular spread of the deflected beam. The angle $\Delta\theta$ by which the deflected beam can be changed by changing the acoustic frequency

Δf is given by,

$$\Delta\theta = \frac{1}{2}\frac{\lambda \Delta f}{v} \qquad \text{Eq. 3.7.2.}$$

Normally, the deflector is operated in the condition where the divergence of the incident beam is much smaller than the spread of the acoustic beam (Gordon 1967, Randolph and Morrison 1971). The divergence of the deflected beam is therefore equal to the incident beam and is given by,

$$\delta\phi = \frac{\alpha \lambda}{W} \qquad \text{Eq. 3.7.3.}$$

where W is the beam width and α is a multiple factor which depends on the shape of the optical beam and the resolution criterion used. Using Raleighs criterion, $\alpha = 1$ for a rectangular beam and 1.22 for a circular beam. For a gaussian beam $\alpha = 1.27$ where W corresponds to a decrease in intensity to $\hat{I}_o/_{e^2}$. The maximum number of resolvable spots is therefore given as

$$N = \frac{\tau \Delta f}{\alpha} \qquad \text{Eq. 3.7.4.}$$

where $\tau = W/v$ is the transit time of the acoustic wave across the optical beam. For high speed and high resolution the interaction bandwidth thus needs to be maximized.

For the two-dimensional case the resolution that can be achieved by the composite order is thus given by

$$N_1 N_2 = \frac{\Delta f_1 \tau_1 \Delta f_2 \tau_2}{\alpha^2} \qquad \text{Eq. 3.7.5.}$$

where the subscripts relate the various parameters to each orthogonal dimension.

3.8. Bandwidth

Since the acousto-optic deflection of the composite beam is essentially the product of two single-dimensional acousto-optic

interactions, the variation of intensity with frequency of the composite order in each of the two dimensions is merely the product of the bandwidths achieved by the two first order beams deflected in each co-ordinate. The methods of achieving a satisfactory bandwidth from different transducer configurations is thus considered and reviewed for a single-dimensional deflector. In this case the deflected first order intensity, under normal bragg diffraction conditions, and in the limit of weak scattering, can be expressed as (Cohen and Gordon 1965, Pinnow 1971a) ,

$$\frac{I_1}{\hat{I}_o} \propto \left(\frac{\sin X}{X}\right)^2 \cdot \left(\frac{\sin mY}{Y}\right)^2 \qquad \text{Eq. 3.8.1.}$$

where the first term gives the response of a transducer element and the second term indicates the response of a transducer array. Also $\Gamma \simeq \gamma$ since ξ is assumed negligible.

3.8.1. Single Transducer

For a single transducer the second term in Eq. 3.8.1. is equal to unity and in the first term,

$$X = \tfrac{1}{2}\gamma L \qquad \text{Eq. 3.8.1.1.}$$

where L is the transducer length and

$$\gamma = K\left(\frac{K}{2k} - \sin\theta_o\right) / \cos\theta_o \qquad \text{Eq. 3.8.1.2.}$$

here, θ_o is the bragg angle.

It is convenient to define the upper and lower bandwidth limits when the quantity X is equal to $\pm \tfrac{1}{2}\pi$. This means that the intensity of the deflected beam has been reduced to 0.405, or approximately -4 dB , of its maximum value. Thus from Eq. 3.8.1.1. and Eq. 3.8.1.2.

$$\tfrac{1}{2}\gamma L = \tfrac{1}{2}K\left(\frac{K}{2k} - \sin\theta_o\right)L/\cos\theta_o \qquad \text{Eq. 3.8.1.3.}$$

Eq. 3.8.1.3. is quadratic in acoustic frequency , f, and a solution is given for this by

$$f = f_o + f_o\left(1 + \frac{(\frac{1}{2}\gamma L)\ 2\lambda_o \cos\theta_o}{n\pi L \sin^2\theta_o}\right)^{\frac{1}{2}} \qquad \text{Eq. 3.8.1.4.}$$

where $f_o = \frac{n v}{\lambda_o} \sin\theta_o$

By remembering that $\sin\theta_o = \frac{\lambda}{2\Lambda} = \frac{\lambda_o f_B}{2 n v}$ we obtain

$$f_o = \frac{1}{2} f_B$$

By substituting in the limits for $\frac{1}{2}\gamma L$ into Eq. 3.8.1.4. and assuming that $\cos\theta_o \simeq 1$, the -4dB frequency limits are given by,

$$f_{-4dB} = \frac{1}{2} f_B\left(1 + (1 \pm \frac{8\pi}{Q})^{\frac{1}{2}}\right) \qquad \text{Eq. 3.8.1.5.}$$

where $Q = \frac{L K^2}{k} = \frac{2\pi L \lambda_o f_B^2}{n v^2}$

Klien and Cook (1967) have defined the quantity Q in the above manner. They have defined that when $Q > 4\pi$ the acousto-optic interaction is clearly within the bragg regime and efficient diffraction of light can be achieved into the first order. Scattering into other orders becomes increasingly difficult as Q becomes large. For $Q < 0.5$ the interaction is essentially within the Raman-Nath regime and the diffraction of light into orders other than the first becomes significant. From Eq. 3.8.1.5. it can be seen that when $Q = 8\pi$ the lower frequency limit is equal to half the bragg frequency. If the deflector is adjusted so that the bragg angle is satisfied for this frequency then Q becomes 2π. This frequency is called the minimum bragg frequency —

$$f_{BM} = \frac{v}{\sqrt{\frac{\lambda_0}{n} L}} \qquad \text{Eq. 3.8.1.6.}$$

and below this frequency the device is operating outside the bragg regime. Thus, when $Q = 8\pi$ the maximum bandwidth that can be achieved with a single transducer is

$$\Delta f = \sqrt{2}\, f_{BM}$$

and for higher values of Q, although the interaction will be moved further into the bragg regime, the available bandwidth will be decreased.

For a given bragg frequency and a given bandwidth the value of Q, for operation to occur within the bragg regime, is given by

$$Q = 8\pi \left(1 - \left(1 - \frac{1}{2}\left(\frac{2\,\Delta f}{f_B}\right)^2\right)^2\right)^{-\frac{1}{2}} \qquad \text{Eq. 3.8.1.7.}$$

3.8.2. Planar Transducer Array

When the acoustic transducer consists of an array of m elements in which each element is driven with a constant phase increment with respect to its neighbour the acoustic beam can be steered so as to approximately track the bragg angle over a particular range of acoustic frequencies. When successive transducer elements are driven with a phase increment of π radians the far field pattern of the acoustic energy consists of two major lobes as shown in Fig. 3.8.2.1. in which the angle they subtend from the normal varies inversely with the acoustic frequency. This transducer configuration has been considered by Gordon (1966). In Eq. 3.8.1. the properties of the array are governed by the second term. If d is the separation

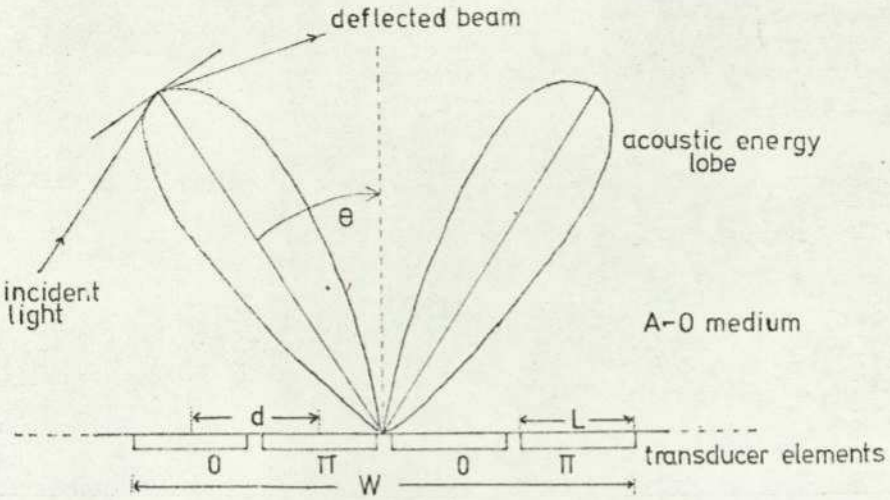

Fig. 3.8.2.1. Planar transducer array with π phase shift between elements and resulting polar plot of acoustic lobe.

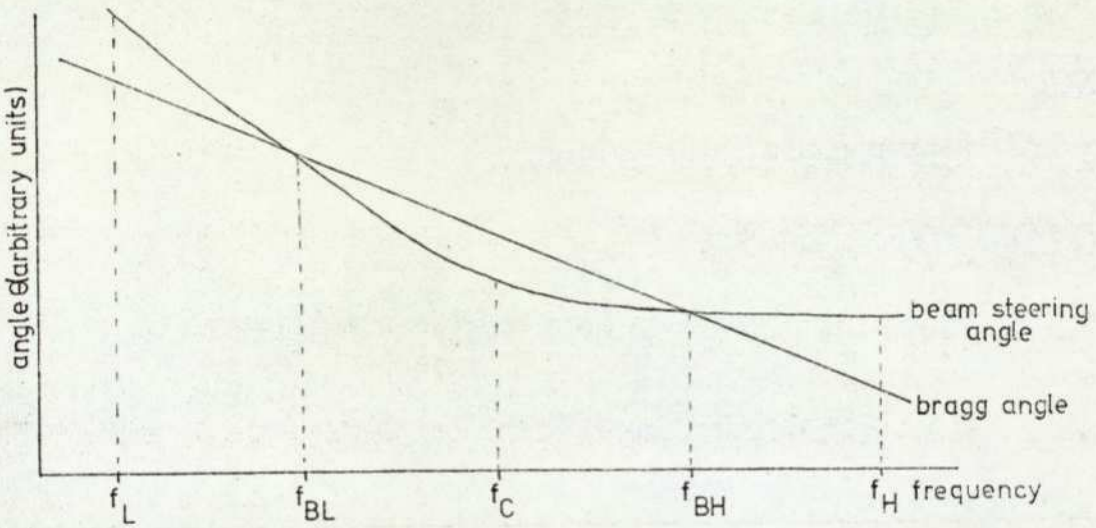

Fig. 3.8.2.2. Approximate bragg angle beam steering by planar array.

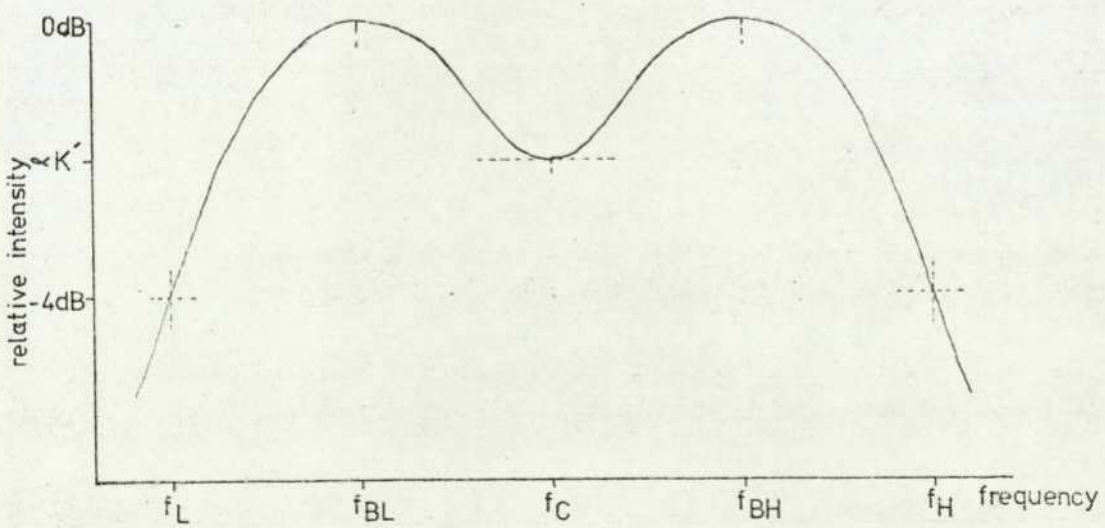

Fig. 3.8.2.3. Variation of the relative intensity of the deflected optical beam with frequency using the planar array.

between the elements then,

$$Y = \frac{1}{2}(\gamma d + \pi)$$

The interaction is at an optimum when $\gamma d = -\pi$. Since the optical beam interacts with only one of acoustic lobes the acoustic energy in that lobe is only 0.405, or approximately -4 dB, of the total acoustic energy supplied. Because the angle between the lobe and the normal varies inversely with frequency the acoustic beam satisfies the bragg condition exactly at two frequencies only as shown in Fig. 3.8.2.2. The resulting variation of intensity with frequency will appear similar to that as shown in Fig. 3.8.2.3. The intensity at the centre frequency will be reduced somewhat, the value of which is given by

$$I_{1(f_C)} \propto \left(\frac{\sin K'\pi}{K'\pi}\right)^2$$

and corresponds to the condition $\frac{1}{2}(\gamma d + \pi) = -K'\pi$. The centre frequency is thus given by

$$f_C = f_o \pm f_o\left(1 - \left(\frac{m+2K'}{m}\right).\frac{\lambda_o}{\Pi d \sin^2\theta_o}\right)^{\frac{1}{2}} \qquad \text{Eq. 3.8.2.1.}$$

where $f_o = \frac{\Pi v}{\lambda_o \sin\theta_o}$

f_C is equal to f_o when

$$\Pi d \sin^2\theta_o = \lambda_o\left(\frac{m+2K}{m}\right) \qquad \text{Eq. 3.8.2.2.}$$

or

$$m d = W = \frac{\lambda_o v^2}{\Pi f_o^2}(m+2K) \qquad \text{Eq. 3.8.2.3.}$$

where W is the total length of the transducer array, assuming that the spacing between the elements is negligible. Referring to Eq. 3.8.1.6. the minimum bragg frequency can be defined for the transducer array as,

$$f_{BM} = \frac{v}{\sqrt{\frac{\lambda_o}{\Pi} W}} \qquad \text{Eq. 3.8.2.4.}$$

Substituting Eq. 3.8.2.3. into Eq. 3.8.2.2. gives the centre frequency as

$$f_C = f_o = f_{BM}\,(m+2K')^{\frac{1}{2}} \qquad \text{Eq. 3.8.2.5.}$$

The two frequencies at which the bragg condition is satisfied exactly is given when

$$m\,Y = 0$$

or when

$$f_B = f_C\left(1 \pm \left(1 - \frac{\lambda_o}{\Pi d \sin^2\theta_o}\right)^{\frac{1}{2}}\right) \qquad \text{Eq. 3.8.2.6.}$$

Substituting Eq. 3.8.2.2. into Eq. 3.8.2.6. and re-arranging one obtains

$$f_B = f_{BM}\left((m+2K')^{\frac{1}{2}} \pm (2K')^{\frac{1}{2}}\right) \qquad \text{Eq. 3.8.2.7.}$$

The upper and lower -4 dB frequencies are given when

$$m\,Y = \tfrac{1}{2}\pi$$

or when

$$f_{-4dB} = f_C\left(1 \pm \left(1 + \frac{(1-m)}{m}\cdot\frac{\lambda_o}{\Pi d \sin^2\theta_o}\right)^{\frac{1}{2}}\right) \qquad \text{Eq. 3.8.2.8.}$$

Substituting Eq. 3.8.2.2. into Eq. 3.8.2.8. and re-arranging one obtains

$$f_{-4dB} = f_{BM}\left((m+2K')^{\frac{1}{2}} \pm (1+2K')^{\frac{1}{2}}\right) \qquad \text{Eq. 3.8.2.9.}$$

Thus the available bandwidth that can be obtained from a planar transducer array is

$$\Delta f = 2\,(1+2K')^{\frac{1}{2}}\, f_{BM} \qquad \text{Eq. 3.8.2.10.}$$

If the value of K' is made equal to $\frac{1}{2}$ then the intensity at the centre frequency will be a -4 dB point also. The bandwidth obtained is then given by

$$\Delta f = 2\sqrt{2}\; f_{BM}$$

and is twice that which can be obtained from a single transducer.

Alphonse (1975) has considered the planar transducer array by examining the behaviour of the acoustic far field. Similar results were obtained and he has demonstrated experimentally the behaviour of a four element transducer bonded to lead molybdate. However, with four or less elements the lower -4dB frequency limit is below the minimum bragg frequency and for three and two elements so is the lower bragg frequency. The full available bandwidth can only be utilised when five or more elements are used. For five elements the maximum fractional bandwidth of 1.15 is realised and decreases as the number of elements increase, that is, for a fixed total array length. For example, for a fractional bandwidth of 0.67 the number of elements is 17. The first term in Eq. 3.8.1. will reduce the available bandwidth to a small extent when only a small number of elements are used. So, although it has been shown that an increase in the bandwidth is possible when a planar transducer array is used compared to that of a single transducer, a reduction in the scattering efficiency also occurs. Gordon (1966) has shown that the efficiency-bandwidth product for a planar array is essentially the same as that of a single transducer. Although here the element length to element separation ratio L/d is assumed to be unity he has shown that it should be ideally 0.742 for an optimum efficiency-bandwidth product.

3.8.3. Stepped Transducer Array

A method of achieving first order acoustic beam steering so as to obtain a large interaction bandwidth and yet overcome the loss in interaction efficiency as experienced with the planar array is to use a stepped transducer array. Here the transducer elements are arranged in the form of a staircase on the interaction medium so that a fixed acoustic delay exists between each element with respect to

its neighbour. With the elements driven with the correct electrical phase the lobe of the far field acoustic energy distribution can be made to vary about the transducers' normal in which the steering angle varies inversely with respect to the acoustic frequency. The arrangement is shown in Fig. 3.8.3.1. and such a device was first investigated and demonstrated by Korpel (1966) for producing the horizontal deflection in a television projection display. In this application, the step height was made equal to half an acoustic wavelength of the centre frequency and the elements were driven π radians out of phase. Coquin et al (1970) have examined this arrangement and have shown that the tolerance on phase shift between each sound column, and hence variations in step height, is not critical. Indeed, by using a stepped transducer array device and by varying the electrical phase to each element they have been able to achieve near perfect first order beam steering over a wide fractional bandwidth. Also, they have shown that even at large scattering efficiencies the arguments relating to weak scattering efficiencies are still valid.

Pinnow (1971a) and Sittig (1972) have considered the case where the step height is an integral number of acoustic half-wavelengths,

$$H = p \frac{\Lambda_c}{2} \qquad \text{Eq. 3.8.3.1.}$$

where Λ_c is the acoustic wavelength at the centre frequency and P is an integer and the steering angle is given by,

$$\theta = \frac{p\, v}{2\, d} \left(\frac{1}{f} - \frac{1}{f_c} \right) \qquad \text{Eq. 3.8.3.2.}$$

In this case the values in Eq. 3.8.1. are given by

$$X = \frac{\pi L}{\lambda} \sin\theta_o$$

$$Y = \frac{\pi d}{\lambda} \sin(\theta_o - \theta) \qquad \text{Eq. 3.8.3.3.}$$

Because the acoustic beam steering angle is inversely proportional

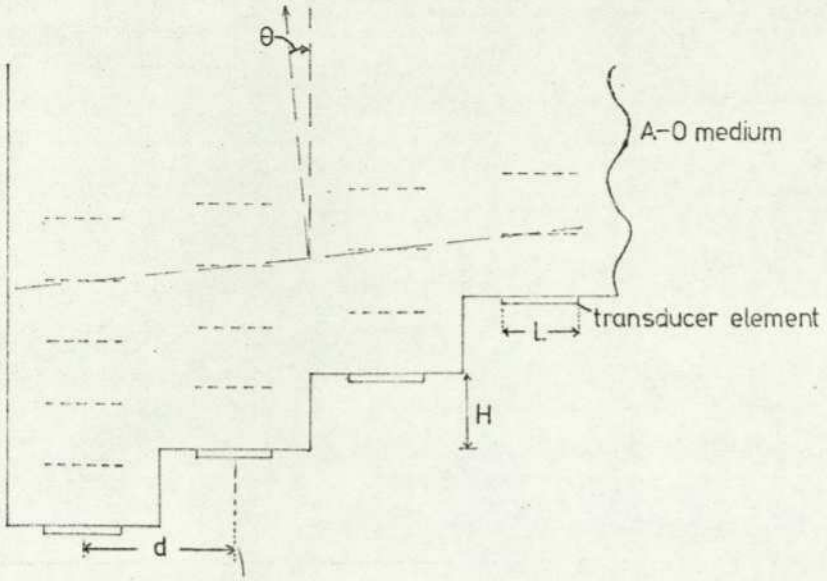

Fig. 3.8.3.1. Geometry of the stepped transducer array showing the beam steering capability.

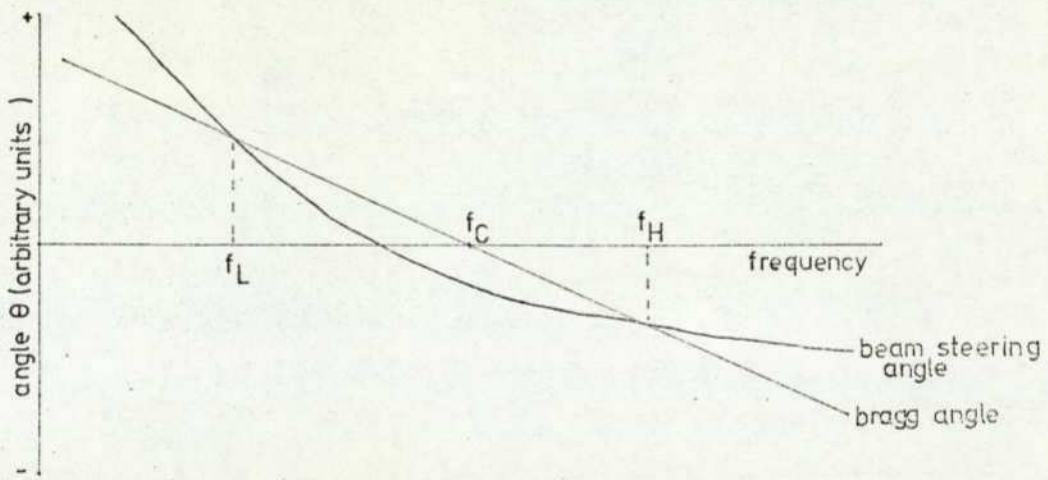

Fig. 3.8.3.2. Approximate bragg angle tracking of the stepped array.

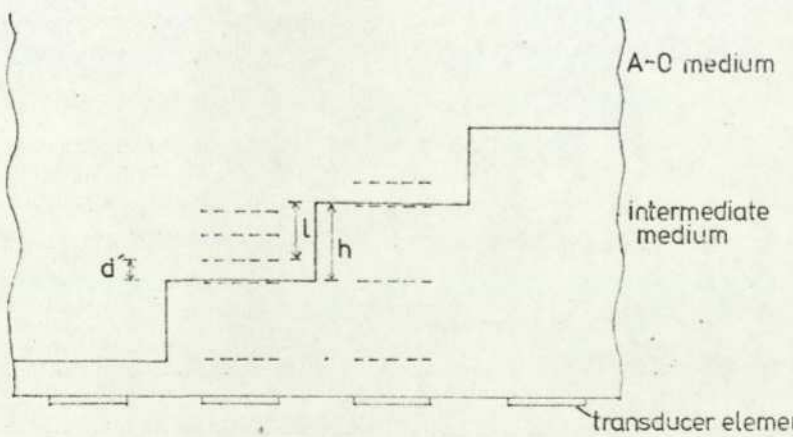

Fig. 3.8.4.1. Modified stepped transducer array for liquid inter--action medium.

to frequency the resultant acoustic beam, as in the case of the planar transducer array, will only track the bragg angle approximately and will satisfy it exactly at only two frequencies as shown in Fig. 3.8.3.2. It has been shown (Pinnow 1971a) that the element length is given by

$$L = \frac{2 k v^2 \Pi}{\lambda_o (f_H - f_L)} \left(\frac{1}{f_H} + \frac{1}{f_L} \right) \qquad \text{Eq. 3.8.3.4.}$$

and the element separation is given by

$$d = \frac{p L}{2 k} \frac{(f_H - f_L)}{(f_H + f_L)} \qquad \text{Eq. 3.8.3.5.}$$

where f_H and f_L are the frequencies at which exact bragg angle tracking occurs. The centre frequency is given by

$$f_C = \frac{1}{2}(f_H + f_L) \qquad \text{Eq. 3.8.3.6.}$$

At the bragg frequencies the intensity of the deflected beam is reduced somewhat due to the first term in Eq. 3.8.1. The value of k is given when

$$I_{1(f_B)} \propto \left(\frac{\sin k\pi}{k\pi} \right)^2 \qquad \text{Eq. 3.8.3.7.}$$

In the previous two cases fractional bandwidth decreased as the transducer length was increased for a given centre frequency. In this case the fractional bandwidth is much less dependent of the length of the array. The obtainable bandwidth is essentially dependent upon the element length, element separation, and step height. So long as Eq. 3.8.2.4. is satisfied the length can be increased as required so that the interaction efficiency can be increased. Also due to the fact that the step height is not limited to merely one acoustic half wavelength the elements are electrically fed with a phase of π if p is an odd integer or are fed in phase if p is an even integer. However, for solid interaction mediums the acoustic

frequency is usually above 100 M Hz. The acoustic wavelength is thus about 20 μm or less. Consequently, manufacturing difficulties accompany this type of configuration when large element arrays are required.

3.8.4. Stepped Array for Liquid Deflectors

Liquids, in particular water, have been used as the interaction medium in a number of devices and the stepped transducer array was first demonstrated (Korpel 1966) using such a medium. The transducers were bonded to an intermediate material, in this case glass, so that a reasonable transducer bandwidth could be obtained. The steps were made on the glass-air boundary and the boundary between the glass and water was plain. Vorshol et al (1975) have suggested that a planar transducer array be bonded to the plain side of the intermediate material and that the stepped side is in direct contact with the liquid. The arrangement is shown in Fig. 3.8.4.1. Although the design considerations given by Pinnow (1971a) essentially hold true, the height of the steps are no longer an integral number of half wavelengths long.

The transit time of an acoustic wavefront between the steps in the intermediate material is given by,

$$\tau = h / v_m \qquad \text{Eq. 3.8.4.1.}$$

The same transit time taken by the acoustic wavefront in the liquid to travel the distance d' is given by,

$$\tau = d' / v_l \qquad \text{Eq. 3.8.4.2.}$$

Consequently, the effective step height between the acoustic columns is,

$$l = h - d' = h(1 - v_l / v_m) \qquad \text{Eq. 3.8.4.3.}$$

and the associated acoustic phase difference is thus given by,

$$\emptyset = \frac{2\pi h}{\Lambda_l} (1 - v_l/v_m) \qquad \text{Eq. 3.8.4.4.}$$

If the elements of the planar transducer array are driven with a phase increment of $n\pi$ radians with respect to their neighbours the effective step height is an integral number of half wavelengths and the actual step height formed on the intermediate material is given by

$$h = \frac{n \frac{\Lambda_l}{2}}{(1 - v_l/v_m)} \qquad \text{Eq. 3.8.4.5.}$$

Hence, the integer p in Pinnows' analysis is replaced here by

$$p' = \frac{n}{(1 - v_l/v_m)} \qquad \text{Eq. 3.8.4.6.}$$

The interaction efficiency and available fractional bandwidth for this configuration are the same for the conventional arrangement. However, it does make the manufacture of both the steps and the transducer array somewhat easier.

3.8.5. Tilted Transducer Array

It has been shown by Tsai et al (1976) and by Kim (1976) in work concerning bragg deflection in thin films by using surface acoustic waves that a large bandwidth and reasonable efficiency can be achieved by using an array of transducers in which the propagation direction of each element is tilted with respect to its neighbour. The elements have staggered centre frequencies and are tilted so that at its centre frequency the acoustic wave generated by an element satisfies the bragg condition.

When applied to bulk acousto-optic deflectors it appears as the arrangement shown in Fig. 3.8.5.1. Here, two elements are considered. The incident light first passes through the sound column 1 and the emerging zero and first order beam amplitudes are given by,

$$E_0 = \hat{E}_o \exp\left(j \tan^{-1}\left(\frac{\gamma_1}{2\Gamma_1}\tan \Gamma_1 L_1\right)\right) . \left(1 - \delta_1^2\right)^{\frac{1}{2}}$$

$$E_1^{(1)} = j \hat{E}_o \delta_1$$

where $\delta_1 = \frac{\gamma_1}{2\Gamma_1} \sin \Gamma_1 L_1$

The amplitude of the light deflected into the first order by the second sound column 2 is given by,

$$E_1^{(2)} = E_0|_{L_1} . j \delta_2 \exp j(\gamma_1 d + \phi - \tfrac{1}{2}\gamma_2 L_2)$$

The term ϕ accounts for the difference in phase between the two interactions. The net deflected beam amplitude is therefore given by,

$$E_1^{(T)} = E_1^{(1)} + E_1^{(2)}$$

$$= j \hat{E}_o \left(\delta_1 + \delta_2 (1 - \delta_1^2)^{\frac{1}{2}} \exp(j\theta)\right)$$

where $\theta = \tan^{-1}\left(\frac{\gamma_1}{2\Gamma_1}\tan \Gamma_1 L_1\right) + \gamma_1 d - \frac{1}{2}\gamma_2 L + \phi$

The resulting intensity of the first order is then given by,

$$I_1^{(T)} = E_1^{(T)} . E_1^{(T)*}$$

Although this arrangement has been successfully demonstrated in thin film devices a number of disadvantages occur when applied to a bulk acousto-optic device. Since the transducer centre frequencies are different, then the thickness of each element will also differ. Consequently, with the same electric field applied to each element the phase of the acoustic wave emerging from each transducer with respect to each other will be different and will vary as the frequency varies. The variation of the phase of a generated acoustic wave with

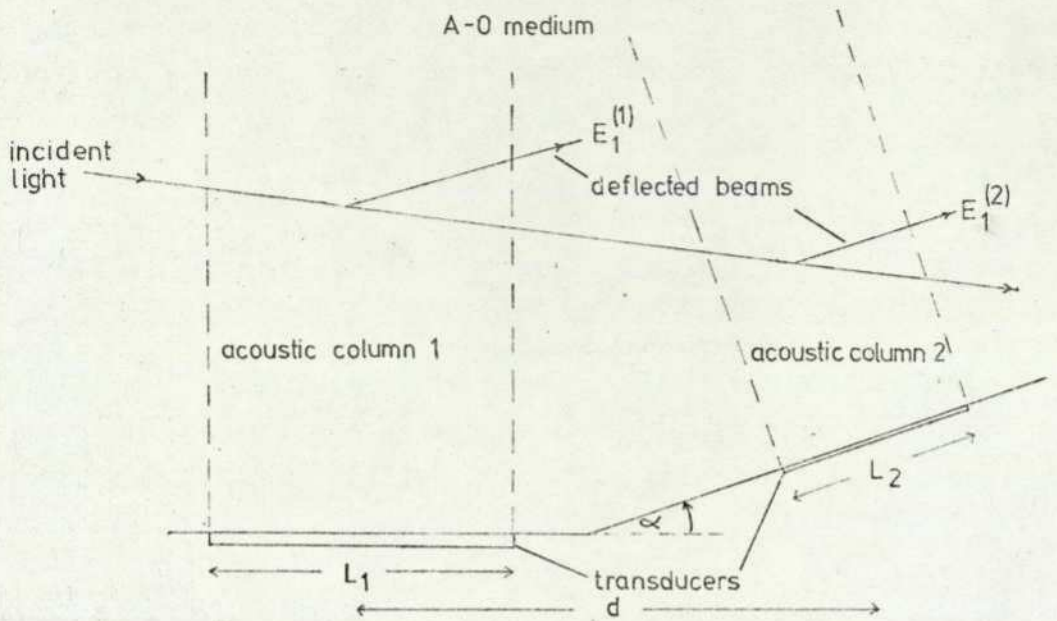

Fig. 3.8.5.1. Schematic arrangement for a tilted transducer array.

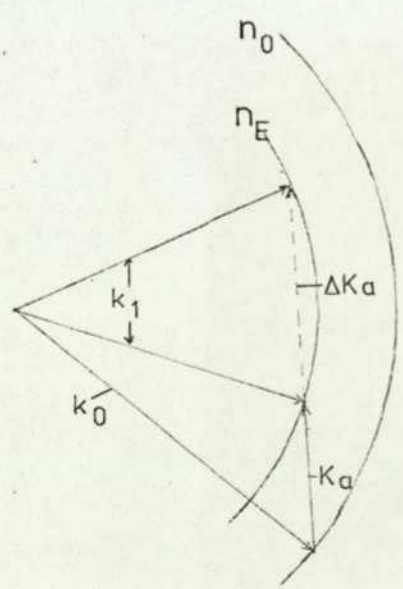

Fig. 3.9.1. Wave vector summation for diffraction in anisotropic media.

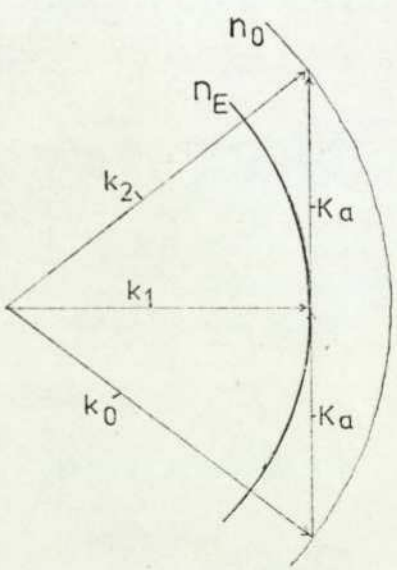

Fig. 3.9.2. Light deflection into 2nd order in anisotropic media.

respect to the frequency-thickness product has been shown by Sittig (1969). Also an additional phase factor is introduced because the element centres are at different heights from each other. Also in this arrangement the angle of tilt, α, is quite small. Consequently, if the transducers are made from piezo-electric platelets the separation length d has to be quite large so that the grinding and polishing of the second transducer does not damage the first transducer. Thus, these three effects contribute to the phase factor $\emptyset$ and unless compensated for will severely effect the bandwidth. For thin film devices these effects are not so serious and can be compensated for electrically by the use of transmission lines (Tsia et al 1976). It should also be mentioned that the interaction bandwidth is also dependent upon the direction in which the light enters the deflector.

The complicated nature of this arrangement really precludes it as a practical system. Although the phase terms could be compensated for by introducing an acoustic delay in the form of a step, a stepped tilted array would be somewhat beyond present technology and may only become viable when the conventional stepped array can be manufactured with relative ease.

3.9. Diffraction in Anisotropic Media

It has been shown by Dixon (1967a) that the acousto-optic interaction becomes significantly different when it takes place in an optically birefringent material and the acoustic wave is, in general, in the form of a shear wave. If the incident light beam in the interaction medium is the ordinary ray the diffraction process causes the polarization of the diffracted wave to rotate by 90° with respect to the incident beam and thus the diffracted beam becomes

the extraordinary ray. The interaction can be represented in terms of the wave-vector summation and is shown in Fig. 3.9.1. for single-dimensional deflection. The vector summation can be approximated for large variations in the acoustic wave vector and consequently the bandwidth of such an interaction is considerably larger than that of 'normal' bragg deflection. This type of deflection has been reviewed extensively by Uchida and Ohmachi (1969), Warner et al (1972), Uchida and Niizeki (1973), and Chang (1976). The theoretical analysis of the diffraction process has been given by Parygin and Chirkov (1975).

In the two-dimensional case the interaction is no longer the superposition of two similar effects. Assuming that the two sound columns are shear waves the incident ordinary wave will be deflected to become the extraordinary wave by one sound column. The other sound column will deflect this first order beam into the composite order. The polarization of this order will then be the same as that of the incident beam. The interaction bandwidth achieved by the second deflection is not the same as that achieved by the first deflection. However, so long as the momentum conservation considerations are satisfied, a composite order can still be obtained.

It has been demonstrated by Chang and Hecht (1975) that when the interaction has been adjusted so that the first order diffracted wave is at right angles to the acoustic beam, light from the first order can be efficiently deflected into the second order as shown in Fig. 3.9.2. The amount of light that can thus be deflected into the second order is dependent upon the amount of light deflected into the first order. High scattering efficiencies are preferred here to minimize the first order deflected light. For a given acoustic

bandwidth and a given optical aperture the resolution obtained is reported to have been increased over that of first order deflection. The polarization of the second order beam is the same as that of the incident light beam.

This arrangement can be applied to the two-dimensional case. Since the second order beam is of the same polarization as the incident beam the second order beam becomes the incident beam for deflection in the orthogonal dimension. The need for high scattering efficiencies here is twofold. Firstly, to obtain efficient deflection of light into the second orders and secondly, to obtain efficient deflection into the composite order. The scattering efficiency to the second orders as well as the scattering from the second orders to the composite order are both proportional to a $\sin^4 x$ relationship. Thus, the scattering efficiency from the incident beam to the composite order is proportional to a $\sin^8 x$ relationship and unless high scattering efficiencies are achieved the light deflected into the composite order will consequently be small.

The problem with this type of deflection is that the interaction is entirely dependent upon the natural birefringence of the material. For most suitable materials this means that the acoustic frequency must be in the G Hz region and difficulties arise in trying to produce efficient broadband transducers at such frequencies.

Warner et al (1972) have pointed out that the arguments relating to birefringent deflection are equally applicable to materials that exhibit optical activity. Paratellurite, TeO_2, is such a material which has an extremely high figure of merit, M_2. Its crystal class is tetragonal and for light propagating near to the optic axis efficient deflection can be obtained by a shear wave propagating along the [110] axis. Due to its crystal symmetry efficient deflection can be obtained with the sound propagating in the orthogonal direction.

In this material the difference in the refractive indices associated with the optical activity is such that for optical frequencies the acoustic frequency is below 100 M Hz. Since at these frequencies the acoustic wave is comparatively easy to produce, a two-dimensional deflector utilizing the second order beam could be realised using this material. As mentioned previously the composite order can be achieved when only the first orders are used and an X-Y device using this material in this way has been demonstrated by Uchida (1973).

4. The Generation of Bulk Acoustic Waves

4.1. Introduction

Any device that can produce a mechanical force and thus force a displacement can be used as an acoustic generator. The generation of bulk acoustic waves within a delay medium for frequencies of 1 M Hz and above is best accomplished using single crystal piezo-electric transducers. These consist of thin platelets bonded onto the delay medium and electrically driven by a r.f. voltage. In this section the theoretical behaviour of such a transducer is considered. These piezo-electric layers have previously been analyzed by considering a single mode, one-dimensional theory developed by Mason (1948) and the equivalent circuit model has been extended to account for the effects of electrode and bonding layers by Sittig (1969), and Reeder and Winslow (1969). An analytic approach has been given by Berlincourt (1964) for an unbounded, single mode resonator and by Foster et al (1968) for the bonded multimode case with special reference to cadmium sulphide and zinc oxide. For the satisfactory design and determination of performance of a transducer, knowledge of properties such as acoustic velocity, electro-mechanical coupling factor, electrical impedance as well as bandwidth and insertion loss is required. The analytic approach has been followed here which is applicable for transducers made from any crystalline material.

4.2. Definitions

When a body is deformed by the application of a force the distances between points in the body subject to the force are different from those between the same points when the force is removed. The

difference in distance between those points is called the particle displacement and, in co-ordinate form, is defined, according to the IRE standards on piezo-electric crystals (1949) as,

$$u_i \qquad i = 1,2,3 \qquad \text{Eq. 4.2.1.}$$

The various points on the body are displaced differentially with distance. This is called the strain (Nye 1957, Musgrave 1970, Federov 1968) and, in tensor form, is given as,

$$S_{ij} = \frac{1}{2}\left(\frac{\partial u_i}{\partial x_j} + \frac{\partial u_j}{\partial x_i} \right) \qquad \text{Eq. 4.2.2.}$$

The subscripts run from 1 to 3. The strain tensor is also symmetric,

$$S_{ij} = S_{ji} \qquad \text{Eq. 4.2.3.}$$

The stress, the differential force per unit area, within a deformed body is, in tensor form, symmetrical and is defined as,

$$T_{ij} = T_{ji} \qquad \text{Eq. 4.2.4.}$$

In a non-piezo-electric material the stress and strain are linearly related. The constant of proportionality expressing stress in terms of strain is called the stiffness and is denoted as C, so that

$$T_{ij} = C_{ijkl}\, S_{kl} \qquad \text{Eq. 4.2.5.}$$

In a strongly piezo-electric material the elastic and dielectric linear effects are coupled to each other. It is possible to write the constituent relationships for a general piezo-electric material in a form which makes any two of the quantities - stress, strain, electric field or electric flux density independent (Holland and Eernisse 1969). For the purposes here the following constituent

relations are used (Mitchell 1972)

$$T_{ij} = C^{\varepsilon}_{ijkl} S_{kl} - e_{mij} E_m \qquad \text{Eq. 4.2.6.}$$

$$D_n = e_{nkl} S_{kl} + \varepsilon^{s}_{nm} E_m \qquad \text{Eq. 4.2.7.}$$

where e is the piezo-electric co-efficient tensor and C^{ε} is the stiffness at constant electric field.

The electric field is given by,

$$E_i = - \frac{\partial \phi}{\partial x_i} \qquad \text{Eq. 4.2.8.}$$

where ϕ is the electric potential

A further important equation used here is the statement of Newton's equation of momentum conservation. Given in differential form the equation is,

$$\frac{\partial T_{ij}}{\partial x_j} = \rho \frac{\partial^2 u_i}{\partial t^2} \qquad \text{Eq. 4.2.9.}$$

From these definitions and equations we are now able to proceed in tackling the problem of analyzing the piezo-electric transducer. Although these equations have merely been stated here a more detailed treatment may be found in the references cited.

4.3. Acoustic Wave Velocity

The transducer geometry to be considered is shown in Fig. 4.3.1. The theoretical model consists of a piezo-electric layer with two perfectly conducting electrodes completely covering the faces. The plate is assumed to be infinite in its lateral dimensions. Thus variations can only occur in the direction normal to the transducer faces, i.e. in the x_1 direction and variations in the x_2 and x_3

directions are assumed to be zero. The plate thus vibrates in the thickness mode. It is also assumed that the bottom face is rigidly bonded onto the delay medium and that the surface of the top electrode is free and is undisturbed. The acoustic wave generated by the transducer when an alternating voltage is applied to the electrodes will thus propagate across the bonded face and into the delay medium.

Since variations can only occur in the x_1 direction the constituent relations, Eq. 4.2.6. and Eq. 4.2.7., can be written as,

$$T_{i1} = C^{\varepsilon}_{i1k1} S_{k1} - e_{1i1} E_1 \qquad \text{Eq. 4.3.1.}$$

$$D_1 = e_{1k1} S_{k1} + \varepsilon^{s}_{11} E_1 \qquad \text{Eq. 4.3.2.}$$

and the equations of motion can be written as,

$$\frac{\partial T_{i1}}{\partial x_1} = -\rho \omega^2 u_i \qquad \text{Eq. 4.3.3.}$$

Sinusiodal variation with time has been assumed here. Use is also made of the electrostatic equation,

$$\text{Div } D = \frac{\partial D_1}{\partial x_1} = 0 \qquad \text{Eq. 4.3.4.}$$

Due to the symmetry of the strain tensor and also due to the symmetry of the stiffness tensor ; C_{ijkl} and C_{jilk} are identical, the strain can be written here as,

$$S_{k1} = \frac{\partial u_k}{\partial x_1} \qquad \text{Eq. 4.3.5.}$$

Substituting Eq. 4.2.8. and Eq. 4.3.5. into Eq. 4.3.1. and Eq. 4.3.2. one obtains,

$$T_{i1} = C^{\varepsilon}_{i1k1} \frac{\partial u_k}{\partial x_1} + e_{1i1} \frac{\partial \phi}{\partial x_1} \qquad \text{Eq. 4.3.6.}$$

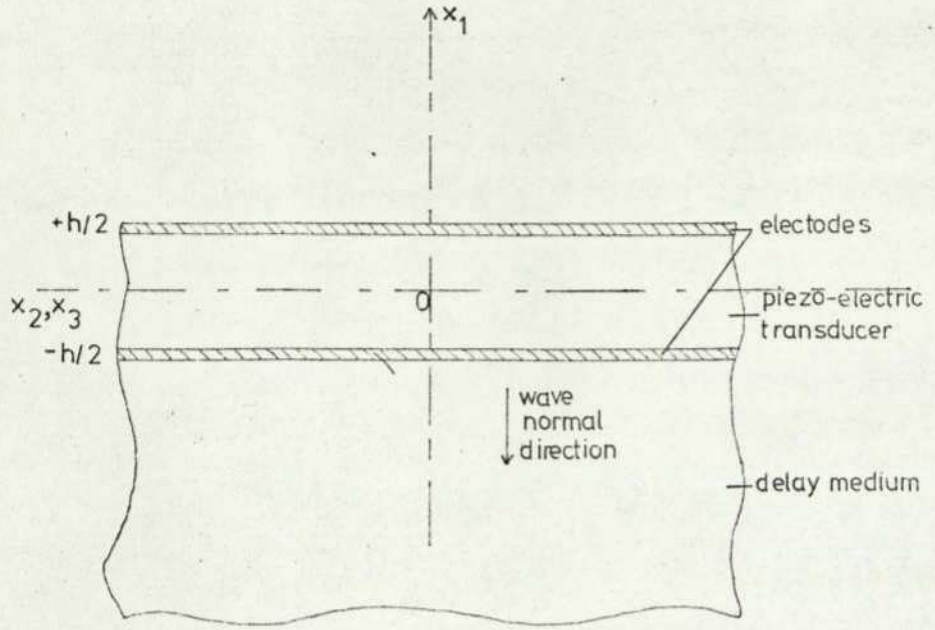

Fig. 4.3.1. The transducer geometry for the generation of bulk acoustic waves.

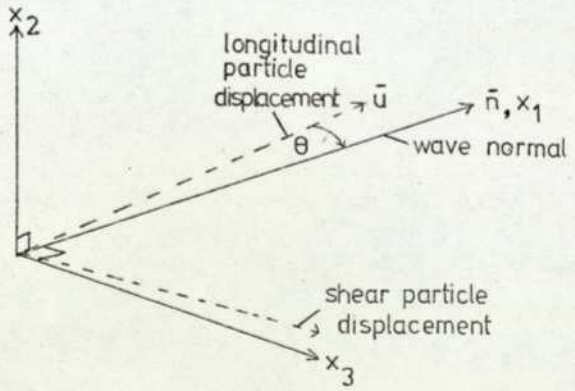

Fig. 4.4.1. Illustration of the possible deviation between the particle displacement and wave normal directions.

$$D_1 = e_{1k1}\frac{\partial u_k}{\partial x_1} - \varepsilon^s_{11}\frac{\partial \phi}{\partial x_1} \qquad \text{Eq. 4.3.7.}$$

Substituting Eq. 4.3.6. and Eq. 4.3.7. into Eq. 4.3.3. and Eq. 4.3.4. one obtains,

$$C^E_{i1k1}\frac{\partial^2 u_k}{\partial x_1^2} + e_{1i1}\frac{\partial^2 \phi}{\partial x_1^2} + \rho\omega^2 u_i = 0 \qquad \text{Eq. 4.3.8.}$$

$$e_{1k1}\frac{\partial^2 u_k}{\partial x_1^2} - \varepsilon^s_{11}\frac{\partial^2 \phi}{\partial x_1^2} = 0 \qquad \text{Eq. 4.3.9.}$$

Substitution of Eq. 4.3.9. into Eq. 4.3.8. yields,

$$\overline{C_{i1k1}}\frac{\partial^2 u_k}{\partial x_1^2} + \rho\omega^2 u_i = 0 \qquad \text{Eq. 4.3.10.}$$

where $\overline{C_{i1k1}} = C^E_{i1k1} + \dfrac{e_{1i1}\, e_{1k1}}{\varepsilon^s_{11}}$

By assuming that the particle displacement varies sinusiodally with distance Eq. 4.3.10. can be re-arranged and written in the form (Tiersten 1963),

$$\left| \frac{\overline{C_{i1k1}}}{\rho} - \delta_{ik}v^2 \right| u_k = 0 \qquad \text{Eq. 4.3.11.}$$

where δ_{ik} is the Kronecker delta and $v^2 = \omega^2/\kappa^2$

The solution to the determinant in Eq. 4.3.11., known as Christoffels Equation, yields three eigen roots. These correspond to the square of the velocities of the three waves which may propagate within the material. The direction of the particle displacements associated with each of the three waves is given by the eigenvectors, u_k. Thus, for a given acoustic wave velocity $v^{(l)}$ there corresponds a particle displacement vector $u_k^{(l)}$, where l denotes the wave under consideration and takes on values of 1 to 3.

4.4. Particle Displacement Angle

In an isotropic material the direction of one of the particle displacement vectors is in the same direction as that of the wave normal. This wave is called the longitudinal wave. The particle displacement vectors associated with the other two waves are orthogonal with respect to the wave normal direction and are orthogonal with respect to each other. These are transverse, or shear waves.

In an anisotropic medium, although all the particle displacement vectors are orthogonal with respect to each other, the particle displacement vector associated with the longitudinal wave may deviate by an angle θ from the wave normal direction as shown in Fig. 4.4.1. Also, one of the shear wave displacement vectors may not be orthogonal to the wave normal direction. In this case the waves are termed quasi-longitudinal or quasi-shear. The value of θ can be determined from the vector product between the wave normal vector $\bar{n}$ and the longitudinal particle displacement vector as,

$$\theta = \cos^{-1}\left[\frac{(\bar{u}_{(long)} \cdot \bar{n})}{|\bar{u}_{(long)}|}\right] \qquad \text{Eq. 4.4.1.}$$

This property is important in so far as if the transducer, say, is such that it generates a quasi-longitudinal wave, and it is bonded onto a delay medium which is isotropic, there will be generated within the delay medium not only the longitudinal wave but also shear waves too. Some power is then lost from the wanted wave into unwanted modes due to mode conversion. This effect will be enhanced if the delay medium is anisotropic also.

4.5. Transducer Impedance

In order to determine the electrical properties of the transducer, solutions for both the stress and particle displacement are required. The analysis here is similar to that given by Foster et al (1969). The particle displacements can be expressed in the form,

$$u_k^{(l)} = u^{(l)} a_k^{(l)} \exp j\omega\left(t \pm \frac{x_1}{v^{(l)}}\right) \qquad \text{Eq. 4.5.1.}$$

Here, $a_k^{(l)}$ are the unit vectors describing the directions of the particle displacements and $u^{(l)}$ are the magnitudes of the displacements. The magnitudes can be described in the form of,

$$u^{(l)} = A^{(l)} \sin K^{(l)} x_1 + B^{(l)} \cos K^{(l)} x_1 \qquad \text{Eq. 4.5.2.}$$

The unknown amplitudes, $A^{(l)}$ and $B^{(l)}$, will be determined so as to satisfy the appropriate boundary conditions.

The stress can be expressed in the form,

$$T_{i1}^{(l)} = T^{(l)} a_i^{(l)} \qquad \text{Eq. 4.5.3.}$$

Thus, by substituting Eq. 4.5.2. into Eq. 4.3.6. and Eq. 4.3.7. the magnitude of the stress can be found to be,

$$T^{(l)} = \omega z^{(l)} \left(A^{(l)} \cos K^{(l)} x_1 + B^{(l)} \sin K^{(l)} x_1 \right) - \frac{e^{(l)} D_1}{\varepsilon_{11}^{s}} \qquad \text{Eq. 4.5.4.}$$

in which $z^{(l)} = \rho . v^{(l)}$ are the acoustic impedances associated with each wave and $e^{(l)} = e_{1k1} \cdot a_k^{(l)}$ are the effective piezoelectric coefficients.

The stress at the transducer - delay medium interface must be continuous across the boundary if the transducer is rigidly bonded onto the delay medium. Thus the stress at $x_1 = -h$ must satisfy the boundary condition,

$$T_{i1}(-h) - j\omega z_d^{(i)} u_i(-h) = 0 \qquad \text{Eq. 4.5.5.}$$

where use has been made of Eq. 4.3.1. without the piezo-electric contribution and $z_d^{(i)}$ are the acoustic impedances associated with the three waves propagating within the delay medium. The stress at the transducer - top electrode interface, $x_1 = h$, must satisfy the condition,

$$T_{i1}(h) = 0 \qquad \text{Eq. 4.5.6.}$$

This will be true if the thickness of the top electrode is negligible compared to the acoustic wavelength. It is also the optimum and most desirable condition since it is required that the acoustic energy should propagate into the delay medium and not leak out into the top electrode material. Before use is made of Eq. 4.5.5. it is convenient to refer the acoustic impedances to the axes as defined in the transducer medium by the particle displacement unit vector, $a_k^{(l)}$. Thus Eq. 4.5.5. can be expressed as,

$$T^{(l)}(-h) - j\omega z'_{d_{ml}} u^{(m)}(-h) = 0 \qquad \text{Eq. 4.5.7.}$$

where $z'_{d_{ml}} = z_d^{(i)} . \varepsilon_{ij} . a_i^{(m)} . a_j^{(l)}$

The particle displacement at the boundaries can be expressed in terms of the stress by using Eq. 4.5.2. and Eq. 4.5.4. together with the boundary conditionsto obtain,

$$u^{(l)}(-h) = \frac{1}{\omega z^{(l)}} \left(T^{(l)}(-h) \cot 2\gamma^{(l)} - \frac{e^{(l)} D_1 \tan \gamma^{(l)}}{\varepsilon_{11}^s} \right) \qquad \text{Eq. 4.5.8.}$$

$$u^{(l)}(h) = \frac{1}{\omega z^{(l)}} \left(\frac{e^{(l)} D_1 \tan \gamma^{(l)}}{\varepsilon_{11}^s} + \frac{T^{(l)}(-h)}{\sin 2\gamma^{(l)}} \right) \qquad \text{Eq. 4.5.9.}$$

where $\gamma^{(l)} = \omega h / v^{(l)}$

Consequently the substitution of Eq. 4.5.8. into Eq. 4.5.7. yields the following set of simultaneous equations for the stress at the

boundary, $x_1 = -h$,

$$T^{(l)}(-h) - j \frac{z_{d_{ml}} \cot 2\gamma^{(m)} T^{(m)}(-h)}{z^{(m)}} + j \frac{z_{d_{ml}} e^{(m)} D_1 \tan \gamma^{(m)}}{z^{(m)} \varepsilon_{11}^s} = 0 \qquad \text{Eq. 4.5.10.}$$

This corresponds to the stress within the transducer medium. However, the stresses excited within the delay medium are directed along the principal geometrical axes in Fig. 4.3.1., assuming that the delay medium material to be isotropic. Relating the stress $T^{(l)}(-h)$ to these axes yields, then, the stress within the delay medium,

$$T_d^{(l)} = a_l^{(m)} T^{(m)}(-h) \qquad \text{Eq. 4.5.11.}$$

Consequently, the acoustic power densities of the waves within the delay medium are thus given by,

$$P_a^{(l)} = \frac{T_d^{(l)} \; T_d^{(l)*}}{2 \; z_d^{(l)}} \qquad \text{Eq. 4.5.12.}$$

The voltage across the transducer is the potential difference between the electrodes at $x_1 = h$ and $x_1 = -h$. Thus, from Eq. 4.3.2., the potential at each boundary may be expressed as,

$$\phi(h) = \frac{e^{(l)} \cdot u^{(l)}(h)}{\varepsilon_{11}^s} - \frac{D_1 \; h}{\varepsilon_{11}^s} \qquad \text{Eq. 4.5.13.}$$

$$\phi(-h) = \frac{e^{(l)} \cdot u^{(l)}(-h)}{\varepsilon_{11}^s} + \frac{D_1 \; h}{\varepsilon_{11}^s} \qquad \text{Eq. 4.5.14.}$$

The potential difference can be obtained by substituting Eq. 4.5.8. and Eq. 4.5.9. into Eq. 4.5.13. and Eq. 4.5.14. to give,

$$\begin{aligned} \phi &= \phi(h) - \phi(-h) \\ &= \frac{2 D_1 h}{\varepsilon_{11}^s} \left(1 - k^{(l)2} G^{(l)} \frac{\tan \gamma^{(l)}}{\gamma^{(l)}} \right) \end{aligned} \qquad \text{Eq. 4.5.15.}$$

where $$G^{(l)} = 1 + \frac{T^{(l)}(-h) \; \varepsilon_{11}^s}{2 \; e^{(l)} \; D_1}$$

and $k'^{(l)2} = \dfrac{e^{(l)2}}{\varepsilon_{11}^{s}\rho\, v^{(l)2}}$. $k'^{(l)}$ is the electro-mechanical coupling factor. This parameter indicates the measure of the strength of electro-elastic coupling in a given material. The electric flux density is related to the electric current by,

Eq. 4.5.16.

$$D_1 = \frac{I}{j\ \omega\ (\text{Area of transducer})}$$

Thus by combining Eq. 4.5.15. and Eq. 4.5.16. the electrical impedance of the transducer is given by,

$$Z = \frac{1}{j\ \omega\ C_o}\left(1 - k'^{(l)2} G^{(l)} \frac{\tan \gamma^{(l)}}{\gamma^{(l)}}\right) \qquad \text{Eq. 4.5.17.}$$

where $C_o = \dfrac{\varepsilon_{11}^{s}}{2\,h}$. (Area of transducer) .

C_0 is the transducers' static capacitance.

In general, the transducers' electrical properties are usually best represented in terms of its admittance, the equivalent circuit of which is shown in Fig. 4.5.1. A method of solution for the stress, $T^{(l)}(-h)$, in Eq. 4.5.10., is given in Appendix B.

4.6. Insertion Loss

The one-way insertion loss is defined as the ratio of the maximum power that the electrical source can deliver compared to that of the power associated with the emergent acoustic wave. It is thus required in practice that this loss should be a minimum over the operating frequency range of the transducer. Onoe (1962) has considered this loss in relation to ultrasonic delay lines.

Here, the insertion loss is considered for the theoretical circuit as shown in Fig. 4.6.1. A current source I_0 with an internal

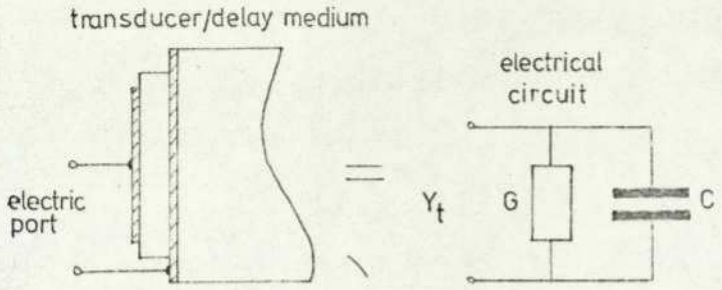

Fig. 4.5.1. Equivalent electrical circuit of the piezo-electric transducer.

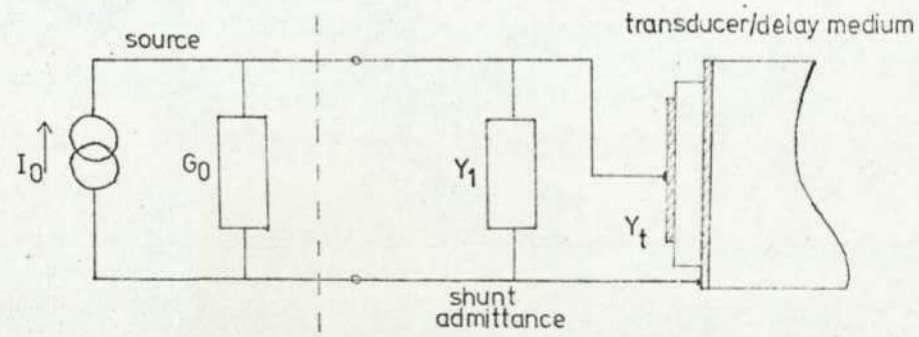

Fig. 4.6.1. Theoretical circuit for estimation of the one-way insertion loss.

conductance G_o feeds the signal to the transducer Y_t . Across the transducer is placed a shunt admittance Y_1 to compensate for the transducers' self capacitance. Assuming no excess losses, the insertion loss is zero when all of the available electrical power is absorbed by the conductance part of the transducers' admittance. This can be achieved by matching the source and transducers' conductances and tuning out the suseptance of the transducer by a parallel inductor. This will be true at a single frequency only and over a frequency range the insertion loss will vary, its variation being dependent on the behaviour of the transducers' electrical properties.

The maximum power that the source can deliver under matched conditions is thus

$$P_{max} = \frac{I_o^2}{4\ G_o} \qquad \text{Eq. 4.6.1.}$$

The power associated with the acoustic wave is equal to the power dissipated in the transducers' conductance.

Thus,
$$P(G) = \frac{I_o^2\ G}{(G_o + Y_1 + Y_t)^2} \qquad \text{Eq. 4.6.2.}$$

The insertion loss IL, in decibels, is consequently given as,

$$IL = 10 \log_{10}(T) \qquad \text{Eq. 4.6.3.}$$

where
$$T = \frac{P_{max}}{P(G)} = \frac{(G_o + Y_1 + Y_t)^2}{4\ G_o\ G}$$

In general more than one type of wave may be excited within the delay medium. Hence the power delivered into the conductance is equal to the sum of the powers of the waves generated as represented in Eq. 4.5.12.,

$$P(G) = P_a^{(l)} = P_L + P_{S1} + P_{S2} \qquad \text{Eq. 4.6.4.}$$

where P_L is the power of the longitudinal wave and P_{S1} , and P_{S2} are the powers of the shear waves. Consequently, the power loss, PL,

associated with each wave is,

$$PL_L = P(G) / P_L$$
$$PL_{S_1} = P(G) / P_{S_1} \qquad \text{Eq. 4.6.5.}$$
$$PL_{S_2} = P(G) / P_{S_2}$$

Hence the absolute one-way insertion loss associated with each acoustic wave can be expressed as,

$$IL_L = 10 \log_{10} (PL_L . T)$$
$$IL_{S_1} = 10 \log_{10} (PL_{S_1} . T) \qquad \text{Eq. 4.6.6.}$$
$$IL_{S_2} = 10 \log_{10} (PL_{S_2} . T)$$

4.7. Electrode and Bonding Layers

The analysis has considered the arrangement where the top electrode and bonding layer thicknesses were negligible compared to the acoustic wavelength. In practice this may not necessarily be true and the electrodes and bonding layer thicknesses may become comparable to the acoustic wavelength, especially at high frequencies. It has been shown by Sittig (1969) that the bandwidth and insertion loss may be severely affected when the electrode and bonding layer acoustic impedances are considerably mismatched with respect to the transducer and delay medium impedances, and when their thicknesses are in the order of a quarter of a wavelength.

Consistent with the analysis here, the effective acoustic impedance 'seen' by the transducer when an intermediate layer exists between the transducer and delay medium is given by,

$$z_d^{(l)} = z_f^{(l)} \left[\frac{z_d^{(l)} \cos 2\gamma_f^{(l)} + j\, z_f^{(l)} \sin 2\gamma_f^{(l)}}{z_f^{(l)} \cos 2\gamma_f^{(l)} + j\, z_d^{(l)} \sin 2\gamma_f^{(l)}} \right] \qquad \text{Eq. 4.7.1.}$$

where $\gamma_f^{(l)} = \omega h_f / v_f^{(l)}$

The subscript 'f' denotes the properties associated with the layer and z_f is the layers' acoustic impedance. When the thickness, $2h_f$, of the layer is negligible compared to the acoustic wavelength the effective acoustic impedance, z_d' , is essentially the same as that of the delay medium. When the thickness is equal to a quarter of a wavelength the effective impedance becomes significantly different and is equal to,

$$z_d'^{(l)}\left(\frac{\lambda}{4}\right) = \frac{z_f^{(l)2}}{z_d^{(l)}} \qquad \text{Eq. 4.7.2.}$$

When the layer is such that it is equal to a half of a wavelength, and multiples thereof, the effective impedance becomes equal to the impedance of the delay medium again. Sittig (1969) has extensively investigated the effects of multiple intermediate layers and although to some extent the layer thicknesses can be adjusted so as to optimise the response (Kossoff 1966) in general the resulting response may be considerably deformed when the acoustic mismatch is severe.

It can be shown that the effective acoustic impedance of the top electrode is given by,

$$z_t'^{(l)} = z_t^{(l)} \tan 2\gamma^{(l)} \qquad \text{Eq. 4.7.3.}$$

where z_t is the acoustic impedance of the top electrode material. When the film thickness is equal to a half of a wavelength the impedance becomes equal to zero. Reeder and Winslow (1969) have shown that at this frequency the insertion loss is greatly reduced. However, a severe reduction in bandwidth also occurs. Use has been made of multiple layers on the top electrode to obtain low insertion loss, narrow bandwidth transducers (Haydl et al 1964).

Thus, for an efficient wideband transducer response it is most desirable that both the top electrode and intermediate layers should be acoustically 'thin'. This is certainly true for the top electrode and its effect can be further minimized by using a material whose

acoustic impedance is greatly mismatched to that of the transducer. Where the acoustic impedances of the bonding and intermediate layers are mismatched to the delay medium the condition that the layers should be acoustically 'thin' is equally important. If these layers, however, have an acoustic impedance nearly equal to that of the delay medium then this condition may be relaxed somewhat (Larson and Winslow, 1971).

4.8. Impedance Matching Networks

Impedance matching the transducer to the source by a suitable electrical network may cause problems especially at high frequencies when the physical shape and dimensions of the arrangement and other constraints may be factors for consideration. The simple circuit in Fig. 4.6.1. may be used so long as the conductance of the transducer can be made to be reasonably closely matched to that of the source. Although the transducer can be driven without any impedance matching network present a considerable reduction in the efficiency will result (this assumes that the source can be operated under such conditions). Parallel tuning is more desirable than series tuning because in the latter the resistance and losses associated with the inductor reduce the overall conversion efficiency and the inclusion of series resistance into the circuit also tends to reduce the available bandwidth.

The conductance, and also the bandwidth, of the transducer is dependent on its electro-mechanical coupling factor. For low coupling factors ($K' \backsim 0.15$) the parallel capacitance of the transducer becomes significantly large compared to the conductance. Consequently, operation over only a narrow bandwidth will result when used in the circuit in Fig. 4.6.1. Methods of obtaining broadband matching have

been extensively investigated and reviewed by Matthaei (1964). He has also given extensive data on impedance transforming networks by using LC ladder filters. Theoretical considerations for matching networks have been given by Schwartz (1969). Reeder and Winslow (1969) have reviewed methods of broadband matching especially relating to transducers operating in the microwave region.

When the value of the electromechanical coupling factor is large ($K' \backsim 0.5$) the conductance becomes consequently large. If the design criterion demands a fixed transducer area the transducers' impedance at frequencies above 100 M Hz may only be a few ohms and series lead inductances will become significant. The impedance may be raised, however, by segmenting the transducer and connecting the elements in series. The impedance will then be increased in proportion to the square of the number of elements. Also the parallel capacitance is reduced. A reasonably large bandwidth can then be achieved even when the simple circuit of Fig. 4.6.1. is used or even when the transducer is driven untuned (Sittig 1969). However, if segmentation is not possible or desirable then the use of more complicated networks such as the ladder filters or transformers, as mentioned above, must be employed.

4.9. Acoustic Wave propagating in an arbitary direction

In sections 4.3. and 4.5. the analysis was related to the cartesian co-ordinate system as shown in Fig. 4.3.1. In order to find the behaviour of a transducer material whose geometrical axes do not coincide with the crystallographic axes as shown, the material's tensor properties must consequently be related to the new co-ordinate system. The translation of tensors from one co-ordinate system to

another has been extensively dealt with, for example, by Jeffreys (1931) and Nye (1957). The arrangement that has been considered is essentially one-dimensional and the tensors describing the properties of the stiffness, piezo-electric coefficient, and permittivity can be transformed in the following way to give,

$$C_{i1k1} \rightarrow C_{ijkl} \cdot n_j \cdot n_l$$

$$e_{1k1} \rightarrow e_{ijk} \cdot n_i \cdot n_k$$

$$\varepsilon^s_{11} \rightarrow \varepsilon^s_{ij} \cdot n_i \cdot n_j$$

The quantity n is a unit vector pointing in the direction of the plate normal and defines the direction of propagation of the acoustic wave normal. The analysis given can then be applied to a crystalline material of any orientation with respect to its crystallographic axes.

4.10. Further Comments

The theoretical behaviour of the piezo-electric transducer has been considered in this section and the equations describing its behaviour have been given. The theoretical model has been assumed to be lossless so that the theoretical results will yield the optimum performance. In practice, properties such as the dielectric loss and acoustic attenuation within the transducer together with the acoustic attenuation in the electrode material and bonding layers and electrical losses due to the finite resistance of the thin electrode layers all contribute to a reduction in the transducers' performance.

The appropriate equations must be solved numerically and a computer program to calculate the acoustic velocity, the particle displacement angle, and the electro-mechanical coupling factor is given in Appendix C. The results obtained for the materials used in

this work are given in the next section. Also, Appendix D gives a computer program to calculate the transducers' electrical admittance, the difference in phase between the acoustic wave and the electrical drive voltage, and the absolute one-way insertion loss. The results obtained for the transducers used in this work, bonded onto various delay mediums, are given in the following sections. The effects due to the finite thickness of the electrodes and bonding layers, as discussed in Section 4.7. have been neglected since the subject has been adequately dealt with elsewhere. It is obvious, though, that the theory used here can be extended to account for these effects.

The tuned insertion loss has been calculated for the circuit as given in Fig. 4.6.1. Although in practice, as discussed in Section 4.8., and also in the following sections, this may not necessarily be a feasible way of matching the transducer to the source in some cases it at least gives one some idea of the operational bandwidth of the transducer.

5. Materials

5.1. Introduction

In this section suitable materials for both the acousto-optic interaction medium and the transducer are briefly reviewed and the properties of the crystalline materials used in this work are considered. Because of the availability of materials to the author during the course of this work the emphasis is placed on materials exhibiting ordinary or normal bragg diffraction where the acoustic wave involved in the diffracting process is a longitudinal wave. The solid crystalline materials used were lead molybdate and lithium niobate. Their acoustic properties are presented and their X-ray laue patterns are given. The directions of the axes of the lithium niobate crystal with respect to the X-ray apparatus are given so that 35^{o} rotated Y-cut longitudinal acoustic transducers may be obtained.

5.2. Interaction Medium Requirements

The materials that have been investigated whose properties are suitable for the acousto-optic interaction medium are numerous. Basically, all suitable materials are required to be of good optical quality and to have low optical and acoustic attenuations. Also, for large aperture deflectors, it is required that the materials that are suitable are obtainable in reasonably large sizes. It has not been until recent years that the evaluation of suitable materials could be reasonably accurately predicted (Pinnow 1970). Beforehand, selection was based on availability and intuition. A review by Dixon (1967b) gives a comprehensive list of the physical properties of some materials, some of which are isotropic and some which are crystalline. Further

suitable materials have been developed since then and they have been extensively reviewed by Pinnow (1971) and by Uchida and Niizeki (1973) in which a comprehensive summary of glasses and new crystalline materials that have been discovered and developed are given. Also a paper by Gottlieb et al (1974) has summarized the acousto-optic properties of some chalcogenide crystals.

It has been shown in Eq. 3.4.3. that the material constants can be grouped together to form a figure of merit. This is the commonly used figure of merit which indicates the usefulness of a given material where the scattering efficiency is of importance. Thus,

$$M_2 = \frac{n^6 p^2}{\rho v^3}$$

A number of further figures of merit have been introduced which may be used to classify materials when other properties such as bandwidth, aperture, and acoustic power density are important. These have been summarized in a review by Chang (1976). Gordon (1966) has shown that where the bandwidth is of importance M_2 should be modified to

$$M_1 = \frac{n^7 p^2}{\rho v}$$

Also, it has been shown by both Dixon (1967b) and Pinnow (1970) that where the optical beam is circular in cross section the acoustic beam height across the optical aperture is proportional to the acoustic velocity. The figure of merit,

$$M_3 = \frac{n^7 p^2}{\rho v^2}$$

has been proposed. A fourth figure of merit has also been proposed by Chang (1976) in which the acoustic power density is taken into consideration. Thus,

$$M_4 = \frac{n^8 p^2 v}{\rho}$$

Another factor which affects the behaviour of an acousto-optic deflector is the thermal properties of the interaction medium. Eschler (1976) has incorporated a thermal figure with the figure of merit so as to give an overall figure of merit for materials

$$M_{Tot} = M_2 \cdot M_{therm}$$

where M_{therm} is a factor which relates the thermal conductivity, thermal expansion and the temperature change in the material's refractive index. This is of importance when distortion of the deflected beam, caused by acoustic power loss at the transducer and absorbtion within the delay medium, may become severe. Usually, the figures of merit are all given relative to those of fused quartz which, in general, has been used as a reference material.

Another property which must also be considered that is not included in the figures of merit is the acoustic attenuation (Pinnow 1970). Liquids, for example, have a relatively large figure of merit, M_2 . Solid materials usually have a lower figure of merit but also have a lower acoustic attenuation. In their studies on liquid interaction mediums Fukumoto and Watanabe (1970) have proposed a further figure of merit to include the acoustic attenuation of the medium. The figure of merit, M_2 has been modified to

$$M_a = M_2 / v \alpha_o \quad \therefore n^6 p^2 / \rho v^4 \alpha_o^2$$

for where both efficiency and resolution are of importance. A high figure of merit and low acoustic loss are, in general, not compatable properties and a trade-off between the two must be made when operation at high frequencies is required. Extensive information relating the figure of merit and acoustic attenuation has been given by Pinnow, and Uchida and Niizeki as already referenced.

Where an interaction medium is required suitable for application to a single device X-Y deflector one requires the material to have good acousto-optic figures of merit in both the orthogonal directions. It is clear that since the interaction is essentially the product of two single-dimensional deflections as shown in Section 3.3., the overall figure of merit for a suitable material is given by the product of the figures of merit in each orthogonal dimension, i.e.

$$M_i(X\text{-}Y) = M_i(X) . M_i(Y)$$

Also, the acoustic attenuation in each direction should be sufficiently small at the operating frequencies used.

It has become common practice in the literature to quote the figures of merit of materials relative to those of fused quartz. The values for fused quartz are given in Appendix E.

5.3. Liquids

As mentioned, liquids have a higher figure of merit (M_2) than most solids and the properties relevant to acousto-optic deflection of some liquids have been examined by Uchida (1968) and by Fukumoto and Watanabe (1970). Longitudinal acoustic waves are the only type of wave that can be supported in a liquid and, thus, liquids are only suitable for normal bragg diffraction. There are some liquids that have a very high figure of merit, M_2, i.e. n-Propyl Iodide. However, the associated large value of acoustic attenuation limits their use to low acoustic frequencies and precludes them as a practical interaction medium. Water, however, has a lower M_2 than most liquids but is preferable due to its lower value of acoustic attenuation and has been widely used for experimental purposes (i.e. Korpel et al 1966). Water has been used as the interaction medium during this work for use in preliminary experiments.

5.4. Lead Molybdate

One solid material that has been shown to have good acousto-optic properties is lead molybdate ($PbMoO_4$) and was first discovered by Pinnow et al (1969). The acoustic, optical, and thermal properties have been investigated by Coquin et al (1971) . The material is a tetragonal crystal and belongs to the crystal point group 4/m. The growth conditions for this material have been studied by Bonner and Zydzik (1970). It is optically uniaxial and is transparent for optical wavelengths between 0.4μm and 4μm . Acousto-optic deflection has been achieved by causing a longitudinal acoustic wave to propagate along the crystallographic z axis and the optical beam to propagate near the plane z = 0. In this configuration it has been reported (Pinnow 1969) that the figures of merit are high (relative to fused quartz, M_2 = 23.7) and that the deflection efficiency is essentially independent of the optical polarization when the optical wavelength used is 632.8 nm. With a longitudinal acoustic wave propagating in the X-Y plane efficient diffraction can also be obtained with light polarized in the X-Y plane although the figure of merit, M_2 = 16, is somewhat less than that in the first configuration. The material is thus useful as the interaction medium in a two-dimensional deflector. The acoustic losses reported by Coquin et al (1971) have shown that the material is useful for acoustic frequencies of up to 500 M Hz.

From the results given by Coquin et al (1971) the acoustic velocities of both longitudinal and shear waves propagating in the bulk medium of $PbMoO_4$ are given in Fig. 5.4.1., Fig. 5.4.3., and Fig. 5.4.5. for waves propagating in the planes X =0, Y = 0,and Z = 0 respectively. In Fig. 5.4.2., Fig. 5.4.4. and Fig. 5.4.6. the variation of the magnitude of the angle between the wave normal and the longitudinal waves' particle displacement is given for the different planes. The

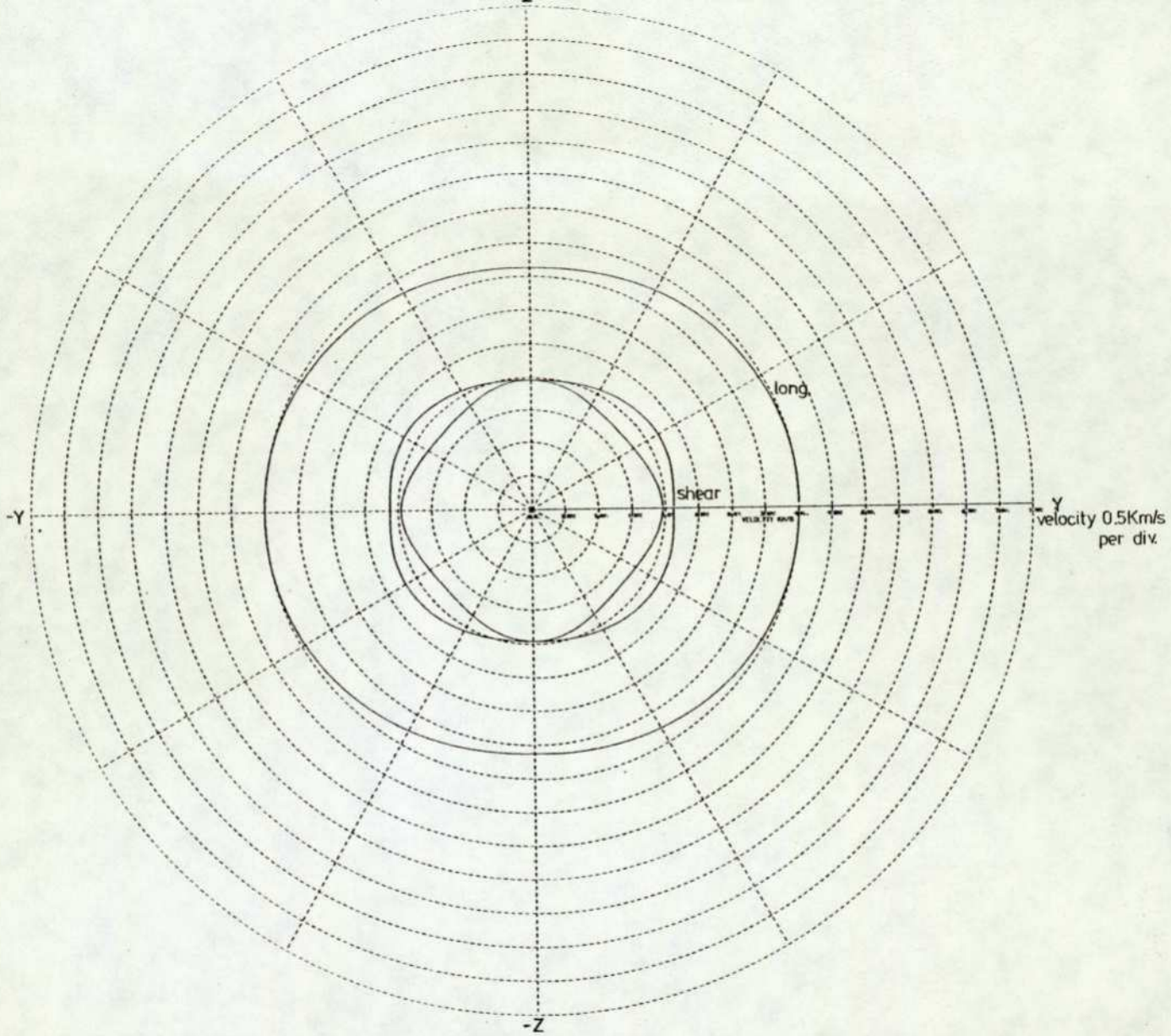

Fig. 5.4.1. Acoustic velocity surfaces for $PbMoO_4$ in the crystallographic plane x=0.

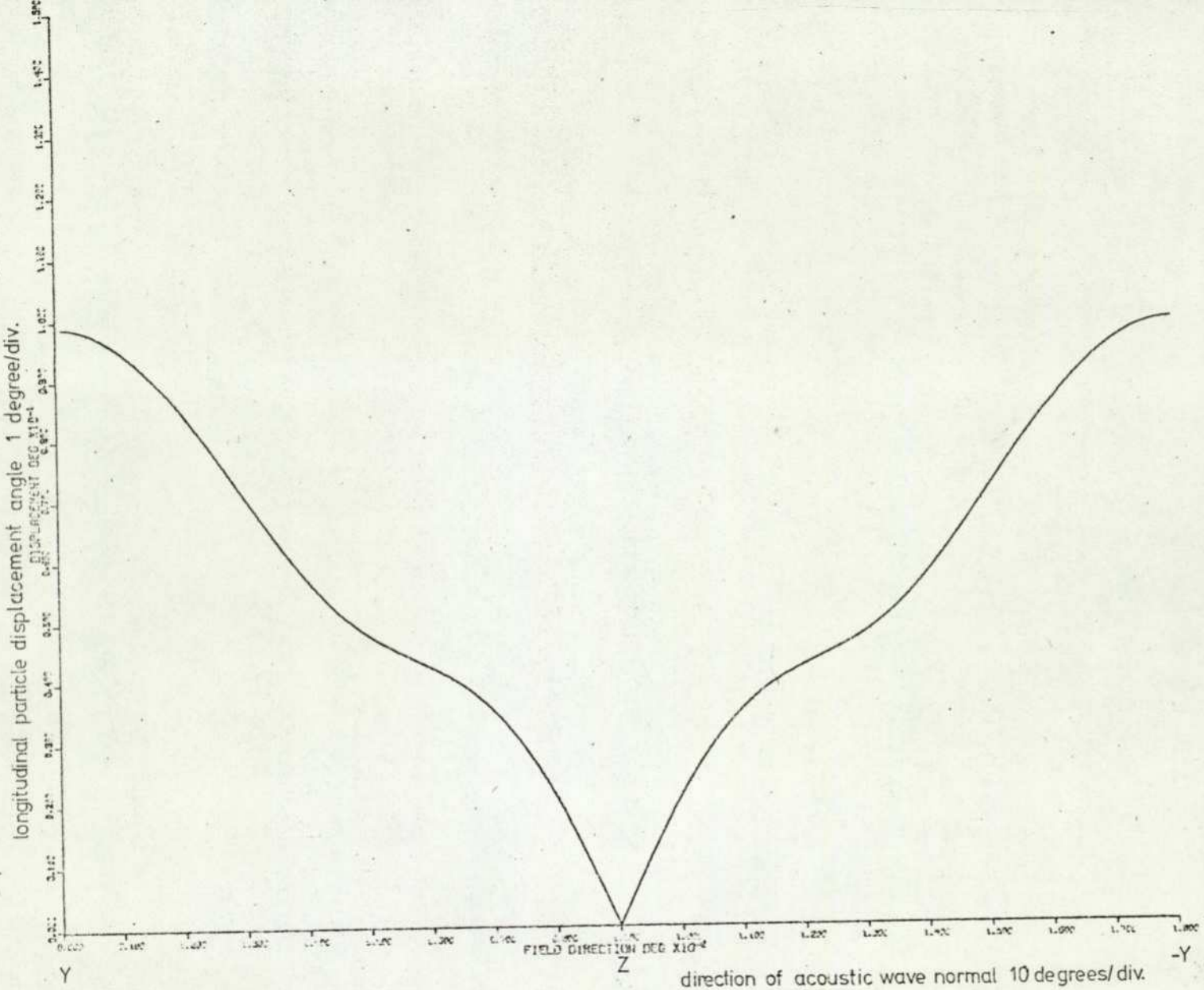

Fig. 5.4.2. Magnitude of particle displacement angle in $PbMoO_4$ in the crystallographic plane x=0.

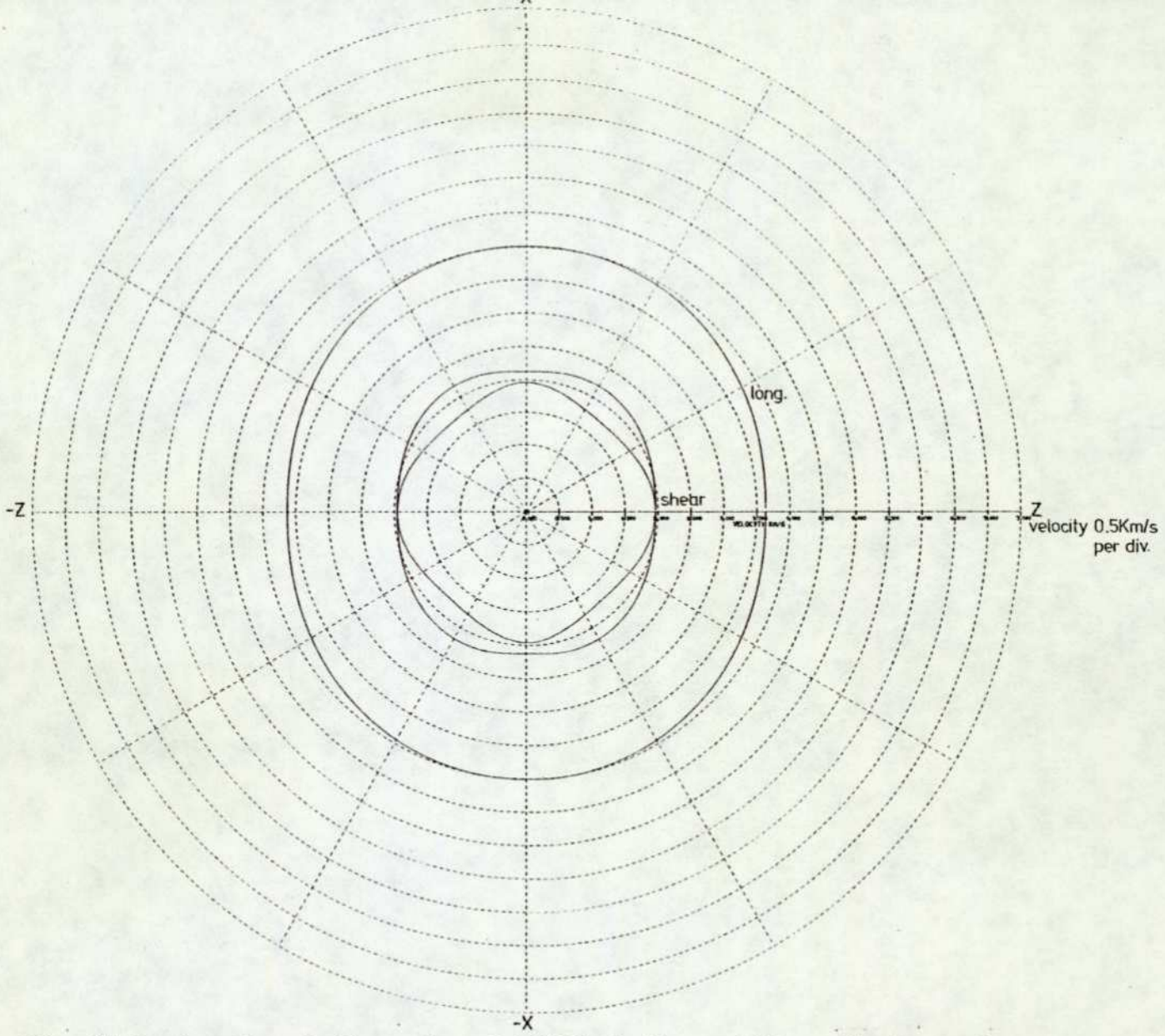

Fig. 5.4.3. Acoustic velocity surfaces for $PbMoO_4$ in the crystallographic plane y=0.

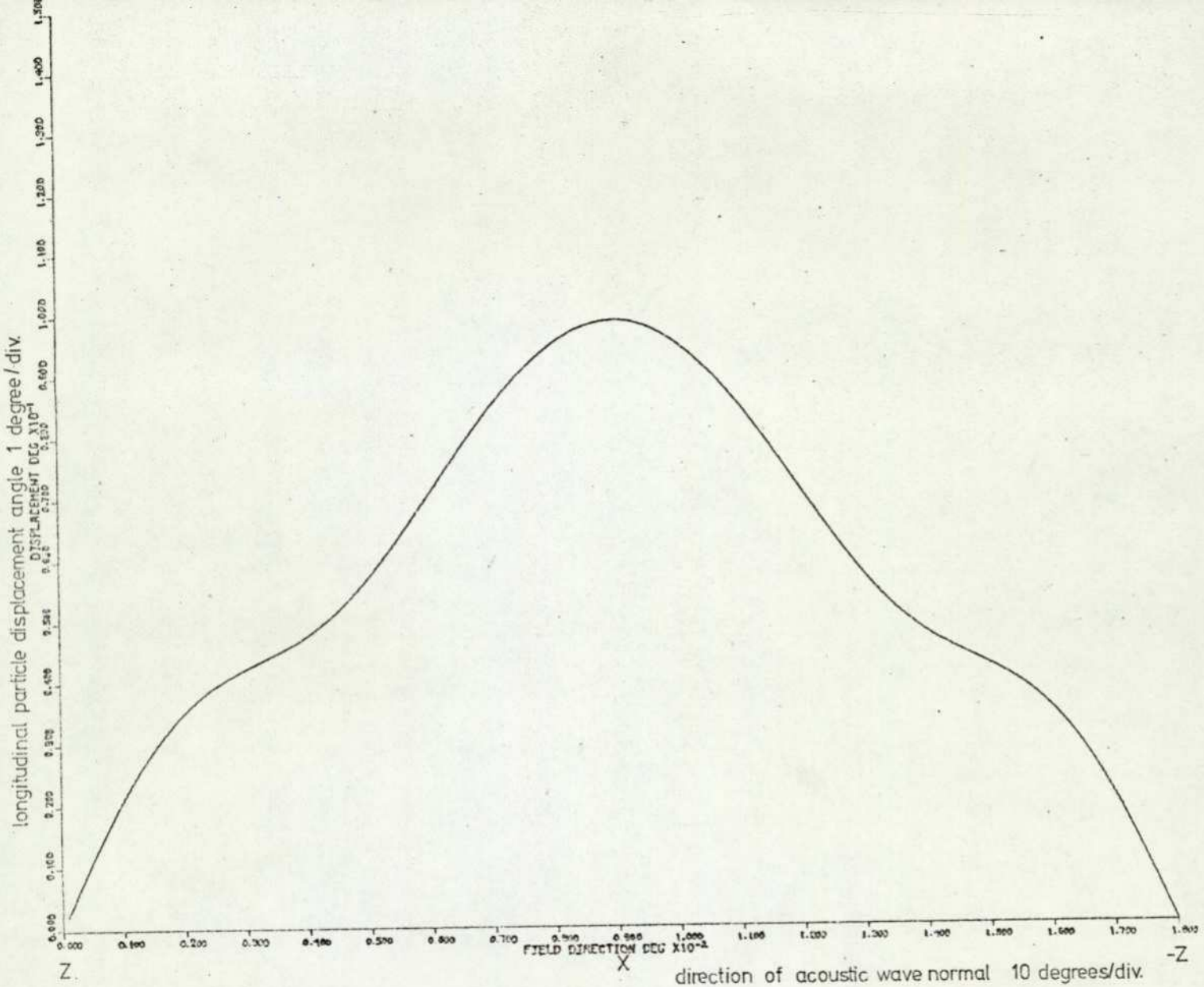

Fig. 5.4.4. Magnitude of particle displacement angle in $PbMoO_4$ in the crystallographic plane y=0.

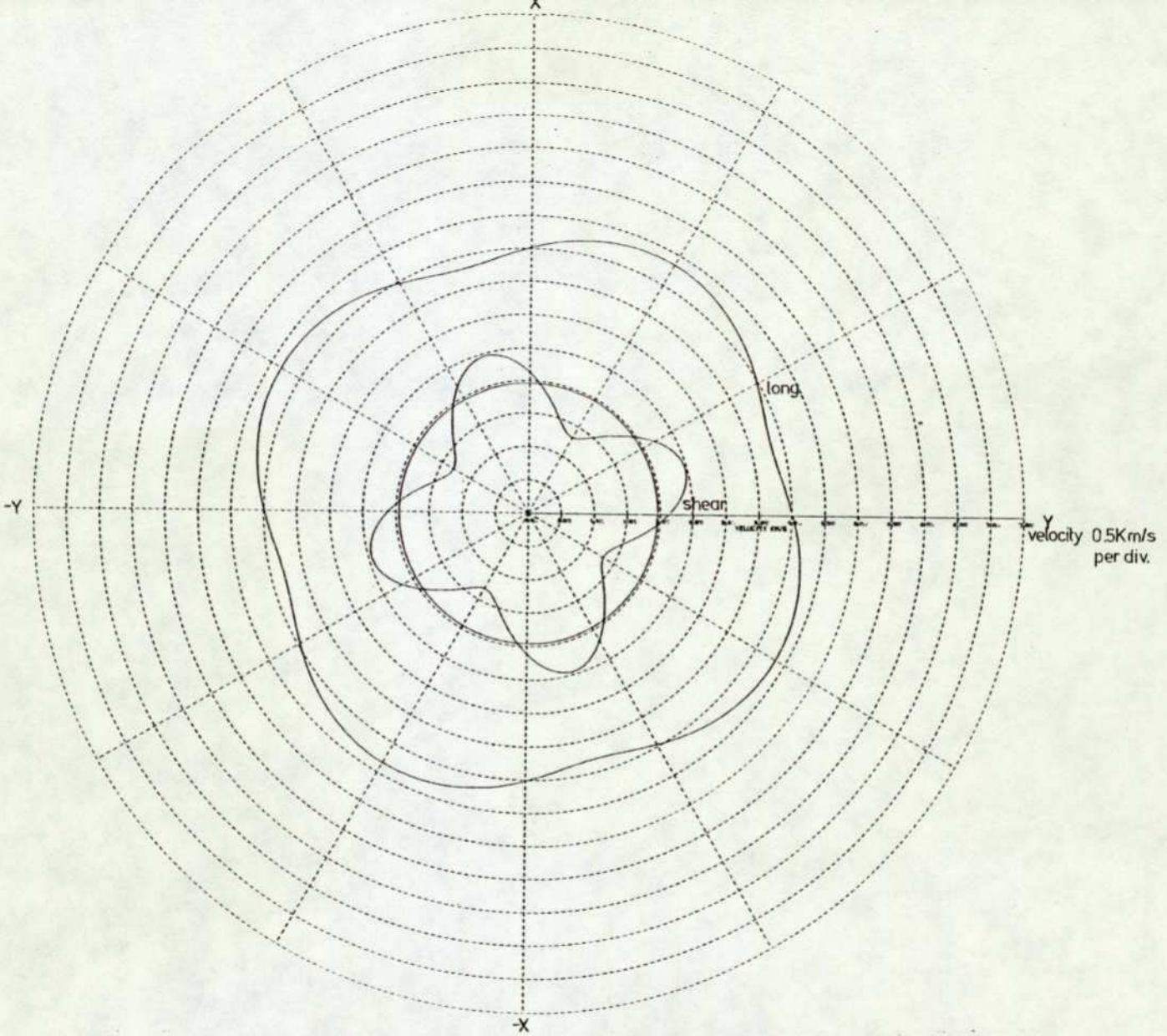

Fig. 5.4.5. Acoustic velocity surfaces for $PbMoO_4$ in the crystallographic plane z=0.

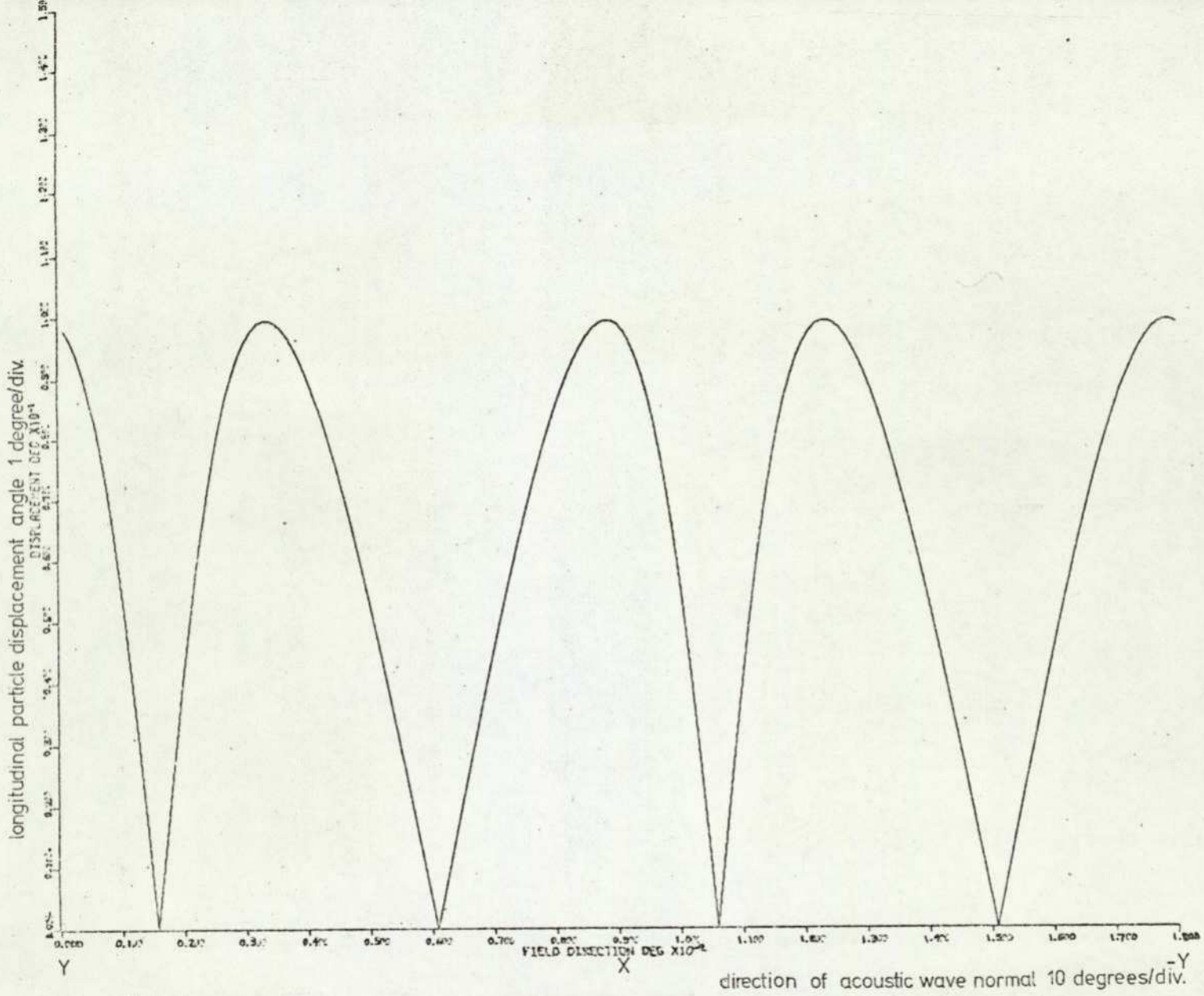

Fig. 5.4.6. Magnitude of particle displacement angle in $PbMoO_4$ in the crystallographic plane z=0.

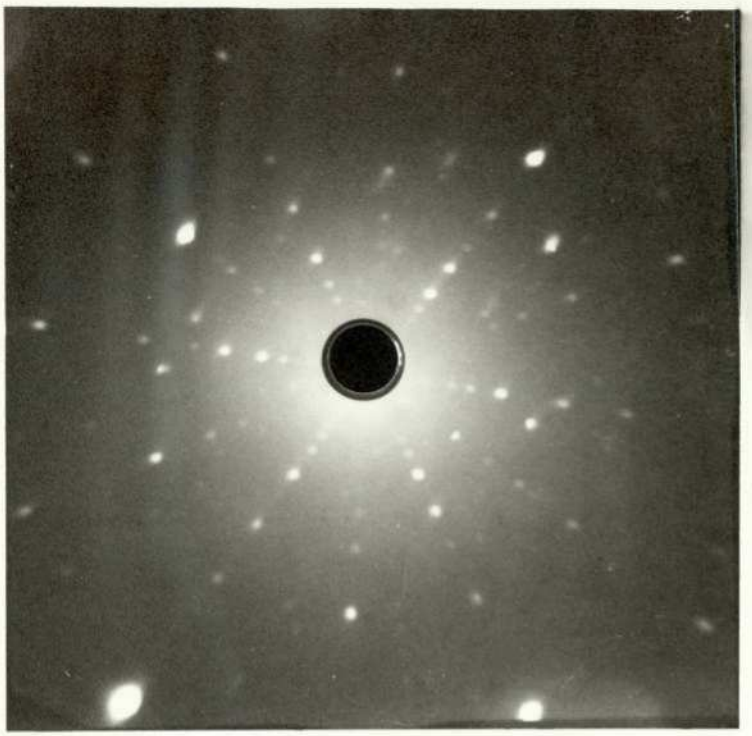

Plate 5.4.1. X-ray laue pattern of $PbMoO_4$ along crystallographic z axis.

variation of the longitudinal velocity in $PbMoO_4$ for waves propagating in the planes considered varies from 3.63 Km/s in the z direction to 4.34 Km/s in the X-Y plane. The z axis is an acoustic axis and the longitudinal wave here is a pure mode. It can be seen that in the XY plane the particle displacement angle varies considerably although there are directions in the positive XY quadrant at 29^{o} and at 74^{o} from the x axis in which a pure mode can propagate. The magnitude of this angle can change by up to 10^{o} and the generation of unwanted modes when a longitudinal transducer is attached to the medium in these directions may become severe.

The lead molybdate boule obtained for this work was about 2.5 cm long and about 2.7 cm in diameter. The material is comparatively soft in nature and is easily susceptible to chipping and cracking which can be caused by sudden thermal changes. The crystal is grown by pulling from a melt and the crystallographic z axis may lie at an angle of up to 30^{o} with respect to the longitudinal axis of the boule (Bonner and Zydzik 1970). Observations taken from a X-ray laue back scatter photograph showed that for the material to be used the z axis lay about 20^{o} off from the boules' longitudinal axis. The laue pattern obtained along the z axis is shown in Plate 5.4.1. Determination of the X and Y axes, however, can not be easily achieved and can really only be found by a more detailed X-ray study. Information about these crystallographic axes can not be readily obtained from the X-ray pattern and unlike lithium niobate there are no markings or indications on the side of the boule to assist with orientation.

5.5. Acoustic Transducer Materials and Requirements

It has not been until recent years that transducer materials have been discovered that are suitable for high frequency, wideband applications. Such materials have been reviewed extensively by Meitzler (1971). The application demands a material with properties such as a low permittivity and a high electromechanical coupling factor together with low acoustic and electrical losses. To date, the most successful transducers that can be fabricated are those which can be made from piezo-electric platelets. Typical materials that can be used for this purpose are lithium niobate ($LiNbO_3$), lithium tantalate ($LiTaO_3$), and lithium iodate ($LiIO_3$) for the generation of longitudinal and shear waves, and barium sodium niobate ($Ba_2NaNb_5O_{15}$) and lithium gallate ($LiGaO_2$) for the generation of longitudinal waves. Acoustic transducers can also be fabricated using materials such as cadmium sulphide (CdS) and zinc oxide (ZnO) which can be deposited by evaporation techniques onto the substrate material (Foster et al 1968). One advantage here is that the bonding layer is eliminated between the substrate and transducer. However, comparatively thick films with low conversion losses may be difficult to achieve and also the electromechanical coupling factor, and consequently the associated fractional bandwidth is lower (Reeder and Winslow 1969). Transducers fabricated from piezo-electric crystal platelets are thus preferred for their lower conversion losses and higher coupling factors, and they are usable over broader fractional bandwidths for frequencies up to about 1 G Hz.

5.6. Lithium Niobate

The acoustic transducer material that has been used for this work is lithium niobate ($LiNbO_3$). It is a trigonal crystal and belongs to the crystal point group 3m. Conditions for growth and its crystal

structure have been examined by Nassau et al (1966b). Comprehensive information concerning the properties of this material have been given by Milek and Neuberger (1972).

The properties of lithium niobate relevant to its application as an ultrasonic transducer have been extensively investigated by Warner et al (1967) and their variation with temperature has been studied by Smith and Welsh (1971). The material also has low dielectric losses (Nassau et al 1966a) and acoustic losses (Spencer et al 1967). From the results for the elastic, piezo-electric and dielectric properties as measured by Warner et al (1967) the variation of the acoustic velocity, the magnitude of the particle displacement angle, and the electromechanical coupling factor in the planes $x = 0$, $y = 0$, and $z = 0$ are shown in Fig. 5.6.1. to Fig. 5.6.9. respectively. Although the most useful cuts can be obtained from orientations in the plane $x = 0$ the variation of the various parameters are shown for the planes $y = 0$ and $z = 0$ for completeness. Spencer (1967) has shown plots of the velocity for lithium niobate but the plot for the plane $x = 0$ has been given with the axes incorrectly orientated.

There are a number of useful cuts which can be obtained from this material. Shear mode transducers can be obtained from the X-cut or the 163^{o} rotated Y-cut orientations. For longitudinal mode transducers there are two suitable orientations. The Z-cut generates a pure longitudinal wave and the 35^{o} rotated Y-cut generates a quasi-longitudinal wave. The 35^{o} rotated Y-cut has been used for this work because of its associated high electromechanical coupling factor and also because the acousto-optic diffraction process for normal bragg diffraction requires the use of longitudinal waves for the interaction mediums used. For this orientation the longitudinal acoustic velocity is 7.4 K m/s and has an electromechanical coupling factor of 48.7%. The relative permittivity at constant strain for a platelet

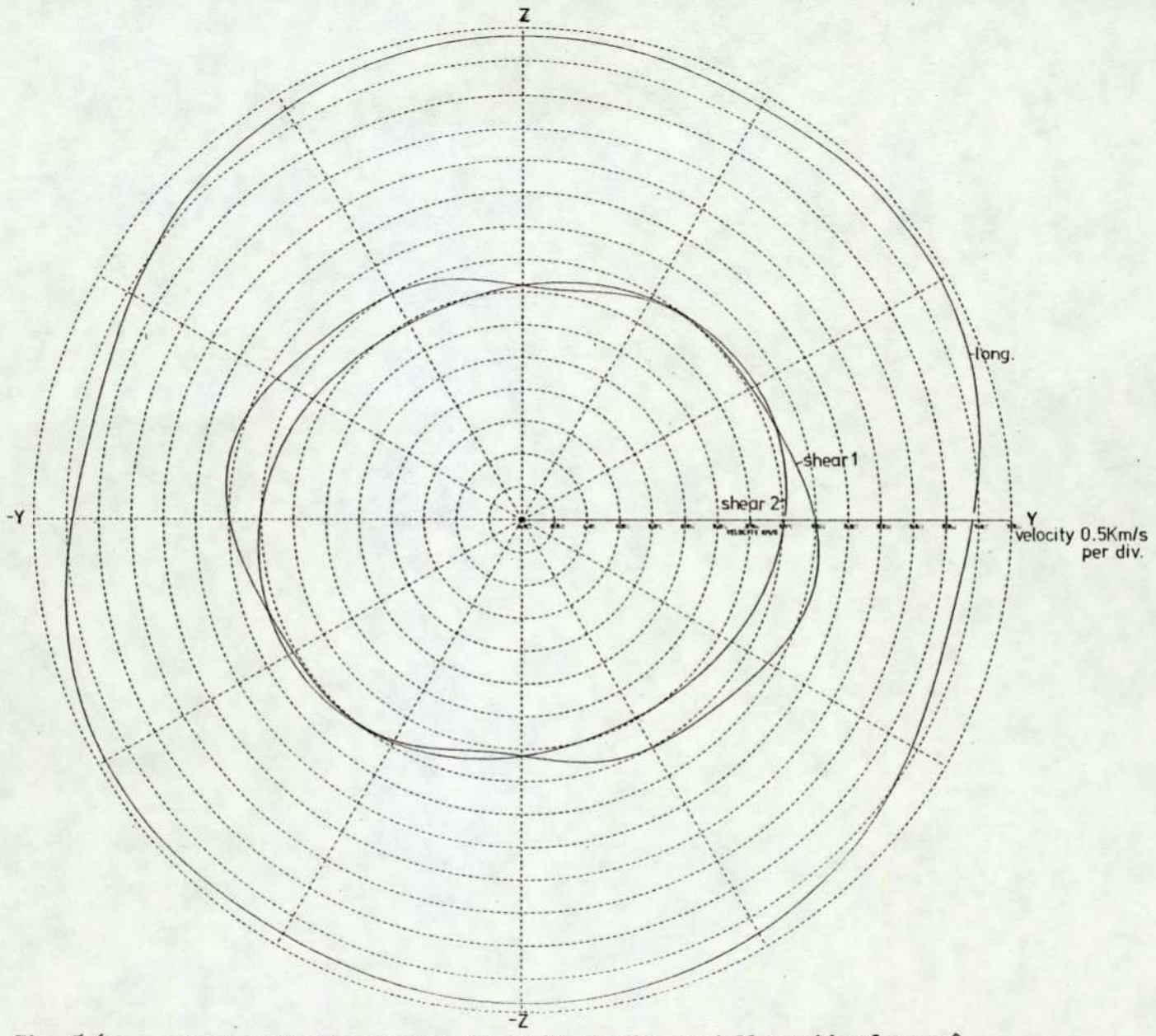

Fig. 5.6.1. Acoustic velocity surfaces for $LiNbO_3$ in the crystallographic plane x=0.

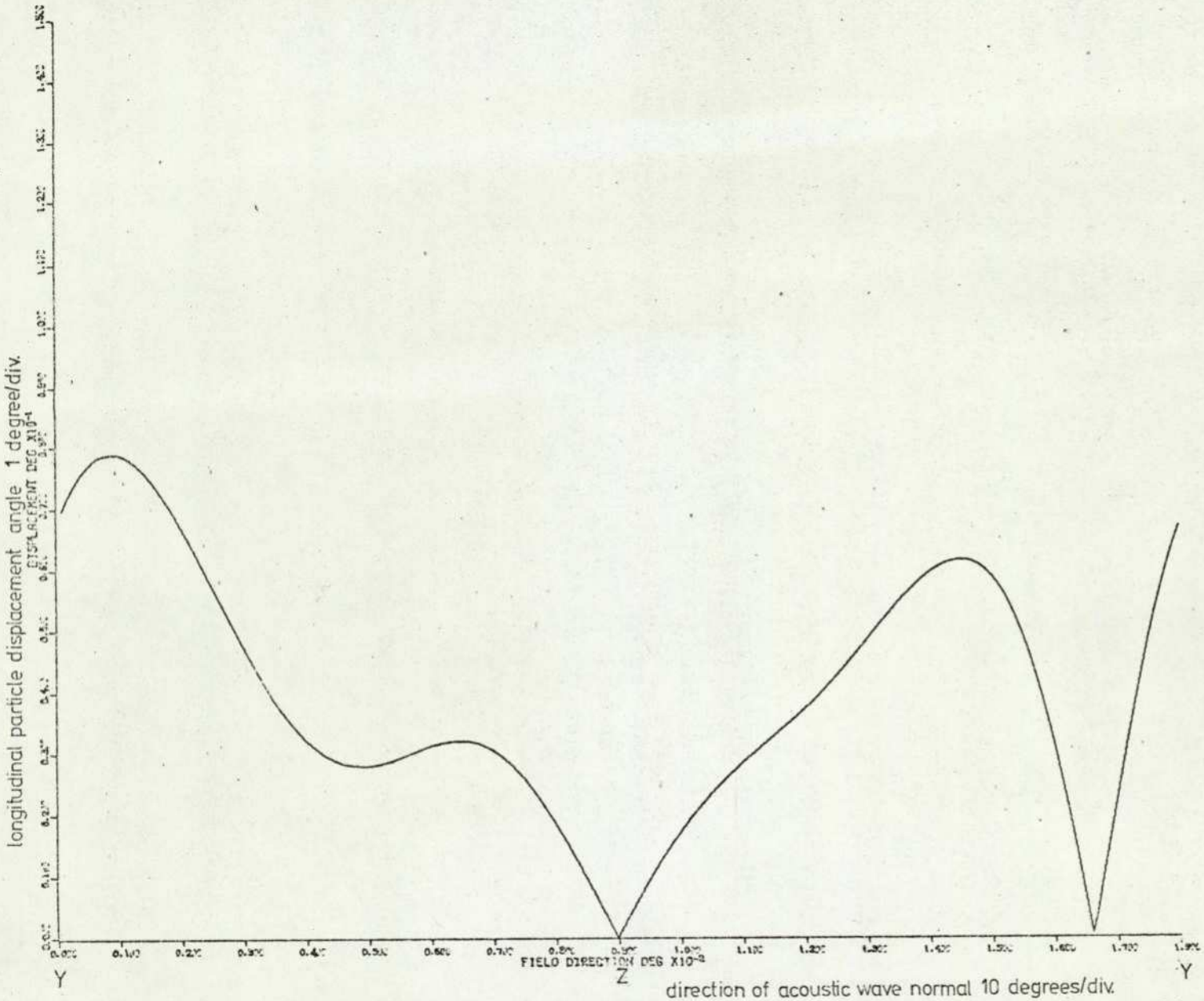

Fig. 5.6.2. Magnitude of particle displacement angle in $LiNbO_3$ in the crystallographic plane x=0.

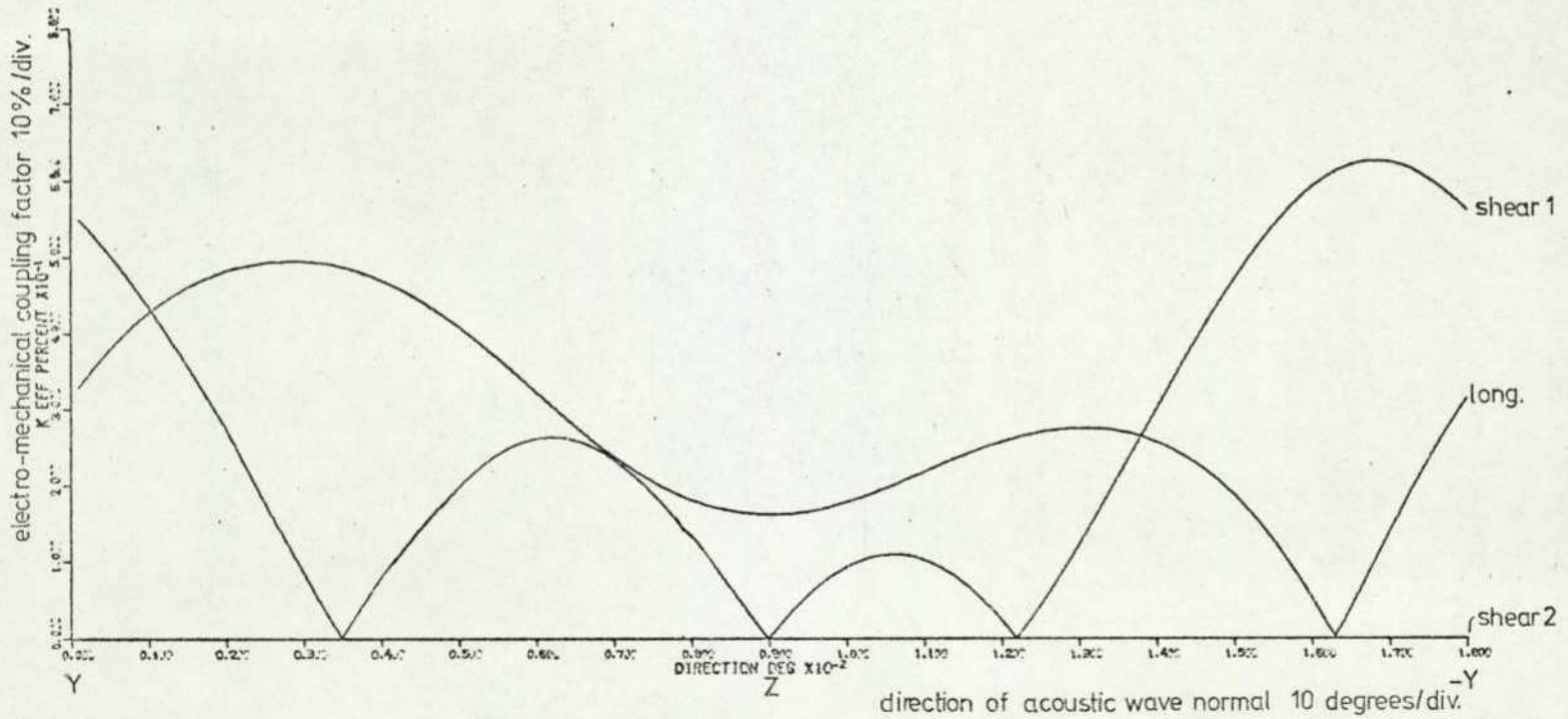

Fig. 5.6.3 Variation of electro-mechanical coupling factor, k', for $LiNbO_3$ in the crystallographic plane x=0.

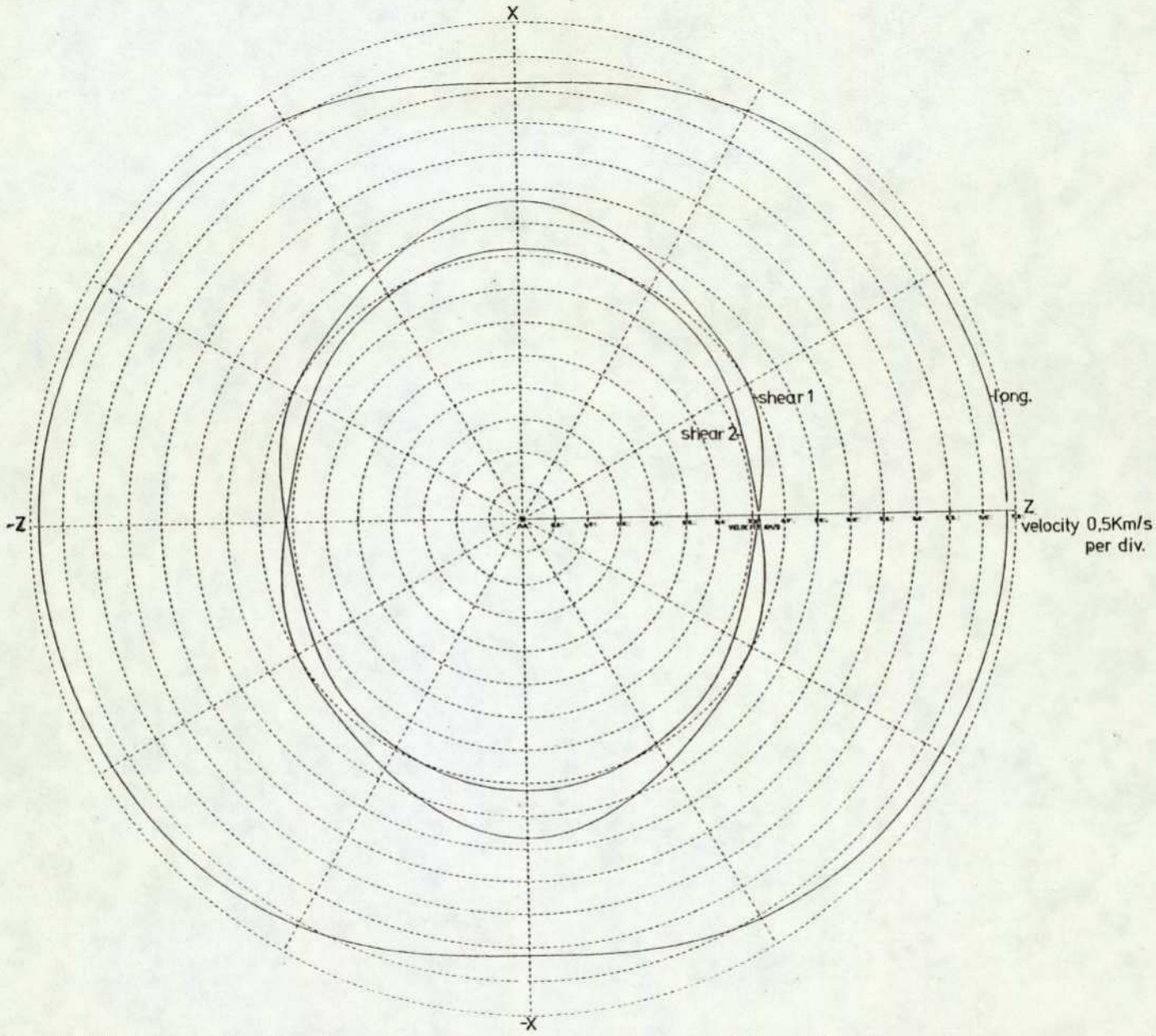

Fig. 5.6.4. Acoustic velocity surfaces for $LiNbO_3$ in the crystallographic plane y=0.

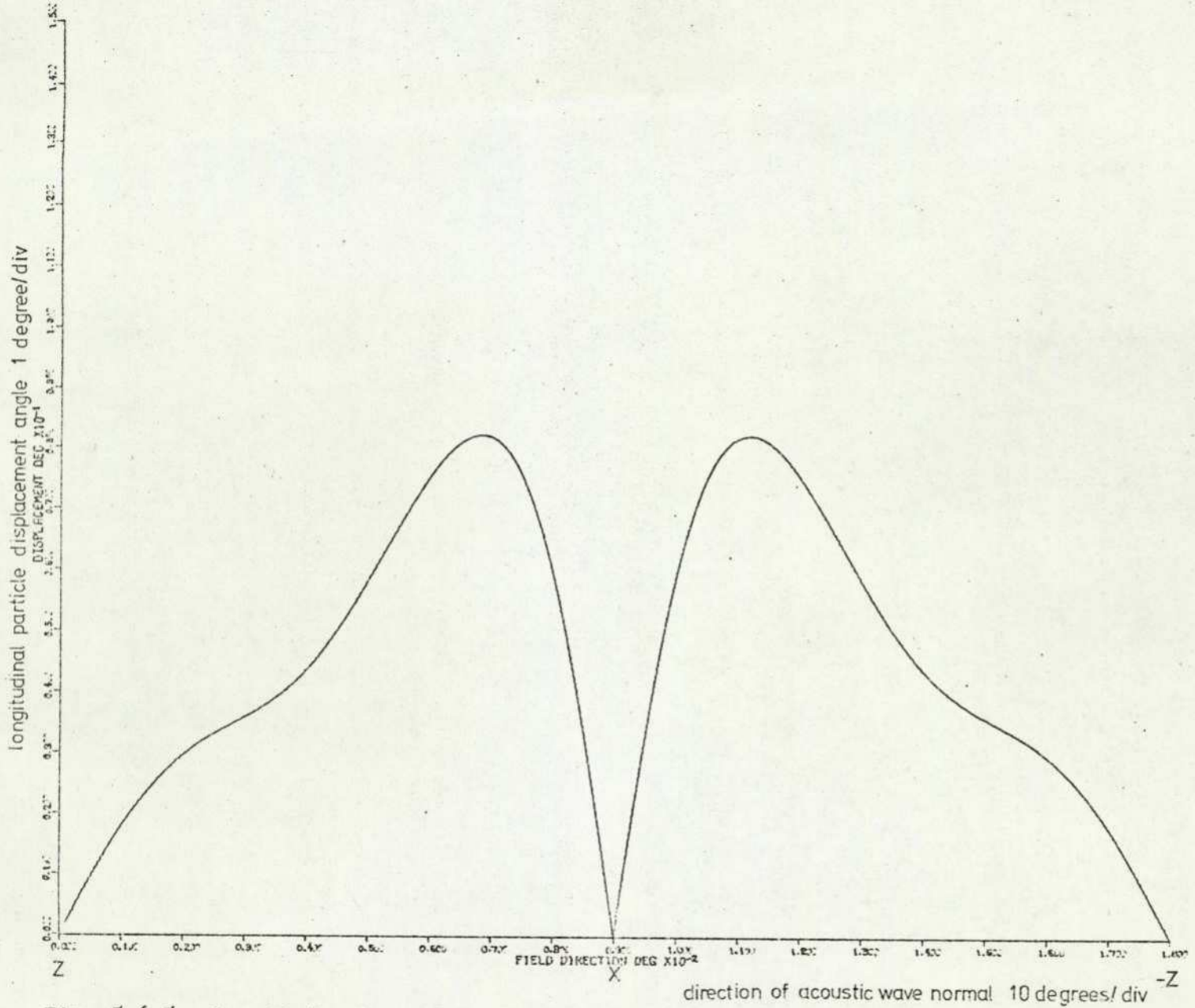

Fig. 5.6.5. Magnitude of particle displacement angle in $LiNbO_3$ in the crystallographic plane y=0.

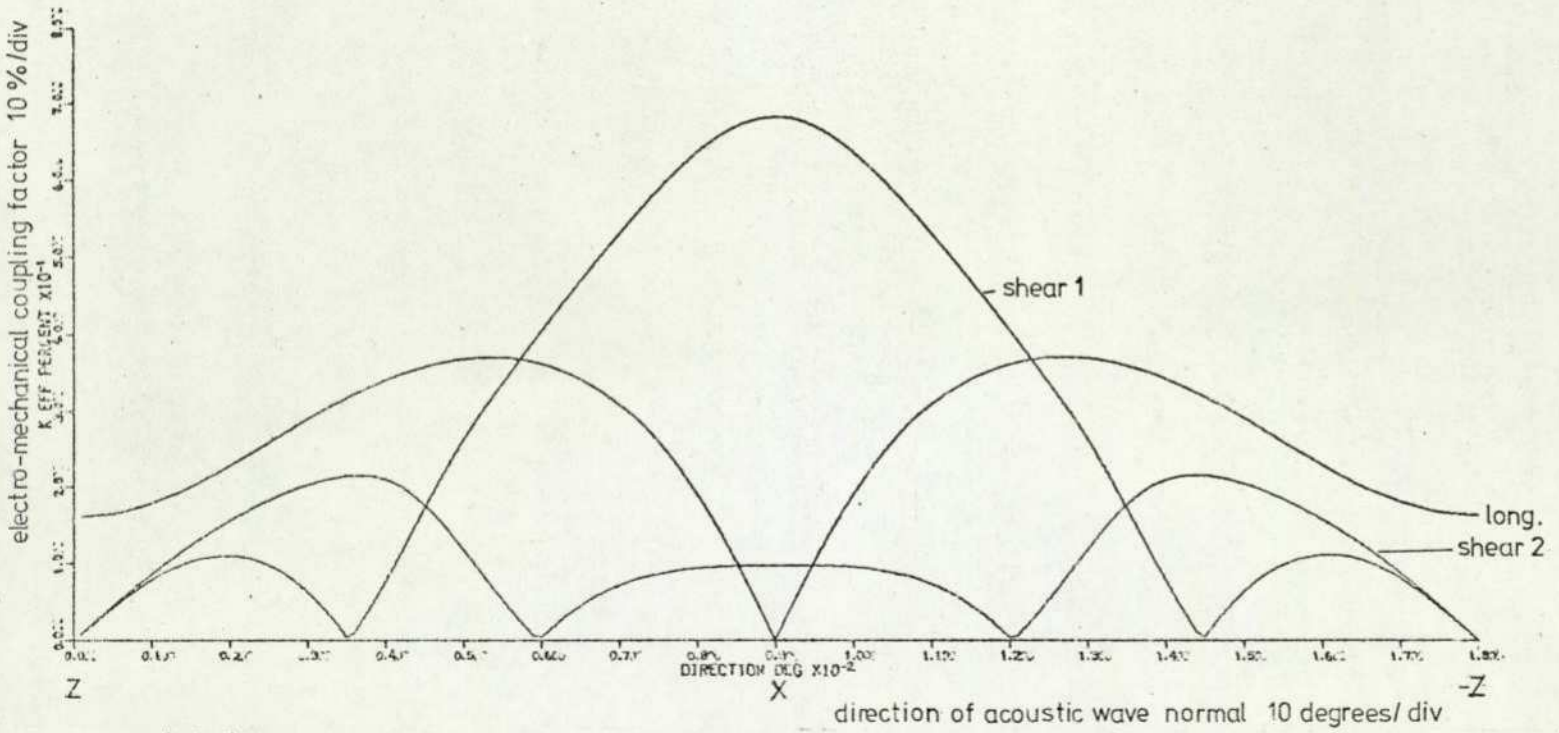

Fig. 5.6.6. Variation of electro-mechanical coupling factor, k', for $LiNbO_3$ in the crystallographic plane y=0.

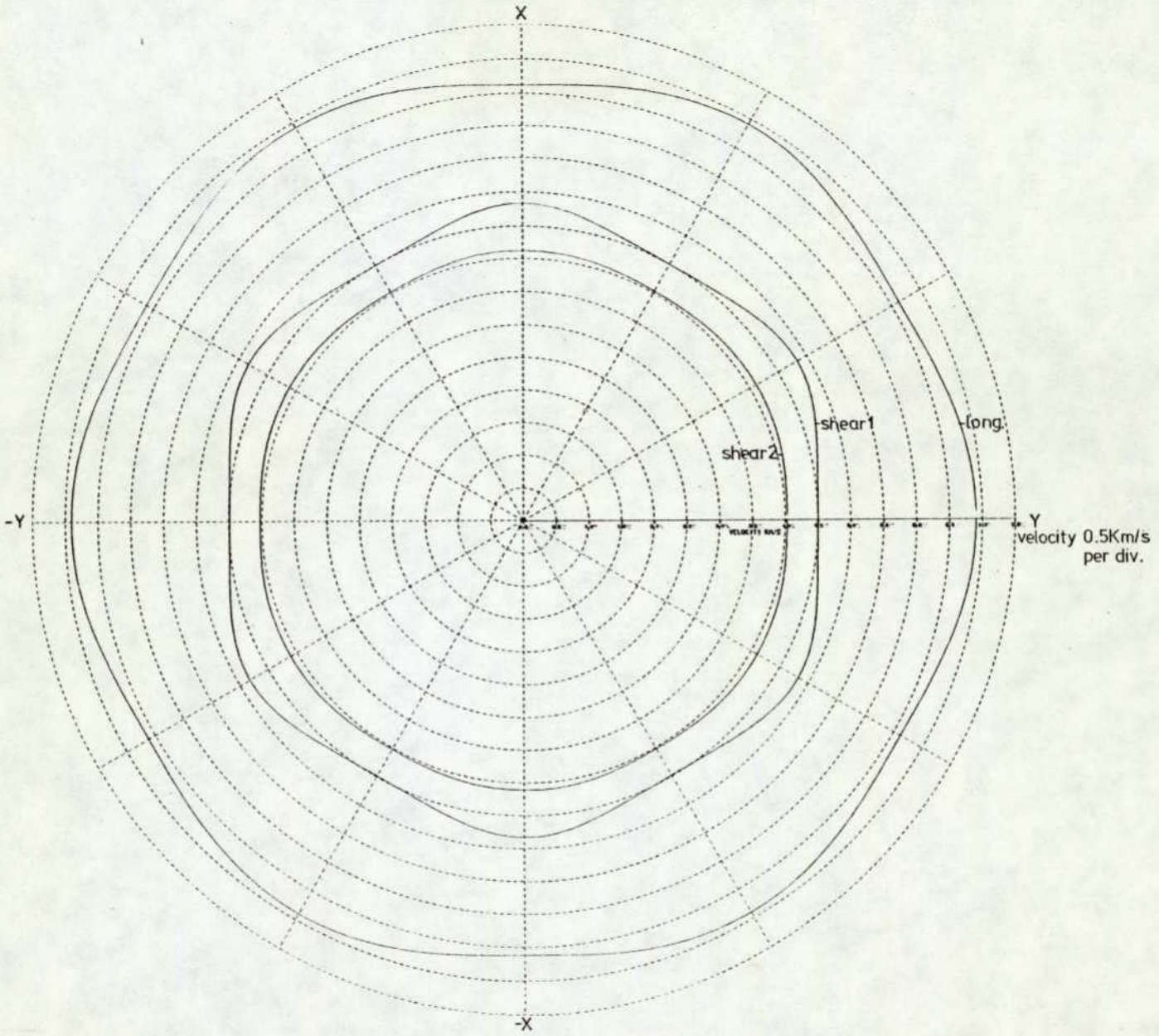

Fig. 5.6.7. Acoustic velocity surfaces for $LiNbO_3$ in the crystallographic plane z=0.

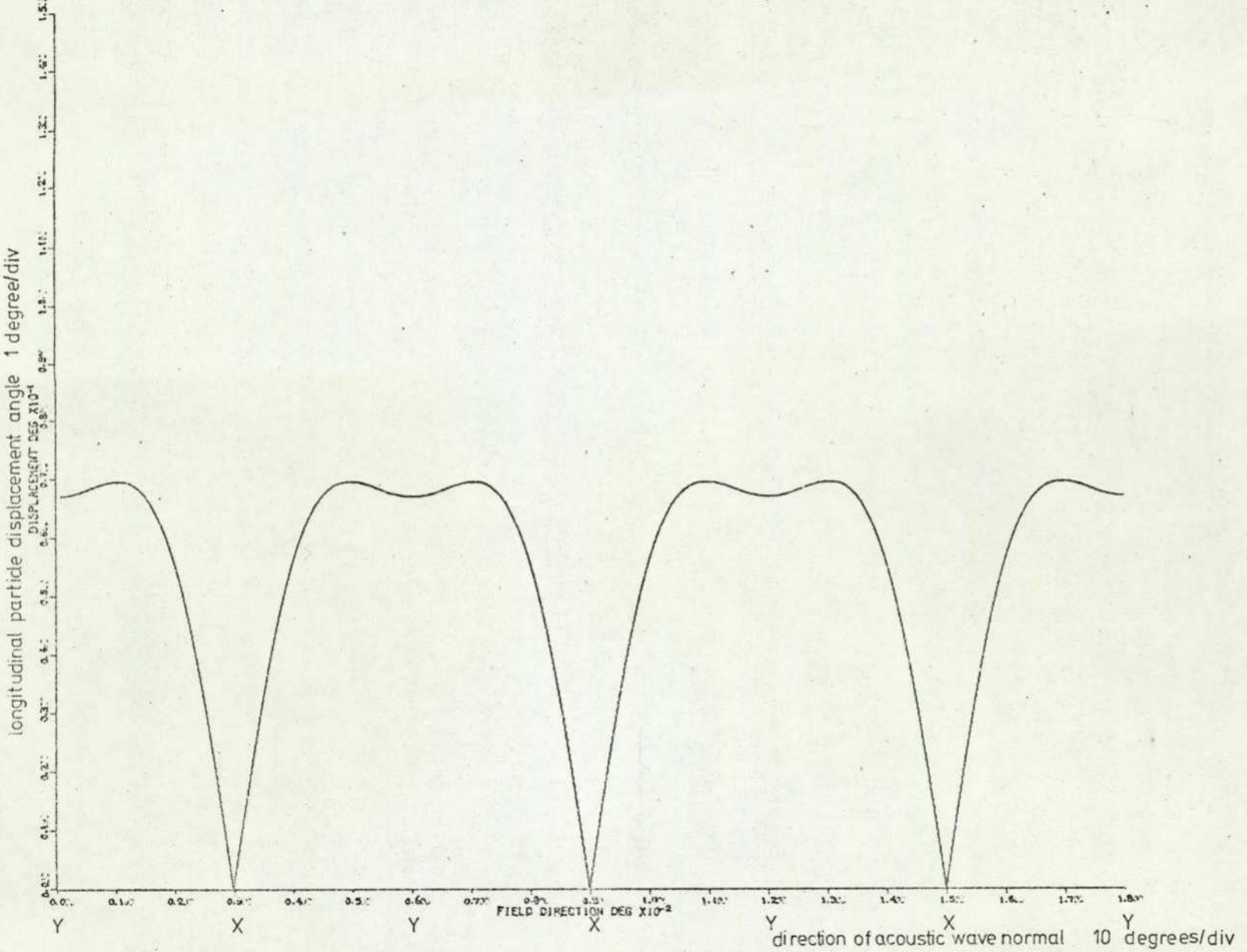

Fig. 5.6.8. Magnitude of particle displacement angle in $LiNbO_3$ in the crystallographic plane z=0.

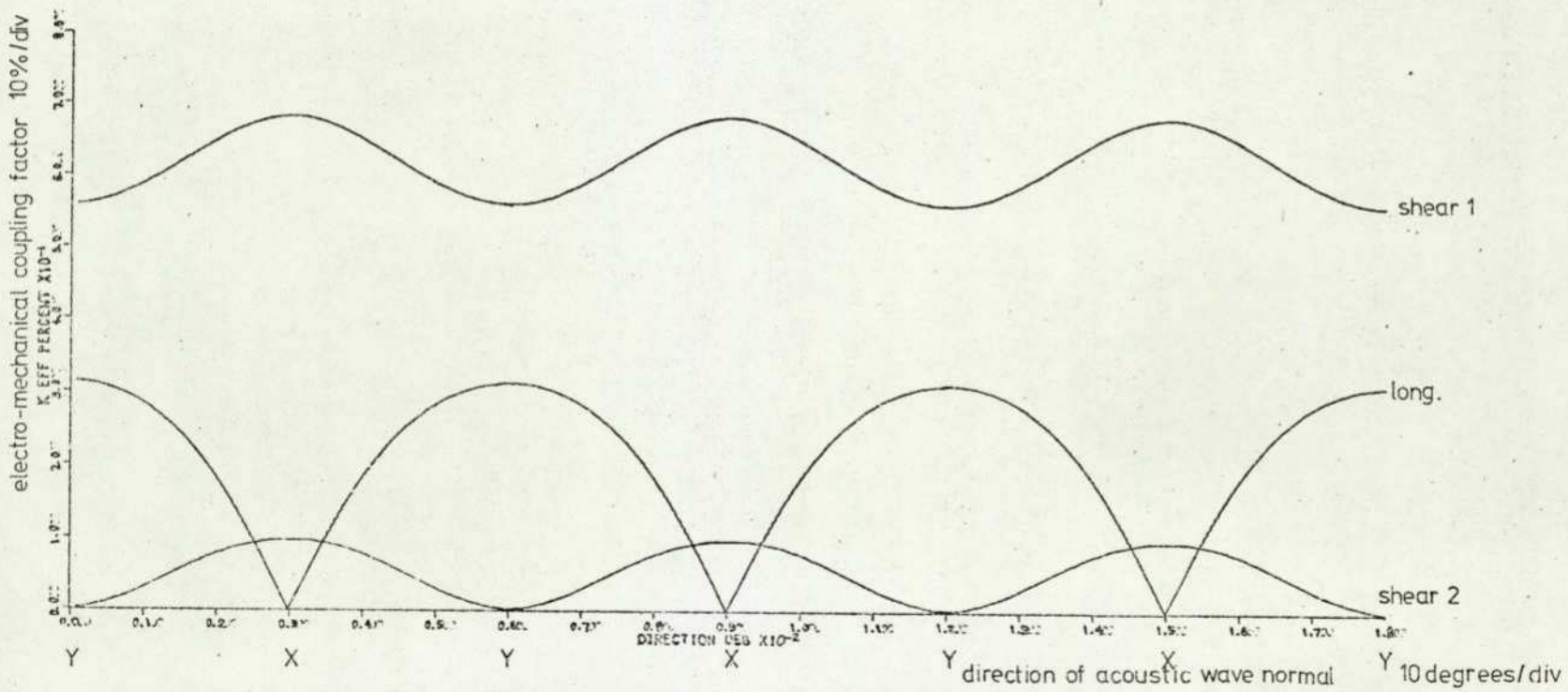

Fig. 5.6.9. Variation of electro-mechanical coupling factor, k', for $LiNbO_3$ in the crystallographic plane z=0.

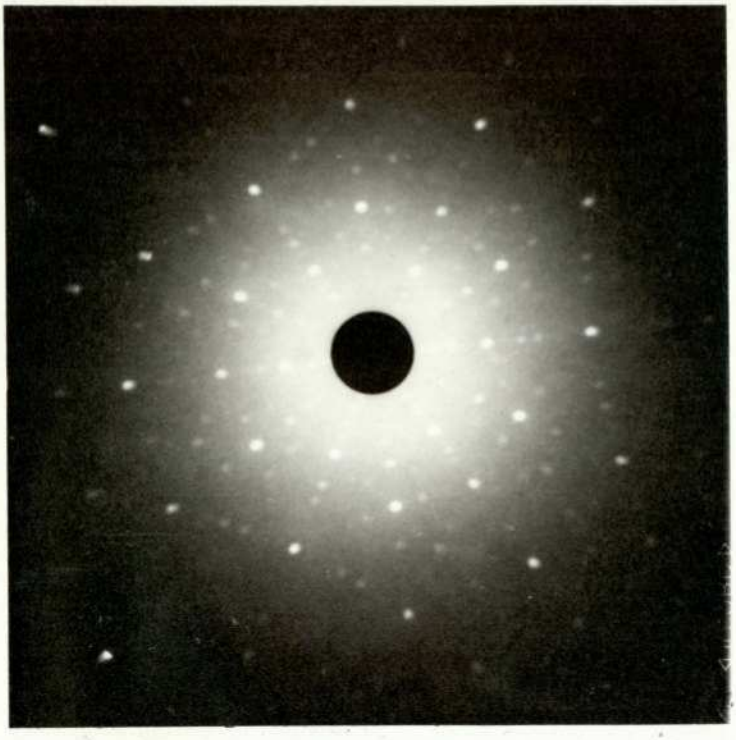

Plate 5.6.1. X-ray laue pattern for $LiNbO_3$ along the crystallographic z axis.

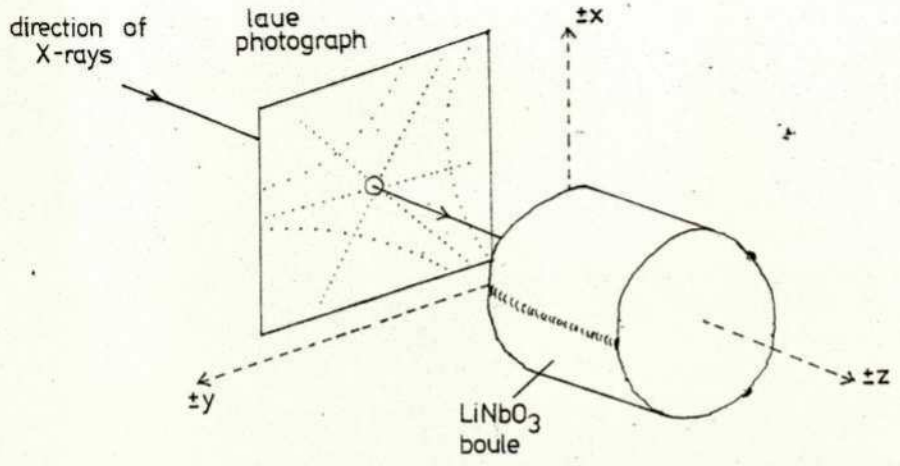

Fig. 5.6.10. Orientation and axis directions for the $LiNbO_3$ boule with respect to the x-raying equipment.

of this orientation is 39. These properties have been summarized by both Uchida and Niizeki (1973) and Chang (1976). The particle displacement angle, although significant, is not too large and is 3.8^{o}.

Plate 5.6.1. shows the laue back scatter pattern taken along the crystallographic z axis of the material and has been given by Nassau et al (1966a). The crystal is grown by pulling from a melt and this axis is usually parallel to the longitudinal axis of the boule. This was found to be so for the material obtained for this work. This department had had some prior experience with this material in connection with work concerned with electro-optics. However, some confusion existed in determining the sense of the directions of the crystallographic axes with respect to the photograph and the X-ray equipment. Fig. 5.6.10. is thus given to indicate the appropriate directions of the axes. For this work it was not important to know the true sign of each axis but merely to know the signs of the axes in relation to each other. Also there are markings on the side of the boule which indicate the position of the crystallographic y axis.

For the purposes of the X-ray studies and the cutting the crystals were mounted onto a balsa wood block which, in turn, was mounted onto a Logitech goniometer. With the crystals correctly orientated the goniometer was transfered from the X-ray equipment to the departments' Meyer and Burger AG QS2 quartz crystal cutting machine and the crystals were then cut to the required shape, size, and orientation.

The values for the appropriate material co-efficients used for calculating the various material parameters are listed in Appendix E.

6. Primary Practical Considerations

6.1. Introduction

In this section some general practical considerations are outlined which, basically, are relevant to any form of acousto-optic device. The methods of bonding piezo-electric platelets to the substrate medium are reviewed and the methods of reducing the thickness of the transducer to its final dimension are discussed. The evaporation of good adhering, conducting films are considered together with the grinding and polishing of the appropriate components and surfaces. Methods of removing the acoustic energy from the delay medium are also considered. These practical aspects are considered in relation to the facilities and the technology that were available in the Department for the subsequent manufacture of acousto-optic devices.

6.2. Bonding Methods and Materials

The problem of bonding acoustic transducers onto a delay medium is one which occurs in the manufacture of ultrasonic delay lines as well as for acousto-optic purposes when piezo-electric platelets are used to excite the bulk acoustic wave. In both cases the bonding layer should be acoustically thin and have negligible effect on the transducers' performance if the layers' acoustic impedance is mismatched to that of the transducer and delay medium. Acoustically thick bonds can be used when the bonding materials' acoustic impedance is closely matched to that of the piezo-layer and substrate. Also the bonding layer should have a good tensile strength and low acoustic loss. One of the advantages of bonded piezo layers over that of evaporated thin film transducers is that their

power handling capability is much greater.

6.2.1. Organic Adhesives

Until recent years the most common bonding materials were viscous greases and oils, inorganic solders, cured materials, and low melting point transparent solids. These materials have been used without difficulty for low frequency applications (below 100 M Hz) and for single high frequency applications. The acoustic impedance mismatch for these materials compared to the transducer and substrate may be as high as 12:1 and for acoustic frequencies above 100 M Hz this means that the bonding layer must be in the order of 0.1 μm . McSkimin (1957) has used a variety of oils and greases to measure the acoustic properties of small samples of materials. Single frequency operation was used for experiments over a wide temperature range. He has also used a silver paste-solder bond for fundamental frequencies up to 60 M Hz. Cured materials such as epoxy resin have been used (Beecham 1969) for frequencies above 100 M Hz. However, careful control from contamination must be observed and 'flat' surfaces must be achieved in order to obtain ultrathin bonds. Chang (1976) has reported using epoxy resin as the bonding medium for use at frequencies up to 160 M Hz without too much difficulty. Low melting point transparent solids have been widely used for bonding purposes. Salol (Phenyl Salicylate) which has a melting point of 43^{o}c has been widely used for acoustic bonding purposes for frequencies of up to 350 M Hz (Maydan 1970). Phenol (Phenyl Benzoate) is another low melting point solid (melting point 71^{o}c) and has acoustic properties similar to Salol. Stilbene (2-diphenyl ethylene), with a melting point of 124^{o}c, is also another suitable bonding material (Obukhovskii et al 1969).

6.2.2. Cold Weld Bonding

Sittig and Cook (1968) have shown that a transducer can be bonded onto the substrate using a cold weld method. They evaporated 10 nm of chromium and then 200 nm of gold onto both the transducer and delay medium ; 200 nm of indium was then deposited onto each of these films and the plated faces were pressed together at room temperature while still under vacuum with a pressure of 'several thousand' p.s.i. Retention of vacuum prevents exposure of the films to the air which would otherwise cause the film surfaces to oxidise and prevent bonding. Warner and Meitzler (1968) have examined the experimental behaviour of transducers operating in the fundamental mode at around 300 M Hz using this type of bond and have reported that the performance using this technique was superior to other forms of bonding. Sittig (1969) has compared the performance of bonds made from epoxy resin to those made using the indium cold weld method. Illustrations of the vacuum arrangement are given as well as for the jigs used for reducing and polishing the transducers to their final thickness. An experimental aluminium-indium bond is reported between lithium niobate and sapphire operating at around 800 M Hz. The applied pressure was between 2000 - 4000 p.s.i. An insertion loss of 10 dB, which was mainly due to diffraction, was achieved. Metals other than indium may also be used such as lead, tin,or germanium - gold alloy (Reeder and Winslow 1969). However, depending on the layers' thickness, their bulk acoustic attenuation may become significant at frequencies above 0.3 G Hz. A review of bonding methods using the indium cold weld technique as well as the low melting point transparent solids has been given by Meitzler (1971).

The cold weld method has been used to produce bonds which do not use indium. Knox (1973) has used gold as the bonding material. By evaporating 20 nm of chromium, 200 nm of aluminium, and then 50 - 100 nm of gold, lithium niobate was bonded onto paratellurite under a pressure of 1200 p.s.i. for a period of about 1 hour. Huang et al (1974) have used an all gold bond to produce a transducer operating at frequencies in the range 1 - 10 G Hz. They have been able to reduce the final thickness of the transducer to 0.25 μm by using the ion milling technique. Chang (1976) has reported to have been able to achieve bonds by using aluminium as the bonding material using the cold weld method. Aluminium is a better acoustic match than gold compared to commonly used substrate and transducer materials and is therefore more preferable.

The optical contact bonding method, which is generally applied for bonding glass samples, has been modified for transducer bonding purposes (Eschler 1976). Electrode layers of gold of not more than 20 nm thick were evaporated onto the very flat and smoothly polished surfaces that were to be bonded. The deposited surfaces were mated under a pressure of 1400 - 3400 p.s.i. and the gold films fused together. The voltage was applied to the thin base electrode by further evaporating a supply electrode 0.5 μm thick around the transducer. The base electrode thickness is limited by the permissible ohmic losses and the bonding method is therefore suitable for low power applications only.

6.2.3. Ultrasonic Bonding

Another method of bonding has been that of welding the two metallized surfaces together ultrasonically. Larson and Winslow (1971)

have bonded transducers using indium, silver, and gold as the bonding materials. By using a static pressure of 2000 - 4000 p.s.i. the piezo layer and substrate were heated to above 100°C in air and a longitudinal ultrasonic wave of 0.4 watts at 18 K Hz frequency was applied for periods between ¼ hour to 2 hours, depending on the materials used. The final reducing of the transducer was achieved by r.f. sputter machining which produced thicknesses down to about 3 μm . A two-way insertion loss of only 6 dB was achieved for barium sodium niobate bonded to sapphire with silver at frequencies around 500 M Hz. Uchida et al (1973) have managed to obtain acoustic wave generation at a centre frequency of 1 G Hz using lithium niobate platelets bonded to quartz using the ultrasonic bonding method and reducing the transducer to a final thickness of 2.5 - 3 μm by means of r.f. sputter machining. A 1.5 dB fractional bandwidth of 0.13 and an insertion loss of 5 dB was achieved. The substrate and transducer were raised to 300°C during the bonding period and the bond material was gold. The bonding of materials at elevated temperatures, however, means that the thermal coefficient of expansion of both materials must be reasonably matched otherwise damage due to thermal stresses may occur.

For the majority of the time in which this work was undertaken the Departments' evaporation plant was out of commission. When re-installed it suffered from the not unexpected teething troubles. Usage, and the running, of the equipment was therefore limited and experimentation and the development of the cold weld method or that of ultrasonic bonding could not be undertaken. This course of action, due to the associated problems, was considered unrealistic here although the cold weld method, to date, is probably the best

method of bonding. The methods of bonding open to the author were thus limited to using epoxy resin or the low melting point solids.

6.3. Film Adhesion

Besides requiring the bond to have a good tensile strength it is also necessary for the deposited metal films to have good adhesion to the surfaces to be bonded. To obtain good adhesion it is usually necessary to first deposit a thin layer of a good adhering metal, about 10 - 50 nm thick. Chromium or titanium are, in general, suitable candidates (Larson and Winslow 1971). The choice is, to some extent, dependent on the substrates and electrode and bonding materials to be used. Chromium is the most often used since it is generally easier to evaporate under vacuum than titanium. However, where silver films are to be used titanium may be a better choice (Sittig 1969). Uchida et al (1973) have used a nickel-chromium alloy for this purpose to ensure adhesion of gold films on lithium niobate and quartz. Alphonse (1975) has suggested that the substitution of molybdenum for chromium may provide better adhesion for films on lead molybdate although chromium has been used elsewhere (Pinnow et al 1969 , Heynau and Bernard 1971).

The adhesion of the top electrode, usually aluminium for a good conducting and good acoustically mismatched film, is sufficient without the need for any prior film since the surface is usually mechanically free.

Throughout this work, where needed, chromium has been used to ensure the adhesion of subsequent films onto the substrates since this could be evaporated without too much difficulty by the evaporation equipments used.

6.4. Transducer Thickness Reduction

As mentioned in section 6.2. final reduction of the thickness of transducers required to operate at frequencies above 300 M Hz may be achieved by processes such as r.f. sputter machining or ion milling. For a 35^{o} rotated Y-cut lithium niobate transducer this means that its thickness at 300 M Hz is about 10 μm . To reduce the transducer to this thickness or for transducer operation below this frequency mechanical lapping methods are employed. The mechanical process entails placing the workpiece in an appropriate jig and then grinding and polishing the whole assembly on a suitable lapping surface until the transducer has been reduced to its required thickness. Precision jigs suitable for this purpose have been discussed and illustrated by Bennett and Wilson (1966), Sittig (1969) and Larson and Winslow (1971). The reduction process starts with an initial transducer thickness anywhere between 1.3 mm (Uchida et al 1973) and 100 μm (Larson and Winslow 1971). The layer is then reduced by lapping either by hand or by machine with the aid of a suitable slurry. An abrasive and a liquid are mixed to form a slurry and the lapping surface is in the form of a flat glass plate or a soft metal surface. The abrasive usually consists of a diamond compound, alumina, or silicon carbide powder. In this manner platelets can be brought down to a thickness in the range of 6 - 10 μm . A final thickness of 2 μm has been achieved using mechanical methods by Wilson (1967).

For this work the reducing process was done with the aid of an existing jig originally designed for polishing purposes. The maximum acoustic centre frequency used in this work was 135 M Hz and consequently the minimum transducer thickness was about 21 μm . The reduction

was therefore done entirely mechanically. The thickness of the lithium niobate slices that could be obtained by sawing from the boule was about 1.5 mm. Thinner slices were liable to crack before the sawing was completed. For the first devices, prior to bonding, the thickness of the platelets were ground down by hand on silicon carbide paper to between 0.7 - 1 mm. For the final devices, however, the material was ground down by hand to a thickness around 300 μm . This was done partly to reduce the amount of material to be removed while the workpiece was attached to the jig and partly because the thinness of the platelet allowed it to be somewhat more flexible and thus take up some of the curvature between the surfaces to be bonded. Platelets thinner than this, however, were too difficult to handle. After bonding the workpiece was attached to the jig and the transducers were lapped down by hand on a flat glass plate to about 100 μm using a slurry of Emery 303 abrasive mixed with water, to 50 μm with Emery 304 abrasive, and down to 21 μm with carborundum powder grade 12000C6 for the higher frequency devices. This was about the minimum thickness that could be obtained using this apparatus, below this the edges of the transducer began to chip and break. Grinding was stopped when the transducer had reached the appropriate thickness and, for the lower frequency devices, the surfaces were finished by briefly grinding with the next finer powder.

Polishing the final surfaces was not attempted. Problems were encountered with the Departments' polishing machine due to vibration and contamination of the polishing laps and it was feared that the layers would be severely damaged if this machine was used. Polishing by hand on a 'Pellon' pad would have caused an unacceptable rounding of the surfaces. The surfaces were thus left with a mat finish

Plate 6.4.1. The grinding jig and adaptor used in fabricating the transducers for the acousto-optic devices.

the granulation of which was a micron or less being negligible compared to the acoustic wave-length. For the lead molybdate devices the clearance of the existing jig was insufficient and an adaptor to obtain this was therefore made. The jig and adaptor are shown in Fig. 6.4.1. The workpiece was placed on an aluminium plate which was screwed to the central column of the jig. The methods of alignment and the measurement of the transducers' thickness are discussed in the sections concerning the devices.

6.5. Polishing Lead Molybdate

Of the materials used in this work the lead molybdate samples were the only ones which required surfaces to be of a good optical finish. Since the crystallographic x and y axes were not easy to ascertain the material was cut so that the sides perpendicular to the plane z = 0 were arbitarily orientated. Due to the shape of the boule it was also necessary to maximize the size of the samples to be cut. Two rectangular solids were obtained from the boule each 1.8 cm x 1.0 cm x 0.9 cm and the smaller end faces were polished. The samples were blocked up with soft flint glass (J. M. Ley, Private communication) fixed together with epoxy resin and the lead molybdate samples were placed in the middle and fixed with paraffin wax (melting point 49^{o}C).

The assembly was then ground down by hand on a flat glass plate using a slurry of Emery 304 abrasive until a good mat finish was obtained. The surface was then polished on a 'Pellon' pad using a slurry of Linde 0.3 alumina abrasive. A flatness to within about a micron could be achieved. During the polishing process it was noticed that small chippings from around the edges of the lead

molybdate were causing scratches to be formed on the polished surfaces. Subsequently,edges of the surfaces were bevelled to try and prevent this. No special precautions were taken to ensure that opposite faces were parallel. This was difficult to achieve by hand polishing and the samples' surfaces were not at all parallel. This was convenient here to some extent since due to the high refractive index considerable reflections occurred at each polished surface and the multi-reflected light was therefore reflected outside the deflection area although some slight distortion of the optical beam may occur due to refracton. Ideally, the surfaces should be optically flat and parallel and the reflection losses reduced by the use of thorium flouride (Thf_4) anti-reflection coatings (Pinnow et al 1969). Although the samples here were polished on a 'Pellon' pad the polished surfaces contained sleeks (J. M. Ley et al 1971), in retrospect, it would have been better to finally polish the specimens on a pitch lap to eliminate these. However, such a suitable lap was not available at the time.

The other four sides to which the transducers and absorbers were to be attached were ground down with carborundum 12000 C6 abrasive on a flat glass plate and left with a mat finish.

6.6. Acoustic Absorbers and Heat Sinks

Broadband acousto-optic deflectors require the use of travelling acoustic waves. Once the sound has propagated through the interaction volume the acoustic energy must be removed from the deflecting medium. Heat produced by the absorption of the acoustic energy within the medium and by acoustic and electrical losses associated with the transducer, electrodes, and bonding layer must also be removed. The sound

energy can be dispersed or absorbed by intercepting the acoustic column with a suitable absorbing medium. The interaction medium is suitably bounded to remove, or at least reduce, the effects due to thermal changes.

In the case of deflectors which use a liquid for the interaction medium a large proportion of the acoustic energy is dissipated within the material as the sound propagates across the optical aperture due to the materials' high acoustic attenuation. The remaining acoustic energy is then dispersed by placing a suitable material in the path of the sound column and deflecting the sound in a direction well outside the bragg angle, thus rendering it harmless with respect to the interaction process. The sound will therefore be essentially absorbed within the liquid. Where the power density of the sound is high the acoustic losses may cause a differential temperature gradient within the liquid and optical spot distortion and displacement of position of the deflected beam will result due to turbulence and non-uniform refractive index variations.

In the case where the interaction medium is a solid it is required that the acoustic wave should propagate through the face opposite that to which the transducer is bonded into a suitable material which acts as the absorber and heat sink. The ratio of the transmitted power to that of the incident power which propagates across the boundary is given by the expression,

$$\frac{P_a \text{ (transmitted)}}{P_a \text{ (incident)}} = \frac{4\, z_1\, z_2}{(z_1 + z_2)^2} \qquad \text{Eq. 6.6.1.}$$

where z_1 and z_2 are the acoustic impedances of the interaction medium and absorbing medium respectively. For the transmission of maximum

acoustic power the acoustic impedance of the absorbing material must be closely matched to that of the interaction medium. The absorber has to be bonded onto the medium and the arguments relating to the bonding of the transducer are equally applicable here. However, the arrangement can be made so that the requirements are less stringent. The two materials can be bonded together with epoxy (Pinnow et al 1969) and the acoustic properties of the bond can be improved by loading the resin with lead, antimony, or silver (Uchida and Niizeki 1973). However, due to the acoustic mismatch of the epoxy some of the energy will inevitably be reflected. The reflected wave can be rendered harmless in a similar way to that in the liquid devices by tilting the boundary at a suitable angle with respect to the transducers' surface. This angle should be at least 5 or 6 times the bragg angle. It is also important that the thermal expansion of the heat sink and interaction medium should be closely matched. The epoxy bond is usually cured at an elevated temperature and the inclusion of thermal stresses in the bond after cooling may otherwise cause damage to the deflecting medium (Coquin et al 1971).

Where excessive heat dissipation occurs within the interaction medium the induced deformations, similar to the case in the liquid deflectors, will cause deformation of the acoustic grating and de-focusing of the optical beam. Coquin et al have measured significant thermal constants of lead molybdate and have estimated the order of magnitude of the resulting effects. Uchida and Niizeki (1973) have examined the temperature distribution in paratellurite deflectors with respect to time and deflection efficiency. Eschler (1976) has examined the thermal behaviour of one-dimensional acousto-optic deflectors for different heat sinking configurations. With slit aperture deflectors additional heat sinks placed on the sides of

the interaction medium were advantageous. Conversely, for symmetrical aperture devices the omission of these heat sinks is desirable. The use of an intermediate material between the transducer and deflecting medium to act as a heat sink and so reduce the effects caused by losses at the transducer was also found to be advantageous.

The method of dispersing the acoustic wave in the water device built during this work was as already described. The absorbers and heat sinks for the lead molybdate devices were aluminium terminations bonded to the sides opposite the transducers (see Section 7.2. and Section 8.5.1.).

The thermal behaviour and methods of heat sinking for solid two-dimensional deflection devices has not been considered in detail here and was an area considered to be beyond the bounds of this present work. The extent to which heat sinking was provided for the experimental devices was subject to the devices' physical state and performance subsequent to the fabrication of their transducers.

7. Experimental Water Cell

7.1. Introduction

The fabrication and performance of a two-dimensional acousto-optic deflector using water as the interaction medium is described in this section. The construction of a device capable of having a capacity in the order of 50 x 50 spots was attempted. The use of a liquid confined the acoustic frequencies to not greater than 50 M Hz due to acoustic attenuation considerations and water was used for this initial device in the hope that the practical aspects, in respect to the fabrication of the transducers, were not too demanding. Taking into consideration the material parameters and the possible transducer bandwidth the resolution may be achieved with an optical aperture of 5 mm and an acoustic bandwidth of at least 15 M Hz with centre frequencies between 22 - 50 M Hz in each dimension. The initial centre frequencies for the horizontal and vertically deflecting transducers were chosen to be 30 M Hz and 45 M Hz respectively although, as will be mentioned, lower frequencies had to suffice. A stepped array for the vertically deflecting transducer was also attempted. The construction of the cell is therefore discussed along with the fabrication of the two transducers and the practical difficulties encountered are outlined. The optical and electrical arrangements are also considered. The performance of the device which could be achieved in practice and its theoretical and potential performance are also compared.

7.2. Cell Construction

The construction of the water cell X - Y deflector is shown in Fig. 7.2.1. The base 1 and back 2 were made of aluminium and the

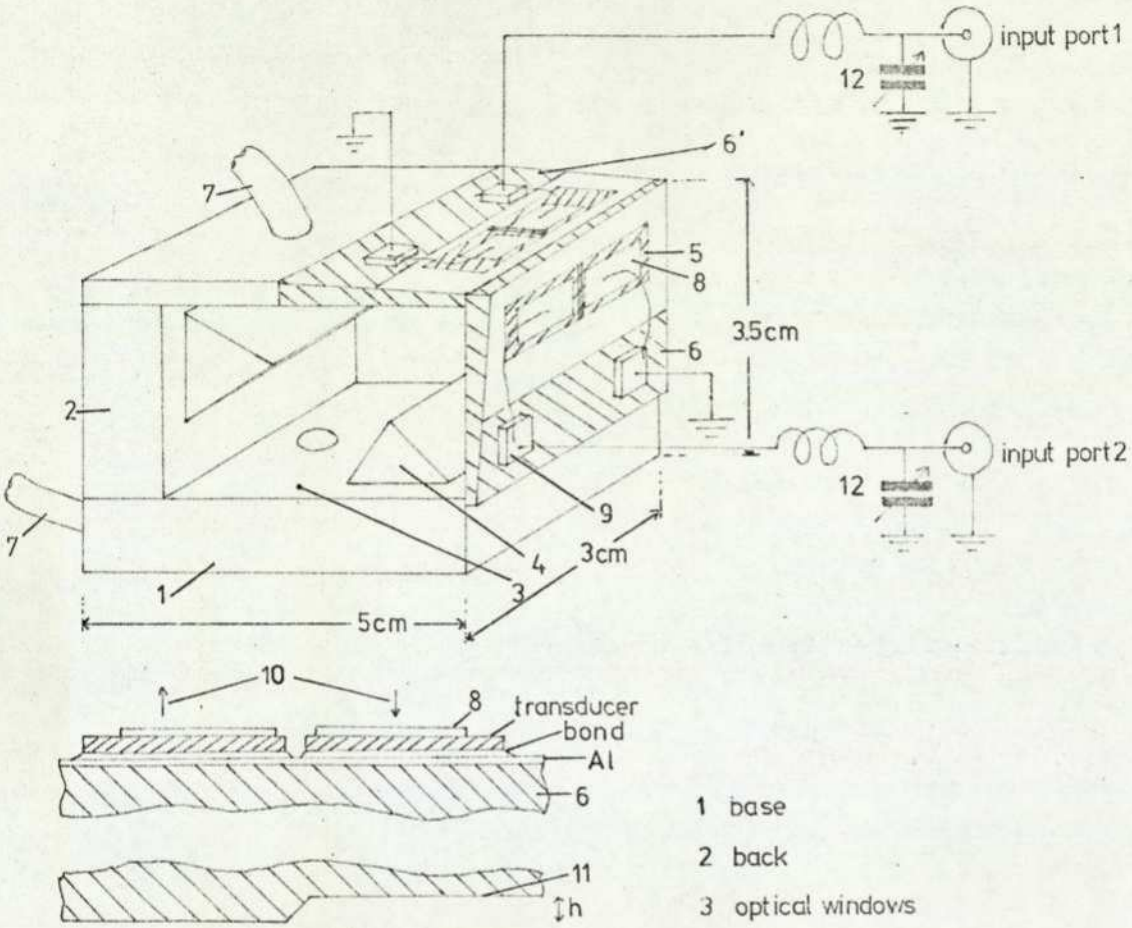

1 base
2 back
3 optical windows
4 perspex wedges
5 transducers
6 glass intermediate medium
7 inlet and outlet
8 top electrode
9 terminals
10 transducer polarisation
11 step in underside of 6'
12 tuning networks

Fig. 7.2.1. Details of the physical construction of the experimental water cell and its' transducers.

optical windows 3 were made from glass. The dispersion of the acoustic energy was achieved using perspex wedges 4. The transducers 5 were mounted onto an intermediate medium 6 of glass to broaden the bandwidth of the transducer response (Korpel et al 1966, Reeder and Winslow 1969). The $LiNbO_3$ transducer in direct contact with the liquid would have resulted in a very narrow bandwidth due to the high acoustic impedance mismatch (Drozhzhin et al 1975). The intermediate medium was wedged in both its length and breadth, by an angle of about 1.2^{o} and 4.6^{o} respectively, so as to destroy the Q of the plate and also to direct unwanted acoustic energy, caused by reflection within the intermediate layer, beyond the bragg angle. An inlet and outlet hole 7 were provided in the base and top of the cell to allow the insertion of the liquid. Electrical contact to the transducers was made by a connecting wire between the top electrode 8 and a $\frac{1}{4}$" square terminal 9 made from copper clad board. The wires were soldered to the terminals and attached to the transducer electrode with silver paste. The whole arrangement was glued together using epoxy resin.

The transducers were divided into two elements to increase the electrical impedance and the directions of polarisation 10 of the plates were inverted with respect to one another so that the resulting acoustic waves generated in the glass medium were in phase. The transducer producing the horizontal deflection was thus a planar array with each element driven in phase and its behaviour corresponds to a single transducer. The transducer associated with the vertical deflection was arranged in a similar way except that a step was formed in the underside of the glass intermediate layer 11 thus making this transducer become a stepped array as discussed in section 3.8.4.

The device was fixed with epoxy resin onto an aluminium chassis

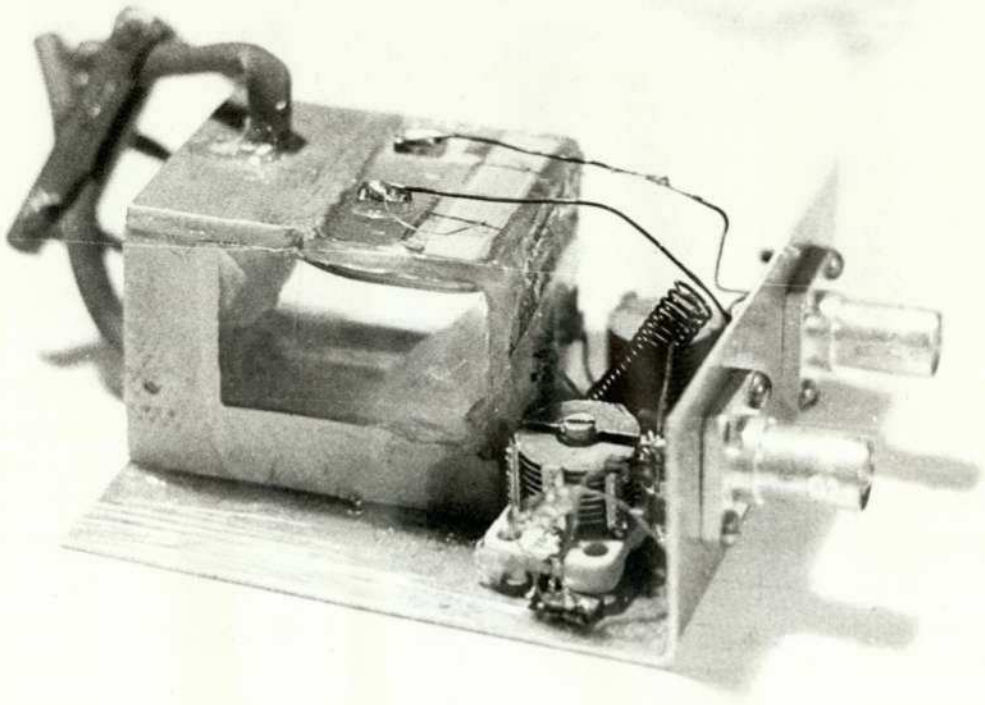

Plate 7.2.1. The experimental water cell two-dimensional deflector.

and, together with the tuning elements 12, connected to two B.N.C. sockets. The complete device is shown in Plate 7.2.1.

7.3. Transducer Fabrication

The intermediate glass layer was wedged by grinding the material down at the appropriate angles on silicon carbide paper and on a flat glass plate. The surface was then polished using the Departments' existing polishing machine. The surface curvature, however, was significant and the flatness was only to within 2 - 3 μm . One side of the $LiNbO_3$ 2 cm x 0.8 cm platelets were also polished to a flatness of about 1.5 μm for later alignment. An aluminium ground electrode about 0.5 μm thick was then evaporated onto the appropriate area of the glass medium. The polished $LiNbO_3$ surfaces were then bonded onto the intermediate layers using epoxy resin (Araldite adhesive AY103, hardner HY 956). The adhesive and hardner were mixed together in the ratio of 5 - 1 by weight or 4 - 1 by volume on a clean glass slide using a clean wire spatula. A drop of the mixture was applied between the surfaces and they were pressed together to allow the epoxy to spread between them. The arrangment was heated to about 60 - 70^{o}c to reduce the viscosity of the epoxy and the surfaces were then pressed together using a hydraulic jig with a pressure equivalent to 1000 p.s.i. (Sittig 1969).

For the side transducer, the glass and $LiNbO_3$ platelet were placed under the hydraulic jig and heated using a hot air blower.

Pressure was then applied with the heating process still maintained. The epoxy was allowed to cure while the pressure was still applied for about 1 hour. The arrangement was then fixed to the jig, aligned (discussed later), and the reducing process followed as discussed in section 6.4. A 2 cm length, 33 M Hz centre frequency transducer,

corresponding to a plate thickness of 100 μm was attempted. The thickness of the plate was monitored by observing the transducers' edges using a travelling microscope. When the transducer had reached a thickness of about 150 μm cracks appeared in its surface and these spread as the reduction continued. The reduction process was consequently stopped when the plate had reached a thickness of 137.5μm $\pm$ 3μm due to the excessive cracking. The cause of this was attributed to mechanical stresses produced in the bond by the presence of the static pressure during the curing period of the epoxy resin.

For fabrication of the top transducer the hot-air blower was not available. The arrangement was thus heated in an oven to the required temperature to reduce the viscosity of the epoxy. The glass medium and transducer were then transferred to the hydraulic jig and the pressure was applied for one minute. The pressure was then released and the bonded materials were returned to the oven to allow the epoxy to cure.. However, the heating rate of the oven was slow and the epoxys' viscosity was not reduced sufficiently to provide a very thin bond. Although reduction of the transducer to about 70 μm , corresponding to a centre frequency of 45 M Hz, was attempted the final average thickness of the platelet was about 85 μm as determined from the impedance measurements. This was a result of the transducer surfaces being non-parallel. However, no apparent damage had occurred to the platelets.

Normally, for the purposes of polishing and grinding, the materials were fixed with paraffin wax to an aluminium base which was subsequently screwed to the central column of the grinding jig (section 6.4.). Since the melting point of the wax (49^{o}c) was less than the epoxy's curing temperature the glass-transducer had to be reattached and aligned with respect to the jig before the reduction process. The arrangement was mounted onto the jig as before and the

top surface of the transducer was aligned by eye to the rim of the jig. The transducers' top surface was then briefly polished so that reflection of light from both the top and bottom surfaces could be achieved. Using a laser and by observing the reflected light from the two surfaces the transducer could be aligned by performing the necessary adjustments to the jig. The jigs' adjustment screws, however, provided an insufficiently fine control and a parallelism of not better than about 1 mR could be achieved. Consequently, the transducers surfaces varied in height over their area by about $\pm$ 10 μm and this method of transducer manufacture using this jig would thus be unsuitable for devices operating at higher frequencies.

Prior to fabrication of the top transducer a step was produced in the underside of the glass medium. From section 3.8.3. and Eq. 3.8.4.6., for an acoustic centre frequency of 45 M Hz and an optical wavelength of 633 nm, with upper and lower bragg frequencies of 51.5 M Hz and 38.5 M Hz respectively for a 1.5 dB reduction in intensity ($K' = 0.3$), a step height of 89 μm was required. By fixing a metal guide in the appropriate position to the glass with epoxy resin the step was produced by grinding the glass medium on the edge of a glass plate with Emery 304 abrasive. No precautions were taken to ensure parallelism with the adjacent surface area. The metal guide was subsequently removed using Dichloromethane to dissolve the epoxy resin. The actual step height, over the appropriate area, was 90 $\pm$ 10 μm measured using a micrometer.

Prior to bonding and evaporating the surfaces in question required cleaning. The materials were placed in a solution of 'Decon Concentrate' for 24 hours and then thoroughly washed with deionised water for $\frac{1}{2}$ hour. The samples were then placed in a desicator containing silica gel and warmed in an oven to dry. Although a more rigorous

method of cleaning may be desirable this method was considered sufficient here.

Finally, aluminium electrodes were vacuum deposited onto the top area of the top transducer of 5 mm width and 2 cm length. Due to the poor condition of the side transducer the top electrode was produced using the silver paste. Evaporation of a top electrode here was not attempted for fear of the top and ground electrodes shorting.

7.4. Optical and Electrical Arrangement

The optical and electrical setup is shown in Fig. 7.4.1. The laser light source (λ = 633 nm) is followed by a beam expanding lens arrangement. The acousto-optic deflector is then included in the optical beam path. The deflector is followed by a telescope arrangement to produce the optical far-field pattern and to magnify the angle of deflection. The resulting image is formed at the detector (Photo-diode or screen).

The two r.f. signal generators are connected to two broadband r.f. power amplifiers (see Appendix F) via the variable attenuators. The r.f. power meter serves to monitor the power delivered to the deflector by each amplifier. The outputs of the amplifiers are then taken to the inputs of the device.

To obtain deflection the r.f. power was applied to the device and vertical and horizontal adjustment, both in position and inclination,was then performed so that the optical beam was positioned within the interaction volume and so that the beam satisfied the bragg angle with respect to each sound column.

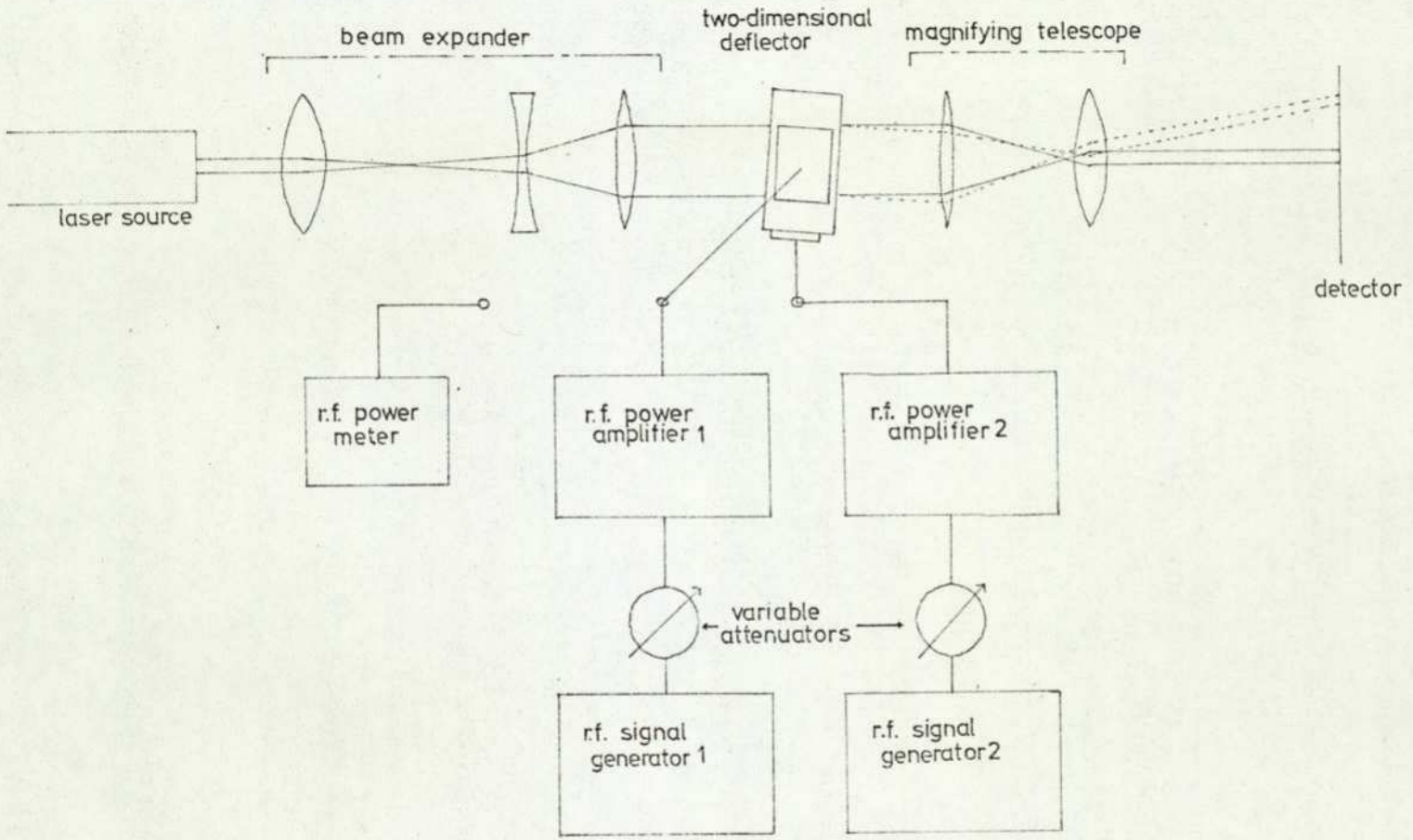

Fig. 7.4.1. Schematic arrangement of the optical and electrical setup.

7.5. Performance

7.5.1. Electrical Response

The theoretical performance of lithium niobate bonded to sheet glass is shown in Fig. 7.5.1.1. The variation of the normalised conductance and capacitance with the frequency-thickness product is shown together with the tuned one-way insertion loss for a transducer matched to the source at the centre frequency. The maximum - 4 dB fractional bandwidth is 0.69 thus requiring a centre frequency greater than 22 M Hz for a bandwidth of 15 M Hz. The choice of the centre frequencies and aperture of the device, as mentioned in the introduction, were thus determined by this requirement.

The measured electrical parameters of each transducer are shown in Fig. 7.5.1.2. and Fig. 7.5.1.3. The conductance and capacitance for each transducer, measured at the copper clad board terminals, vary in a similar fashion to that in Fig. 7.5.1.1. However, the presence of the bond in series with the transducer has reduced the net capacitance and narrowed the peak in the variation of the conductance. The loading of the side transducer by the silver paste top electrode has contributed in broadening its response (Alphonse 1976). The very narrow response of the top transducer is attributed to the suspected 'thick' bond produced and together with the higher frequency operation the attenuation of the bonding material has become significant.

For the measurement of the transducers' electrical properties a Hewlett-Packard 4815A vector impedance meter was used. The values of the capacitances and conductances illustrated were calculated from the measured phase and magnitude of the impedances. This equipment was used for all subsequent electrical measurements for frequencies up to 108 M Hz.

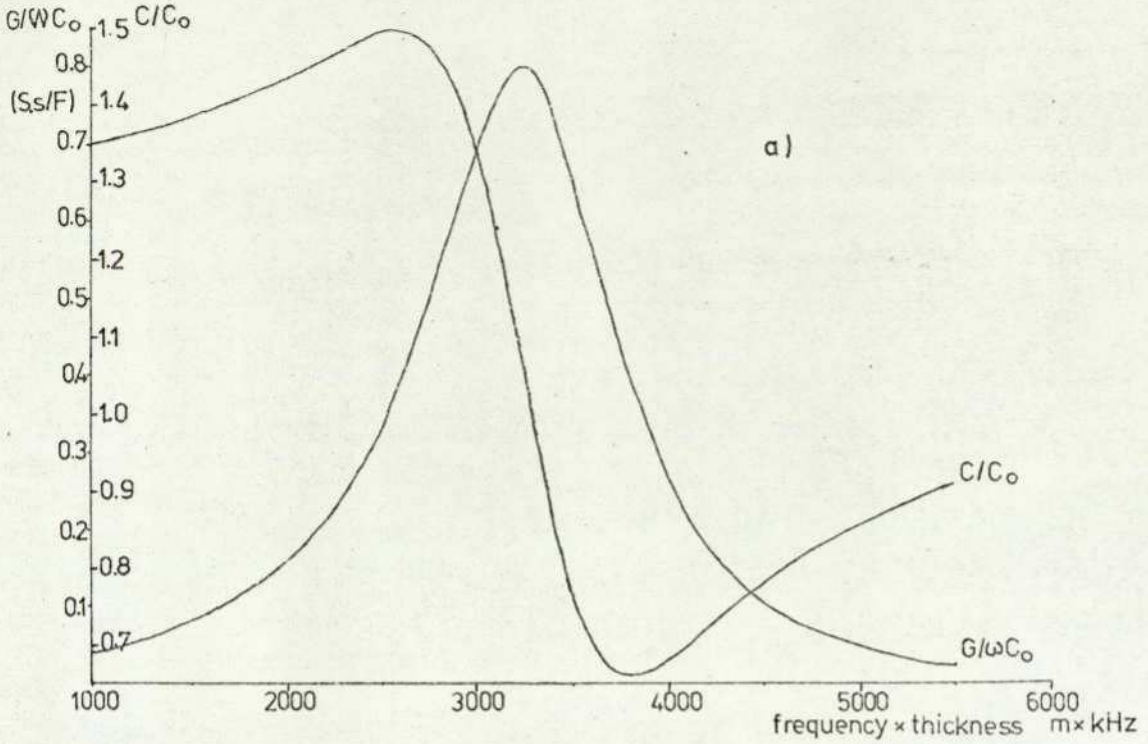

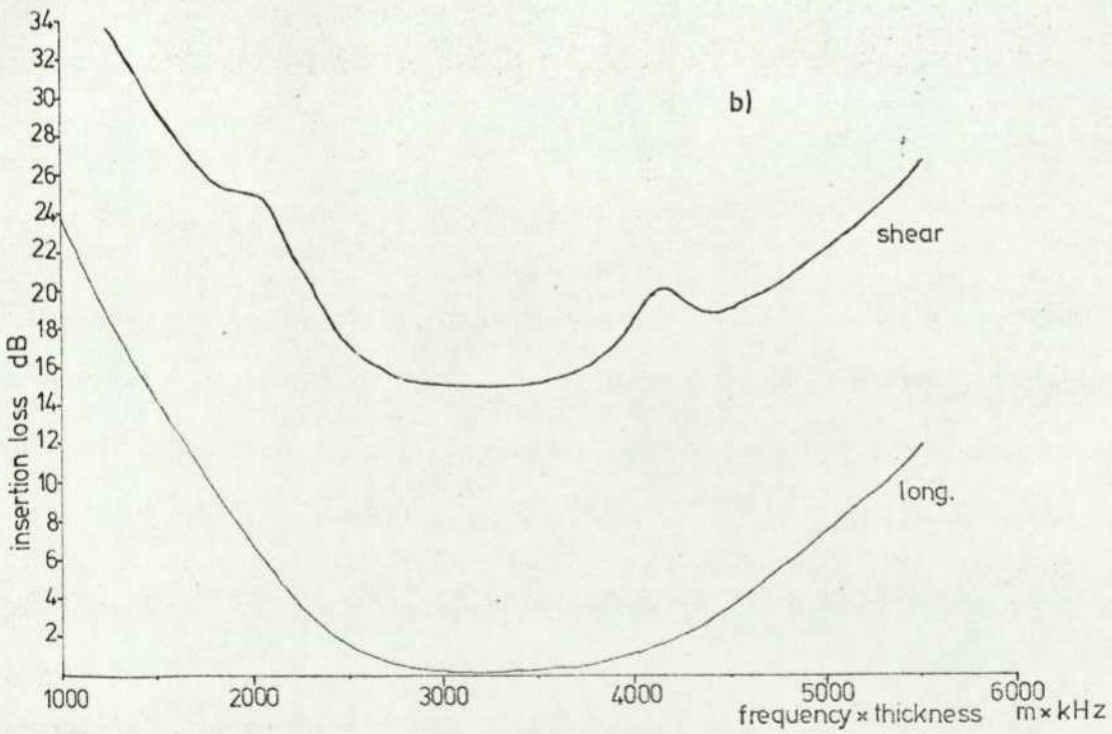

Fig. 7.5.1.1. Theoretical response of 35° y-cut $LiNbO_3$ transducer bonded to sheet glass; a)the normalised electrical properties, b)the tuned one-way insertion loss.

7.5.2. Efficiency

The tuning elements in Fig. 7.2.1. were adjusted experimentally so that at 30.5 M Hz, for the side transducer, and 38 M Hz, for the top transducer, the input impedance to each port was 50 Ω . With the device driven at these frequencies the relative intensity of the zero and first order beams versus applied power in each co-ordinate, with diffraction in the orthogonal dimension equal to zero, is shown in Fig. 7.5.2.1. A 1 mm diameter optical beam was used positioned close to the glass-water boundary. Due to the curvature of the bonded surfaces of the glass and transducer and the subsequent variation in bond thickness, together with the physical condition of the transducers, the efficiency varied across the transducers' width. Fig. 7.5.2.1. shows the deflection efficiency for the optical beam placed in the optimum position. The side transducer was tuned to a higher frequency than the centre frequency to allow deflection to occur even further into the bragg regime.

For the case where the bond is perfect the power required to deflect 50% of the incident light into each first order, including a 4.75 dB loss at the glass-water interface and an estimated loss of 0.4 dB due to attenuation in the glass and water, is 212 mW and 266 mW for the side and top transducers respectively. An applied power of 2.06 W and 0.95 W , corresponding to transducer losses of 9.9 dB and 5.5 dB, was required by the side and top transducer respectively to achieve this percentage deflection. The excessive losses related to the side transducer are a result of acoustic energy lost from the back of the piezo-electric platelets into the silver past electrode and also to dispersion of the wave due to the cracked surfaces, together with the acoustic attenuation of the bond material. The losses associated with the top transducer are mainly due to the attenuation of the epoxy resin bond.

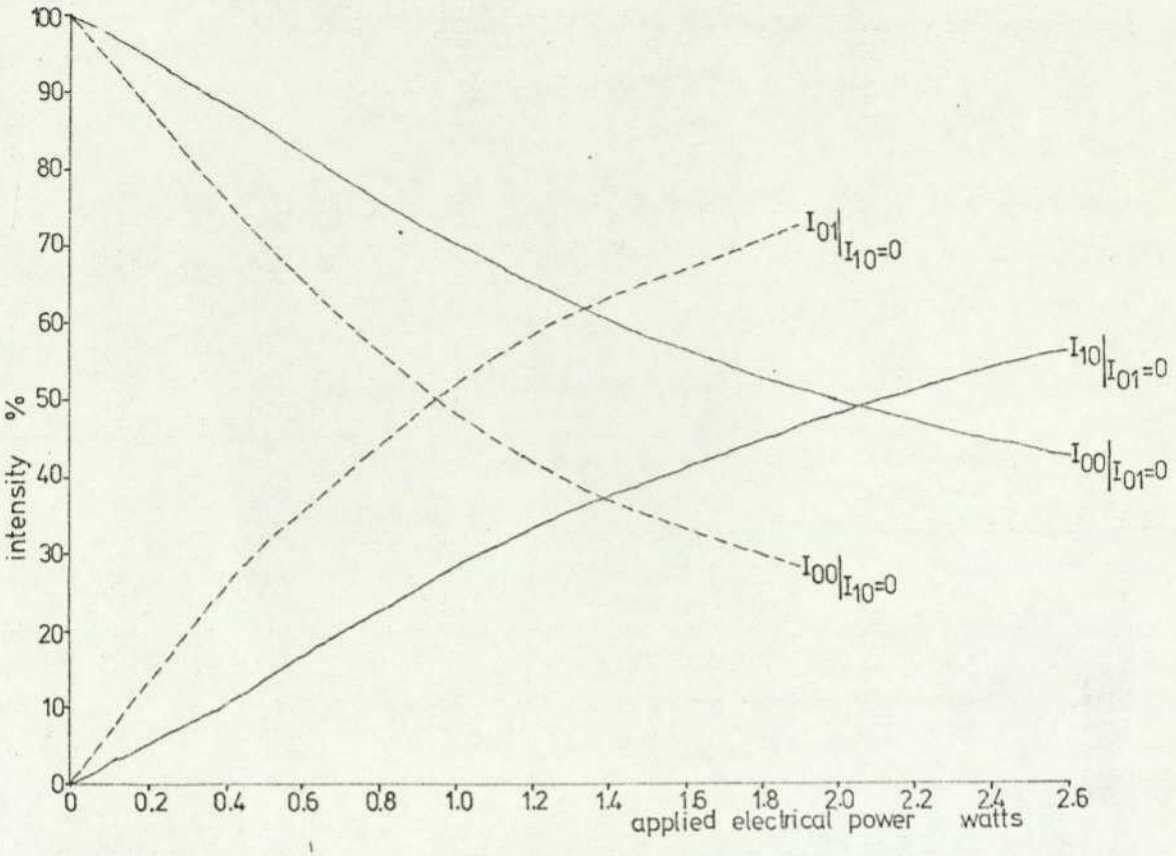

Fig. 7.5.2.1. Variation of the incident and first order beams with applied electrical power for zero deflection in the orthogonal dimension.

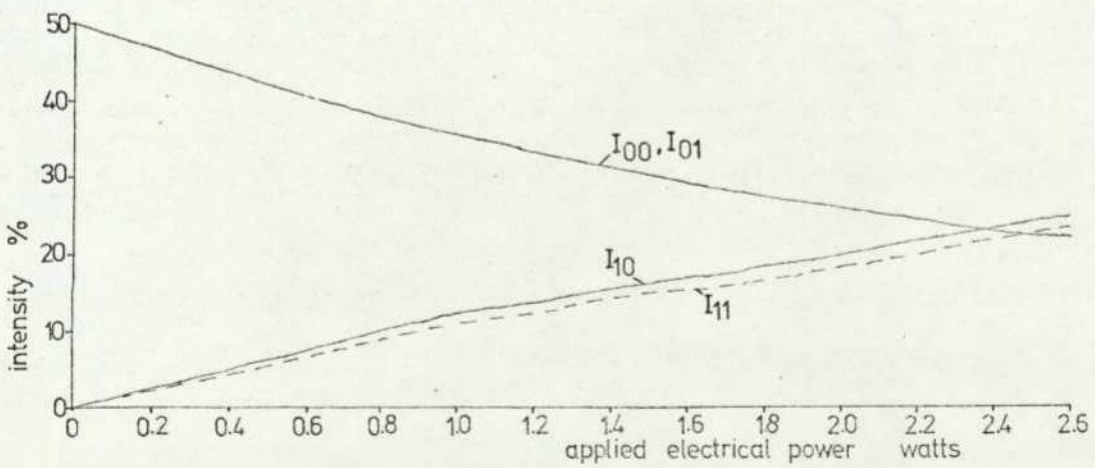

Fig. 7.5.2.2. Variation of the four main orders with applied electrical power to the horizontally deflecting transducer with initial deflection in the vertical dimension of 50%.

For deflection in both co-ordinates the optical beam was re-positioned and the cell adjusted to optimise deflection of light into the composite order. To achieve 50% deflection of light into the vertical co-ordinate an increase of applied power by 1 dB to 1.2 W was required to compensate for the acoustic attenuation of the water. The variation of the orders, I_{00}, I_{01}(vertical), I_{10}(horizontal), and I_{11}, are shown in Fig. 7.5.2.2. in relation to the power applied to the side transducer. To deflect 25% of the incident light into each order an increase in power of 1 dB to 2.6 W to the side transducer was also required due to losses in the water. The application of a total power of up to 3.8 W to the device began to cause turbulence and, together with increased deflection into higher orders, accounts for the slight difference in variation between I_{10} and I_{11}. The heat and turbulence caused by the losses prohibited increased light deflection above this level into the composite order.

7.5.3. Bandwidth

The variation of intensity with frequency for each first order beam is shown in Fig. 7.5.3.1. and Fig. 7.5.3.2.. Also shown are the theoretical bandwidths for each transducer arrangement for comparison. The cell was adjusted so that the horizontal deflection bragg angle was satisfied at 29.5 M Hz. Although lower than the frequency to which the transducer was tuned and higher than the layers' centre frequency this adjustment provided the most satisfactory bandwidth. Modulation of the response has occurred due to interference between multi-directed acoustic waves caused by the piezo layers' non-parallelism (Cohen and Gordon 1966) and also as a result of the cracked surfaces. The non-parallel surfaces have produced, across the optical aperture, a frequency dependent phased array causing

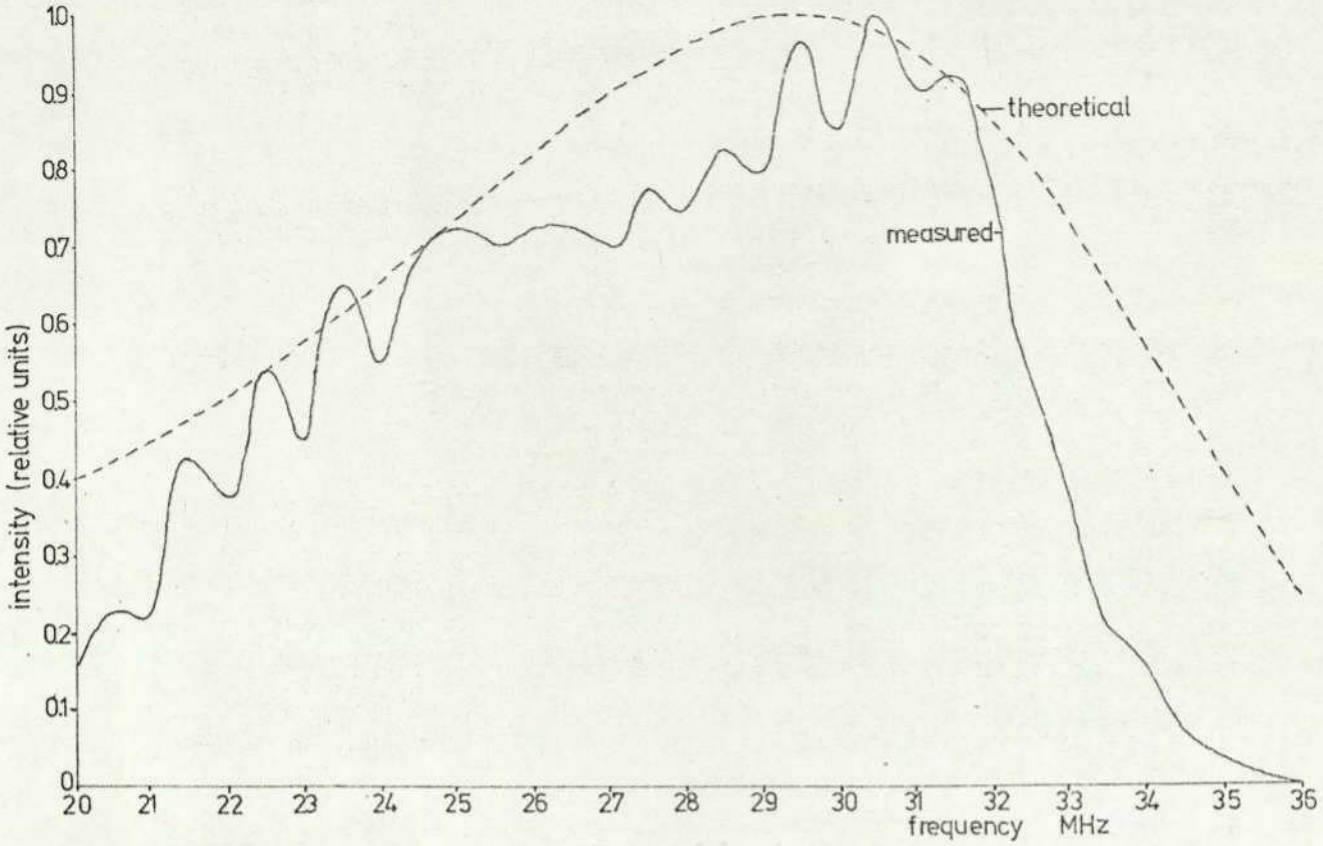

Fig. 7.5.3.1. Theoretical and measured optical bandwidths related to the horizontally deflected order.

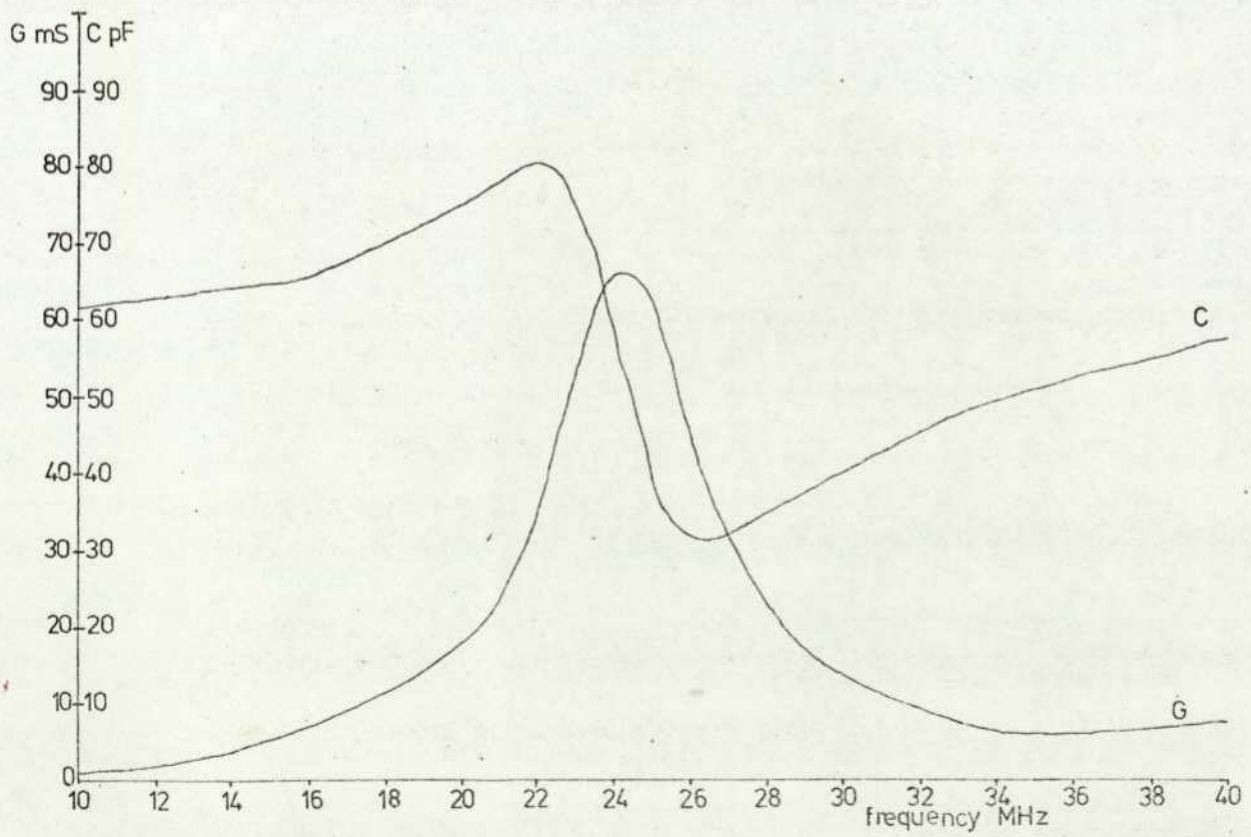

Fig. 7.5.1.2. Electrical response of the transducer associated with the horizontal deflection.

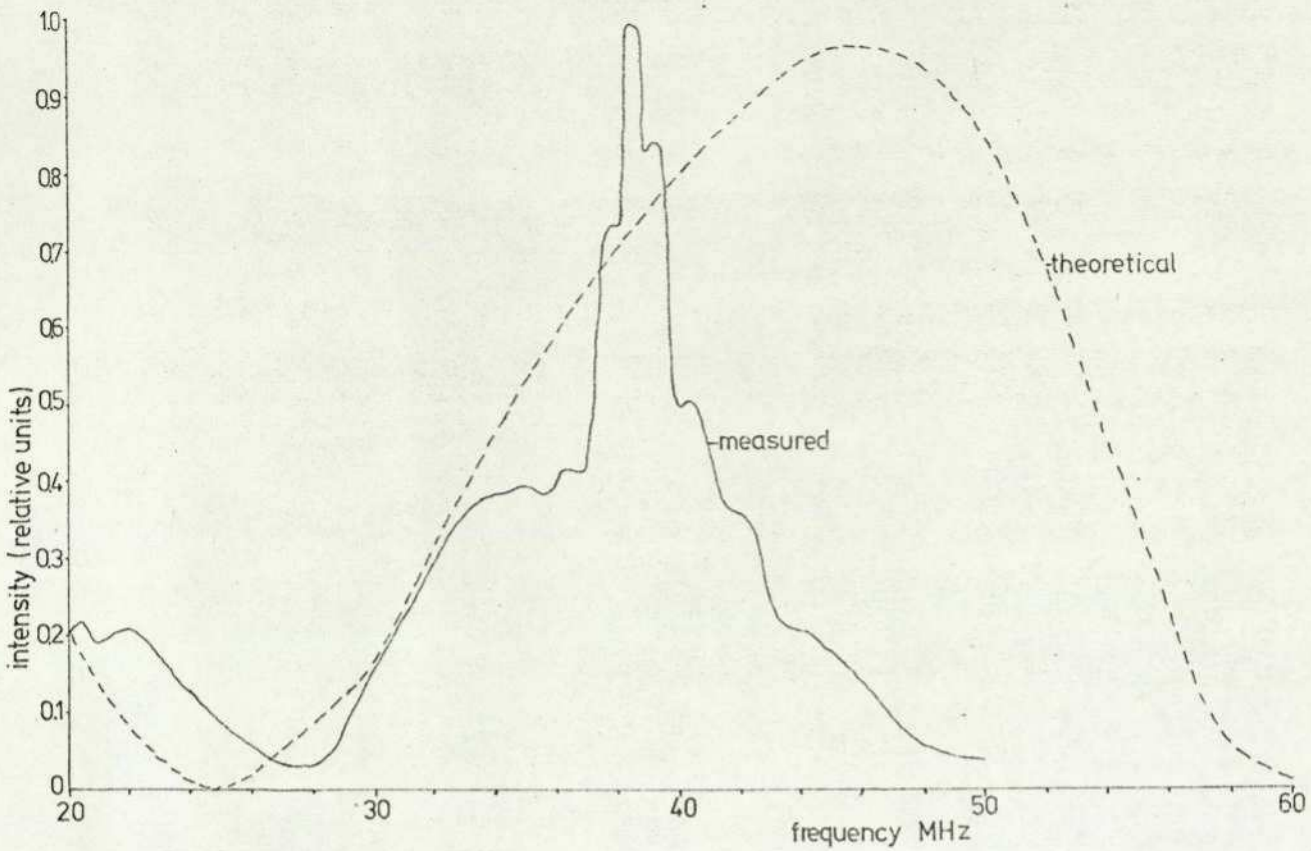

Fig. 7.5.3.2. Theoretical and measured optical bandwidths related to the vertically deflected order.

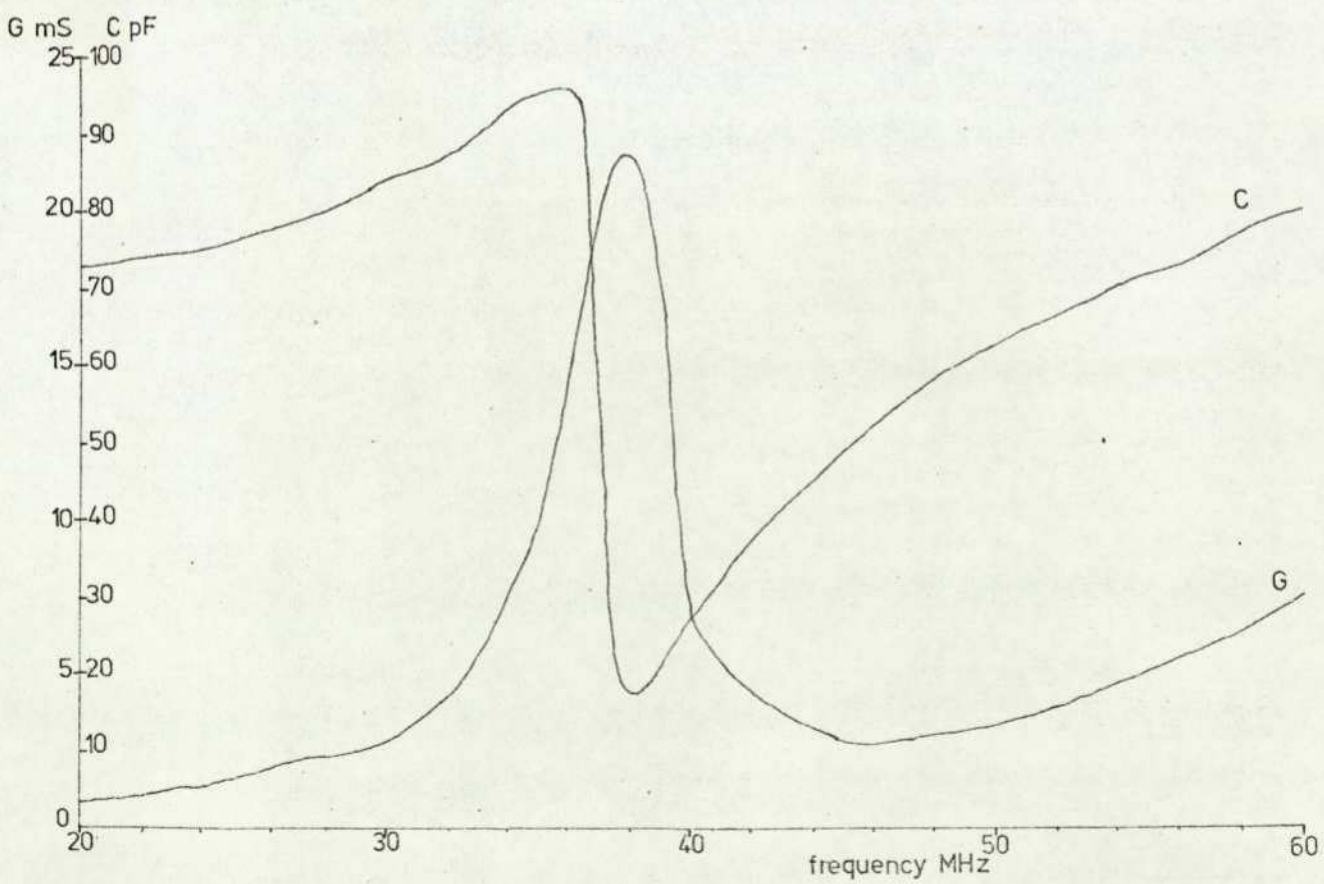

Fig. 7.5.1.3. Electrical response of the transducer associated with the vertical deflection.

constructive and destructive interference of the acoustic energy lobe. The high frequency response reduces sharply as a consequence of the tuning arrangement used (Matthaei 1964). The upper and lower -4 dB frequencies were 33 M Hz and 21.5 M Hz respectively resulting in a bandwidth of 11.5 M Hz.

The interference associated with the side transducer is evident in the response concerning deflection in the vertical co-ordinate. The cell was adjusted so that the bragg angle was satisfied at 38.5 M Hz as this was the lower bragg frequency for the designed transducer geometry. The resulting bandwidth has been severely narrowed by the inclusion of the 'thick' bond and it can be seen to vary in relation to the electrical response (Fig. 7.5.1.3.). The optical bandwidth does, to some extent, begin to follow the theoretical response at the lower frequencies and suggests that the high frequency response has been altered by virtue of the frequency dependence of the bonds' attenuation (Pinnow 1970) and possible electrical losses. The bandwidth achieved was 7.2 M Hz with upper and lower -4 dB frequencies of 41.2 M Hz and 34 M Hz respectively.

It is pointed out that the intensity variation of the composite order will vary by an amount of up to -8 dB when the vertical and horizontal transducers are driven between the frequency limits mentioned.

7.5.4. Display

The resulting display produced by the device is shown in Plate 7.5.4.1. for an incident optical beam diameter of 1 mm. The transducers were driven at their tuned frequencies with a power of about 1 watt. The deflection of light into the composite order only for operation of the device well within the bragg regime can clearly

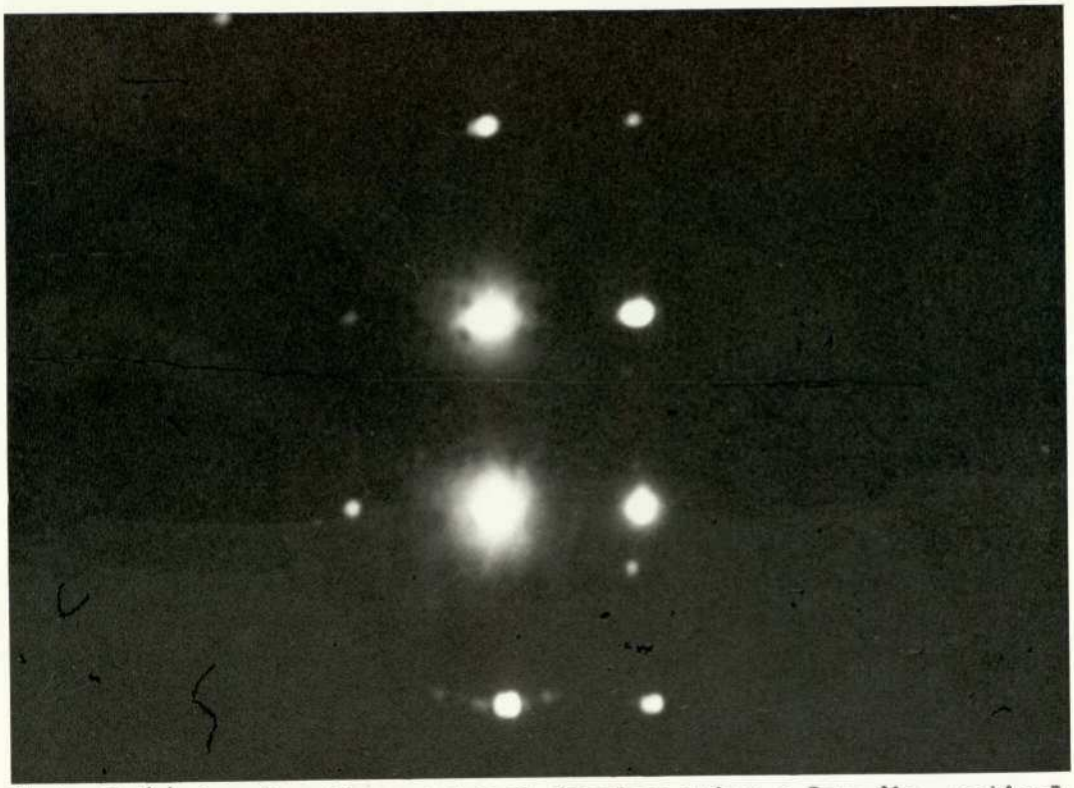

Plate 7.5.4.1. Resulting optical display using a 1mm dia. optical beam. Power to each transducer is 1 watt. The bragg condition is satisfied in each coordinate. The largest spot, due to over-exposure, is the incident order.

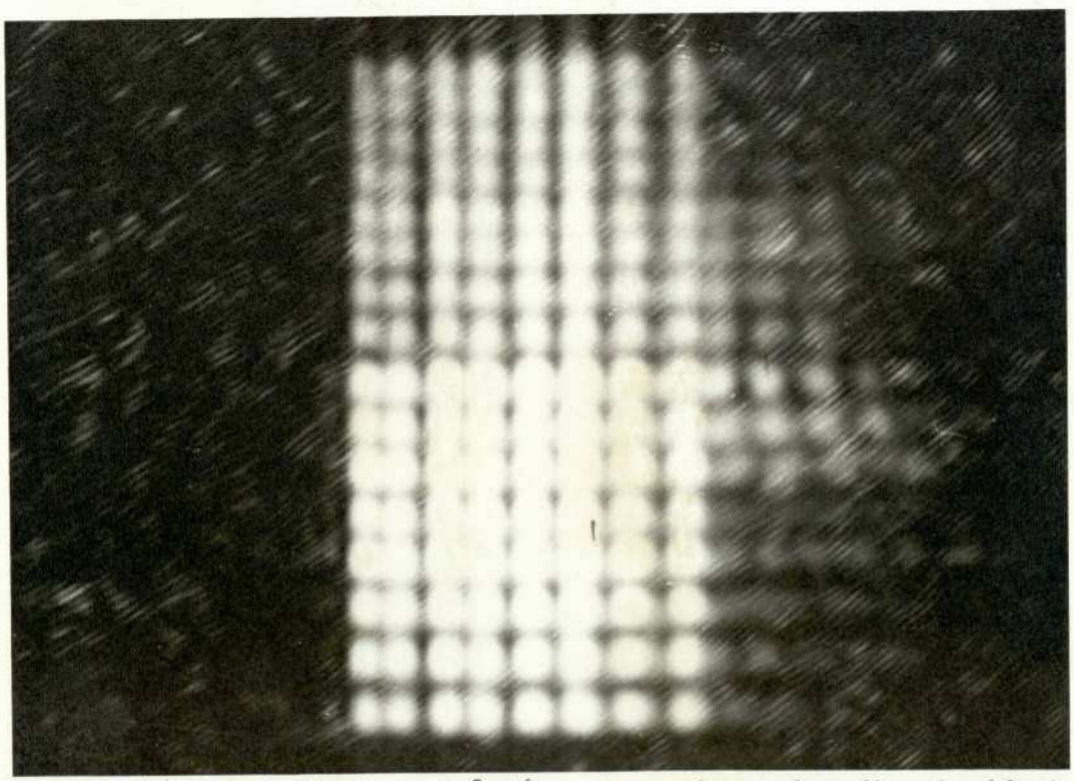

Plate 7.5.4.2. A display of 8x16 spots, using a 3mm dia. incident optical beam, by the composite order.

be seen. Although a significant deflection of light appears to have occurred into the 2nd and -1st order in the vertical co-ordiante this is misleading and is due to the γ function of the photographic film. However, it can be seen that deflection into higher composite orders will occur if the interaction approaches the Raman-Nath regime. The vertical deflection -1st order is also accompanied by some light scattered by the multi-directed waves produced by the top transducer.

With the optical beam width increased to approximately 3 mm the display shown in Plate 7.5.4.2. was achieved. Two stepped frequency generators (see Appendix G) which were originally designed for use at high frequencies (f > 100 M Hz) were briefly modified to operate within the range of frequencies required for this device. Without serious modification to the generators a display of 16 x 8 spots was produced to demonstrate the X-Y control of the composite order. To the right of the display deflection due to the multi-directed acoustic wavefront is in evidence here also. The operating frequency ranges in the horizontal and vertical directions were approximately 4.5 M Hz and 9 M Hz respectively and the spot period was about 17μs / spot. Although the frequency range used in the Y direction was greater than the -4 dB bandwidth the generator output was not linear over the range and has compensated for the otherwise limited response. The distinct drop in intensity of the upper half of the display is due to the generator output.

Suitable sweep generators were not available at the time to demonstrate the entire capacity of the device although a total of 38 x 24 spot resolution could have been expected using a full 5 mm optical aperture.

8. Methods and Experiments Pertaining to the Realisation of a Two-Dimensional Acousto-optic Deflector using Lead Molybdate and the Consequent Performance of Such a Device

8.1. Introduction

In section 7 the performance of the water cell device was dependent upon the quality of the bonding process and the subsequent fabrication of the transducers. Where the interaction medium is a solid material the higher frequency operation demands that the quality of these processes is even greater. It was therefore necessary to develop, as far as possible, procedures for obtaining satisfactory bonding and transducer fabrication. Before discussing the two lead molybdate devices that were constructed the attempts at trying to achieve success regarding this aspect are first considered. The authors' attempts at trying to produce a metallic bond, albeit unsuccessful, are described. The performance of a transducer bonded with epoxy and with phenyl salicylate are also discussed and compared.

Of the lead molybdate devices constructed one used epoxy resin as the bonding material and the other used phenyl salicylate. The construction and performance of each device is described. Using this material a capacity of up to 200 x 200 spot resolution can be anticipated for the size of material available and for a transducer centre frequency of less than 200 M Hz. The device using epoxy as the bonding material is herein after referred to as Deflector 1 and the other device as Deflector 2.

8.2. Attempted Metallic Bonding

An attempt was made at trying to achieve a bond using a low melting-point metal as the bonding medium. The materials to be bonded

were a 35^{o} rotated Y-cut $LiNbO_3$ transducer and a delay medium of X-cut $LiNbO_3$. Subsequent to the evaporation of approximately 20 nm of chromium a 0.5 μm film of gold was evaporated onto the surfaces to be bonded. The evaporation equipment was then brought to atmospheric pressure and solder (plumbers) was then placed in the vacuum chamber. Being a tin alloy and having a farily low melting point, as well as being a soft material, this was considered to be a reasonable substitute for indium. The use of tin in place of indium has been suggested by Reeder and Winslow (1969). With the chamber pressure reduced to 10^{-6} torr a 0.6 μm film of solder was then deposited onto the surfaces. With the vacuum chamber brought to atmospheric pressure the samples were then removed from the chamber and the two surfaces brought into contact with each other.

With the two materials placed in the hydraulic rig, and with a polished aluminium plate placed on top of the transducer, a pressure equivalent to 2000 p.s.i. was applied. Connected between the aluminium plate and the evaporated electrode was the output of a r.f. amplifier driven, untuned, at a frequency corresponding to the centre frequency of the $LiNbO_3$ platelet thus using the platelet to simulate the ultrasonic bonding method. The voltage across the transducer was about 5 Volts r.m.s. The arrangment was also warmed using a hot-air blower to about 40 - 50^{o}c and was left for a period of about one hour.

Adhesion between the two surfaces appeared to have been achieved. The transducer was further secured by applying a small amount of epoxy around its edges. The arrangement was then attached to the grinding jig and the grinding process proceeded with. However, by the time the transducer thickness had reduced to 150 μm slurry could be seen to flow under the transducer and the grinding process was

stopped. Upon dissection it was found that although the two solder films had adhered the chromium film which was originally fixed to the transducer had become completely detached.

On a subsequent attempt about 0.85 μm of solder was vacuum deposited onto the surfaces and they were left under pressure for a period of two hours. During the process the transducer had cracked, however, and upon examination of the bond the chromium film originally fixed to the X-cut $LiNbO_3$ delay medium had become detached. The two solder films, however, appeared to have bonded together.

Due to the problems associated with the vacuum plant and the physical environment this line of approach was discontinued. However, the fact that adhesion of the films was achieved suggests that bonding by this method may be realisable. The poor adhesion of the chromium to the surfaces may be related to their cleanliness. However, a fellow colleague found that titanium films evaporated from the systems' electron gun facility were contaminated (M.F. Ahmed- Private Communication) and consequently the chromium films evaporated here using this same facility may have also been contaminated. The evaporation of chromium from plated tungsten rods onto previously cleaned surfaces appeared to have adhered well and would suggest that cleanliness was not entirely responsible for the bond failure although the method of cleaning, as described in Section 7.3., may not have been entirely adequate here.

It was hoped to attempt this method of bonding near room temperature and within a vacuum. Due to the inconsistent functioning of the vacuum plant available this course was abandoned.

8.3. Comparison between Epoxy Resin Bonding and Phenyl Salicylate Bonding

Limited to the above mentioned bonding materials the behaviour of a transducer bonded with each material is examined and its performance,

together with the bonds' properties, are illustrated.

8.3.1. Epoxy Resin Bonding

In the construction of the water cell the epoxy bond was included in the electrical circuit of the transducer. For the manufacture of transducers requiring separate elements the bonds' inclusion will be a necessity. The electrical behaviour of the epoxy resin used in this work was therefore examined. Two polished plates, one of copper and the other of aluminium, were bonded together and the electrical behaviour of this 'capacitor' was measured over the frequency range 1 - 108 M Hz. The two plates were placed together with a small amount of the resin between them and the arrangement was placed in an oven heated to 50 - 60^{o}c to cure the epoxy. The thickness of the bond was measured by breaking the two plates apart and observing the epoxy layer edges with a travelling microscope subsequent to the measurements. The variation of the dielectric constant and the loss tangent for four different thicknesses is shown in Fig. 8.3.1.1. and Fig. 8.3.1.2. respectively. The two thicker layers, 63 μm and 35 μm , were measured as described and the two thinner layers, 21 μm and 11.5 μm , were estimated both from optical and electrical measurements.

In the frequency range 10 - 45 M Hz the relative permittivity has a value of approximately 4 and the loss tangent has a minimum between 0.1 - 0.3. Above 50 M Hz the loss tangent increases rapidly and the value of the permittivity changes. The behaviour of each quantity is dependent upon the thickness of the bond layer. Although variations in the adhesive-hardner ratio may have produced some effect the properties of the epoxy may have altered near the metal surfaces due to its chemical reaction with those materials and would account for the rapid increase in the loss tangent and the increased variation in the permittivity with the reduced thickness. At higher frequencies

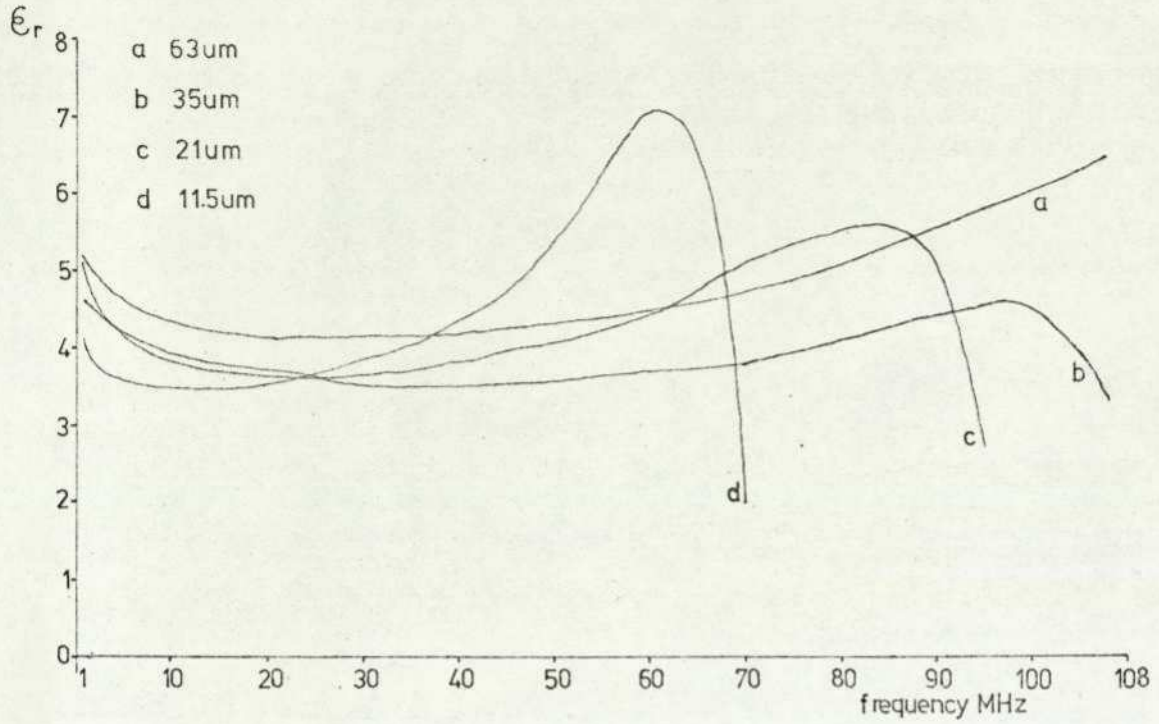

Fig. 8.3.1.1. Relative permittivity versus frequency of the epoxy resin used (Araldite adhesive AY103, hardener HY956) for various thicknesses between an aluminium and copper plate.

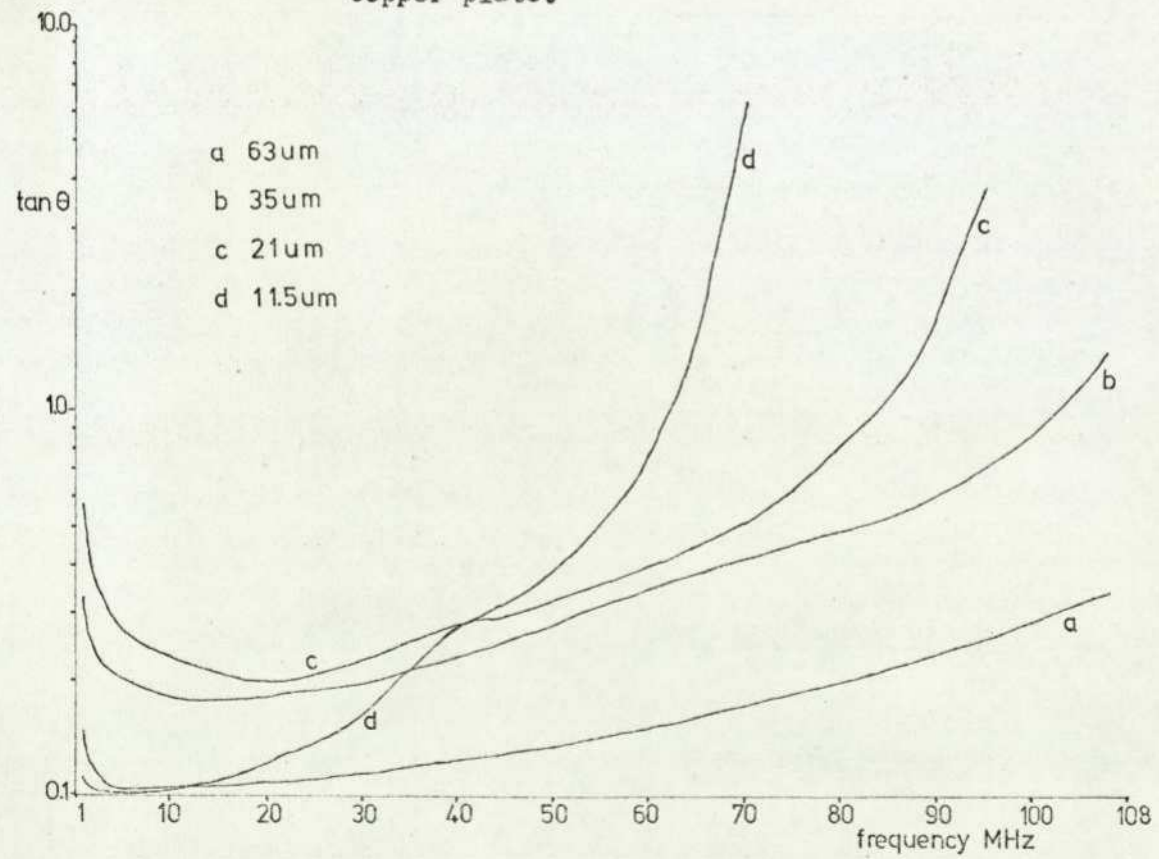

Fig. 8.3.1.2. Corresponding variation in loss tangent with frequency of the epoxy resin for the various thicknesses.

the permittivity became negative and the behaviour of the arrangment was therefore inductive due to possible absorbtion resonance.

To examine the acoustic behaviour of the epoxy bond a single-dimensional acousto-optic deflector was constructed using an unknown sample of soft flint glass as the interaction medium. Here, a 0.95 μm layer of silver was deposited onto the delay medium and a single 15 mm x 5 mm transducer platelet. However, the evaporation process produced conglomerations on the silver films and, without wishing to delay matters by re-evaporating the films, these had to be subsequently cleaned up. This was achieved by removing the particles with a razor and smoothed by gently rubbing the surfaces on a dry tissue. In view of the state of the films the bonding pressure was limited to about 100 p.s.i. The method of manufacture was similar to that described in section 8.5.2. and the transducer was reduced (section 6.4.) to a thickness of 60 μm . It was evident at this thickness that the particles in the deposited films had not been entirely removed since non-parallelism of the transducer surfaces could readily be observed. Two aluminium electrodes, 6.5 mm x 2 mm and 0.2 μm thick, were evaporated onto the top of the transducer so that the final arrangement represented a two-element planar array (section 3.8.2.).

This construction eliminated the epoxy bond from the electrical circuit. The measured electrical performance of the transducer is shown in Fig. 8.3.1.3. For compairson there is also shown the theoretical response of a 35^{o} rotated Y-cut $LiNbO_3$ transducer with epoxy resin as the delay medium. Although the transducer was bonded to a glass delay medium the platelet essentially 'sees' a delay medium of epoxy resin due to the bonds' high value of acoustic attenuation. Between a thickness-frequency product of 3340 and 3660 the permittivity becomes negative and the transducer thus becomes inductive. The plate has a

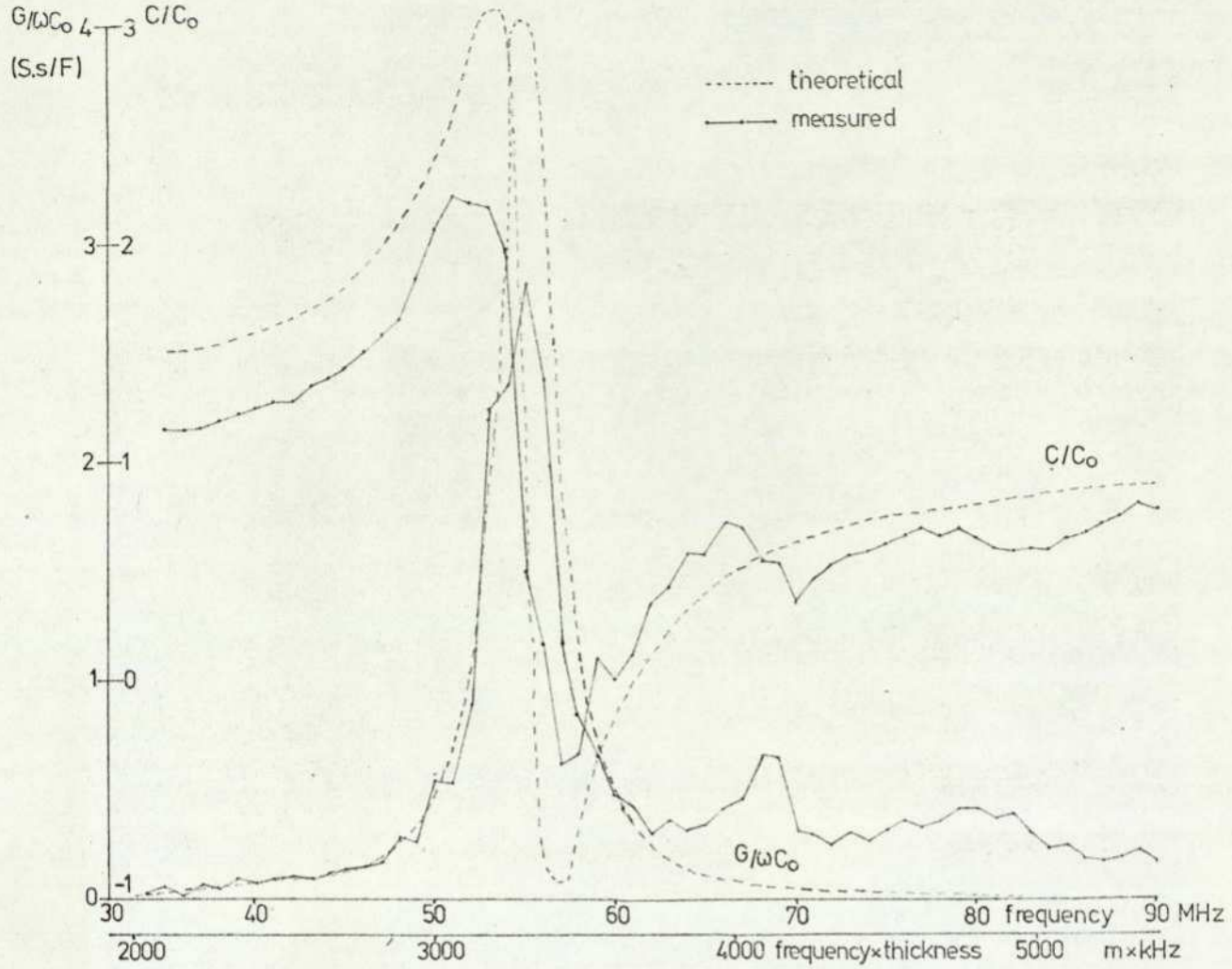

Fig. 8.3.1.3. Theoretical electrical response of 35° y-cut $LiNbO_3$ transducer bonded to epoxy and measured response of a transducer epoxy bonded to glass.

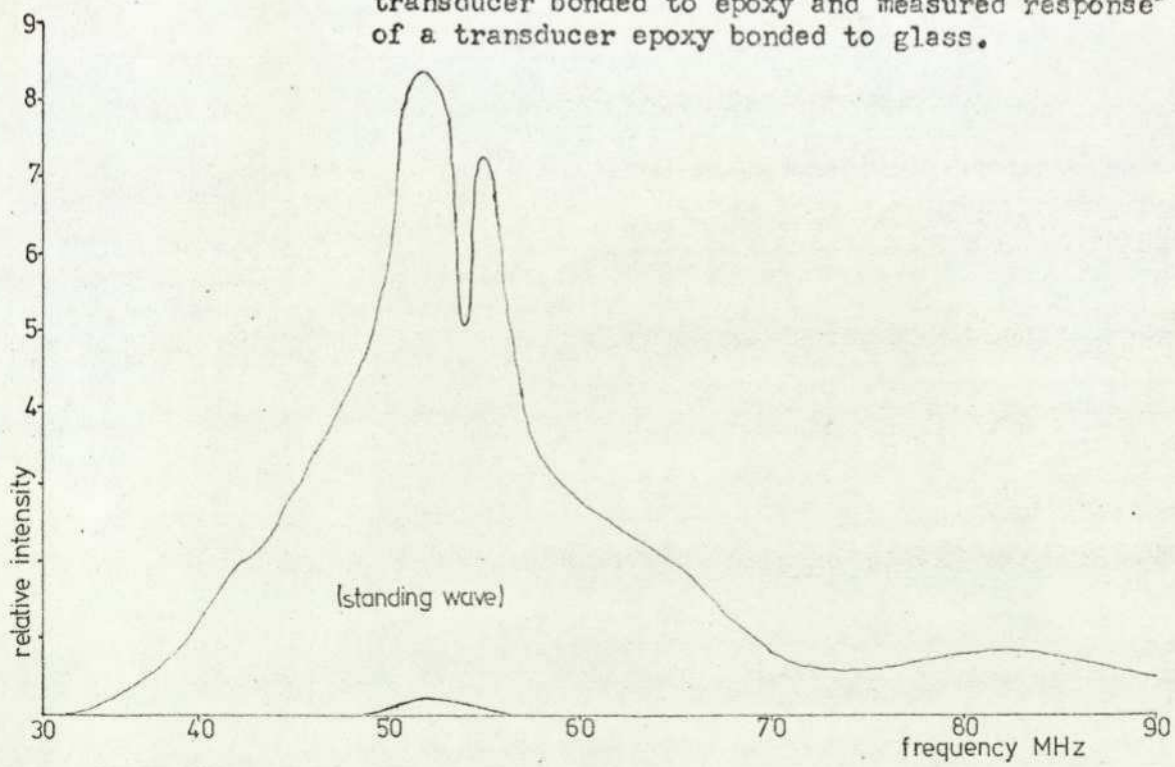

Fig. 8.3.1.4. Envelope of the intensity of the deflected first order with frequency of the device with the epoxy bonded transducer.

pure conductance at these two frequencies. The high measured value of conductance at the higher frequencies is due to the non-parallelism of the plate and indicates that resonance has occurred over areas of the transducer which are of a smaller thickness than the average value.

The optical performance, using a He-Ne 633 nm wavelength laser, is shown in Fig. 8.3.1.4. Within the glass medium, although terminated with an aluminium heat sink, a standing wave existed and the envelope of the response is transducer limited. The curvature between the bonded surfaces was such that the effective acoustic column length inside the glass is no longer the same as that of the transducers' top electrode. The bonds' attenuation has reduced the effective interaction length and the sound intensity varies along the length. The deflection was such that the interaction was essentially within the Raman-Nath regime and, together with the acoustic losses, the peak deflected light with an applied power of 3 Watts driven untuned at the centre frequency was only 4%.

The electrical and acoustic performance of the epoxy bond measured here indicates that the use of this bonding material at higher frequencies would be undesirable unless the bond thickness can be made ultra-thin i.e. $\simeq 0.1\mu m$. The characteristics here give a clear indication of the behaviour of the water cell transducers discussed in section 7. Electrical losses due to the evaporated films are essentially negligible. A single-dimensional water cell device using aluminium as the intermediate medium and epoxy as the bonding material constructed by D. K. K. Wong (1977) supervised by the author still had an insertion loss of approximately 4 dB at 30 M Hz. The estimated attenuation constant for the epoxy used here is thus in the order of 10^7 dB / cm G Hz^2. Although the use of an alternative grade of epoxy may have improved matters it was considered that the advantage would be negligible if the bonding thickness using the existing epoxy could

not to be made ultrathin and the curvature of the surfaces to be bonded reduced.

8.3.2. Phenyl Salicylate Bonding

The alternative method of bonding open to the author was the use of the low melting point solids. Phenyl Salicylate (Salol) was chosen for its lowest melting point (43^{o}C) to minimize problems due to thermal effects caused while bonding. To examine the behaviour of a device using this material for bonding a similar device to that used to examine the epoxy resin bond was constructed. The interaction medium was a similar piece of soft flint glass also terminated with an aluminium heat sink. An aluminium film, approximately 0.5 μm thick, was evaporated onto the transducer surface only and the flint glass surface was ground flat (section 6.4.). The two surfaces were placed together under a pressure of approximately 100 p.s.i. The 'salol' crystals were placed around the edges of the transducer and the arrangement was heated to $55^{o}C$ in an oven. The bond is formed by the 'salol' seeping between the two surfaces by capillary action (Sullivan 1962). The assembly was left to cool for a period of about 2 hours for the cement to harden. Using this procedure the salol does not harden immediately below the melting point but only when the arrangement has been cooled to room temperature for some time. This virtually eliminates any induced stresses produced during the bonding using an elevated temperature. The transducer was fabricated and reduced, as discussed in section 6.4. and section 8, to a thickness of 42 μm . The top electrode, although of similar dimensions, was made using silver paste. Evaporation of aluminium or tin electrodes could not be achieved since the heat produced within the vacuum chamber was sufficient to melt the bond.

The electrical response of the transducer is shown in Fig. 8.3.2.1. Similar to the epoxy resin device a standing wave existed within the glass medium and this factor is evident in the impedance measurements. The normalized conductance and capacitance, measured point by point, clearly show this. Also shown is the average variation of the electrical properties. The response, although affected by the bonds attenuation and the loading of the silver paste, is considerably broader over this frequency range and is an improvement compared to the epoxy resin device. The effect of the standing wave on the impedance suggests that the acoustic losses of the bond are considerably lower than that of the epoxy resin bond.

The optical bandwidth shown in Fig. 8.3.2.2. re-affirms the improved performance of the device using this bonding material. The envelope of the standing wave response is shown and the device was operational over a fractional bandwidth of 0.6 tuned to a centre frequency of 81 M Hz. The reduced losses improved the effective interaction length and the device was able to operate well within the bragg regime.

The efficiency of the device has also been improved over that of the epoxy resin device. A peak deflection of 14% of the incident light from a He-Ne laser was achieved with the application of 3 watts pulsed electrical power. For continuous operation, however, the device could be operated with no more than 0.5 - 0.75 watts, corresponding to a power density of 2 - 3 watts / cm^2. Heating, due to the acoustic losses of the bond and acoustic energy absorbed by the silver paste electrodes, was sufficient to temporarily melt the cement. Degradation in performance, after allowing the cement to reset, was not noticeable.

Although an improved performance is achieved using 'salol' as the bonding medium the temperature dependence of the material does not permit the evaporation of a top electrode and limits the maximum power

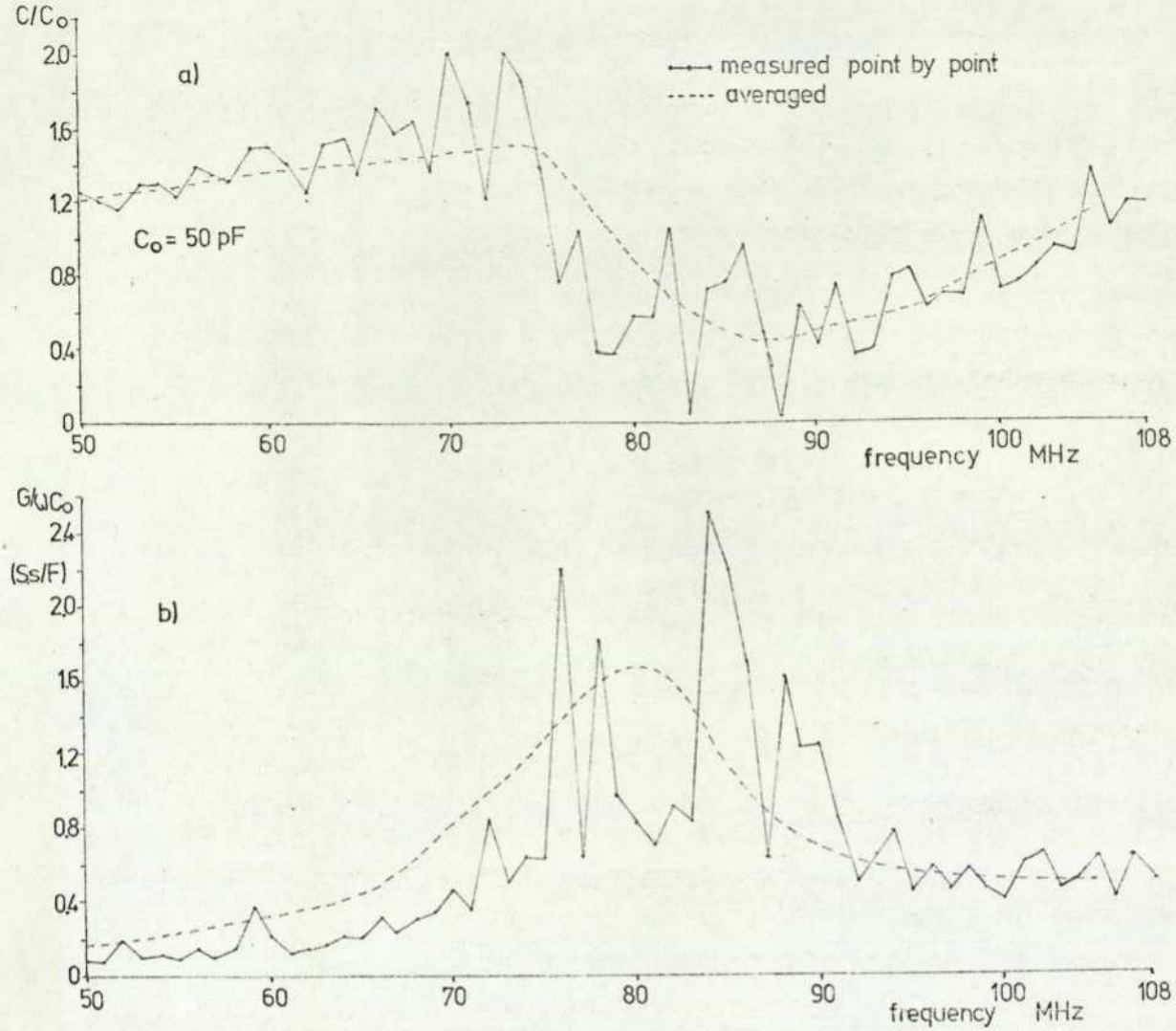

Fig. 8.3.2.1. Measured electrical performance of 'salol' bonded 35° y-cut $LiNbO_3$ transducer on glass. The averaged values illustrate the trend of the properties. a) the normalised capacitance, b) the normalised conductance.

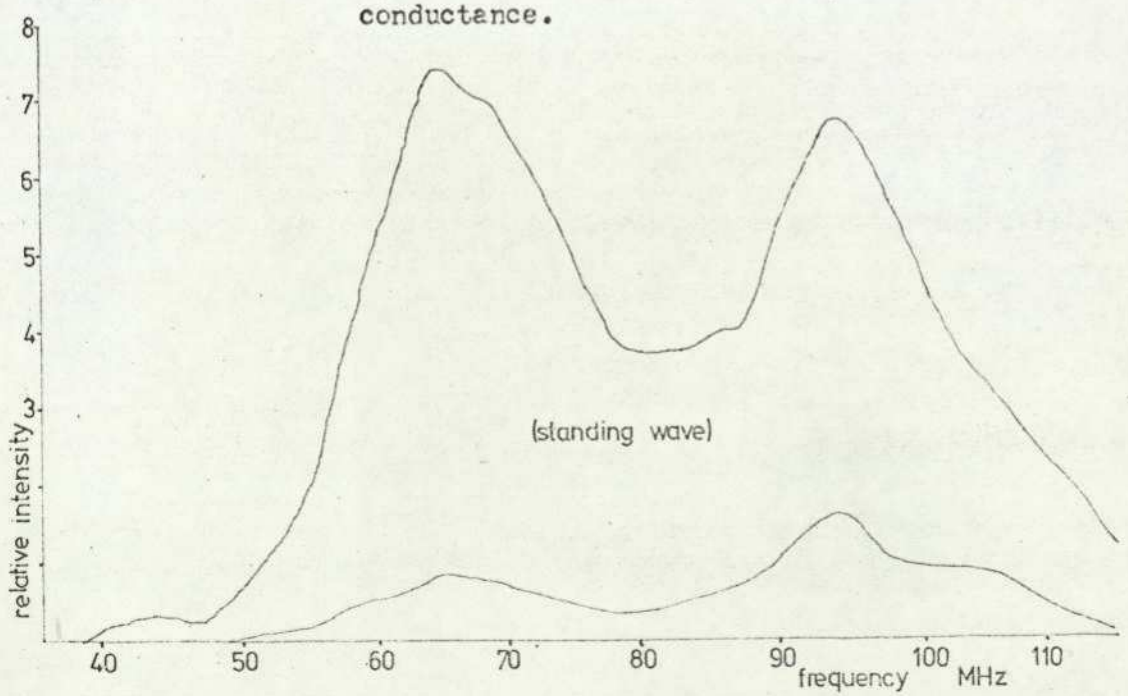

Fig. 8.3.2.2. Envelope of the intensity of the deflected first order with frequency of the device with the 'salol' bonded transducer.

handling capability of the transducer. These restrictions are not imposed with epoxy as the bonding material although, acoustically, the bond will have a considerably increased loss. The physical properties of the flint glass interaction medium are not essential for comparison purposes although the measured values of refractive index and longitudinal acoustic velocity for the samples used were 1.485 $\pm$ 0.2% and 5.36 Km/s $\pm$ 1% respectively yielding a minimum bragg frequency of 65 M Hz.

8.4. Lead Molybdate Design Considerations

The size of the $PbMoO_4$ samples determined the capacity, access time, efficiency and bandwidth that can be obtained using this material as the interaction medium. As already mentioned in section 6.5. the dimensions of the samples were 1.8 x 1.0 x 0.9 cm. The 1.0 x 0.9 cm optical faces allow an aperture of about 0.8 cm in diameter and the 1.8 cm sample length allows a maximum interaction length of 1.6 cm.

Using He-Ne laser light of 633 nm wavelength propagating near the plane z = 0, polarised parallel to this plane, and for sound propagating along the z axis, using the full aperture, the maximum access time is 2.2 μs . The minimum bragg frequency given by Eq. 3.8.1.6. is 56 M Hz. The transducer thickness must therefore be less than 54 μm . The power required to deflect 70% of the incident beam into the first order,with the light polarized in the plane z = 0 (Appendix A) is given by Eq. 3.4.3. to be 1.12 watts, assuming the sound column to be generated by a single transducer with a length-width ratio of 2 : 1.

Similarly, for the same optical arrangement but with the sound propagating in the plane z = 0 nearly orthogonal to the light direction,

the maximum access time, using the full aperture is 1.85 μs corresponding to the largest longitudinal velocity in this plane. The corresponding minimum bragg frequency is 66 M Hz resulting in a maximum transducer thickness of 44 μm . The power required to deflect the same amount of light in this plane using the same geometry is, theoretically, 1.65 watts.

The electrical properties of a 35^{o} rotated Y-cut $LiNbO_3$ transducer bonded to $PbMoO_4$ with the plate normal parallel to the z axis and the x or y axis is shown in Fig. 8.4.1. Also, in Fig. 8.4.2. there is shown the theoretical one-way insertion loss for such a transducer. The $PbMoO_4$ particle displacement angle in the x or y direction was assumed to be zero for these calculations. The various properties in each direction differ only slightly and the optimum -4 dB fractional bandwidth is approximately 0.79. The power associated with the shear wave generated is 15 dB below the longitudinal wave power and is of little significance. This level may be reduced, however, due to the finite particle displacement angle in the x or y directions (Fig. 5.4.6.). To make use of the potentially available bandwidth a transducer centre centre frequency in excess of 75 M Hz is required.

It has been shown by DeBenedictis and Lucero (1974) that dispersion with optical wavelength of the refractive indices and elasto-optic coefficients, P_{13} and P_{33},of $PbMoO_4$ occur. The figure of merit, M_2, associated with a z propagating acoustic wave and for x or y polarised light, has been shown to increase by a factor of 3 when an optical wavelength of 441.6 nm, obtained from a He-Cd laser, is used compared to that when He-Ne laser light is employed. This is a result of the increased value of the ordinary refractive index and the coefficient P_{13} at this optical wavelength. Irrespective of the change in material parameters (given in Appendix E) Eq. 3.4.3. shows that the

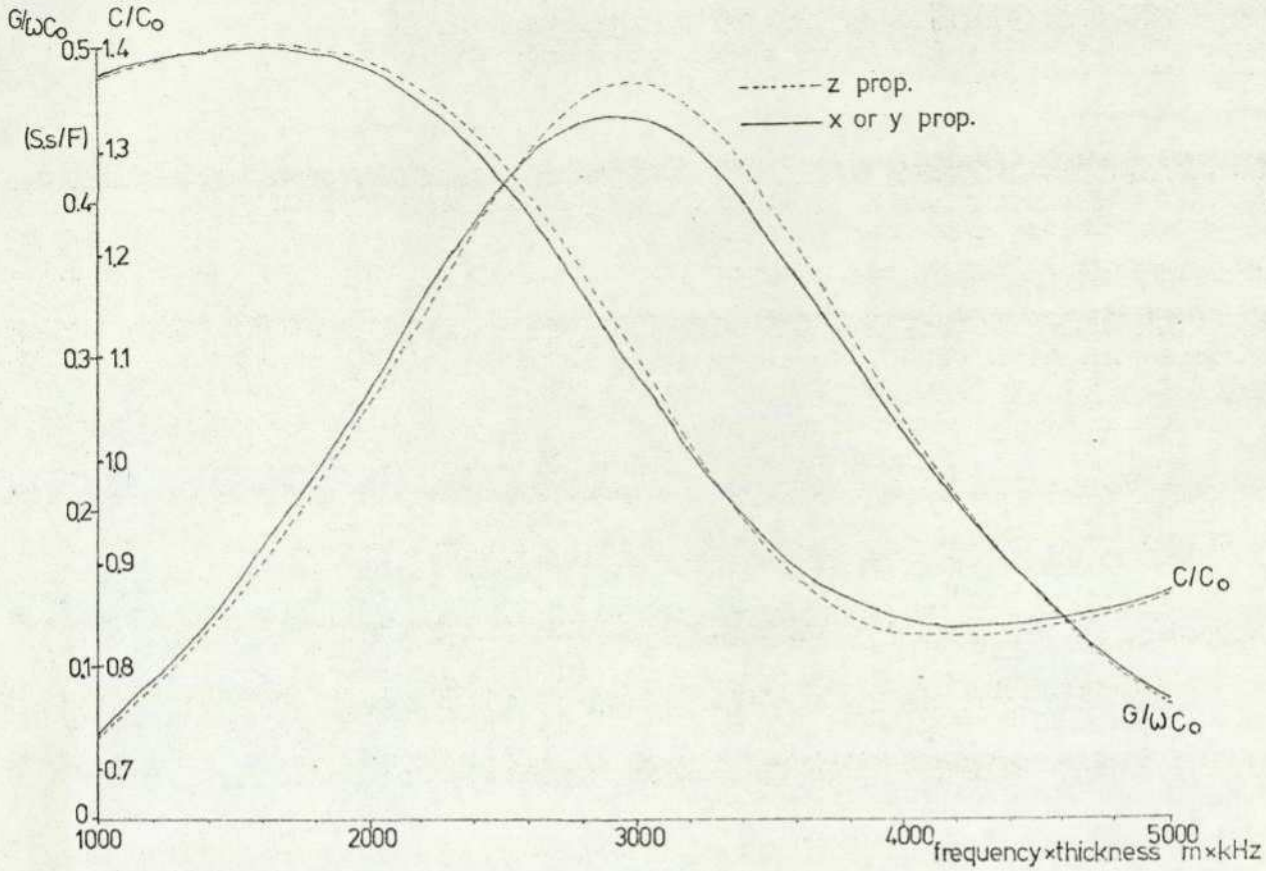

Fig. 8.4.1. Theoretical electrical response of 35° y-cut $LiNbO_3$ transducer bonded to $PbMoO_4$ for the acoustic wave propagating in the appropiate directions.

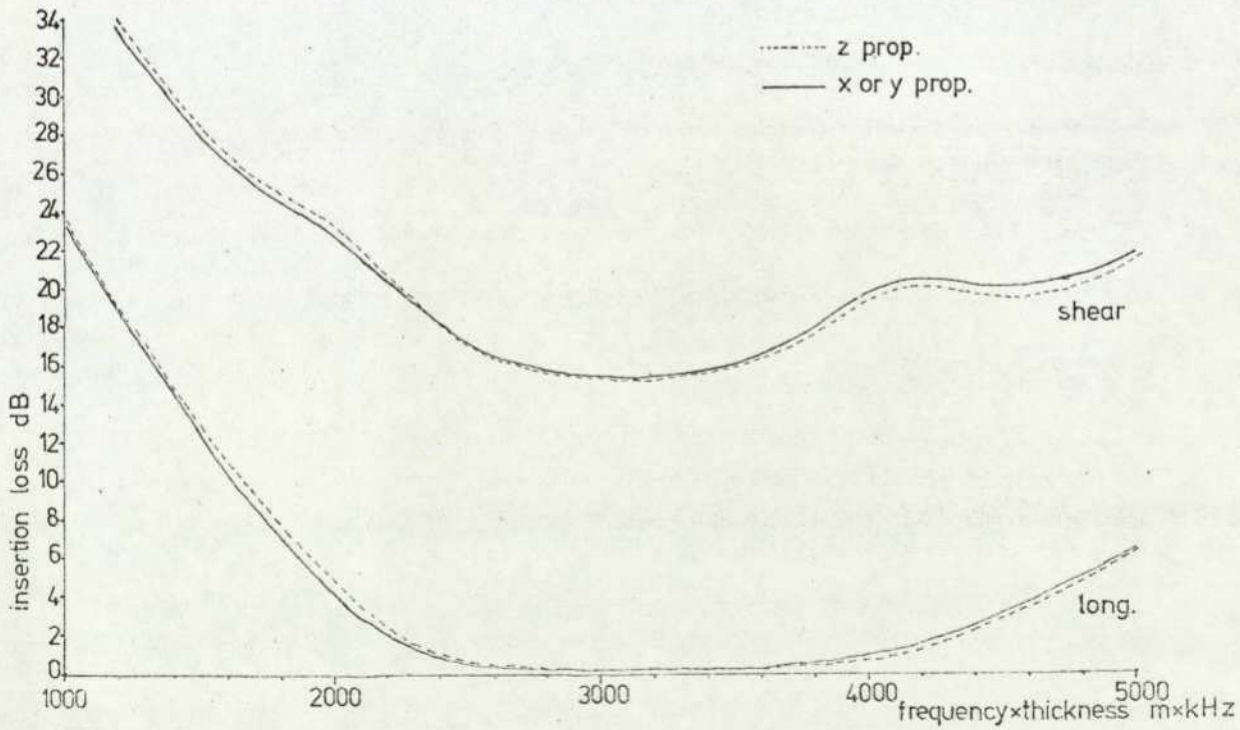

Fig. 8.4.2. Theoretical tuned one-way insertion loss for 35° y-cut $LiNbO_3$ transducer bonded to $PbMoO_4$ for the acoustic wave propagating in the appropiate directions.

efficiency increases by a factor of 2 when this shorter wavelength is used. The figure of merit associated with the deflection by an x or y propagating acoustic wave involves the ordinary refractive index and an increase in M_2 here may also be anticipated. Although the value of the relevant elasto-optic coefficient P_{11} is not known at this wavelength an overall increase in the figure of merit of 2 or greater may be expected. The total increase in the deflection efficiency of 7.8 dB and 6 dB respectively may thus be expected and may be useful where excessive acoustic losses occur. The corresponding minimum bragg frequencies for z propagating and x or y propagating sound are 69.5 M Hz and 82.5 M Hz respectively.

8.5. Device Construction and Transducer Fabrication

The construction of the lead molybdate devices is illustrated and the method of fabricating the transducers is described. The bonding of the appropriate components and the condition and quality of the final devices is also discussed.

8.5.1. Device Construction

The basic construction of the $PbMoO_4$ device is shown in Fig. 8.5.1.1. Aluminium heat sinks 1 are bonded to the back faces of the sample 2 with the same epoxy resin used for the transducer bonding. The metal surfaces were polished, albeit with up to a 4μm curvature, and bonded under 1000 p.s.i. pressure using a hydraulic jig with the assembly heated to about 60^{o}C with a hot air blower. The materials were then transferred to an oven, heated to about the same temperature, to cure. Coquin et al (1971) have observed damage to $PbMoO_4$ samples due to the difference in thermal expansion between $PbMoO_4$, in the plane normal to the z axis, and aluminium when the bonded surfaces

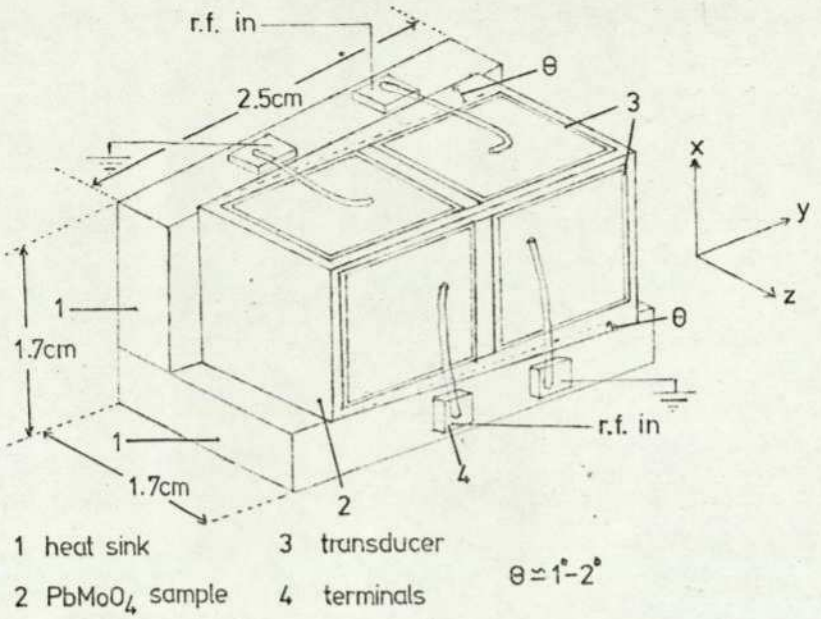

Fig. 8.5.1.1. Basic construction of the $PbMoO_4$ devices.

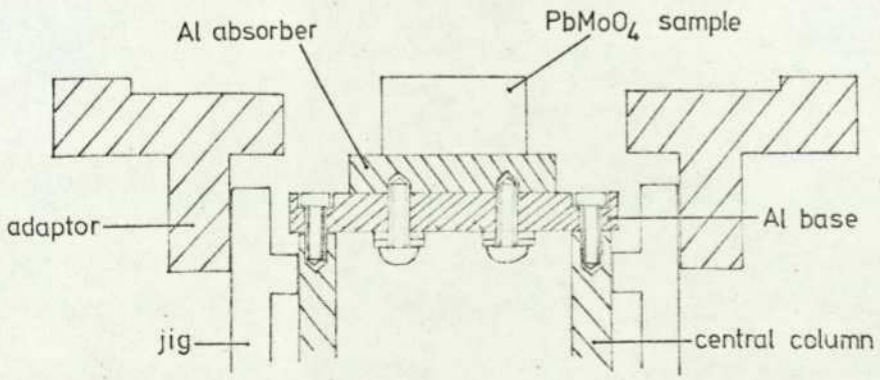

Fig. 8.5.2.1. Method of alignment and attachment of device to jig for fabrication of transducers.

are cooled from an elevated temperature. Kovar was suggested as an alternative. This risk was taken here, however, and no damage occurred to the samples. The thermal expansion of $PbMoO_4$ in the plane parallel to the z axis closely matches that of aluminium however. The size of the heat sinks and the order in which they were bonded was such that allowance was made for the fabrication of each of the two transducers 3. These were attached to the faces opposite the heat sinks. These faces were tilted between 1^o-2^o longitudinally (Pinnow et al 1969) and laterally with respect to the opposite faces. Contact to the transducer was made with wires via $\frac{1}{4}$" square copper clad board terminals 4.

8.5.2. Method of Alignment

Prior to bonding, two screw threads were produced in the back of the aluminium heat sinks so that the assembly could be attached to the grinding jig without the use of an adhesive. The assembly was screwed to an aluminium base as shown in Fig. 8.5.2.1. which was subsequently screwed to the central column of the jig. The surface on the $PbMoO_4$ to which the transducer was to be bonded was then ground flat. The aluminium base could then be removed and the transducer bonded to the $PbMoO_4$. The base was then returned to the central column of the jig. In the hope that no misalignment to the jig occurred the subsequent fabrication of the transducer would allow its faces to remain parallel to each other. The removal of the device from the jig was thus made simple. Further heat sinking could be added if required.

8.5.3. Deflector 1 : Transducer Arrangement and Fabrication

For this device epoxy resin was used as the transducer bonding material. In view of the performance of the previous devices bonded with epoxy an acoustic centre frequency of 90 M Hz corresponding to a transducer thickness of about 33 μm was aimed for. This would allow the device to operate within the bragg regime and yet minimize losses due to the bond. The transducers were also arranged so that they consisted of two elements with the polarisation of one element inverted with respect to the other. With electrical contact made to the top electrodes the behaviour would be similar to that of a single transducer and the impedance would also be raised in value. The 4 dB loss associated with a planar transducer array (section 3.8.2.) would also be overcome.

The surfaces to be bonded were initially cleaned in the same manner as for the fabrication of the water cell transducers (section 7.3.). An aluminium electrode of approximately 0.5 μm was deposited onto the $PbMoO_4$ surface. Both elements of the transducer were bonded simultaneously to one of the $PbMoO_4$ surfaces as in section 7.3. except that the assembly was quickly heated to reach about $60^{o}C$ within about 5 minutes using the hot air blower and the 1000 p.s.i. pressure was applied for 1 minute only. The grinding process was followed as in section 6.4. and satisfactory reduction to a thickness of 60 μm was achieved. The transducer thickness was monitored by observing acousto-optic diffraction at the plates' fundamental and harmonic resonant frequencies. Two aluminium foil electrodes temporarily placed on to the top of the transducers were driven with a r.f. signal and a He-Ne laser was passed through the deflection medium while still attached to the jig. Below 60 μm , however, the transducer began to crack and by the time the thickness was reduced

to 35 μm their condition was somewhat dire.

The same procedure was followed for the fabrication of the second transducer. Again, reduction to about 50 μm was satisfactory but below this excessive cracking occurred. The top electrodes were formed from self-adhering aluminium foil. The use of silver paste or the evaporation of electrodes was considered pointless due to the transducer's poor condition. This cracking is attributed to the considerable difference in the coefficient of thermal expansion between the two materials.

8.5.4. Deflector 2 : Transducer Arrangement and Fabrication

This second device used the low melting point cement 'salol' as the bonding medium. Consideration of the performance of the previous glass device (section 8.3.2.) permitted a higher transducer centre frequency to be tried. Thus a frequency of 150 M Hz, corresponding to a transducer thickness of about 20 μm was attempted here and operation well within the bragg regime could therefore be expected. The transducers were arranged in the form of a single bonded platelet, subdivided into elements, and electrically connected to form a planar array as in section 3.8.2. The 4 dB loss in the interaction efficiency was tolerated assuming the acoustic attenuation of the bond not to be excessive.

The appropriate surfaces were prepared and cleaned as before. A 0.5 μm aluminium electrode was deposited onto the transducer surface only. The evaporation of a film onto the $PbMoO_4$ surface was unnecessary for this transducer configuration and this also minimized the number of evaporation processes. The transducer and $PbMoO_4$ surfaces were placed together and the bonding procedure followed as discussed for the device in section 8.3.2. The method of alignment

and reduction procedure have been discussed in section 8.5.2. and section 6.4. Monitoring of the transducers' thickness was achieved in the same way as described for the fabrication of the transducers for Deflector 1 (section 8.5.3.). Satisfactory reduction to the required thickness was achieved without any damage occuring to the transducers. Removal of excess 'salol' from around the transducers' edges, using acetone, was undertaken during the reduction process to prevent the cement from becoming detached and causing damage to the platelet. Unlike the transducers associated with Deflector 1 no cracking had occurred and the transducers were in a good condition. The final thickness of the plates, estimated from subsequent impedance measurements, was about 25 μm , corresponding to a centre frequency of about 135 M Hz, the error being due to the inaccuracies of the monitoring method.

The transducer bonded to the adjacent $PbMoO_4$ surface was fabricated in the same manner. During the bonding procedure the first transducer had to be kept in position since its bond would melt. A polished aluminium plate was placed on top of the first transducer and secured in position using rubber bands. Degradation in the transducers' subsequent performance was not detectable. For the top electrodes silver paste was used. Initially the top electrodes were arranged so that a two element array could be realised. However, the plates were eventually divided to realise a four element array to increase the transducers impedance. The transducer was segmented using a scalpel (Alphonse 1975) and the silver paste electrodes were divided accordingly.

8.6. Performance

The performance of the two devices, Deflector 1 and Deflector 2,

are described. For the examination of their optical behaviour the optical and electrical arrangement as described in section 7.4. was used with the inclusion of a polarizer between the laser and the beam expanding lens arrangement.

It was expected that for the direction in which the optical beam was propagating the polarization axes would coincide with the normals of the transducers. Upon examination of the two $PbMoO_4$ samples this was not the case. The polarization axes were orientated at almost 45^o with respect to the transducers normals. Separation of the ordinary and extraordinary rays occurred and was partly due to the non-parallelism of the optical faces. However, it was observed that this birefringence was spatially variant across the optical aperture. Operation in both orthogonal directions could be achieved, however, with the light appropriately polarized along one of the polarization axes. Using an aperture of 8 mm considerable distortion to the resulting spot occurred. Satisfactory spot shape could be obtained only when the aperture was reduced to about 4 mm and for the incident beam suitably positioned in an area of the aperture. Although some residual distortion was due to the optical components used in the setup the distortion caused by the $PbMoO_4$ was predominant. Thus, the $PbMoO_4$ samples appeared to be twinned. However, they were nevertheless usable to demonstrate the interaction.

For Deflector 2 the performance of the device with its transducers arranged as a two element array and as a four element array are compared.

8.6.1. Performance of Deflector 1

8.6.1.1. Electrical Response

The electrical response of each of the transducers is shown in

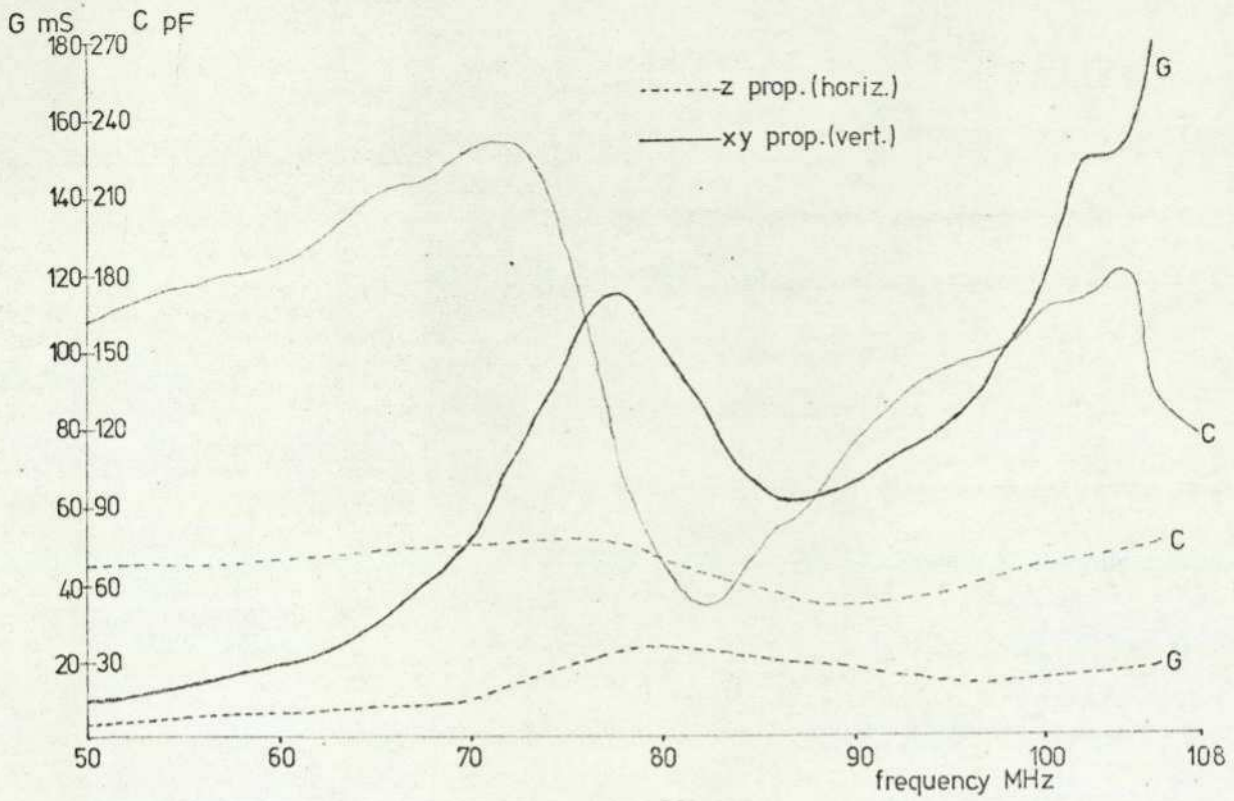

Fig. 8.6.1.1.1. Electrical properties of the transducers associated with Deflector 1. Horizontal deflection is accomplished with the z propagating(in $PbMoO_4$) acoustic wave.

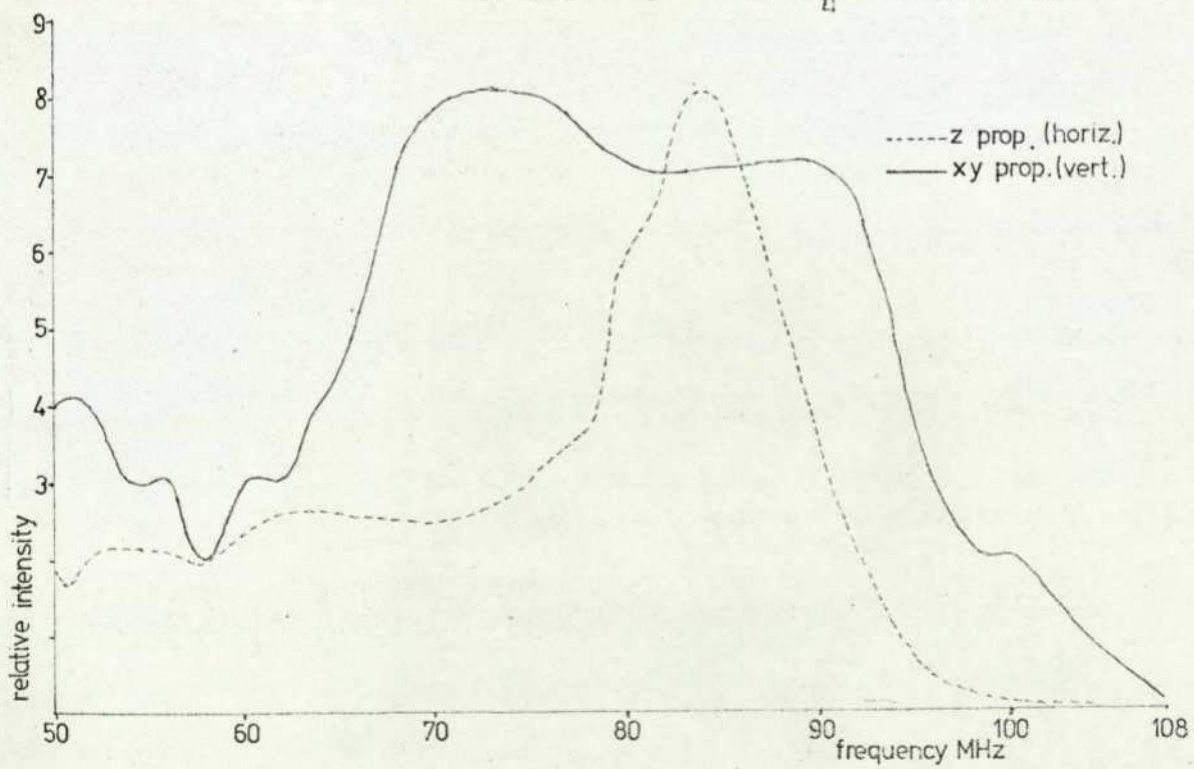

Fig. 8.6.1.3.1. Optical bandwidth of each first order of Deflector 1

Fig. 8.6.1.1.1 in the frequency range between 50 M Hz and 108 M Hz and bears little resemblance to the theoretical curves of Fig. 8.4.1. It can be seen, however, from the curves showing the conductance and capacitance of the transducer bonded to the $PbMoO_4$ face parallel to the assumed z axis that the electrical properties of the epoxy resin, as shown in Fig. 8.3.1.1. and Fig. 8.3.1.2., are beginning to predominate. The lower values of the conductance and capacitance associated with the transducer bonded to the face normal to the z axis are due largely to the improper contact between the aluminium foil top electrode and the $LiNbO_3$ surface. Again, here, the epoxy is responsible for the poor response and the resonance of the transducers is reduced due to the bonds' attenuation. Also, the physical condition of the platelets has contributed to the poor response. Thus, electrical power supplied to the transducer will also be dissipated within the epoxy as well as being delivered to the transducer.

8.6.1.2. Efficiency

The device was bonded to an aluminium chassis and the transducers were connected to two B.N.C. sockets via a tuning network similar in form to those used on the water cell device (section 7.2.). Each port was tuned to 50Ω at a frequency of 85 M Hz. The final device is shown in Plate 8.6.1.2.1.

It can be inferred from the electrical response that the efficiency of the device will be poor. Using a 1 mm beam diameter He-Ne 633 nm laser the light deflected into the first orders by the z propagating and the x or y propagating acoustic wave was approximately 7.5% and 4.5% respectively using an r.f. power of 3 watts. From Eq. 3.4.3.

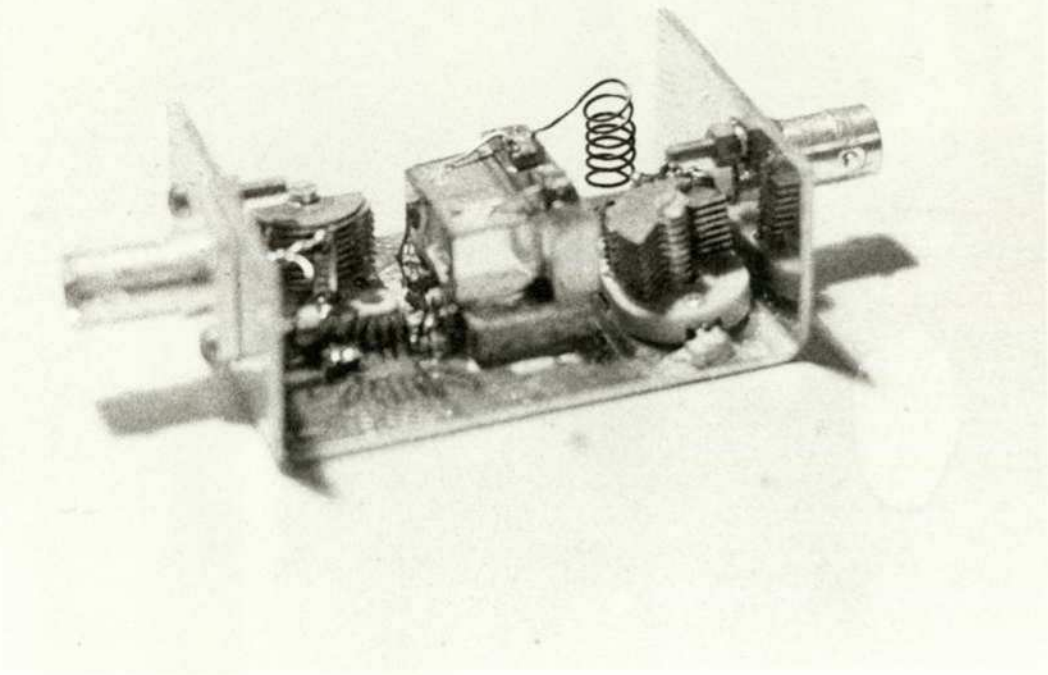

Plate 8.6.1.2.1. The $PbMoO_4$ two-dimensional deflector 1.

the estimated transducer losses were 15.4 dB and 15.9 dB respectively. Inevitably, the transducers efficiency was spatially variant over the aperture and these measured values correspond to the incident beam situated in the optimum position. These losses could be accounted for by energy dissipated in the epoxy, acoustic attenuation of the bond, energy lost into the foil electrodes and dispersion of the sound by the physical state of the transducers. Also, the interaction being near the Bragg-Raman Nath regime boundary, and the bonds' attenuation reducing the effective interaction length, together with the quality of the $PbMoO_4$ all make their contribution to the losses. The amount of light that could be deflected into the composite order was consequently extremely samll.

The excessive losses thus demanded the use of a shorter optical wavelength to improve the percentage deflection of light into the composite order. The interaction will be moved further towards the bragg-Raman Nath boundary however. The percentage deflection of light with power, using a 1 mm diameter beam He-Cd 441.6 nm laser, suitably positioned, is shown in Fig. 8.6.1.2.1. for single-dimensional operation in each co-ordinate. There is a considerable difference in the amount of light deflected from the zeroth order compared to the intensity of the first orders and illustrates that the interaction is not contained within the bragg regime. Nevertheless, approximately a threefold increase in the deflection efficiency is achieved for the first orders. This still meant that not more than 7% of the incident beam could be deflected into the composite order for 3 watts of electrical power applied to each transducer.

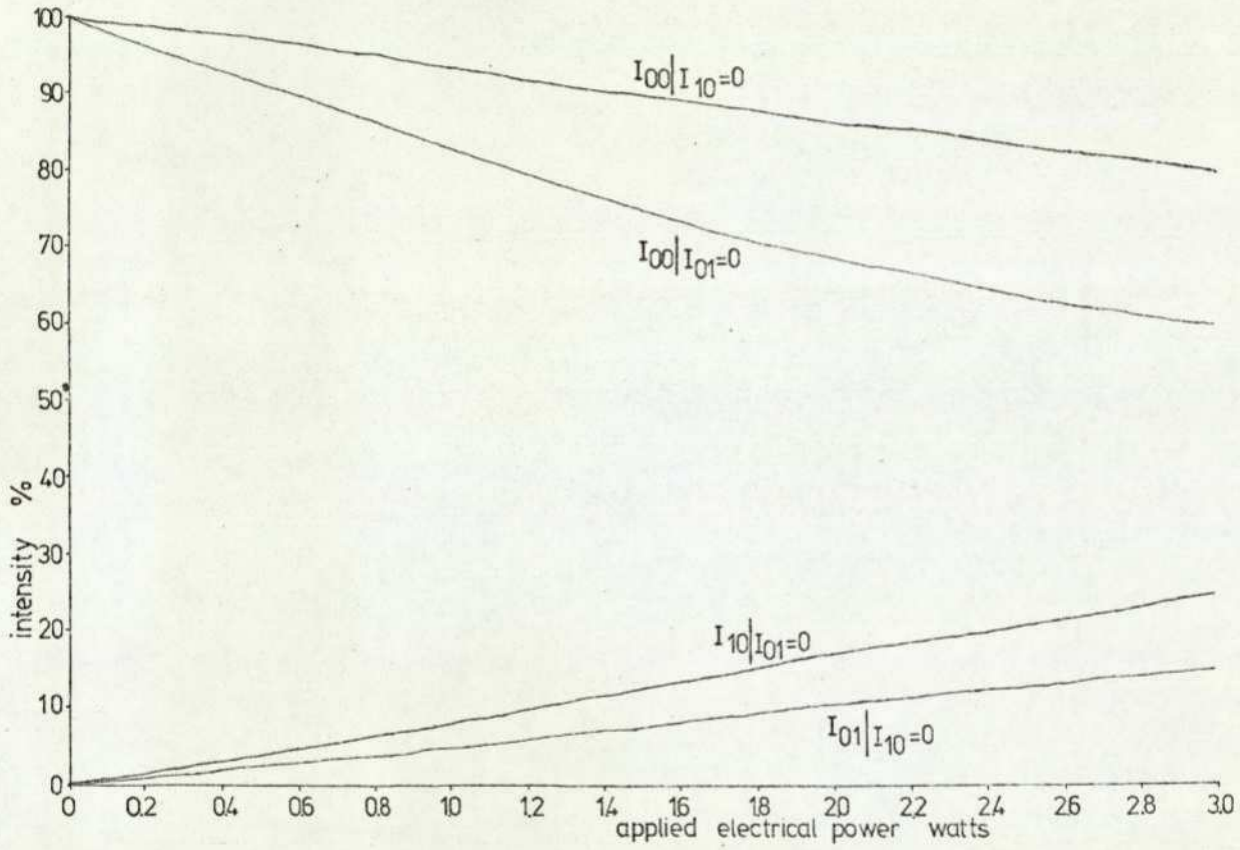

Fig. 8.6.1.2.1. Diffraction efficiency of Deflector 1. Percentage deflection into the orders I_{xy} with applied electrical power is shown.
(f_B=85MHz, λ_o=441.6nm)

8.6.1.3. Bandwidth

Using the He-Cd wavelength light, and without any additional electrical tuning, the bandwidth in each orthogonal direction is shown in Fig. 8.6.1.3.1. The interaction is entirely dependent on the transducer bandwidths. The bragg angles were satisfied at the frequency to which the device was tuned.

The bandwidth associated with the first order deflected by the x or y propagating acoustic wave has a broader response and can be related to the transducers' electrical response in Fig. 8.6.1.1.1. The peak intensity increases slightly as the frequency decreases due to the frequency dependence of the epoxy resins' losses. The -4 dB fractional bandwidth obtained for this case was 0.42.

The response of the first order beam deflected by the z propagating acoustic wave has peaked around the bragg frequency. This is a result of the effective capacitance in series with the transducer by the improper contact of the foil top electrode and this performance is as expected from the transducers' electrical behaviour. The optical deflection, although reduced to 5 dB below the peak deflected intensity, is extended down to 60 M Hz as the losses are reduced with a decrease in frequency. The -4 dB fractional bandwidth here was only 0.174 although a -6 dB fractional bandwidth of 0.45 was obtainable.

8.6.1.4. Display

The excessive transducer losses were such that only about 3% of the applied electrical energy appeared as acoustic energy within the $PbMoO_4$ and observable deflection of light (441.6 nm) could only be satisfactorily achieved when about 2 watts of electrical power was

applied to each transducer. The subsequent heat produced at each of the transducer surfaces caused considerable thermal effects to occur. Controlling the composite order with two stepped frequency generators (Appendix G),both of which were adjusted to scan between the frequencies 70 - 90 M Hz , the display shown in Plate 8.6.1.4.1. could be obtained using an optical aperture of 2 mm. Increasing the aperture further did not increase the resolution but rather decreased it due to the severity of the thermal effects. Also, soon after initially operating the device the optical beams began to wander due to the prism forming heating effect (Coquin et al 1971). Such effects have caused the beam spot shape to become triangular and the heating is also responsible for the distortion to the rectangular array of spots. After operating for about ½ hour the device and the aluminium chassis became almost too hot to touch. The heat sinking provided was thus insufficient for a device being supplied with this amount of power.

With this device interference between the two channels was observed. Plate 8.6.1.4.2. shows that with about 2 watts applied to the vertically deflecting transducer light is deflected not only into the vertical first order but also into the horizontal first order as well. The formation of the two first orders has also caused some scattering of light into the composite order. The port associated with the horizontally deflecting transducer was open-circuited in this instance. The interference occurred, however, irrespective of the value of the ports' termination. Although coupling between the transducers may be due to external means, in which case screening between the two sections would have to be provided, it is possible that coupling has occurred through the interaction medium since each electrode on

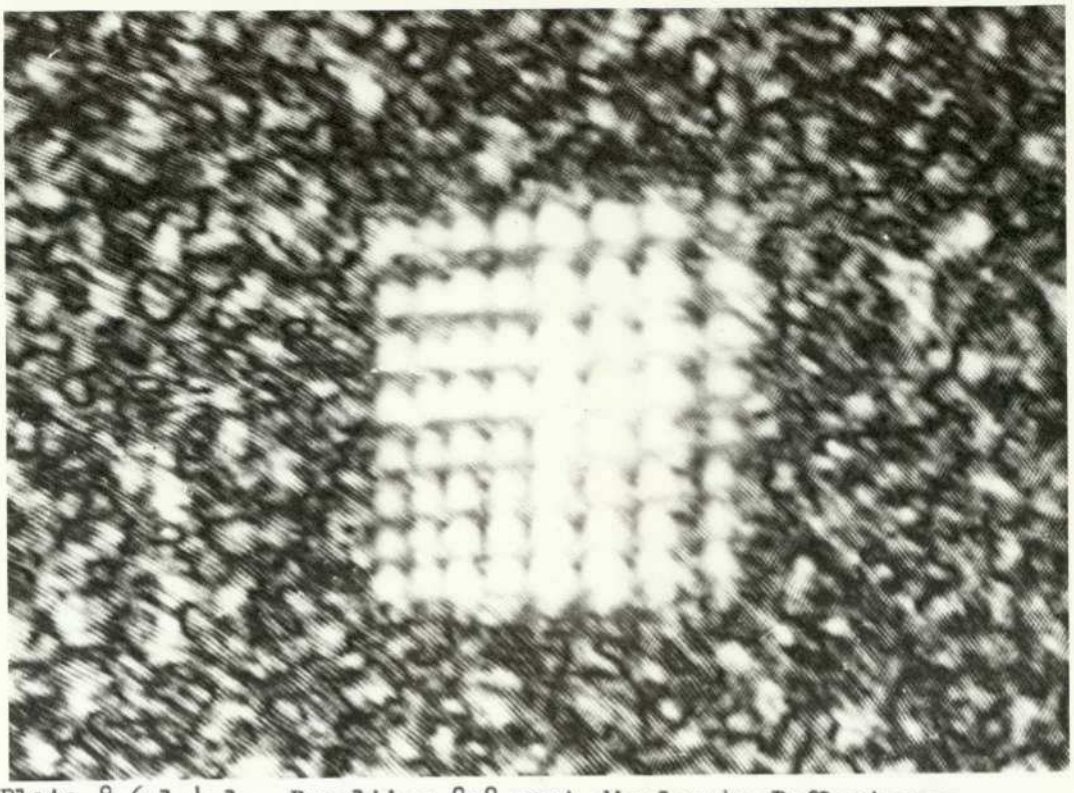

Plate 8.6.1.4.1. Resulting 8x8 spot display by Deflector 1. The resulting distortion is due to extreme thermal effects.

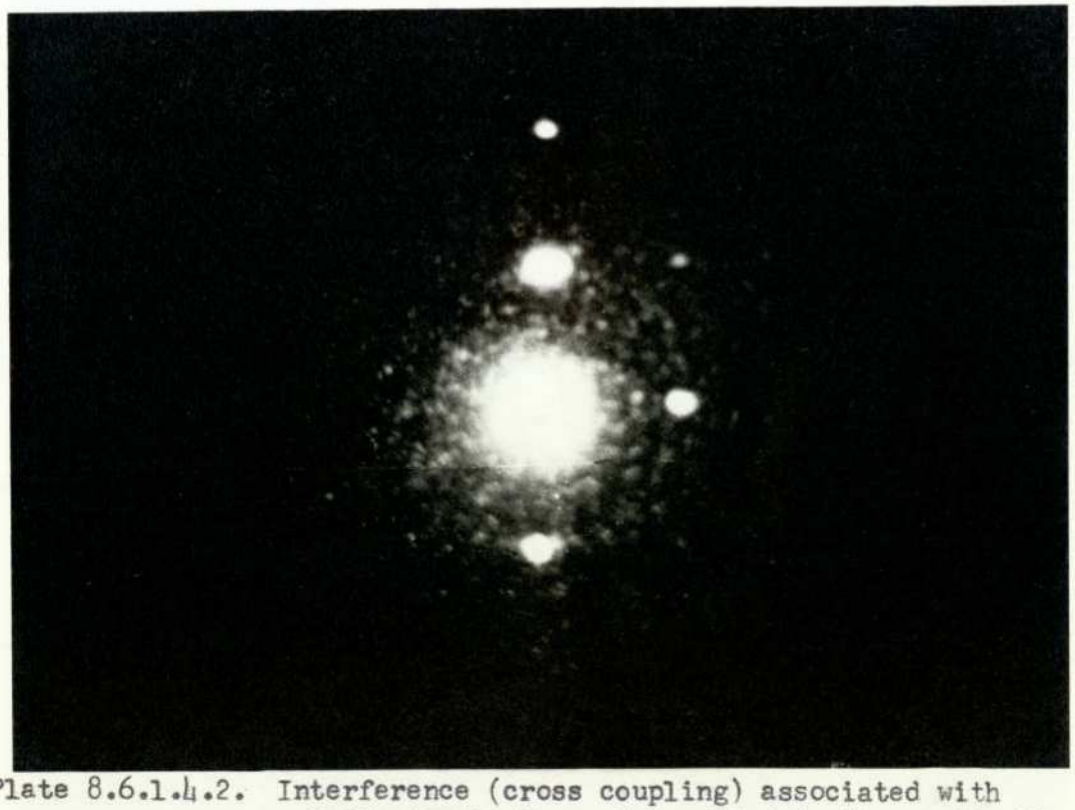

Plate 8.6.1.4.2. Interference (cross coupling) associated with Deflector 1. Power is applied to the vertically deflecting transducer only.

the $PbMoO_4$ surfaces is 'live'. This coupling cannot therefore be avoided and may be an inherent characteristic of the device. Acoustic detection and regeneration of waves by the horizontally deflecting transducer from reflections of the vertically propagating acoustic wave within the interaction medium may also be a possible cause.

8.6.2. Performance of Deflector 2

8.6.2.1. Electrical Response

The electrical response of the transducers associated with Deflector 2 are shown in Fig. 8.6.2.1.1. On the smith chart is shown the impedance of the transducers divided into four elements as well as two elements measured from the copper clad board terminals over the frequency range 50 - 250 M Hz. For this device the transducers electrical circuit does not include the bonding layer.

The high value of the capacitance of the plate has caused the inductance of the connecting wires to become significant. This is clearly shown by the variation of the impedance for the two element arrangement for both transducers. The centre frequency of each transducer can be seen to be about 120-125 M Hz and the magnitude of the resistance at these frequencies (0.9 - 1.2 Ω maximum) is less than that expected from the theoretical response in Fig. 8.4.1.

Dividing the transducers into four elements has reduced the capacitance and also reduced the significance of the connecting wires' inductance. The magnitude of the resistance has also increased, although less than expected, allowance being made for the slight reduction of the top electrode area due to the segmentation. It can be seen from Plate 8.6.2.2.1. that for the four element array power is applied to

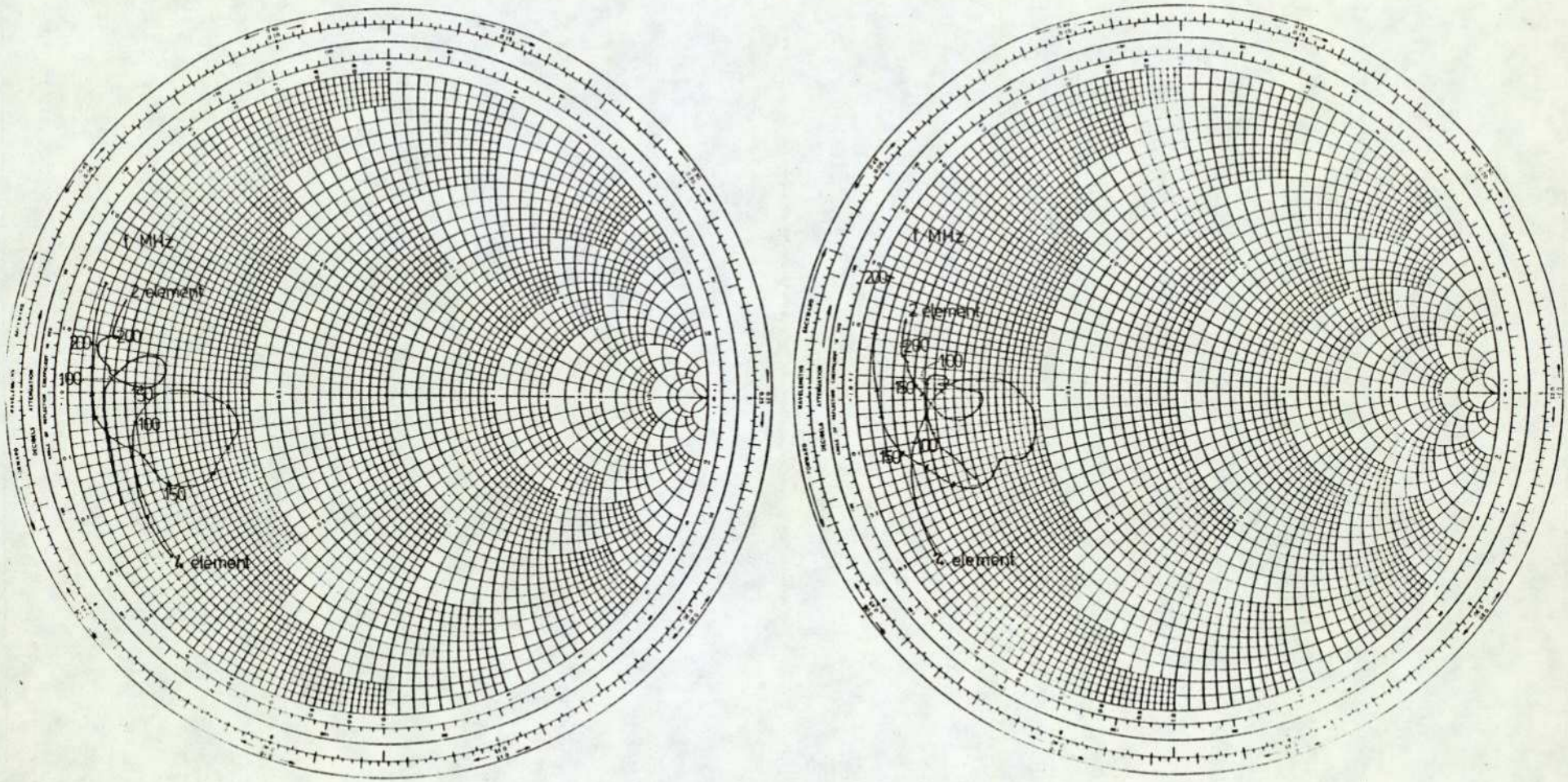

Fig. 8.6.2.1.1. Impedance of the transducers associated with Deflector 2.

a) impedance of transducer associated with the horizontal deflection (z propagating acoustic wave).

b) impedance of transducer associated with the vertical deflection (xy propagating acoustic wave).

the two inner elements while the two outer elements are linked together. This method of connection was done merely for convenience since it eliminated the removal and replacement of the already existing supply wires. The performance of the array is still similar to that described in section 3.8.2. The links' inclusion will increase the series inductance of the arrangement however.

For these measurements use was made of a Hewlett Packard 8410A network analyser, a 8690B 0.1 - 4 G Hz voltage controlled oscillator, and a 8745A S parameter test set used in conjunction with a 8414A polar display.

8.6.2.2. Efficiency

Deflector 2 is shown in Plate 8.6.2.2.1. bonded to an aluminium chassis and connected via two tuning networks to the two B.N.C. sockets. The device was arranged so that additional heat sinking could be provided for the removal of heat. Each transducer was initially tuned to 50 Ω at its centre frequency using a first order tuning network. The variation of intensity of the first order with applied power, for single-dimensional deflection in each co-ordinate, is shown in Fig. 8.6.2.2.1. The intensity variation is shown for both the two element and four element arrangements. The cell was adjusted so that the acousto-optic interaction satisfied the bragg angle in each dimension at the tuned frequencies. Plate 8.6.2.2.2. shows the cell mounted on an adjustable table designed so that the necessary adjustments could be performed. This table was used for alignment and adjustment purposes for all the devices discussed in this work.

Using the He-Cd wavelength light and a 1 mm beam diameter 49% of the incident beam could be deflected into the first order by the

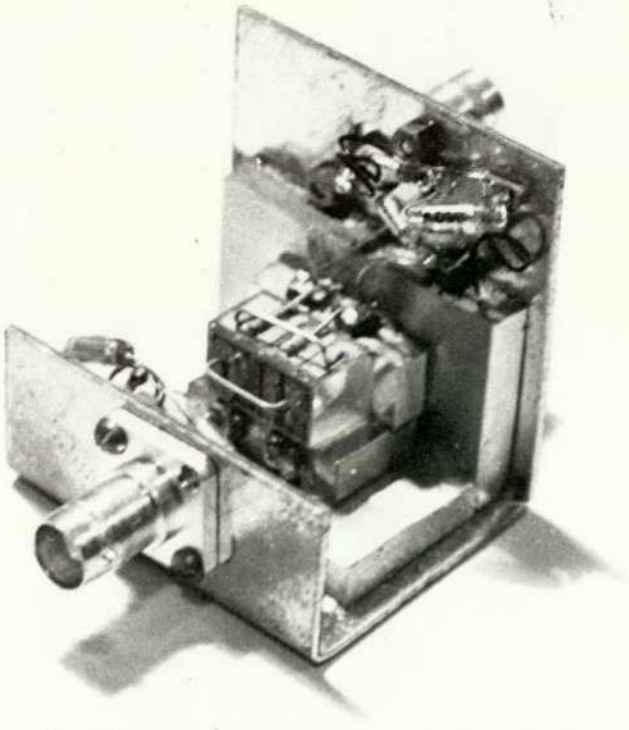

Plate 8.6.2.2.1. The $PbMoO_4$ two dimensional deflector 2.

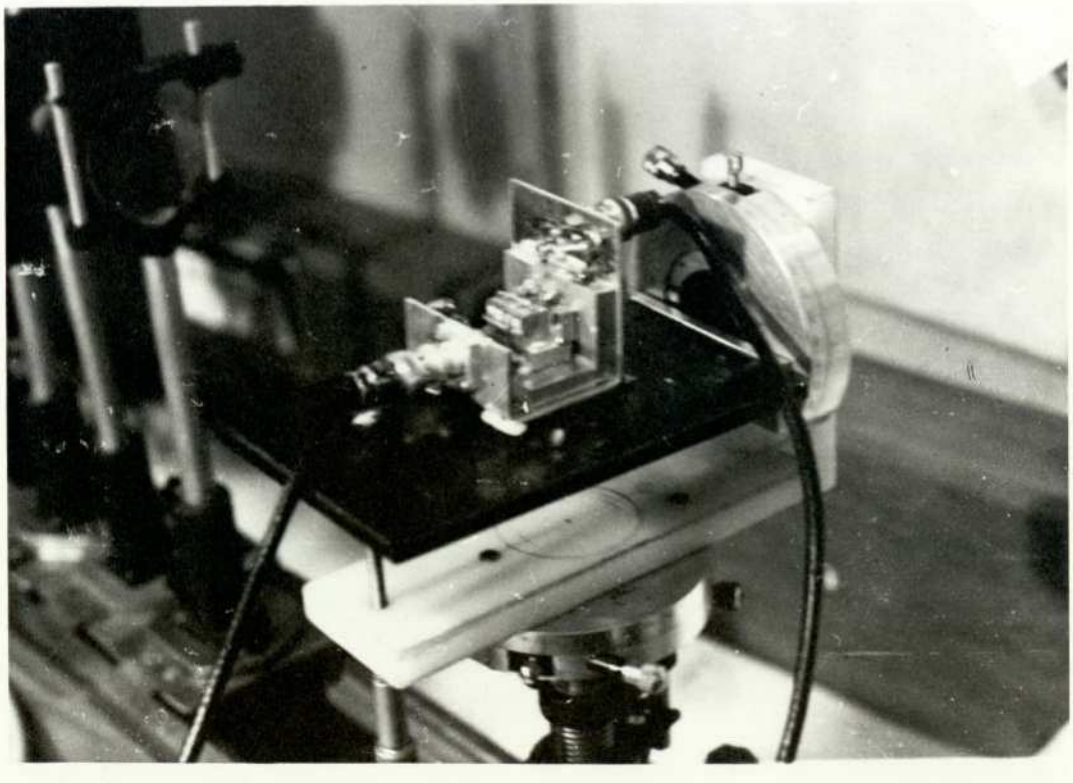

Plate 8.6.2.2.2. Deflector 2 in use mounted on its' adjustable table.

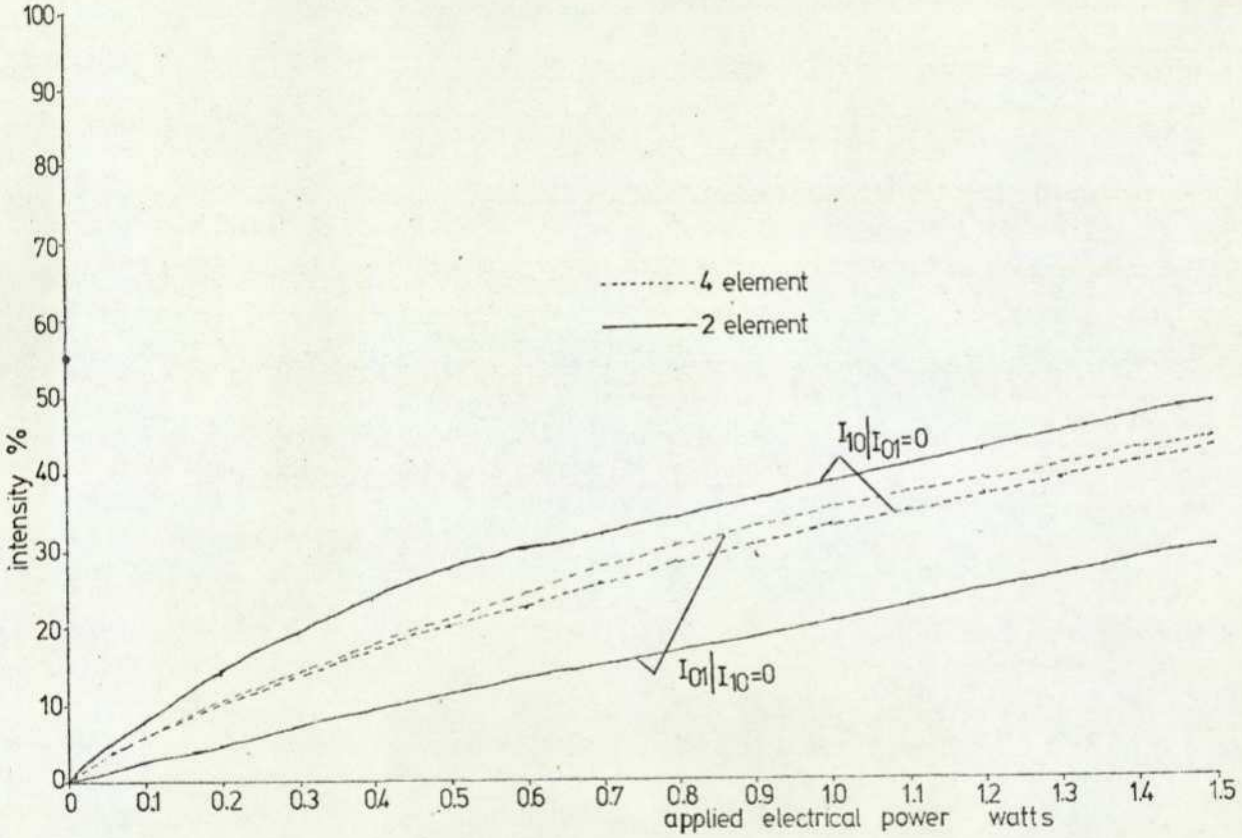

Fig. 8.6.2.2.1. Diffraction efficiency of Deflector 2. Percentage deflection into the two first orders with applied electrical power is shown for both the 2 and 4 element transducer arrangements.

horizontally deflecting transducer (z propagating acoustic wave) arranged as a two element array with an applied electrical power of 1.5 watts. For the same arrangement the vertically deflecting transducer could deflect 30% of the incident beam when operated at the same power level. The bond and the loading of the transducers by the silver paste produced an uneven response across the transducers widths and Fig. 8.6.2.2.1. shows the response for the incident beam placed in the optimum position. The reduced losses of the bond allowed the interaction to occur well within the bragg regime. Continuous operation above 1.5 watts, however, caused the 'salol' bonds to melt due to heat produced by the transducers losses and thus prevented operation above this level. The estimated losses associated with the bond here were about 3 dB, allowing for the 4 dB interaction loss and a 3 - 4 dB loss due to the silver paste loading.

For the four element transducer arrays the device was similarly tuned, aligned, and adjusted. Fig. 8.6.2.2.1. shows that for this arrangement the efficiency in the horizontal dimension has decreased slightly by 0.57 dB and the efficiency in the vertical dimension has increased by 1.7 dB. This measurement was made to investigate to what extent, if any, the electrical losses had on the transducers performance. These losses would appear to have been responsible for the change in efficiency in the vertical dimension although the slightly reduced interaction length, due to the segmenting, may be responsible for the reduced efficiency in the horizontal dimension.

8.6.2.3. Bandwidth

The low impedances of the two element arrays required that the tuning networks would have to match the transducer to near 50Ω over

the desired bandwidth. This could not be achieved with a first order network similar to that used on the water cell device. Instead, a third order network was used, the type of which is described by Matthaei (1964). The interaction bandwidths, for deflection in each dimension, are shown in Fig. 8.6.2.3.1. and Fig. 8.6.2.3.2. The values of the tuning components were determined from the tables given by Matthaei and also by experiment. A centre frequency around 100 M Hz was aimed for which, although lower than the transducers centre frequencies, was attempted to minimise the losses. The interaction - 4 dB fractional bandwidth achieved in the horizontal dimension (z propagating acoustic wave) was 0.36 with a centre frequency of 104 M Hz. The fractional bandwidth in the vertical dimension was 0.48 with a 99 M Hz centre frequency. The bandwidth, however, was essentially dependent on the tuning networks rather than on the response of the transducers.

The segmentation of the transducers to form a four element array was an attempt to increase the transducer impedances so as to ease the tuning and matching problem. Here, as before, a third order tuning network for each transducer was employed which is illustrated in Fig. 8.6.2.3.3. The component values were determined from the tables given by Matthaei (1964) and also by experiment. Fixed values of capacitance were used and the inductors were adjusted to minimise the reflection coefficient. The centre frequencies were higher than before (131 M Hz) and were tried to achieve a larger fractional bandwidth. The tuned impedances, Z_{11} and Z_{22}, of the two ports are shown in Fig. 8.6.2.3.4. over the frequency range 85 - 185 M Hz. The interaction bandwidths are shown in Fig. 8.6.2.3.5. and Fig. 8.6.2.3.6. A -4 dB fractional bandwidth of 0.49 was achieved for deflection in the horizontal dimension and of 0.51 for deflection in the vertical dimension. The

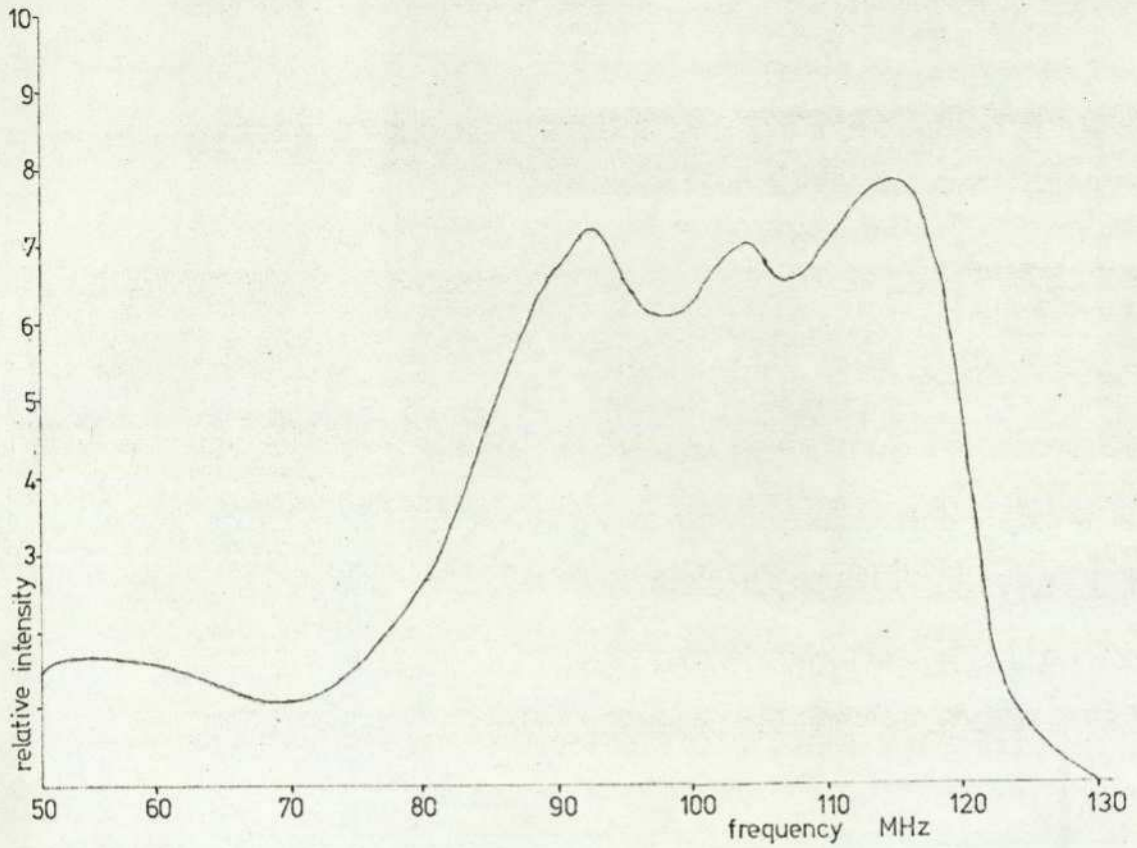

Fig. 8.6.2.3.1. Bandwidth of horizontal first order of Deflector 2 with 2 element transducer array.

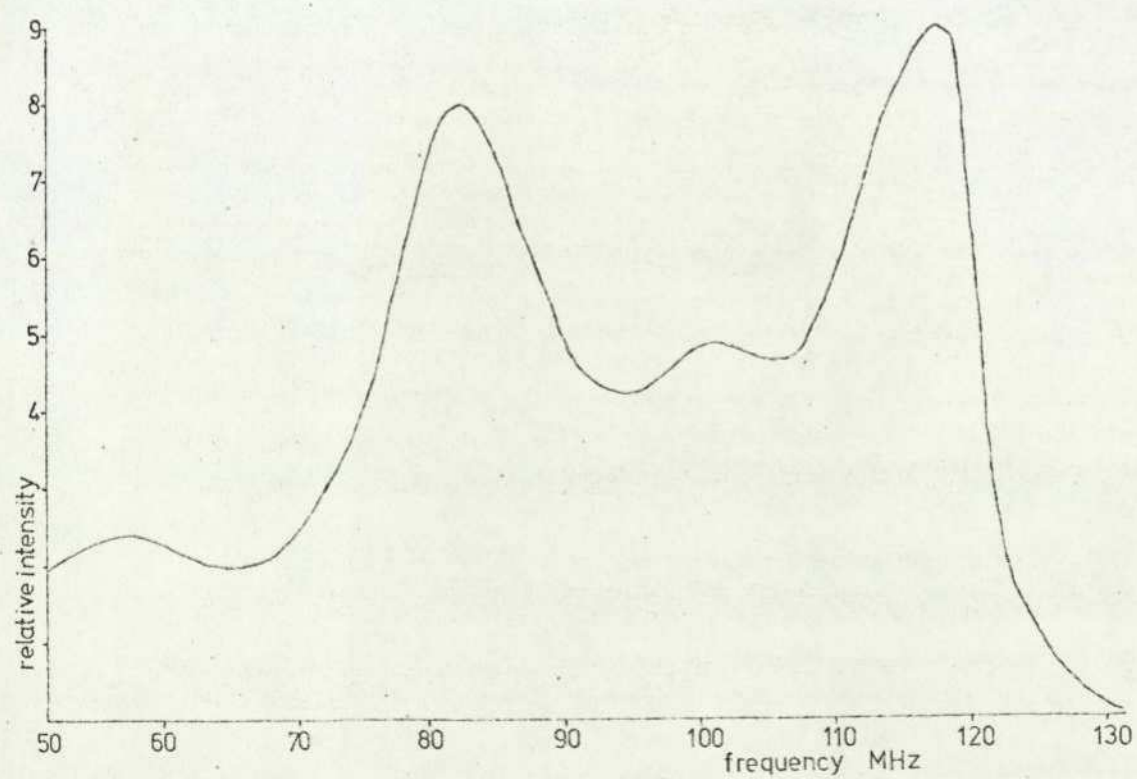

Fig. 8.6.2.3.2. Bandwidth of vertical first order of Deflector 2 with 2 element transducer array.

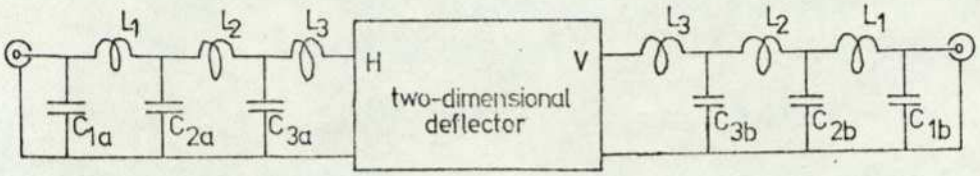

$L_1 \sim 50nH$ $C_{1a} = 18pF$ $C_{1b} = 18pF$ H = horizontally deflecting transducer

$L_2 \sim 30nH$ $C_{2a} = 27pF$ $C_{2b} = 22pF$ V = vertically deflecting transducer

$L_3 \sim 10nH$ $C_{3a} = 33pF$ $C_{3b} = 47pF$

Fig. 8.6.2.3.3. The tuning arrangement for Deflector 2. The capacitors were of fixed values while the the values of the inductances are approximate and were adjusted experimentally.

peak in the interaction bandwidths between 110 - 120 M Hz is due to the transducers centre response and the extended bandwidth above 120 M Hz is due to the response of the tuning networks.

Further segmentation of the transducers to form an eight element array would have been appropriate to increase their impedances and to further extend the bandwidths. However, this was not feasible due to the delicacy of the transducer arrangements.

8.6.2.4. Display

The temperature dependence of the bonding material limited the total amount of power that could be applied to the device. A maximum limit of 1.5 watts was imposed which meant that the average power that could be applied to each transducer was less than 0.75 watts. For X-Y deflection purposes the device was actually driven with between 0.5 - 0.7 watts fed to each transducer. The percentage He-Cd light deflected into the composite order was thus small and in the order of about 4% or less using the four element array transducers. As previously

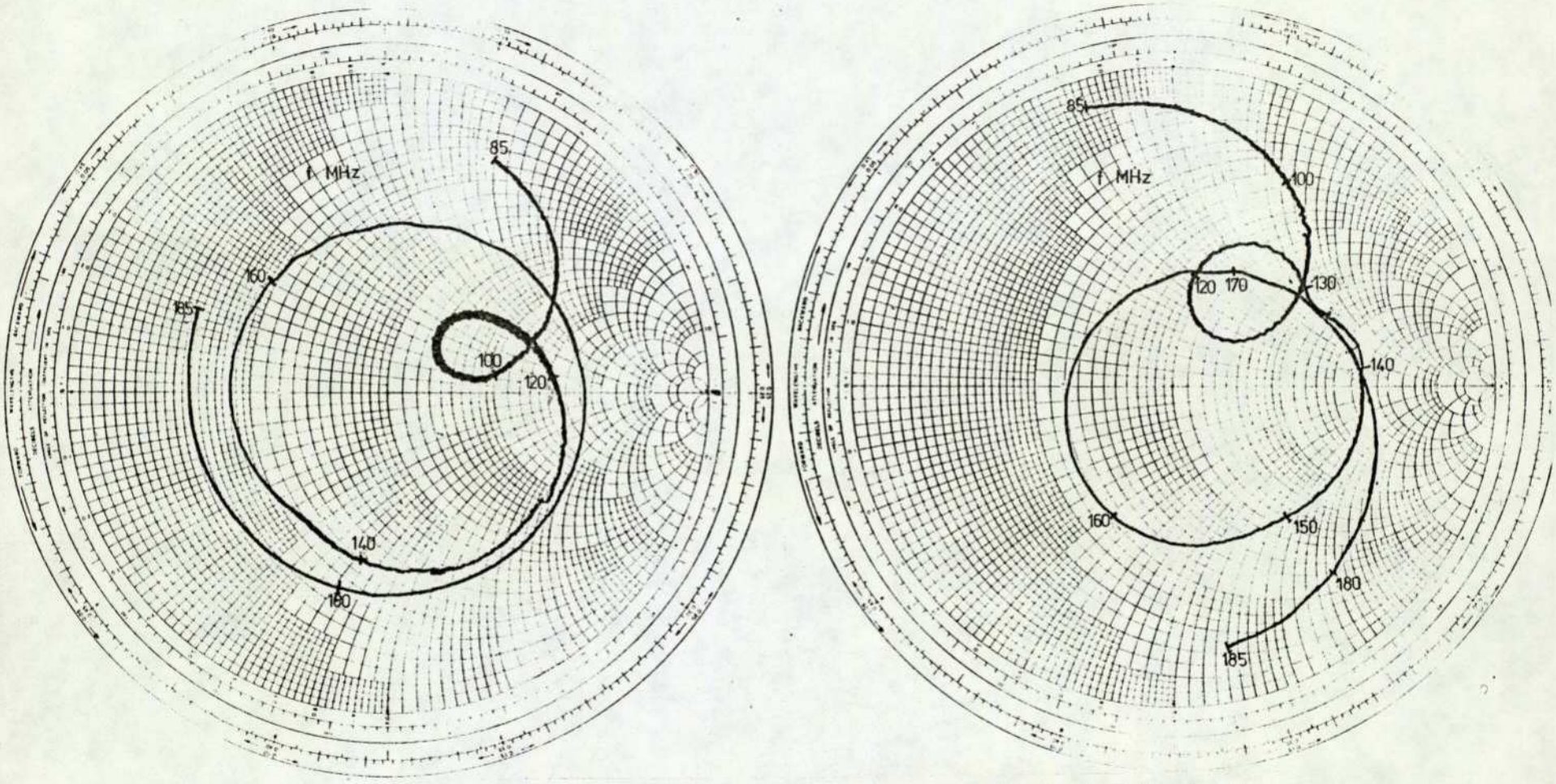

Fig. 8.6.2.3.4. The tuned impedances of the two ports associated with Deflector 2.

a) the port associated with the horizontal deflection.

b) the port associated with the vertical deflection.

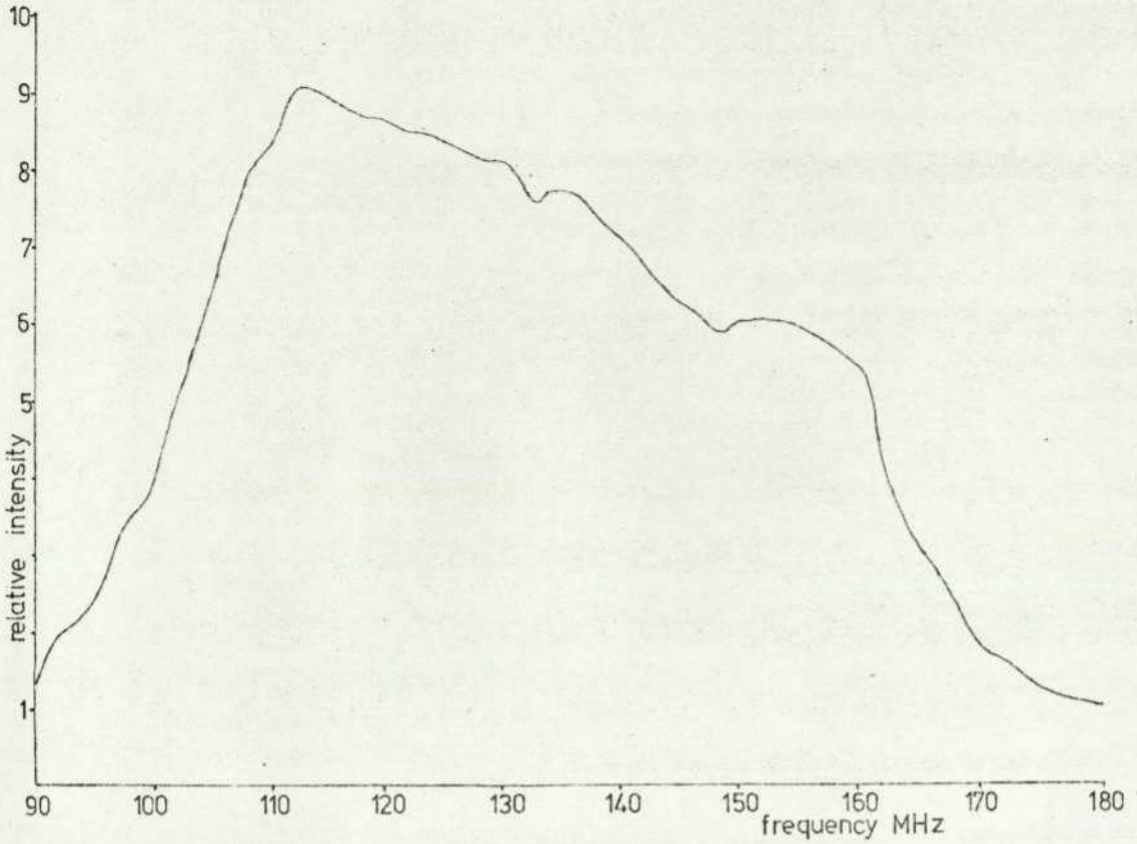

Fig. 8.6.2.3.5. Bandwidth of horizontal first order of Deflector 2 with 4 element transducer array.

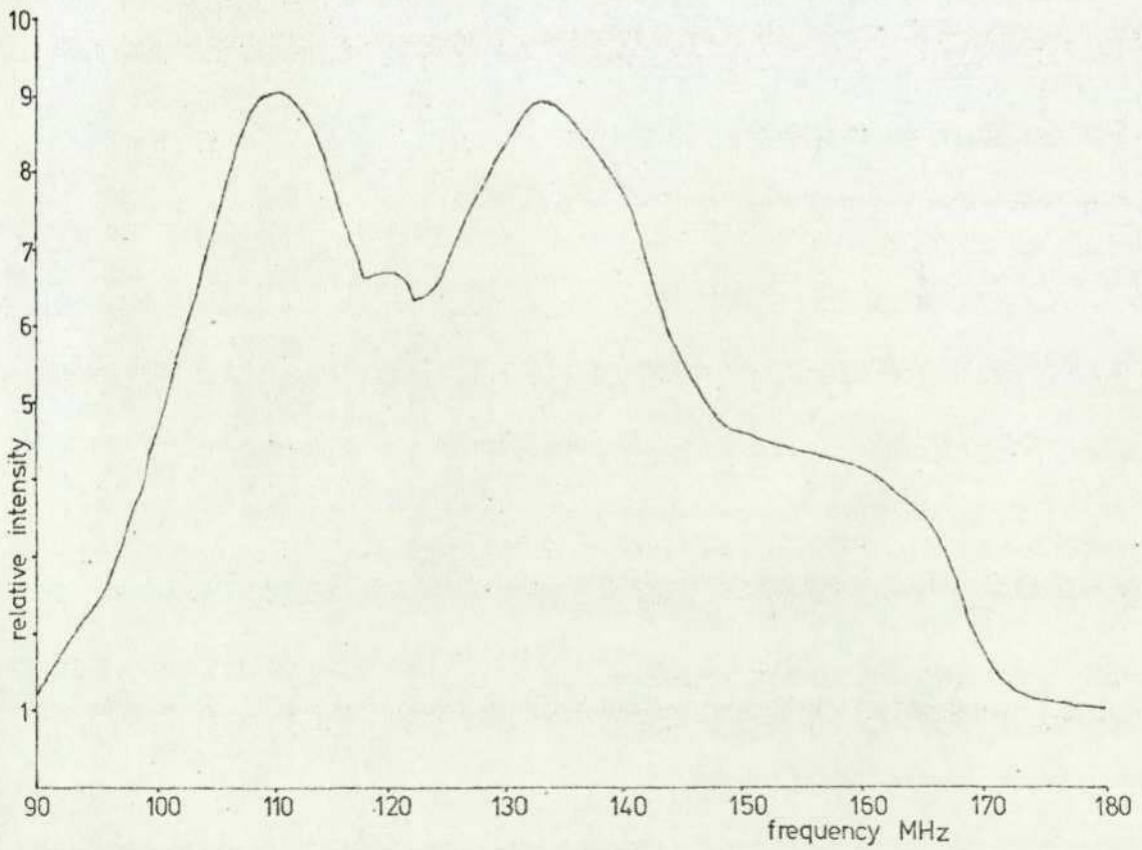

Fig. 8.6.2.3.6. Bandwidth of vertical first order of Deflector 2 with 4 element transducer array.

mentioned the incident optical beam diameter was limited to no more than 4 mm due to the peculiarities of the $PbMoO_4$ samples, although the device was designed to permit an 8 mm diameter beam. The resolution obtained was thus less than desired.

The composite order displaying 256 spot positions is demonstrated in Plate 8.6.2.4.1. Two stepped frequency generators (Appendix G) were used to control the deflection in each dimension, one of which was adjusted to operate between 120 - 155 M Hz for controlling the vertical deflection and the other was adjusted to between 116 - 149 M Hz for the horizontal deflection. Deflection in the vertical dimension was of a good quality. Even with the 4 mm aperture the deflected spot was not accompanied by any spurious scattered light. Some misalignment had occurred during the fabrication of the horizontally deflecting transducer, however, and some spurious deflections did accompany the deflected spot. This, nevertheless, was not severe and did not interfere to any appreciable extent with the composite spot display. Spot distortion was mainly due to the behaviour of the $PbMoO_4$ sample and the residual distortion produced by the optical components in the system. Some thermal effects were noticed especially with the beam placed near the transducers surfaces. With the incident beam positioned elsewhere these were not noticeable with the low electrical applied power. Due to the low level of deflection efficiency some of the spots are partially obscured by the spacial noise caused by light scattered at the various optical surfaces.

Plate 8.6.2.4.2. shows the display with the stepped frequency generators adjusted to produce 1024 spot positions. The resolution is limited by the aperture and frequency range used. It can be clearly seen that there is some non-linearity in the frequency increments of the generators. In the upper right quadrant the spots are just

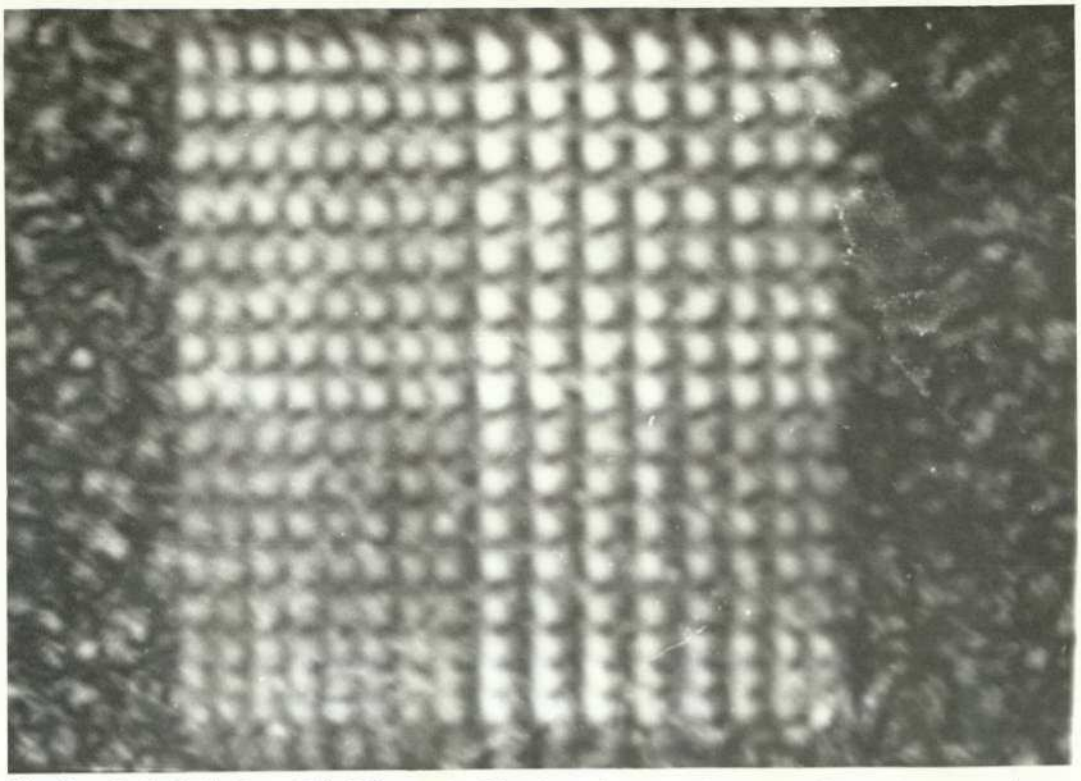

Plate 8.6.2.4.1. 16x16 spot display by Deflector 2. Aperture 4mm, bandwidth 33MHz x 35MHz.

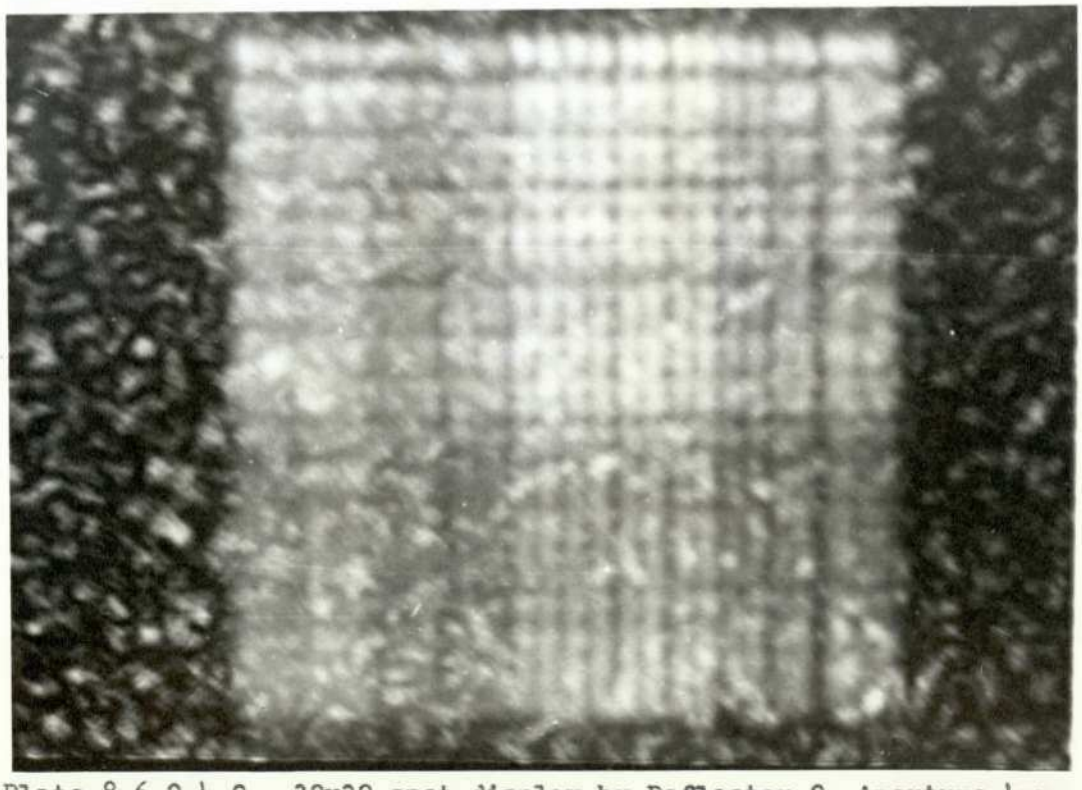

Plate 8.6.2.4.2. 32x32 spot display by Deflector 2. Aperture 4mm, bandwidth 33MHz x 35MHz.

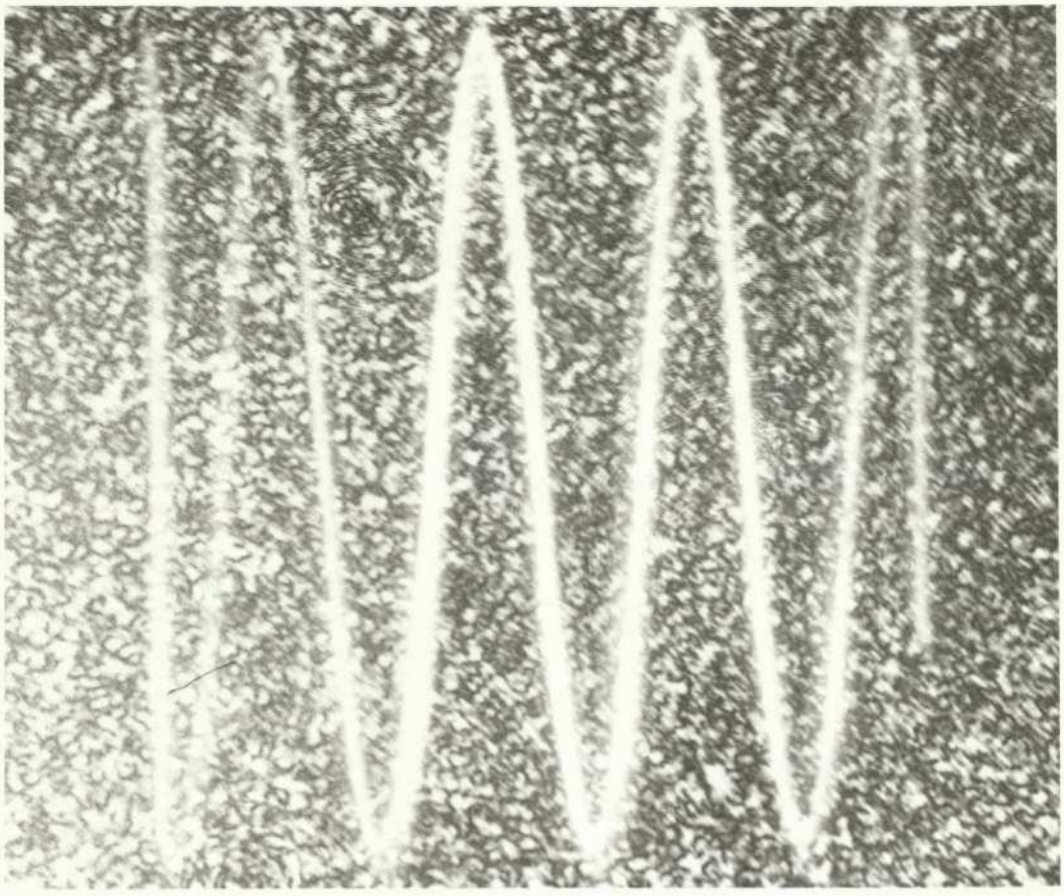

Plate 8.6.2.4.3. Sine wave (400Hz) display by Deflector 2 using full available bandwidth and 4mm aperture.

resolvable while in the lower left quadrant this resolution can not be attained. Again, the intensity of the deflected light is comparable with the quiescent scattering. The deflection speed here was about 10 μs / spot.

To demonstrate the full capacity of the deflector the generators were replaced with two voltage controlled sweep frequency oscillators. The oscillator controlling the vertical deflection was driven with a 400 Hz sine wave signal while the oscillator controlling the horizontal deflection was fed with a sawtooth waveform of 100 Hz. The resulting display is shown in Plate 8.6.2.4.3. The r.f. frequency range in both dimensions was 90 M Hz centred at 130 M Hz in the horizontal and 135 M Hz in the vertical. Although some resolution has been lost in the photographic reproduction process the scale of the deflection and resolution can be inferred from the size of the spacial noise in Fig. 8.6.2.4.3. compared to that in Fig. 8.6.2.4.1. and Fig. 8.6.2.4.2. The available capacity in this instance was of the order of 90 x 90 resolvable spots. Also, unlike Deflector 1, no interference due to cross-coupling was observed with this second device.

9. Discussion

9.1. Introduction

This section commences with a summary of the major aspects of the work undertaken and attempts to relate it to previously reported devices. Some of the aspects relating to device fabrication and performance are discussed in section 9.3. along with the consequent areas of which this work has brought to light. Aspects requiring further investigation are dealt with in section 9.4. and some applications along with the devices' ultimate potential are considered in section 9.5.

9.2. Resume of Work Undertaken

The two-dimensional acousto-optic interaction has been considered in section 3. Where the two sound columns are mutually perpendicular it has been shown that not only is the intrinsic deflection efficiency the same as that of a properly aligned cascaded system, as described by LaMacchia and Coquin (1971) and Chu and Mauldin (1973), but also that the behaviour of the composite order is intrinsically the same in all other respects as well. The interaction is the product of two single-dimensional interactions as given by Eq. 3.3.14 thus allowing the performance of a device, in each co-ordinate, to be designed independently. There is no fundamental reason why the interaction efficiencies should be the same in each co-ordinate however, as stated by LaMacchia and Coquin (1971), apart from mere preference. It is noted that the intensities of the various orders may be related in the form given by Eq. 3.3.15 ,

i.e.

$$I_{00} \cdot I_{11} = I_{01} \cdot I_{10} \qquad \text{(Eq. 3.3.15)}$$

This holds true whether the bragg deflection is exact or otherwise. The effects produced by misalignemt between the two acoustic columns has been illustrated in section 3.6. The most significant form of misalignment is with respect to the orthogonality of the two sound columns, given the premise that bragg deflection is satisfied in each co-ordinate. For the two sound columns orientated other than at 90^{o} with respect to each other the deflection efficiency into the composite order will be degraded and the degradation rapidly increases as the acoustic frequency increases. The interaction has also been considered in terms of the integral equation method which illustrates the conservation of momentum and shows that, for a symmetrical gaussian beam, the dimensions of the two-dimensional interaction volume are related to the optical beam size, i.e. $H = D \simeq Wo$, where D and H are the cross-sectional dimensions of the interaction volume and Wo is the waist of a symmetrical gaussian optical beam.

The interaction bandwidth for various transducer geometries has been considered. The acousto-optic interaction has been analyzed for a planar transducer array and a tilted array as well as for a single transducer and stepped transducer array. Results for the planar transducer array are similar to that given by Alphonse (1975). The available bandwidth is given by,

$$\Delta f = 2 (1 + 2K')^{\frac{1}{2}} f_{BM} \qquad \text{(Eq. 3.8.2.10)}$$

with a centre frequency,

$$f_C = (m + 2K')^{\frac{1}{2}} f_{BM} \qquad \text{(Eq. 3.8.2.5.)}$$

f_{BM} is the minimum bragg frequency and m is the number of transducer elements. K' relates the decrease in intensity at the centre frequency.

Design modifications are given with respect to the stepped array for use with liquids. These modifications have resulted in the step being equal to P' half wavelengths in height, where

$$p' = \frac{n}{\left(1 - v_l / v_m\right)} \qquad \text{(Eq. 3.8.4.6.)}$$

and where the transducer elements are driven with a phase increment of $n\pi$ radians with respect to their neighbour. The use of a tilted transducer array for bulk deflectors has been considered to be impractical in relation to presently available technology.

The theoretical arguments considered in this work are not only relevant to a two-dimensional deflector but may also be extended to include a cascaded deflector system since the condition that the two sound columns should overlap is arbitary.

The necessary considerations regarding the generation of bulk acoustic waves from piezo-electric platelets are discussed in section 4. Although such work has been covered elsewhere in the literature (i.e. Foster et al 1969) it has been put in a form suitable for the work undertaken here. The analysis includes derivation of the acoustic wave velocity, particle displacement angle, coupling factors, admittance, and insertion losses.

The properties of the interaction and transducer materials have been discussed in section 5. The acoustic properties of the two crystalline materials used in this work, lithium niobate and lead molybdate, have been illustrated. X-ray laue patterns are given for both materials and the orientation directions of the lithium niobate for obtaining an oblique transducer cut are identified.

Some of the basic practical considerations relating to various aspects in the fabrication of acousto-optic devices are reviewed in section 6, and the appropriate aspects in relation to this work have

been outlined. The methods of bonding have been reviewed as have the methods of transducer fabrication. Heat sinking and film adhesion, as well as the methods adopted for transducer reduction and polishing the lead molybdate samples have been considered.

The interaction has been initially demonstrated using water as the interaction medium in section 7. Although the devices' performance was not as good as that desired its construction illustrated some of the problems that would exist in fabricating a higher frequency device, especially in view of the practical limitations that were imposed on the author. These problems were of bonding and of transducer fabrication. Nevertheless, the device demonstrated that deflection of light into the composite order at a reasonable efficiency could be achieved in contrast to that achieved by Uchida and Iwasaki (1969) and also that a capacity could be achieved as opposed to single spot deflection as demonstrated by Chu and Mauldin (1973).

In section 8, a description of the authors' attempts at trying to achieve improved bonding, as well as a description of the two devices that were constructed using lead molybdate, is given. Limited to the use of epoxy resin or phenyl salicylate as the bonding material the performance and properties of a transducer bonded to glass using these materials are discussed and compared. Also included is the authors' attempt, although unsuccessful, to produce a metallic bond using solder as the bonding medium and to simulate the ultrasonic bonding method (i.e. Larson and Winslow 1971) by driving the transducer during the bonding period. Two two-dimensional acousto-optic deflectors using lead molybdate as the interaction medium have been constructed using each of the bonding materials available to the author. Deflector 1 used epoxy resin as the

bonding material and the performance of the device was poor due to the dire condition of the transducers and the excessive losses of the bonds. The deflector, however, admirably demonstrated the thermal effects caused by the losses and exhibited a certain amount of cross-coupling between the two transducers. The efficiency and bandwidth was limited by the effects of the bonds and the transducers conditions. Deflector 2 was thus constructed to try and improve the situation. Here the bonding material was phenyl salicylate and the two sound columns were derived from planar transducer arrays. The temperature dependence of the bonding material limited the amount of power supplied to the device and thus limited the amount of light that could be deflected. Its improved performance, however, allowed a reasonable bandwidth to be achieved and thermal effects were not a predominant problem. A capacity of about 90 x 90 just resolvable spot positions could be achieved using only half the available optical aperture and is slightly greater than that achieved by Uchida and Ohmachi (1970) using paratellurite (TeO_2). The full aperture could not be used due to peculiarities associated with the lead molybdate samples. Coupling between the two transducers was not observed with this second device. These two devices also show that the figure of merit, M_2, associated with diffraction of light polarized in the plane $z = 0$ caused by sound propagating in the same plane, also increases for low optical wavelengths and its increase is comparable with that associated with diffraction for z-propagating sound (DeBenedictis and Lucero 1974).

9.3. Aspects Relating to Device Fabrication and Performance

One of the main problems that has existed throughout this work has been that of bonding and is a topic which is not only relevant

to the two-dimensional deflector but also to all other aspects of acousto-optics as well. Although epoxy resin and phenyl salicylate are not suitable for a practical device they have nevertheless been used here since these materials were the only bonding agents that did not require the use of a high technology process. The performance of the departments' vacuum plant was also a factor which limited the scope of experimentation regarding this aspect. The catastrophic condition of the transducers associated with deflector 1 indicates that bonding processes requiring the use of elevated temperatures are not suitable for attaching lithium niobate transducers to lead molybdate. The most suitable bonding method is therefore that of cold weld vacuum bonding (Sittig and Cook 1968), to eliminate any thermally induced stresses. The method of ultrasonic bonding, for example, would not be suitable for the bonding purposes required here since the strength of the lithium niobate platelet would be insufficient to tolerate the stresses caused by the difference between the thermal expansion of the lead molybdate and the transducer. It was thus fortunate that the phenyl salicylate bonds did not solidify until close to room temperature.

Other workers have reported that their bonding methods have been developed to a state of maturity, in particular the cold weld vacuum bond using indium (Alphonse 1975) and an optical-contact bond method using gold (Eschler 1975). The fabrication of two transducers onto a single medium should not then adversely affect device yield as suggested by LaMacchia and Coquin (1971) and the manufacturing process should be no more complex than that in the fabrication of single-dimensional deflectors. Failure during fabrication of one transducer should not affect the condition of the other and thus replacement of the failed transducer should constitute little problem.

Although it has been reported elsewhere that satisfactory bonding using epoxy resin has been achieved for transducers operating above 100 M Hz (i.e. Chang 1976) the success relies on obtaining clean and flat surfaces to achieve ultra-thin bonds. The bonding process must include the resources for grinding, polishing, cleaning, and electrode deposition as well as working in a clean environment. The success of the bonding procedure is inevitably as good as the 'weakest link' in these processes. Although a certain level of cleanliness could be achieved with care the grinding and polishing processes allowed surfaces to have a curvature of no better than 1 - 2 μm . Contamination of evaporated films was also a problem and these additional factors ultimately limited the success and performance of the bonded transducers associated with this work.

Although the method of cleaning the material surfaces during this work, as discussed in section 7.3., may have been insufficient and the reduced adhesion of the deposited films may have contributed to a small extent to the losses the method was considered adequate in view of the other factors which limited the ultimate quality of the process. A more rigorous cleaning method has been discussed by Johnson (1976) and may be more suitable where well established fabrication techniques are employed.

A problem associated with acousto-optic deflectors is thermal stability. This problem also exists for the two-dimensional deflectors. Here there are the additional factors that losses occur at two surfaces (those to which the transducer is bonded) and that an increased power density due to the presence of two sound columns instead of one exists within the interaction medium. Both the transducer losses and the losses due to attenuation associated with

each acoustic wave contribute to heating. Both the refractive index and acoustic velocity are temperature dependent (Coquin et al 1971) and together with optical losses these will affect the beam position, beam shape, efficiency, and deflection angle. It is acknowledged that the heat sinking arrangment associated with Deflector 1 was inadequate for the power levels applied. However, the losses were almost entirely due to the bonding losses and thus in this case bonding was the predominant problem. Deflector 2 only allowed a limited power to be applied but here again over three-quarters of the power was lost at the transducer boundary. These losses could not be adequately anticipated and, with the silver paste top electrodes, the arrangement did not lend itself for removing heat from the transducers back surfaces (i.e. Heynau and Barnard 1971). Although heat sinking is inevitably an important aspect the primary problem here was to first generate an acoustic wave with reasonable efficiency. Even for Deflector 2 less than 20% of the applied electrical power appeared as acoustic power.

It has been mentioned that the lead molybdate samples appeared to be twinned. In retrospect, it would have been advantageous to briefly polish the surfaces normal to the crystallographic z axis, as identified from the X-ray laue photograph prior to further cutting. The materials' quality may then be assessed by viewing the material between crossed polarizers with monochromatic light (Bonner and Zydzik 1970). The anomalies would then have been observable. However, it is unlikely that this would have altered matters since the deflectors' design requirements required the author to use as much of the limited amount of material as there was available.

The transducers were bonded to the lead molybdate in an arbitary direction in the crystallographic plane, z = 0. Although the figure of merit, M_2, associated with sound propagating in this

plane and light polarized in the plane z = 0 is essentially constant for any orientation the deflection efficiency may be reduced due to losses incurred for some orientations. For directions in the plane z = 0 other than those at 29^{o} and 74^{o} from the x axis in the positive x-y quadrant the particle displacement angle is significant and losses due to mode conversion will result. It is thus desirable to propagate the sound in either of the two directions mentioned. Identification of the x or y axes is difficult to ascertain merely from X-ray studies however and for future devices orientation may be accomplished by observing diffraction produced by the Schaefer-Bergmann method (Spencer et al 1967, Uchida et al 1969) prior to cutting the faces of the material normal to these directions.

Interference, in the form of cross-coupling, between the two transducers was observed with Deflector 1. This coupling, however, was not in evidence with Deflector 2. In the case of Deflector 1 electrodes for both transducers were deposited onto the lead molybdate surfaces and were electrically 'live'. For Deflector 2, however, no electrode deposition was performed on the lead molybdate surfaces and the transducers ground electrodes were isolated from the interaction material by the phenyl salicylate bond. This suggests that the electrical properties of the lead molybdate may be significant, although some coupling may have been due to external means. It is desirable that this coupling should be minimized as much as possible and although screening may be provided to reduce external coupling, coupling through the interaction medium may prove problematic. The effect may be reduced, as perhaps has been achieved here, by introducing a dielectric isolating layer of low permittivity between the transducers bottom electrodes and the interaction medium surfaces. The permissable amount of cross-coupling is, to an extent, dependent on the application for which the device is to be used. If this form

of interference is intolerable then the bandwidths over which the transducers are to operate must be separated . This interference was not noticeable with the water cell device mainly because the transducers operated over two different frequency ranges.

The two-dimensional deflector may be considered as a two-port network. Throughout this work the electrical responses of the transducers have been considered as being isolated from each other. The observed coupling between each transducer indicates that this premise is invalid. The electrical properties may be represented in any form associated with two-port network theory although for devices operating above 100 M Hz the S parameter representation would be most appropriate. The amount of cross-coupling would then be given by the values of S_{12} and S_{21}. For the devices operating below 100 M Hz equipment suitable for measuring the devices' electrical properties in this form were not available. Above 100 M Hz, although equipment existed for this purpose the physical arrangements of the measuring equipment and the final two-dimensional lead molybdate deflector were not compatable. It required the inclusion of transmission lines between the deflectors' and instruments' ports and the cancellation of their effects could not be achieved.

Throughout this work the operational bandwidths of the devices has been limited not by the bandwidth of the acousto-optic interaction but by either the transducer behaviour or by the methods of tuning. For both the water cell and Deflector 1 the delay medium to which the transducer was bonded was disguised by the high acoustic losses of the epoxy bonding layer. The transducers responded as though they were bonded to a delay medium of epoxy rather than that of glass or lead molybdate and this is clearly illustrated by the experimental

device used to examine the bonds' behaviour in section 8.3.1. The losses associated with the phenyl salicylate bonds appear to have been less significant in this respect. Thus for Deflector 2 the bandwidth was more dependent on the extent to which the transducer could be tuned to match the source impedance over the operating frequency range. It is of importance, therefore, to obtain a transducer impedance close to that of the source impedance by using series-connected transducer elements to ease the tuning requirements. Minimising losses incurred by tuning the applied power into the resistances of the electrodes and connecting wires will also be achieved.

Further subdivision of the transducers associated with Deflector 2 would have been desirable but as mentioned in section 8.6.2.3. this was not attempted in view of their delicacy. The planar transducer array, as discussed in section 3.8.2., permits up to 17 elements before the interaction bandwidth is limited to an octave frequency range. Thus further segmentation to eight elements of Deflector 2's transducers would have improved tuning and matching yet not have caused a reduction in the operational bandwidths.

The device necessarily needs transducers of large area. Unlike single-dimensional deflectors where tolerance can be afforded with the dimensions of the transducers' width this dimension here is determined by the optical aperture requirements. For the transducers impedances to match the source impedances for broadband operation it will be of greater necessity for the transducers to be subdivided and for the elements to be series-connected for this case than for the single-dimensional deflector case. The impedance, however, may not increase in proportion to the square of the number of series-connected elements as suggested by Alphonse (1975) since this assumes

that electrical coupling via the interaction medium between the elements base electrodes is negligible. This type of coupling between planar electrodes has been considered by Engan (1969). If the electrical properties of the interaction medium are significant then the impedance will be modified accordingly and may account for the difference in the expected and measured impedances of the four element transducers associated with Deflector 2, as shown in Fig. 8.6.2.1.1.

It has been shown that dispersion of the figure of merit, M_2, and consequently the elasto-optic coefficient, P_{11}, with optical wavelength occurs when diffraction is achieved by sound propagating in the crystallographic plane z = 0 in lead molybdate. It is estimated here that the increase in this figure of merit is about the same, or even slightly greater, than that of the figure of merit, M_2, involved with the diffraction produced by a z propagating acoustic wave (DeBenedictus and Lucero 1974). A measurement, by comparing the diffraction at different optical wavelengths, was not undertaken since the peculiarities of the lead molybdate samples would have provided an erroneous and unreliable result.

9.4. Areas for Further Investigation

A more extensive investigation is required to determine the electrical behaviour of the device. Knowledge of the electrical properties of the interaction medium will be required. Electrical measurements of lead molybdate are thus necessary for a device using this material. Even when using other materials knowledge of the permittivity and loss tangent will be needed and appropriate transducer configurations and the use of an isolating intermediate layer between the transducer and delay medium may then be determined. With

the electrical properties of the interaction medium determined the areas worthy of consideration are the coupling between the transducers base electrodes via the interaction medium to determine the consequent modification to the transducers electrical response and also to determine the extent of the cross-coupling between each transducer. Modifications to the structure of the device may result depending on the outcome of these considerations. It may prove advantageous to consider the device primarily as a two port structure as opposed to two single port networks. The design of the device may then be determined from the point of view of its electrical behaviour to minimise cross-coupling effects.

Where transducer bonding and fabrication techniques have been developed to maturity the paramount problem will be that of thermal stability. As has already been mentioned in section 6.6., the thermal behaviour of single-dimensional deflectors has already been extensively studied by Eschler (1976). Application of the work presented there to a two-dimensional deflector would thus yield valuable clues concerning the most favourable geometry of the deflector. He has also introduced a dielectric intermediate material between the transducer and interaction material to aid in the heat sinking and to help in isolating the transducer losses from affecting the acousto-optic diffraction by localised heating. The use of an intermediate material, with regard to a two-dimensional deflector may also help in reducing the electrical cross-coupling besides improving heat dissipation and is an aspect worthy of further investigation.

The geometry of the devices considered in this work were determined by the desired capacity, efficiency, and frequency ranges together with the availability of the appropriate materials. The latter consideration made it necessary to place the two transducers in

close proximity to each other. With regard to thermal considerations and electrical coupling it may be desirable to use more interaction medium than required and to place the transducers so that a reasonable distance exists between each transducer and the 'common edge'. The optical beam would then have to be positioned a distance away from the two transducers and the effect of their losses may be reduced. The device geometry should then be deduced not only from the nature of the acousto-optic interaction but also in terms of the conditions regarding heat dissipation and electrical behaviour to determine the optimum arrangement.

Improvements in bonding and transducer fabrication are areas which require continued investigation. Low-loss bonds and accurate transducer fabrication are aspects which need development to maturity for any practical device and these become increasingly critical as higher frequency operation becomes necessary. The transducers' bandwidth is not only dependent on the effects of electrode and bonding layer thicknesses, as shown by Sittig (1969) but also on the acoustic attenuation of the materials, as illustrated in section 8.3. Thus for devices operating up to 1 G Hz the development of fabricating and bonding techniques and the search for suitable low loss materials may still continue. Transducer fabrication and bonding have been discussed in sections 6.2. and 6.4. and gives an account of the level to which the subject has reached.

The use of alternative solid materials besides lead molybdate may also be considered. All isotropic materials are potentially applicable for use as the interaction medium for a device of this nature operating under normal bragg diffraction conditions. Crystalline materials must have suitable material parameters in orthogonal directions however. Classification of materials using the figure of

merit $M_i(X-Y)$ may be helpful in their selection. Lists of suitable materials for acousto-optic diffraction may be found in section 5.2.

The device may be extended to include the use of birefringent materials. A two-dimensional deflector has previously been demonstrated using a material (TeO_2) which exhibits abnormal or anisotropic diffraction (Uchida and Ohmachi 1970). The extension of thedevice using materials suitable for operating under this condition has already been discussed in section 3.9. Apart from paratellurite, most suitable materials require the use of fairly high operating frequencies (> 100 M Hz). So long as the material has the appropriate parameters and the processes involved in producing high frequency transducers are well established the realisation of a two-dimensional deflector using materials operating in this mode may be investigated.

9.5. Applications and Device Potential

The lead molybdate Deflector 2 described in this work has demonstrated a capacity of about 90 x 90 just resolvable spot positions using a 4 mm optical aperture and operating over a bandwidth, in each co-ordinate, of 90 M Hz. But for the peculiarities of the lead molybdate samples and some difficulty in tuning the transducers to operate over a larger bandwidth a capacity of about 200 x 200 spot positions would have been realised using an 8 mm optical aperture. Using the planar transducer array and with reduced transducer losses to about 1 - 2 dB a deflection efficiency of 70% in each co-ordinate would have been possible with the application of 0.7 watts and 1 watt to the transducers associated with the z propagating and x or y propagating acoustic columns respectively using the He-Cd 441.6 nm wavelength light.

The materials' usefulness is limited by the permissable acoustic attenuation across the optical aperture of the device (Pinnow 1970, Coquin et al 1971). For lead molybdate the material is limited to an upper acoustic frequency of about 500 M Hz. Using the same geometrical arrangement as for Deflector 2 the maximum capacity that could be achieved over a fractional bandwidth of 0.79 would be about 400 x 400 just resolvable spot positions. Although two samples were cut from the lead molybdate boule it could have been possible to obtain only a single sample of dimensions 2.4 x 1.2 x 1.2 cm. For transducer dimensions of 2.2 x 1 x 1 cm a 1 dB increase in the deflection efficiency would have resulted and the increased optical aperture would have provided a 2.5μs access time. However, the resolution would be limited to about the same as before due to the bandwidth being limited by the behaviour of the planar arrays. Thus it would appear that the potentially realisable resolution using this material will be limited to around 400 x 400 resolvable spots, using a transducer length to width ratio of 2 to 1, unless a stepped transducer array is utilised. The resolution may be increased by decreasing the length to width ratio of the planar array but only at a sacrifice to the deflection efficiency.

The obtainable resolution is sufficient for the device to be applied to numerous applications. Hrbek and Watson (1970) have used two acousto-optic deflectors to generate a seven by five spot array simultaneously for producing alpha-numeric characters. The two-dimensional deflector is aptly suited for this low resolution application. Where cascaded systems have been employed in applications such as holographic data storage systems (i.e. Anderson 1968, Pinnow and Williamson 1969, LaMacchia 1970) the two-dimensional deflector has sufficient resolution and speed to directly replace the original deflection system. Also, interference due to cross-coupling associated

with the two-dimensional deflector may not be too problematic if it is below a certain threshold level. However, it is of the utmost importance that thermal stability is maintained in applications of this nature and this may prove to be one of the two-dimensional deflectors' drawbacks. Several memory systems have been proposed in which a two-dimensional deflector may be wholly, or in part, employed as the deflection element within the system (Smits and Gallaher 1967, Rajchman 1970, Lohman 1971).

For laser television and facsimile displays the two-dimensional deflectors' resolution may only reach that required for these applications at the expense of decreased efficiency if planar transducer arrays are used or by increased fabrication complexity if stepped arrays are employed. Although such systems have been described (i.e. Korpel et al 1966, Korpel et al 1969) using single-dimensional deflectors whose resolutions were within that already mentioned, at present, single-dimensional deflectors are now available with resolutions in excess of 1000 and it is unlikely that the two-dimensional deflector will be able to compete directly, in terms of capacity and efficiency, with cascaded systems using these presently available devices. However, it has been shown by Foster et al (1970) that the capacity of a low resolution deflector may be greatly increased when displaying television type encoded information by using a travelling wave acoustic lens. It has been shown that an increase in the resolution of over ten to one can be achieved for one-dimensional line scan optical systems. Thus the two-dimensional deflector may still be able to be applied to this application when incorporated with a travelling acoustic lens, extended to include deflection in both co-ordinates. The resolution demonstrated by Deflector 2, as shown in Plate 8.6.2.4.3. shows that a sufficient capacity can be achieved for the device to be used directly for oscillographic purposes however.

The two-dimensional deflector is ideally suited for use in two component laser doppler velocimeter systems (Farmer and Hornkohl 1973). Used as a beam splitter and frequency shifter the device is superior to that of cascaded systems since all four orders appear to be deflected from a common origin and alignment problems are largely eliminated. Although single frequency operation has been used in previous systems some capacity may be used if required in future systems where more complex signal processing techniques are employed.

The device may also be applied to perform single-dimensional deflection. Using passive optical components the vertical deflection could be transformed into the horizontal plane so that the resolution of the horizontally deflected beam would be greatly increased without adversely affecting the access time. Although this method may prove complex high resolution can be achieved without sacrificing a high speed.

An alpha-numeric display, as demonstrated by Uchida and Ohmachi (1970) using their paratellurite two-dimensional deflector, was intended to be demonstrated using the deflectors constructed during this work. The performance of Deflector 2 together with the stepped frequency generators allowed about 32 x 32 just resolvable spot positions to be displayed as shown in Plate 8.6.2.4.1. and Plate 8.6.2.4.2. It was intended to control the stepped frequency generators from the departments' FM1600B computer via a fast data transfer unit to display an array of 5 x 4 characters. However, failure of certain aspects of the computers' hardware prohibited this exercise to be conducted although the appropriate software was developed to permit the device to perform this function. Nevertheless, alpha-numeric display applications is a function to which the device may possibly be applied.

As to whether the two-dimensional deflector presents a viable

proposition to replace cascaded deflector systems in some applications depends upon the demands of the application. It is unfortunate that the practical difficulties encountered during this work did not permit the construction of a device whose performance, with regard to transducer losses and material quality, was comparable with that which has been attained elsewhere with single-dimensional deflectors. Only when this can be achieved can the two deflection systems be adequately compared and a rational appraisal made. However, from the work undertaken here the potential of a single device x,y deflector may be envisaged to an extent. The compactness of the single device may prove more attractive than a cascaded system in applications where moderate efficiency, capacity, and speed are required so long as the deivces' thermal behaviour and electrical interference are not problematic. For applications that demand high resolution (> 500 spots) and high efficiencies the choice of a cascaded system may still predominate.

10. Conclusion

A two-dimensional acousto-optic light deflector using lead molybdate as the interaction material has been realised, operating under normal bragg conditions in each co-ordinate. Although restricted by fabrication difficulties and material quality the performance of a device constructed by the author has allowed a resolution of about 90 x 90 spot positions to be demonstrated, albeit at a low deflection efficiency, with an access time of about 1 μs in each dimension. The theoretical analysis has shown that for the single device deflector the behaviour of the deflected composite order is, for propertly aligned transducers, the product of two single-dimensional deflections.

It has been unfortunate that due to fabrication difficulties and material quality the devices constructed were unable to be operated to their full advantage. However, it is hoped that the potential of such a device may be envisaged from the results of this present study.

The theoretical work has revealed that composite order deflection, although a rescattering process, will occur so long as the conservation of momentum is accomplished between the acoustic and optical wave vectors and that the propagation directions of the two acoustic columns are correctly aligned. The experimental devices have demonstrated that thermal stability may prove problematic in any practical device and has also uncovered the potential problem of electrical cross-coupling between each transducer. Modification to the devices' construction and fabrication and also its electrical representation may be required pending further investigation.

It is concluded, however, that the two-dimensional deflector appears to qualify for its place within the family of acousto-optic devices and has potential applications where moderate resolution and

efficiency can be tolerated. Lead molybdate has proved to be a suitable material for this device. Nevertheless, it appears unlikely that the device will be able to compete in its own right with cascaded systems in applications where both high resolution and efficiency are required.

Acknowledgements

The provision of research facilities by the head of the Electrical and Electronic Engineering Department, [redacted], and the financial assistance provided by the Science Research Council for the three year period is gratefully acknowledged.

I would like to especially thank Mr. R. J. Webb for his supervision throughout this work and to my colleagues in the computer engineering group who provided the necessary motivation and progressive influence for this work to be completed.

I would also like to thank [redacted] for interesting discussions on X-rays and Hi-Fi, [redacted] for allowing the use of the Mechanical Engineering Departments' polishing facilities, and [redacted] and Rank Xerox Ltd for use of crystal cutting equipment to cut the lead molybdate samples.

Acknowledgements go to [redacted] for her patience and skill in typing this thesis.

A special acknowledgement is given to [redacted] for keeping me alive during this period.

References

Abrahams, S. C. Levinstien, H. T., Reddy, J. M., 1966, 'Ferro-electric Lithium Niobate 5 ; Polycrystal X-ray studey between 24^{o}c and 1200^{o}c', J. Phys. Chem. Solids, Vol. 27, June - July, pp 1019 - 1026.

Adler, R., 1967, 'Interaction between light and sound' IEEE Spectrum, May, pp 42 - 54.

Alphonse, G. A. 1975, 'Broadband Acousto-optic Deflectors : New Results'. Appl. Optics, Vol. 14, No 1, January, pp 201 - 207.

Anderson, L. K., 1968, 'Holographic optical memories for bulk data storage', Bell. Lab. Rec., Vol 46, November, pp 318 - 325.

Baker, C. E., 1968, 'Laser Display Technology', IEEE Spectrum, December, pp 39 - 50.

Beecham, D., 1969, 'Sputter machining of piezo-electric transducers', J. Appl. Physics., Vol. 40, No. 11, October, pp 4357 - 4361.

Beiser, L, 1974, 'Laser scanning systems', in Laser Applications, Vol. 2., Edited by M. Ross, Academic Press.

Bennett, G. A., Wilson, R. B., 1966, 'Precision polishing technique for optics and microwave acoustics', J. Sci. Instrum., Vol. 43, pp 669 - 670.

Berlincourt, D.A., Curran, D. R., Jaffe, H. 1964, 'Piezo-electric and piezo-magnetic materials and their function in transducers', Physical Acoustics, Vol. 1, Part A, Edited by W. P. Mason.

Bonner, W. A., Zydzik, G. J., 1970, 'Growth of single crystal lead molybdate for acousto-optic applications', J. Crystal Growth, Vol. 7, pp 65 - 68.

Born, M., Wolf, E.,1959,'Principles of Optics',New York, Pergamon.

Chang, I. C., Hecht, D. L., 1975, 'Doubling acousto-optic deflector resolution utilising 2nd order birefringent diffraction', Appl. Phys. Lett., Vol. 27, No. 10, November, pp 517 - 518.

Chang, I. C., 1976, 'Acousto-optic devices and applications', IEEE Trans. Sonics and Ultrasonics, Vol. SV-23, No. 1, January pp 2 - 22.

Chen, F. S., et al, 1966, 'Light modulation and beam deflection with Potassium Tantalate Niobate crystals', J. Appl. Phys., Vol. 37, January, pp 388 - 398.

Chu, W. P., Mauldin, L. E., 1973, 'Bragg diffraction of light by two orthogonal ultrasonic waves in water', Appl. Phys. Lett., Vol. 22, No. 11, June, pp 557 - 559.

Cohen, M. G., Gordon, E. I., 1965, 'Acoustic beam probing using optical techniques', Bell system Tech. J., Vol. XLIV, April, pp 693 - 721.

Coquin, G. A., Griffin, J. P., Anderson, L. K., 1970, 'Wideband acousto-optic deflectors using acoustic beam steering', IEEE Trans. Sonics and Ultrasonics, Vol. SU-17, No. 1, January, pp 34 - 40.

Coquin, G. A., Pinnow, D. A., Warner, A. W., 1971, 'Physical properties of lead molybdate relevant to acousto-optic device applications', J. Appl. Phys., Vol. 42, No. 6, May, pp 2162 - 2168.

C.R.C. Handbook, 1973, 'Handbook of tables for applied engineering science : 2nd edition', Edited by R. E. Bolz and G. L. Tuve, The Chemical Rubber Company, Cleveland, Ohio.

Damon, R. W., Maloney, W. T., McMahon, D. H., 1970, 'Interaction of light with ultrasound : Phenomena and applications', Physical Acoustics, Vol. 7, Edited by W. P. Mason and D. N. Thurston, Academic Press.

De Benedictis, L. C., Lucero, J. A., 1974, 'Optical polarization sensitivity of Lead Molybdate', Appl. Phys. Lett., Vol. 25, No 1, July, pp 62 - 64.

Dixon, R. W., 1967a, 'Acoustic diffraction of light in anisotropic media', IEEE J. Quantum Electron., Vol QE-3, February, pp 85 - 93.

Dixon, R. W., 1967b, 'Photo-elastic properties of selected materials and their relevance for applications to acoustic light modulators and scanners', J. Appl. Phys., Vol. 38, December, pp 5149 - 5153.

Drozhzhin, A., Kosovskii, L., Mikhailova, L., 1975, 'Acousto-optic light deflector with 50 positions', Sov. J. Quant. Electron., Vol. 4, No. 7, January, pp 887 - 889.

Engan, H., 1969, 'Excitation of elastic surface waves by spatial harmonics of interdigital transducers', IEEE Trans. Electron. Devices, Vol. ED-16, No. 12, December, pp 1014 - 1017.

E.N.I. Product Bulletin, 'Model 400 AP RF Power Amplifier', Electronic Navigation Industries Inc., 3000 Winton Road South, Rochester, New York, 14623.

Eschler, A., 1976, 'Performance limits of Acousto-optic light deflectors due to thermal effects', Applied Physics, Vol. 9, pp 289 - 306.

Farmer, W. M., Hornkohl, J. O., 1973, 'Two component, self-aligning laser vector velocimeter, Appl. Optics, Vol. 12, No. 11, November, pp 2636 - 2640.

Federov, F. I., 1968, 'Theory of elastic waves in crystals' Plenum Press, New York.

Foster, N. F., et al, 1968, ' Cadnium Sulphide and zinc oxide thin film transducers', IEEE Trans. Sonics and Ultrasonics, Vol. SU-15, No. 1, January, pp 28 - 41.

Foster, L. C., Crumley, C. B., Cohoon, R. C., 1970, 'A high resolution linear optical scanner using a travelling wave acoustic lens', Appl. Optics, Vol. 9, No. 9, September, pp 2154 - 2160.

Fowler, V. J., Schlafer, J. S., 1966, 'A survey of laser beam deflection techniques', Proc. IEEE, Vol. 54, No. 10, October, pp 1437 - 1444.

Fukomoto, A., Watanabe, A., 1970, 'Liquid materials and their figure of merit as acousto-optic deflector', Japan J. Appl. Phys., Vol. 9, No. 6, June, pp 662 - 665.

Gordon, E. I., 1966, 'A review of acousto-optic deflection and modulation devices', Proc. IEEE, Vol. 54, No. 10, October, pp 1391 - 1400.

Gottlieb, M., et al, 1974, 'Acousto-optic properties of some chacogenide crystals', J. Appl. Phys., Vol. 45, No. 12, December, pp 5145 - 5151.

Haydl, W. H., Blötckjaer, K., Quate, C. F., 1964,' Coupling to hypersonic waves', J. Acoust. Soc. Am., Vol. 36, September, pp 1670 - 1677.

Heynau, H. A., Barnard, G. M., 1971, 'An efficient 500 spot acousto-optic deflector', Proceedings of the Technical Program, Electro-optics '71 International Conference, Industrial and Scientific Conference Management Inc., Illinois, pp 146 - 152.

Holland, R., Eernisse, E. P., 1969, 'Design of resonant piezoelectric devices', Research monograph No. 56, The M.I.T. Press, Cambridge, Massachusetts and London, England.

Hrbek, G., Watson, W., 1970, 'A high speed laser alpha-numeric generator', Electro-optical systems design conference, New York, September.

Huang, H. C., et al, 1974, 'Fabrication of submicron $LiNbO_3$ transducers for microwave acoustic (bulk) delay lines', Appl. Phys. Lett., Vol. 24, No. 3, February, pp 109 - 111.

I.R.E. Standards on Piezo-electric crystals, 1949, Proc. I.R.E., Vol. 37, December, pp 1378 - 1395.

Johnson, M. 1976, 'Doped crystals for integrated optics : Investigation by guided wave probe', Ph.D. thesis, University College, London.

Jeffreys, H., 1931, 'Cartesian Tensors', Cambridge University Press, New York, Ch. 1, pp 1 - 11.

Kim, B., Tsai, C. S., 1976, 'High Performance guided-wave acousto-optic scanning devices using multiple surface acoustic waves', Proc. IEEE, Vol. 64, No. 5, May, pp 788 - 793.

Klein, W. R., Cook, B. D., 1967, 'Unified approach to ultrasonic light diffraction', IEEE Trans. Sonics and Ultrasonics, Vol. SU-14, July, pp 123 - 124.

Kulcke, W., et al, 1966, 'Digital light deflectors', Proc. IEEE, Vol. 54, No. 10, October, pp 1419 - 1429.

Knox, J. D., 1973, 'A room temperature non-indium metallic bond tested by welding acoustic shear-wave transducers to paratellurite', R.C.A. Review, Vol. 34, June, pp 369 - 372.

Korpel, A., et al, 1966, 'A television display using acoustic deflection and modulation of coherent light', Proc. IEEE, Vol. 54, No. 10, October, pp 1429 - 1437.

Korpel, A., Lotsoff, S. N., Whitman, R. L., 1969, 'The interchange of time and frequency in television displays', Proc. IEEE, Vol. 57, No. 2, February, pp 160 - 170.

Kossoff, G., 1966, 'The effects of backing and matching on the performance of piezo-electric ceramic transducers', IEEE Trans. Sonics and Ultrasonics, Vol. SU-13, No. 1, March, pp 20 - 30.

LaMacchia, J. T., 1970, 'Optical memories : A progress report', Laser focus, Vol. 6, February, pp 35 - 39.

LaMacchia, J. T., Coquin, G. A., 1971, 'Simultaneous X,Y Acousto-optic deflections', Proc. IEEE, Vol. 59, No. 2, February, pp 304 - 305.

Larson, J. D., Winslow, D. K., 1971, 'Ultrasonically welded piezo-electric transducers', IEEE Trans. sonics and ultrasonics, Vol. SU-18, No. 3, July, pp 142 - 152.

Ley, J. M., Parrish, A. T., Widdis, F. C., 1971, 'The preparation of electro-optic crystals for use in laser modulation', The City Univeristy, Dept. Elect. and Electron. Eng., report, March.

Lohman, R. D., Mezrich, R. S., Stewart, W. C., 1971, 'Holographic mass memory's promise : Megabits accessible in microseconds', Electronics, Vol. 18, January, pp 61 - 66.

Mahajan, V. N., 1975, 'Diffraction of light by sound waves of arbitary standing wave ratio', J. Appl. Phys., Vol. 46, No. 9, September pp 3707 - 3709.

Mason, W. P., 1958, 'Physical acoustics and the properties of solids', D. Van Nostrand Company Inc., Princeton, New Jersey, London.

Matthaei, G. L., 1964, 'Tables of chebyshev impedance transforming networks of low-pass filter form', Proc. IEEE, Vol. 52 , No. 8 , August,pp 939 - 963, also 'Microwave filters, impedance matching networks, and coupling structures', New York, Plenum, 1964.

Maydan, D., 1970, 'Acousto-optical Pulse Modulators', IEEE J. Quantum Electroncis, Vol. QE-6, No. 1, January pp 15 - 24.

McMahon, D. H., 1969, 'Relative efficiency of optical bragg diffraction as a function of interaction geometry', IEEE Trans. sonics and Ultrasonics, Vol. SU-16, No. 2, April, pp 41 - 44.

McSkimin, H. J., 1957, 'Use of high frequency ultrasound for determining the elastic moduli of small specimens', I.R.E. Trans. Ultrason. Eng., Vol. VE-5, August, pp 25 - 43.

Meitzler, A. H. 1971, 'Piezo-electric transducer materials and techniques', in 'Ultrasonic transducer materials', Ed. by Mattiat, O.E., Plenum, New York.

Milek, J. T., Neuberger, M., 1972, 'Handbook of electronic materials : Linear electro-optic modulator materials', Vol. 8., Plenum, London.

Mitchell, R. F., 1972, 'Generation and detection of sound by distributed piezo-electric sources', Phillips Res. Repts. Suppl., No. 3.

Morse, P. M. Feshbach, H., 1953, 'Methods of theoretical physics', McGraw Hill Book Company, New York, Toronto, London.

Musgrave, M. J. P., 1970, 'Crystal Acoustics : Introduction to the study of elastic waves and vibrations in crystals,' Holden-Day Press, San Francisco, Cambridge, London, Amsterdam.

Nassau, K., Levinstien, H. J., Loiacono, G. M., 1966a, 'Ferro-electric Lithium Niobate 1 ; Growth domain structure dislocations and etching', J. Phys. Chem. Solids, Vol. 27, June - July, pp 983 - 988.

Nassau, K., Levinstien, H. J., Loiacono, G. M., 1966b, 'Ferro-electric Lithium Niobate 2 ; Preparation of single domain crystals', J. Phys. Chem. Solids, Vol. 27, June - July, pp 989 - 996.

Ninomiya, Y., 1973, 'Ultra high resolving electro-optic prism array light deflector', IEEE J. Quant. Electron., Vol. 9, No. 8, August, pp 791 - 793.

Nye, J. F., 1957, 'Physical Properties of crystals', Clarendon Press, Oxford, England.

Obukhovskii, Y. A., et al, 1969, 'A high temperature material for acoustic bonding', Soviet Physics-Acoustics, Vol. 14, No. 4, April - June, pp 525 - 526

Onoe, M., 1962, 'Relationships between input admittance and transmission characteristics of an ultrasonic delay line', I.R.E. Trans. Ultra-son. Eng., Col. UE-9, December, pp 42 - 46.

Papoulis, A., 1968, 'Systems and transforms with applications to optics', McGraw Hill Book Company, New York, Maidenhead.

Parygin, V. N., Chirkov, L. E., 1975, 'Diffraction of light by ultrasound in an anisotropic medium', Sov. J. Quant. Electron., Vol. 5, No. 2, August, pp 180 - 184

Pinnow, D. A., Williamson, S. R., LaMacchia, J. T., 1969, 'Acousto-optic light deflection : The design and operation of a simple X-Y deflection system', J. Opt. Soc. Am., Vol. 15, No. 4, April, pp 490.

Pinnow, D. A., et al, 1969, 'Lead Molybdate : A melt grown crystal with high figure of merit for acousto-optic applications', Appl. Phys. Lett., Vol. 15, No. 3, August, pp 83 - 86.

Pinnow, D. A., 1970, 'Guidelines for the selection of acousto-optic materials', IEEE J. Quant. Electron., Vol. QE-6, No. 4, April, pp 223 - 238.

Pinnow, D. A., 1971a, 'Acousto-optic light deflection'. Design considerations for first order beam steering transducers', IEEE Sonics and Ultrasonics, Vol. SU-18, No. 4, October, pp 209 - 214.

Pinnow, D. A., 1971b, 'Elasto-optical materials', in C.R.C. Handbook of Lasers, Ed. by R. J. Presley, The Chemical Rubber Company.

Quate, C. F., Wilkinson, C. D. W., Winslow, D. K, 1965, 'Interaction of light and microwave sound', Proc. IEEE, Vol. 53, October, pp 1604 - 1623.

Randolph, J., Morrison, J., 1971, 'Modulation transfer characteristics of an Acousto-optic deflector', Appl. Optics, Vol. 10, pp 1383 - 1385 also 'Rayleigh equivalent resolution of acousto-optic deflection cells', Appl. Optics, Vol. 10, pp 1453 - 1454.

Rajchman, J. A., 1970, 'Promise of optical memories', J. Appl. Phys., Vol. 41, pp 1376 - 1383

Reeder, T. M., Winslow, D. K. 1969, 'Characteristics of microwave acoustic transducers for volume wave excitation', IEEE Trans. Microwave theory and Techniques, Vol. MTT-17, No. 11, November, pp 927 - 941.

Schwartz, E., 1968, 'Broadband matching of resonant circuits and circulators', IEEE Trans. Microwave theory and Techniques, Vol. MTT-16, March, pp 158 - 165.

Sittig, E. K., Cook, H. D., 1968, 'A method for preparing and bonding ultrasonic transducers in high frequency digital delay lines', Proc. IEEE, Vol. 56, August, pp 1375 - 1376.

Sittig, E. K., 1969, 'Effects of bonding and electrode layers on the transmission parameters of peizo-electric transducers used in ultrasonic digital delay lines', IEEE. Trans. Sonics and Ultrasonics, Vol. 50-16, No. 1, January, pp 2 - 10.

Sittig, E. K., Warner, A. W., Cook, H. D., 1969, 'Bonded piezo-electric transducers for frequencies beyond 100 M Hz', Ultrasonics, Vol. 7, No. 2, April, pp 108 - 112.

Sittig, E. K., 1972, 'Elasto-optic light modulation and deflection' in 'Progress in optics', Vol. X, Ed. Wolf, North-Holland Publishing Co., Amsterdam.

Smit, F. M., Gallaher, L. E., 1967, 'Design considerations for a semi-permanent optical memory ', Bell syst. Tech.J.,Vol 46, pp 1267-1278.

Spectron, 1976, 'Two-dimensional bragg cell has 32 mm clear aperture', Spectron Development Laboratories Inc., Tullahoma, Tenn., in Laser Focus, No. 7, July, 1976, pp 36.

Spencer, E. G., Lenzo, P. V., Ballman, A. A., 1967, 'Dielectric materials for electro-optic, elasto-optic and ultrasonic device applications', Proc. IEEE, Vol. 55, No. 12, December, pp 2074 - 2108.

Soro Electro-optics, 1974, 'XY Acousto-optic laser deflector DXY', Bulletin MD 821, Soro Electro-optics, 17 Av. du Mal de Lattre de Tassigny, 92100 Boulogne s/Seine, France.

Sullivan, P. F., 1962, 'Bonding methods and a bonding clamp for ultrasonic measurements', J. Acoust. Soc. Am., Vol. 34, No. 12, December, pp 1879 - 1882.

Tiersten, H. F. 1963, 'Thickness vibrations of piezo-electric plates' J. Acoust. Soc. Am., Vol. 35, No. 1, January, pp 53 - 58.

Tsai, C. S., et al, 1976, 'Wideband Guided-wave acousto-optic bragg diffraction and devices using multiple tilted surface acoustic waves', Proc. IEEE, Vol. 64, No. 3, March, pp 318 - 328.

Uchida, N., 1968, 'Elasto-optic coefficients of liquids determined by ultrasonic light diffraction method', Japan J. Appl. Phys. Vol. 7, No. 10, October, pp 1259 - 1266.

Uchida, N., Iwasaki, H., 1969, 'Two-dimensional acousto-optic deflector', Japan J. Appl. Phys., Vol. 8, pp 811.

Uchida, N., Ohmachi, Y., 1969, 'Elastic and photo-elastic properties of TeO_2 single crystal', J. Appl. Phys., Vol. 40, November, pp 4692 - 4695.

Uchida, N., 1970, 'Acousto-optical pattern display using pulse modulated ultrasound', Opto-electronics, Vol. 2, February, pp 43 - 45.

Uchida, N., Ohmachi, Y., 1970, 'Acousto-optical light deflector using TeO_2 single crystal', Japan J. Appl. Phys., Vol. 9, Pt. 1, pp 155 - 156.

Uchida, N., Niizeki, N., 1973, 'Acousto-optic deflection materials and techniques', Proc. IEEE, Vol. 61, No. 8, August, pp 1073 - 1092.

Uchida, N., Fukunishi, S., Saito, S., 1973, 'Performance of single crystal $LiNbO_3$ transducers operating above 1 G Hz', IEEE Trans. Sonics and Ultrasonics, Vol. SU-20, No. 3, July, pp 285 - 287.

Voshol, C. P. L., Spiekerman, A. J. G., 1975, 'Acousto-optic laser beam deflector with modified phased-array transducer', IEEE Trans. Sonics and Ultrasonics, Vol SU-22, No. 2, March, pp. 143.

Warner, A. W., Onoe, M., Coquin, G. A., 1967, 'Determination of elastic and piezo-elastic constants for crystals in class (3m)', J. Acoust. Soc. Am., Vol. 42, No. 6, pp 1223 - 1231

Warner, A. W., Meitzler, A. H., 1968, 'Performance of bonded single crystal $LiNbO_3$ and $LiGaO_2$ as ultrasonic transducers operating above 100 M Hz', Proc. IEEE, Vol. 56, August, pp 1376 - 1377.

Warner, A. W., White, D. L., Bonner, W. A., 1972, 'Acousto-optic light deflectors using optical activity in paratellurite' J. Appl. Phys., Vol. 43, November,

Wilson, R. B., 1967, 'Precision polishing of thin single crystal layers', J. Sci. Instrum., Vol. 44, February, pp 159.

Wong, D. K. K., 1977, 'Water cell acousto-optic deflector', B.Sc. Project Report No. 970, The City University, Electrical and Electronic Engineering Dept., London.

Wright, S., Wilson, M. G. F., 1973, 'New form of electro-optic deflector'. Electron. Lett., No. 8/9, Vol. 9, May, pp 169 - 170.

Zenith Bulletin, 'DV-150 Voltage Controlled oscillator and D-150R Acousto-optic deflector', Zenith Radio Corporation, 2001N, Janice Ave., Melrose Park, Illinios, 60160.

Appendix A

The Elasto-optical Effect

The refractive index, and hence the permittivity, of a material can be described in terms of the index ellipsiod,

$$B_{ij}\, x_i\, x_j = 1 \qquad i,j = 1 \to 3$$

where x_i are the crystallographic axes and B_{ij} is the impermeability tensor. For an undisturbed crystalline material,

$$B_{ij} = 1/n^2_{ij}$$

which, with respect to the crystallographic axes, is zero for $i \neq j$.

When a strain is applied to the material the impermeability tensor is given by (Nye 1957),

$$B_{ij} = 1 / n^2_{ij} + P_{ijKL}\, S_{KL}$$

where S is the induced strain and P is the elasto-optic tensor. The above may be written in the matrix form,

$$B_i = 1 / n^2_i + P_{ij}\, S_j \qquad i,j = 1 \to 6$$

The index ellipsiod is thus given by

$$B_1x_1^2 + B_2x_2^2 + B_3x_3^2 + 2B_4x_2x_3 + 2B_5x_3x_1 + 2B_6x_1x_2 = 1$$

where
$$\begin{bmatrix} B_1 \\ B_2 \\ B_3 \\ B_4 \\ B_5 \\ B_6 \end{bmatrix} = \begin{bmatrix} 1/n_1^2 \\ 1/n_2^2 \\ 1/n_3^2 \end{bmatrix} + \begin{bmatrix} P_{11} & \cdots & P_{16} \\ \cdot & & \cdot \\ \cdot & & \cdot \\ \cdot & & \cdot \\ \cdot & & \cdot \\ P_{61} & \cdots & P_{66} \end{bmatrix} \cdot \begin{bmatrix} S_1 \\ S_2 \\ S_3 \\ S_4 \\ S_5 \\ S_6 \end{bmatrix}$$

In the absence of a shear wave S_4, S_5 and S_6 are equal to zero. If a longitudinal wave is the only type of wave present then S_1, S_2,

and S_3 are the only strains that may exist.

For a material of the 4/m crystal class, such as $PbMoO_4$, the relevant elasto-optic coefficients are,

$$P_{ij} = \begin{bmatrix} P_{11} & P_{12} & P_{13} & 0 & 0 & P_{16} \\ P_{12} & P_{11} & P_{13} & 0 & 0 & -P_{16} \\ P_{31} & P_{31} & P_{33} & 0 & 0 & 0 \\ 0 & 0 & 0 & P_{44} & P_{45} & 0 \\ 0 & 0 & 0 & -P_{45} & P_{44} & 0 \\ P_{61} & -P_{61} & 0 & 0 & 0 & P_{66} \end{bmatrix}$$

and the static reciprocal permittivities are given by

$$1/n_i^2 = \begin{bmatrix} 1/n_o^2 \\ 1/n_o^2 \\ 1/n_e^2 \end{bmatrix}$$

The refractive indices are given by the semi-major and minor axes of the central elliptic section when the ellipsiod is intersected by a plane normal to the light direction. Consider, for example, that the light is propagating along the y axis, polarized parallel to the x axis, and a z propagating strain, S_3, is also present. The ellipse is then given by

$$\left(1/n_o^2 + P_{13}\, S_3\right)x_1^2 + \left(1/n_e^2 + P_{33}\, S_3\right)x_3^2 = 1$$

At optical frequencies $\varepsilon = n^2$

therefore the ellipse becomes

$$x_1^2/\varepsilon_1' + x_3^2/\varepsilon_3' = 1$$

where $\varepsilon' = \varepsilon + \Delta\varepsilon$

ε is the static permitivitty and

$\Delta\varepsilon$ is the change in permitivitty due to the acoustic disturbance.

Consequently, the permittivity associated with the optical wave is

and by using the binomial theorem,

$$\varepsilon_1 + \Delta\varepsilon_1 = n_o^2 \left(1 - n_o^2 P_{13} S_3 + \cdots \right)$$

The fractional change in permitivitty is thus given by

$$\left| \frac{\Delta\varepsilon_1}{\varepsilon_1} \right| \simeq n_o^2 P_{13} S_3$$

Similarly, for a strain wave, S_1, propagating in the x direction,

$$\left| \frac{\Delta\varepsilon_1}{\varepsilon_1} \right| \simeq n_o^2 P_{11} S_1$$

In general, when diffraction is produced by a longitudinal strain wave the fractional change in permitivitty is given by

$$\left| \frac{\Delta\varepsilon}{\varepsilon} \right| = n^2 P S$$

where the coefficients depend upon the nature of the material, the direction of propagation, and polarization direction of the optical beam, and the propagation direction of the longitudinal acoustic wave.

The actual change in the refractive index is given by

$$n + \Delta n = (1/n^2 + P S)^{-\frac{1}{2}}$$

$$\text{or } |\Delta n| \simeq \frac{n^3 P S}{2}$$

Appendix B

Solution for the Acoustic Stress

Recalling Eq. 4.5.10. the stress at the transducer-delay medium boundary is given by,

$$T^{(l)}(-h) - j\,\frac{z_{d_{ml}}\cot 2\gamma^{(m)}}{z^{(m)}}\,T^{(m)}(-h) + j\,\frac{z_{d_{ml}}\,e^{(m)}D_1\tan\gamma^{(m)}}{z^{(m)}\,\varepsilon_{11}^{s}} = 0 \qquad \text{Eq. B.1.}$$

and from Eq. 4.5.15. the stress can be represented in the form,

$$T^{(l)}(-h) = \left(G^{(l)} - 1\right)\frac{2\,e^{(l)}D_1}{\varepsilon_{11}^{s}} \qquad \text{Eq. B.2.}$$

substitution of Eq. B.2. into Eq. B.1. yields,

$$H^{(l)}e^{(l)} - j\,X_{lm}e^{(m)}H^{(m)} + j\,Y_{lm} = 0 \qquad \text{Eq. B.3.}$$

where $H^{(l)} = G^{(l)} - 1$

$$X_{lm} = \frac{z_{d_{ml}}\cot 2\gamma^{(m)}}{z^{(m)}}$$

and $$Y_{lm} = \frac{z_{d_{ml}}\,e^{(m)}\tan\gamma^{(m)}}{2\,z^{(m)}}$$

Eq. B.3. can be further reduced to the form,

$$U_{lm}H^{(m)} = W_l \qquad \text{Eq. B.4.}$$

where $U_{lm} = e^{(m)}\left(\delta_{lm} - j\,X_{lm}\right)$

and $W_l = j\,Y_{lm}$

The solution to Eq. B.4. for H can be given by,

$$H^{(l)} = V_{lm} W_m \qquad \text{Eq. B.5.}$$

where $U_{il} V_{jm} = \delta_{lm}$

Thus, the stress is therefore given by

$$T^{(l)}(-h) = \frac{H^{(l)} 2 e^{(l)} D_1}{\varepsilon_{11}^*} \qquad \text{Eq. B.6.}$$

Appendix C

Computer Program to Calculate Acoustic Wave Velocity, Particle Displacement Angle and Electro-mechanical Coupling Factor

This computer program was written in order to find the bulk acoustic wave velocity, the angle between the direction of the particle displacement and acoustic wave normal, and the electro-mechanical coupling factor for piezo-electric platelets of varying orientation with respect to the material's crystallographic axes vibrating in the thickness mode. The material coefficients are placed at the beginning of the program and the results are drawn by a graph plotter. The program shown here contains coefficients for lithium niobate. Although, in general, the program will give satisfactory results there will, for some materials, be positions where more than one set of particle displacement eigenvectors will satisfy a given set of eigenvalues. Consequently, anomalous results for the electro-mechanical coupling factor may be given at these positions. However, these anomalies will be quite evident and the correct results can easily be ascertained.

```
      MASTER DAVE
      DIMENSION X(6,6),C(3,3,3,3),GA(3,3),G(3,3),DEL(3,3)
     1,D(3),AMS(3),YY(3),YYA(3),ESP(3,3),EH(3,6),EEH(3,3,3)
     2,AA(3),BA(3,3),CA(3),HK(3,3),RF(3,3),PP(6,6),S(6)
     3,AP(2),E(3,2),DD(2,2),H(3),F(3,2),B(6),BB(3,3)
     4,ANG(360),PHIL(360,3),EH(360,3),DCS(360,3)
     5,VN1(180),VN2(180),W1(360),W2(360)
      COMMON PI,PE,RF
C
C  PROGRAM TO FIND ACOUSTIC VELOCITIES,PARTICLE DISPLACEMENT ANGLE AND
C  ELECTRO-MECHANICAL COUPLING FACTORS
C
COMMENT P=DENSITY
      P=4.63E3
      PI=4.*ATAN(1.)
COMMENT SET STIFFNESS TO ZERO
      DO 1 I=1,6
      DO 1 J=1,6
1     XC(I,J)=0.
C ASSIGN COEFFICIENTS OF STIFFNESS ON R.H.S. OF MATRIX
      XC(1,1)=20.3E10
      XC(1,2)=5.3E10
      XC(1,3)=7.5E10
      XC(1,4)=0.9E10
      XC(3,3)=24.5E10
      XC(4,4)=6.0E10
      XC(6,6)=7.5E10
C GIVE XTAL SYMMETRY ON R.H.S. OF STIFFNESS MATRIX
      XC(2,2)=XC(1,1)
      XC(2,3)=XC(1,3)
      XC(2,4)=-XC(1,4)
      XC(5,5)=XC(4,4)
      XC(5,6)=XC(1,4)
C FILL L.H.S. OF STIFFNESS MATRIX
      DO 2 I=1,6
      DO 2 J=1,6
2     XC(J,I)=XC(I,J)
C SET PERMITTIVITY TO ZERO
      DO 41 I=1,3
      DO 41 J=1,3
41    ESP(I,J)=0.
C ASSIGN RELATIVE COEFFS. OF PERMITTIVITY
      ESP(1,1)=44.
      ESP(2,2)=44.
      ESP(3,3)=29.
C CHANGE PERMITTIVITY FROM RELATIVE TO ABSOLUTE
      DO 42 I=1,3
      DO 42 J=1,3
42    ESP(I,J)=ESP(I,J)*(1.E-9/(36.*PI))
C SET PIEZOELECTRIC COEFFS. TO ZERO
      DO 43 I=1,3
      DO 43 J=1,6
43    EH(I,J)=0.
C ASSIGN PIEZOELECTRIC COEFFS.
      EH(2,4)=3.7
      EH(2,2)=2.5
      EH(3,1)=0.2
      EH(3,3)=1.3
C FILL PIEZOELECTRIC MATRIX
      EH(2,1)=-EH(2,2)
      EH(3,2)=EH(3,1)
      EH(1,5)=EH(2,4)
```

```
      EH(1,6)=-EH(2,2)
C PUT PIEZOELECTRIC MATRIX IN TENSOR FORM
      DO 44 M=1,3
      DO 44 N=1,3
44    EEH(M,N,N)=EH(M,N)
      DO 45 M=1,3
      J=1
      K=2
      L=3
      DO 45 N=4,6
      EEH(M,K,L)=EH(M,N)
      EEH(M,L,K)=EEH(M,K,L)
      NM=J
      J=K
      K=L
45    L=NM
C PUT STIFFNESS IN TENSOR FORM
      DO 3 I=1,3
      DO 3 J=1,3
3     C(I,I,J,J)=XC(I,J)
      JI=1
      K=2
      L=3
      DO 5 M=4,6
      IJ=1
      I=2
      J=3
      DO 4 N=4,6
      C(I,J,K,L),C(J,I,K,L),C(J,I,L,K),C(I,J,L,K)=XC(N,M)
      NM=IJ
      IJ=1
      I=J
4     J=NM
      NMA=JI
      JI=K
      K=L
5     L=NMA
      I=1
      J=2
      K=3
      DO 7 N=1,3
      DO 7 M=4,6
      C(N,N,J,K),C(J,K,N,N),C(N,N,K,J),C(K,J,N,N)=XC(N,M)
      L=I
      I=J
      J=K
7     K=L
COMMENT DEFINE KRONECKER DELTA
      DO 21 I=1,3
      DO 21 J=1,3
      DEL(I,J)=0.
21    DEL(I,I)=1.
      COMMENT ASSIGN WAVE NORMAL
      DO 30 M=1,360
      N=90
      CALL PATH(M,N,D)
COMMENT SOLVE CHRISTOFFEL EQN.
      DO 14 I=1,3
      DO 14 L=1,3
14    GA(I,L)=0.
      DO 20 I=1,3
      DO 20 L=1,3
      DO 20 J=1,3
      DO 20 K=1,3
      GA(I,L)=(C(I,J,K,L)*D(J)*D(K))/D+GA(I,L)
20    CONTINUE
```

```
      BA=0.
      DO 47 I=1,3
      DO 47 J=1,3
47    BA=BA+D(I)*D(J)*FSP(I,J)
      DO 48 L=1,3
      DA(L)=0.
48    CA(L)=0.
      DO 49 L=1,3
      DO 49 J=1,3
      DO 49 K=1,3
      DA(L)=ECH(J,L,K)*D(J)*D(K)+DA(L)
49    CA(L)=ECH(J,K,L)*D(J)*D(K)+CA(L)
      DO 50 I=1,3
      DO 50 L=1,3
50    GA(I,L)=GA(I,L)-DA(I)*CA(L)/(P*BA)
COMMENT FIND COEFFS. OF CHARACTERISTIC EQN.
      XP=0.
      Q=0.
      R=0.
      J=1
      K=2
      L=3
      DO 31 I=1,3
      XP=XP+GA(J,J)
      Q=Q-GA(J,J)*GA(K,K)-GA(J,K)*GA(K,J)
      R=R-GA(I,J)*(GA(2,K)*GA(3,L)-GA(3,K)*GA(2,L))
      NM=J
      J=K
      K=L
31    L=NM
      Y=1.E8
COMMENT FIND 1.ST. EIGENVALUE
COMMENT TOP=F(Y)
23    TOP=-Y**3+XP*Y*Y-Q*Y+R
COMMENT BOT=D.DX(F(Y))
      BOT=-3.*Y*Y+2.*XP*Y-Q
COMMENT USE NEWTON-RAPHSON METHOD
      Y=Y-TOP/BOT
      Z=TOP/BOT
      IF(ABS(Z).LE.1.E2)GOTO25
      GOTO23
COMMENT FIND 2.ND AND 3.RD EIGENVALUES
25    A=(XP-Y)/2.
      XB=ABS(A*A-Q/Y)
      YB=SQRT(XB)
      YY(1)=Y
      YY(2)=A+YB
      YY(3)=ABS(A-YB)
C RE-ORDER EIGENVALUES
      DO 81 I=1,3
81    YYA(I)=GA(I,I)
      DO 80 I=1,3
      DO 80 J=1,3
      IF(YYA(I).GT.YYA(J))GOTO19
      TRA=YYA(I)
      YYA(I)=YYA(J)
      YYA(J)=TRA
19    CONTINUE
80    CONTINUE
      DO 82 J=1,3
      DO 83 I=1,3
83    IF(YYA(J).EQ.GA(I,I))MIX=I
      IF(J.EQ.1)NOW=MIX
      IF(J.EQ.2)KEN=MIX
      IF(J.EQ.3)JON=MIX
82    ANS(MIX)=SQRT(ABS(YY(J)))
```

```
      COMMENT ANS(M,N)=VELOCITY
      C FIND EIGENVECTORS
            IA=1
            JA=2
            KA=3
            DO 28 MM=1,3
            DO 26 I=1,3
            DO 26 L=1,3
      26    G(I,L)=GA(I,L)-DEL(I,L)*(ANS(MM)**2)
            J=1
            K=2
            L=3
            DO 288 JKL=1,3
            HK(J,IA)=G(JA,K)*G(KA,L)-G(KA,K)*G(JA,L)
            NM=J
            J=K
            K=L
      288   L=NM
            NMA=IA
            IA=JA
            JA=KA
      28    KA=NMA
      C NORMALISE EIGENVECTORS
            DO 32 I=1,3
            PO=0.
            DO 33 J=1,3
      33    PO=PO+HK(J,I)**2
            DO 32 K=1,3
            IF(PO.EQ.0.)PO=FLOAT(M)
      32    HK(K,I)=HK(K,I)/SQRT(PO)
      C FIND ELECTRO-MECHANICAL COUPLING FACTORS
            DO 38 I=1,3
      38    AA(I)=0
            DO 39 I=1,3
            AA(1)=AA(1)+HK(I,NOW)*CA(I)
            AA(2)=AA(2)+HK(I,KEN)*CA(I)
      39    AA(3)=AA(3)+HK(I,JON)*CA(I)
            AA(1)=(AA(1)**2)/(BA*P*(ANS(NOW)**2))
            AA(2)=(AA(2)**2)/(BA*P*(ANS(KEN)**2))
            AA(3)=(AA(3)**2)/(BA*P*(ANS(JON)**2))
            DO 40 I=1,3
      40    EM(M,I)=SQRT(ABS(AA(I)))
      C FIND ANGLE BETWEEN WAVE NORMAL AND
      C LONGITUDINAL PARTICLE DISPLACEMENT VECTOR
            UA=0.
            DO 277 I=1,3
      277   UA=UA+HK(I,NOW)*D(I)
            TA=ABS(UA)
            IF(TA.GT.1.)TA=1.
            ANG(M)=ACOS(TA)
      C GIVE ACOUSTIC VELOCITIES
            DO 321 I=1,3
      321   POL(M,I)=SQRT(VV(I))
      30    CONTINUE
            CALL HGBSTART(22HWAVE VELOCITY SURFACES,22)
      C  PLOT ACOUSTIC VELOCITIES
            CALL HGBAXIS(15.0,15.0,13HVELOCITY KM/S,-13,15.0,0.0,0.0,0.0,0.5)
            DO 100 I=1,15
            R=FLOAT(I)
            ST=5.-R
            CALL HGBCIRCLE(15.0,ST,-90.0,270.0,R,R,0.5)
      100   CONTINUE
            DO 101 J=30,330,30
            O=P1*FLOAT(J)/180.
            X=15.0*(1.+COS(O))
            Y=15.*(1.+SIN(O))
```

```
      CALL HGDASHLN(15.0,15.0,X,Y,0.5)
101   CONTINUE
      Q=2./1.E3
      N=1
104   IC=3
      DO 102 M=1,360
      O=PI*FLOAT(M)/180.
      X=15.+Q*POTL(M,N)*COS(O)
      Y=15.+Q*POTL(M,N)*SIN(O)
      CALL HGPLOT(X,Y,IC,0)
      IC=2
102   CONTINUE
      IF(N.EQ.3)GOTO103
      N=N+1
      GOTO104
103   CONTINUE
C  PLOT PARTICLE DISPLACEMENT ANGLE
      CALL HGPAXIS(0.,36.,19HFIELD DIRECTION DEG.,-19,18.,0.,0.,10.)
      CALL HGPAXIS(0.,36.,16HDISPLACEMENT DEG,16,15.,90.,0.,1.)
      IC=3
      DO 200 I=1,180
      X=0.1*FLOAT(I)
      Y=36.+180.*ANG(I)/PI
      IF(Y.GT.51.)Y=51.
      CALL HGPLOT(X,Y,IC,0)
      IC=2
200   CONTINUE
C  PLOT ELECTRO-MECHANICAL COUPLING FACTORS
      CALL HGPAXIS(0.,57.,13HDIRECTION DEG.,-13,18.,0.,0.,10.)
      CALL HGPAXIS(0.,57.,13HK EFF PERCENT,13,8.,90.,0.,10.)
      DO 199 M=1,3
      IC=3
      DO 199 I=1,180
      X=0.1*FLOAT(I)
      Y=57.+10.*EM(I,M)
      IF(Y.GT.65.)Y=65.
      CALL HGPLOT(X,Y,IC,0)
      IC=2
199   CONTINUE
      CALL HGFINISH
      STOP
      END

E SEGMENT, LENGTH  2517, NAME  DAVE
```

```
      SUBROUTINE PATH(M,N,D)
      DIMENSION D(3)
      COMMON PI
C  FIND COSINES FOR PROPAGATION DIRECTION
      ALPHA=PI*FLOAT(M)/180.
      BETA=PI*FLOAT(N)/180.
      D(1)=SIN(ALPHA)
      R=COS(ALPHA)
      D(2)=R*COS(BETA)
      D(3)=R*SIN(BETA)
      RETURN
      END

F SEGMENT, LENGTH    84, NAME  PATH
```

Appendix D

Computer Program to Calculate Transducer Admittance, Acoustic Phase, and Insertion Loss

This computer program was written in order to find the variation of the transducer admittance, the difference in phase between the acoustic wave and the electric drive voltage, and the variation of the one way insertion loss with respect to the frequency times thickness product. The insertion loss has been found for a transducer which is simply tuned by a parallel inductor and fed by a source whose conductance is equal to the maximum value of the transducers' conductance.

```
      MASTER DAVE
      DIMENSION V(3),VD(3),EH(3),EM(3),A(3,3),E(3),Z(3),ZD(3),DEL(3,3),
     1HK(3,3),ZZ(3,3),X(3,3),Y(3),W(3),U(3,3),H(3),G(3),T(3),L(3,3),
     2GAMMA(3),GAM2(3)
     3,PD(3),AR(3,3)
      COMPLEX DEL,U,W,H,G,T,XY,POW
      COMMON PI,V,GAMMA,EM
C
C  PROGRAM TO FIND TRANSDUCER ADMITTANCE AND ACOUSTIC INSERTION LOSS
C
      PI=4.*ATAN(1.)
C  ESP=PERMITTIVITTY,P=TRANSDUCER DENSITY,PD=DELAY MEDIUM DENSITY
      READ(1,10)ESP,P,PD
C  V=TRANSDUCER VELOCITY(LONG,SHEAR1,SHEAR2)
      READ(1,10)(V(I),I=1,3)
C  VD=DELAY MEDIUM VELOCITY(LONG,SHEAR1,SHEAR2)
      READ(1,10)(VD(I),I=1,3)
C  EH=PIEZO-ELECTRIC COEFFICIENTS
      READ(1,10)(EH(I),I=1,3)
C  EM=ELECTRO-MECHANICAL COUPLING FACTORS(LONG,SHEAR1,SHEAR2)
      READ(1,10)(EM(I),I=1,3)
C  A=EIGENVECTORS(LONG,SHEAR1,SHEAR2)
      DO 1 I=1,3
    1 READ(1,10)(A(J,I),J=1,3)
C  M=ANGLE OF Y-CUT
      READ(1,10)M,M,M
   10 FORMAT(3G0.0)
      DO 2 I=1,3
C  Z=TRANSDUCER ACOUSTIC IMPEDENCE
      Z(I)=P*V(I)
C  ZD=DELAY MEDIUM ACOUSTIC IMPEDENCE
      ZD(I)=PD*VD(I)
C  E=EFFECTIVE PIEZO-ELECTRIC COEFFICIENTS
      E(I)=0.
      DO 2 J=1,3
      E(I)=E(I)+EH(J)*A(J,I)
C  DEL=KRONECKER DELTA
      DEL(I,J)=(0.,0.)
    2 DEL(I,I)=(1.,0.)
      CALL COSMIC(M,U)
      DO 3 I=1,3
      DO 3 K=1,3
C  HK=DIRECTION COSINES RELATIVE TO PROPAGATION DIRECTION
      HK(I,K)=0.
      DO 3 J=1,3
    3 HK(I,K)=HK(I,K)+U(J,K)*A(J,I)
C  A=DELAY MEDIUM ACOUSTIC IMPEDENCE AS 2ND ORDER TENSOR
      DO 4 I=1,3
      DO 4 J=1,3
    4 A(I,J)=ZD(I)*REAL(DEL(I,J))
C  ZZ=DELAY MEDIUM ACOUSTIC IMPEDENCE RELATIVE TO TRANSDUCER PARTICLE DIS-
C  -PLACEMENT AXES
      DO 5 I=1,3
      DO 5 J=1,3
      ZZ(I,J)=0.
      DO 5 K=1,3
      DO 5 L=1,3
    5 ZZ(I,J)=HK(I,K)*HK(J,L)*A(K,L)+ZZ(I,J)
C  N=FREQUENCY*DISTANCE
      DO 30 N=1000,2500,50
C  SOLVING TO FIND STRESS
      DO 6 I=1,3
      GAMMA(I)=PI*FLOAT(N)/V(I)
      R=SIN(GAMMA(I))
      IF(ABS(R).EQ.1.)GOTO30
    6 GAM2(I)=2.*GAMMA(I)
```

```
      DO 7 I=1,3
      DO 7 J=1,3
      Y(I)=0.
7     X(I,J)=0.
      DO 8 L=1,3
      DO 8 M=1,3
      Y(L)=ZZ(L,M)*E(M)*TAN(GAMMA(M))/(2.*Z(M))+Y(L)
8     X(L,M)=ZZ(L,M)*COT(GAM2(M))/Z(M)+X(L,M)
      B=0.
      DO 9 I=1,3
      DO 9 J=1,3
      U(I,J)=CMPLX(B,X(I,J))
9     W(I)=-CMPLX(B,Y(I))
      DO 12 I=1,3
      IF(E(I).EQ.0.)E(I)=E(I)+1.E-10
      DO 12 J=1,3
12    U(I,J)=E(J)*(DEL(I,J)-U(I,J))
      CALL PHEW(W,U,H)
      DO 11 I=1,3
      G(I)=H(I)+DEL(1,1)
C  T=STRESS
11    T(I)=H(I)*2.*E(I)/ESP
      CALL GOSH(G,XY)
C  XY=TRANSDUCER ADMITTANCE
      DO 50 I=1,3
50    G(I)=(0.,0.)
      DO 51 I=1,3
      DO 51 J=1,3
51    G(I)=G(I)+T(J)*HK(I,J)
      DO 52 I=1,3
52    T(I)=G(I)
      ABC=AIMAG(T(1))/REAL(T(1))
C  ABC=PHASE BETWEEN ACOUSTIC WAVE AND ELECTRIC DRIVE VOLTAGE
      ABC=180.*ATAN(ABC)/PI
      DO 40 I=1,3
      T(I)=T(I)*CONJG(T(I))
C  PO=MAGNITUDE OF ACOUSTIC POWER(LONG,SHEAR1,SHEAR2)
40    PO(I)=REAL(T(I))/(2.*PO*VO(I))
      AL=0.
      DO 42 J=1,3
42    AL=AL+PO(J)
      DO 41 I=1,3
      IF(PO(I).EQ.0.)PO(I)=1.E-10
C  PO=RELATIVE ACOUSTIC POWER LOSS
41    PO(I)=AL/PO(I)
C  POW=SOURCE RESISTANCE
      POW=(0.0785,0.)*2.*PI*3.6E3
C  YL=1./INDUCTANCE
      YL=0.
      YL=-2.*PI*YL/FLOAT(N)
      G(1)=(0.,1.)*YL
      T(1)=POW*G(1)+(XY*2.*PI*FLOAT(N))
      T(1)=T(1)**2
      T(1)=T(1)/(4.*POW*REAL(XY)*2.*PI*FLOAT(N))
C  SLOS=ELECTRICAL MISMATCH POWER LOSS
      SLOS=CABS(T(1))
      DO 43 I=1,3
      PO(I)=SLOS*PO(I)
43    PO(I)=10.*ALOG10(PO(I))
C  PO=NET ONE-WAY INSERTION LOSS(LONG,SHEAR1,SHEAR2)
30    WRITE(2,20)N,XY,ABC,(PO(I),I=1,3)
20    FORMAT(1H ,I4,3X,6G14.4)
      STOP'IS FINISHED'
      END

MENT, LENGTH  1387, NAME  DAVE
```

```
0141                    SUBROUTINE PHEW(B,C,T)
0142                    COMPLEX B,C,T,ADJ,F
0143                    DIMENSION B(3),C(3,3),T(3),ADJ(3,3)
0144              C  SOLVE MATRIX EQUATION[C]*[T]=[B]
0145                    F=(0.,0.)
0146                    DO 5 I=1,3
0147              5     T(I)=(0.,0.)
0148              C  INVERT MATRIX [C] - FIND ADJOINT
0149                    J=1
0150                    K=2
0151                    L=3
0152                    JA=1
0153                    KA=2
0154                    LA=3
0155                    DO 2 N=1,3
0156                    DO 1 M=1,3
0157                    ADJ(JA,J)=C(KA,K)*C(LA,L)-C(KA,L)*C(LA,K)
0158                    NM=J
0159                    J=K
0160                    K=L
0161              1     L=NM
0162                    NMA=JA
0163                    JA=KA
0164                    KA=LA
0165              2     LA=NMA
0166              C  FIND CONSTANT FACTOR
0167                    DO 3 I=1,3
0168              3     F=ADJ(I,1)*C(1,1)+F
0169                    DO 4 I=1,3
0170                    DO 4 J=1,3
0171              C  GIVE RESULT FOR [T]
0172              4     T(I)=ADJ(J,I)*B(J)/F+T(I)
0173                    RETURN
0174                    END

END OF SEGMENT, LENGTH   295, NAME  PHEW
```

```
0175                    SUBROUTINE GOSH(G,Y)
0176                    COMPLEX A,G,Z,Y
0177                    DIMENSION EM(3),G(3),GAMMA(3),V(3)
0178                    COMMON PI,V,GAMMA,EM
0179                C   TO FIND TRANSDUCER ADMITTANCE Y
0180                    A=(0.,0.)
0181                    DO 1 L=1,3
0182                1   A=A+((EM(L)**2)*G(L)*TAN(GAMMA(L)))/GAMMA(L)
0183                    Y=(1.,0.)
0184                    Z=Y-A
0185                    Y=1./Z
0186                    Y=Y*(0.,1.)
0187                    RETURN
0188                    END
```

END OF SEGMENT, LENGTH 127, NAME GOSH

```
0189                    SUBROUTINE COSMIC(M,D)
0190                    DIMENSION D(3,3)
0191                    COMMON PI
0192                C   TO FIND DIRECTION COSINES IN PLANE X=0.
0193                    A=FLOAT(M)*PI/180.
0194                    D(1,3)=1.
0195                    D(1,1),D(1,2),D(2,3),D(3,3)=0.
0196                    D(2,1),D(3,2)=COS(A)
0197                    D(2,2)=-SIN(A)
0198                    D(3,1)=SIN(A)
0199                    RETURN
0200                    END
```

END OF SEGMENT, LENGTH 113, NAME COSMIC

Appendix E

Material Coefficients

The coefficients of the various parameters of the materials used throught this work are listed below.

Lead Molybdate, $PbMoO_4$

Density[a] $\rho = 6.95 \times 10^3 \text{ Kg/m}^3$

Elastic stiffness constants[a] $\times 10^{10} \text{ N/m}^2$

$c_{11} = 10.92$	$c_{33} = 9.17$
$c_{12} = 6.83$	$c_{44} = 2.67$
$c_{13} = 5.28$	$c_{66} = 3.37$
$c_{16} = 1.36$	

Refractive indices

($\lambda_o = 632.8$ nm)[a]	$n_o = 2.386$	$n_e = 2.262$
($\lambda_o = 441.6$ nm)[b]	$n_o = 2.571$	$n_e = 2.379$

Elasto-optic constants

($\lambda_o = 6.328$ nm)[a] $P_{11} = 0.24$	$P_{33} = 0.3$
$P_{12} = 0.24$	$P_{44} = 0.067$
$P_{13} = 0.255$	$P_{45} = -0.01$
$P_{16} = 0.017$	$P_{61} = 0.013$
$P_{33} = 0.175$	$P_{66} = 0.05$
($\lambda_o = 441.6$ nm)[b] $P_{13} = 0.347$	$P_{33} = 0.276$

Thermal expansion ppm/°C [a] $\alpha_{11} = 10$ $\alpha_{33} = 25$

[c] $\alpha_{11} = 11$ $\alpha_{33} = 28.5$

Lithium Niobate, $LiNbO_3$

Density[d] $\rho = 4.63 \times 10^3$ Kg / m^3

Elastic stiffness constants at constant electric field[e] $\times 10^{10}$ N / m^2

$C^e_{11} = 20.3$ $C^e_{33} = 24.5$

$C^e_{12} = 5.3$ $C^e_{44} = 6.0$

$C^e_{13} = 7.5$ $C^e_{66} = 7.5$

$C^e_{14} = 0.9$

Piezo-electric constants[e] C /m^2

$e_{24} = 3.7$ $e_{31} = 0.2$

$e_{22} = 2.5$ $e_{33} = 1.3$

Relative Permittivity at constant strain[e]

$\varepsilon_{11} = 44$ $\varepsilon_{22} = 44$ $\varepsilon_{33} = 29$

Thermal expansion[f] ppm/°C

$\alpha_a = 16.7$ $\alpha_c = 2$

Water

Density[g] $\rho = 1 \times 10^3$ Kg/m^3

Refractive index[g] $\Pi = 1.33$ velocity[g] $v_l = 1.5 \times 10^3$ m/s

figure of merit[h] $M_2 = 106$ ($\lambda_o = 632.8$nm)

acoustic attenuation[h] $\alpha_o = 2000$ dB /cm GHz^2

Sheet glass.

Density[g] $\rho = 2.5 \times 10^3$ Kg / m^3

Velocity[g] $v_l = 5.9 \times 10^3$ m/s $v_s = 3.0 \times 10^3$ m/s

Acoustic impedance[g] $z = 14.75 \times 10^6$ Kg / s m^2

Epoxy Resin

Velocity[k] $v_l = 2.6 \times 10^3$ m/s Acoustic impedance[k] $z_l = 2.86 \times 10^6$ Kg / s.m^2

Aluminium

Density[g] $\rho = 2.7 \times 10^3$ Kg / m^3

Velocity[g] $v_l = 6.4 \times 10^3$ m/s $v_s = 3.05 \times 10^3$ m/s

Acoustic impedance[k] $z_l = 17.3 \times 10^6$ Kg / s m^2

Acoustic Attenuation[k] $\alpha_{o_l} = 200$ dB / cm.GHz^2

Thermal expansion[a] $\alpha = 24$ ppm/°C

Phenyl Salicylate

Melting point[j] $t_m = 43$ °C

Density[j] 1.167×10^3 Kg / m^3

Figures of merit for fused quartz[K] (absolute)

$M_1 = 7.83 \times 10^{-8}$ m^2.s/Kg $M_3 = 1.3 \times 10^{-11}$ m.s^2/Kg

$M_2 = 1.51 \times 10^{-16}$ s^3/Kg $M_4 = 4.06$ m^4/Kg.s

a) Coquin et al (1971)

b) DeBenedictus and Lucero (1974)

c) Bonner and Zydzik (1970)

d) Milek and Neuberger (1972)

e) Warner et al (1967)

f) Abrahams (1966)

g) CRC Handbook (1973)

h) Pinnow (1970)

j) Obukhovskii (1969)

k) Chang (1976)

Appendix F

The r.f. Power Amplifiers

For this work two wideband R.F. power amplifiers were required to drive the two transducers on the acousto-optic deflectors. The amplifiers obtained for this purpose were Electronic Navigation Industries type 400 AP broadband power amplifiers (ENI Product Bulletin) which could cover a frequency range from 150 K Hz to 300 M Hz. Their gain was nominally 37 dB and could deliver a linear power output of more than 3 watts. The input / output impedance of the amplifiers was 50 Ω and they could be terminated with an arbitary load. The power supply requirements for each amplifier was 22 volts D.C. at 1.3 amps. Consequently, a suitable power supply was built for each amplifier and the amplifiers, together with the power supplies, were housed in an appropriate box. A photograph of the two amplifiers is shown in Plate F1 and the circuit diagram for the power supplies is shown in Fig. F1.

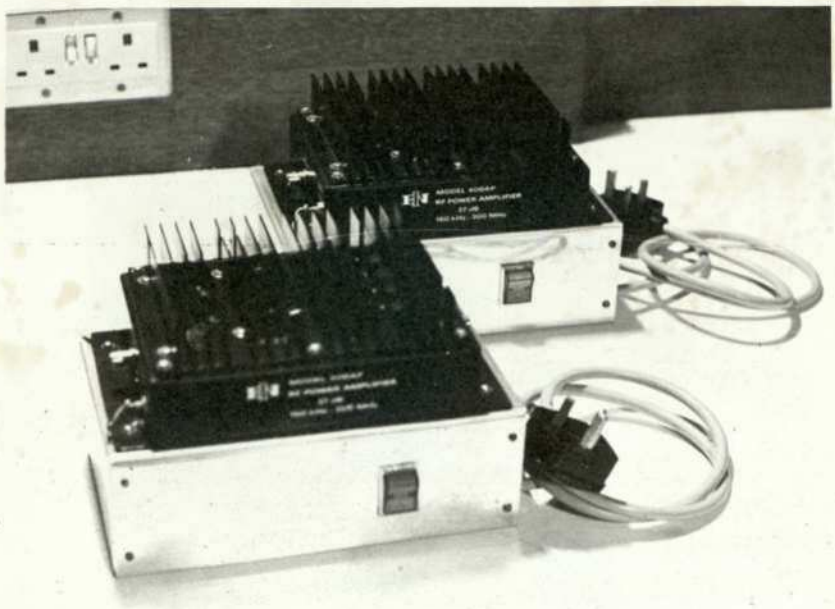

Plate.F.1. The r.f. power amplifiers.

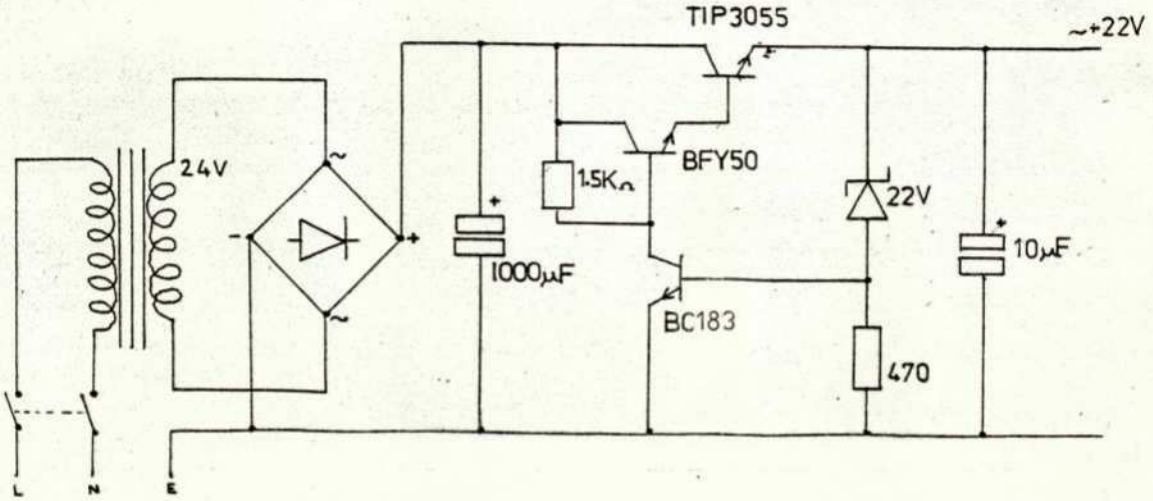

Fig.F.1. Power supply for amplifiers.

Appendix G

The Stepped Frequency Generators

In order to demonstrate the XY capabilities of the two-dimensional acousto-optic deflectors and also to demonstrate the optical resolution that could be obtained by them two stepped frequency generators were constructed to perform this function. There are a number of possible circuit arrangements in which this could be achieved.

For example, for linear optical beam scanning the frequency source would usually consist of an oscillator whose frequency is varied by means of a varactor diode (Zenith Bulletin). For stepped-frequency operation the varactor diode would be controlled, via a suitable isolating network between the control circuitry and the oscillatory circuit, by a D-A convertor which is controlled from logic circuitry. However, in order to obtain reasonably fast switching times of, say, less than 500 ns the minimum switching time would ultimately be limited by the settling time of the D-A convertor and the response of the isolating network, apart from the fact that the Q of the oscillator must be low.

Another method of obtaining stepped deflection would be to provide a number of oscillators, the number being equal to the total number of spot positions, each of which would be tuned to a frequency corresponding to a discreet spot position and suitably isolated from the other oscillators (J. M. Ley Private Communication). The stepped frequency variation would be obtained by switching in the appropriate oscillator. Although fast switching speeds would have been obtained such a system would be both complex and expensive.

In order to considerably reduce the number of components and

yet try to keep switching times below 500 ns the arrangement shown in Fig. G1 was constructed. Only one oscillator is used and although a colpitts oscillator is shown any other type should be equally suitable. The oscillator frequency is altered by the diode-capacitor arrangement across the inductor. Considering the first stage, transistor T_1 is biased so that when the voltage at point A is essentially zero volts it is conducting. This causes the diode D_1 to be forward biased which essentially connects the capacitor C_1 across the inductor. The oscillator frequency is thus essentially altered by the inclusion of C_1. When the voltage at point A is equal to a logic gate output in the '1' state the transistor T_1 is non-conducting. The diode D_1 is then reverse-biased by R_1 which must also discharge the capacitor C_1 in an appropriate short time. The oscillator frequency is thus altered by the effective removal of C_1. The 1 KΩ resistor in series with the collector of T_1 provides some isolation between the resonant circuit and the collector-base capacitance.

The circuit that was constructed used five such stages so that the number of discreet frequency steps was 32. The diodes were chosen so that their reverse-bias capacitance was small and the capacitors C_1 - C_5 were air-spaced trimmers. None of the other components were especially critical. It should be mentioned here that the oscillator voltage across the inductor should be sufficiently small otherwise the diodes will rectify for part of the oscillator cycle. The oscillator output was taken via the resistor R_0 and the capacitor C_0' and this was taken directly to the input of the R.F. amplifier. In retrospect, a buffer stage between the oscillator and amplifier would have been appropriate since variations in amplitude and frequency of the oscillator were noticed when the cables connecting

the two were altered. However, the arrangement was found to be reasonably satisfactory for experimental purposes although some non linearity in spot distribution occurred, as can be seen from Fig. 8.6.2.4.1. and Fig. 8.6.2.4.2. With this system switching times of about 200 ns were achieved. By suitably adjusting the values of the inductor L and the trimmers C_{1-5} and C_0' the generators could be operated with a fractional bandwidth of up to about 0.34 with a centre frequency varying from 25 M Hz to 150 M Hz.

Fig. G.2. shows the logic circuitry which was used to control the stepped frequency generator which consists of a clock, a synchronous binary counter and a Phase locked loop for synchronizing purposes. The power supply circuit used for this equipment is shown in Fig. G.3. A photograph of one of the stepped frequency generators constructed is shown in Plate G.1.

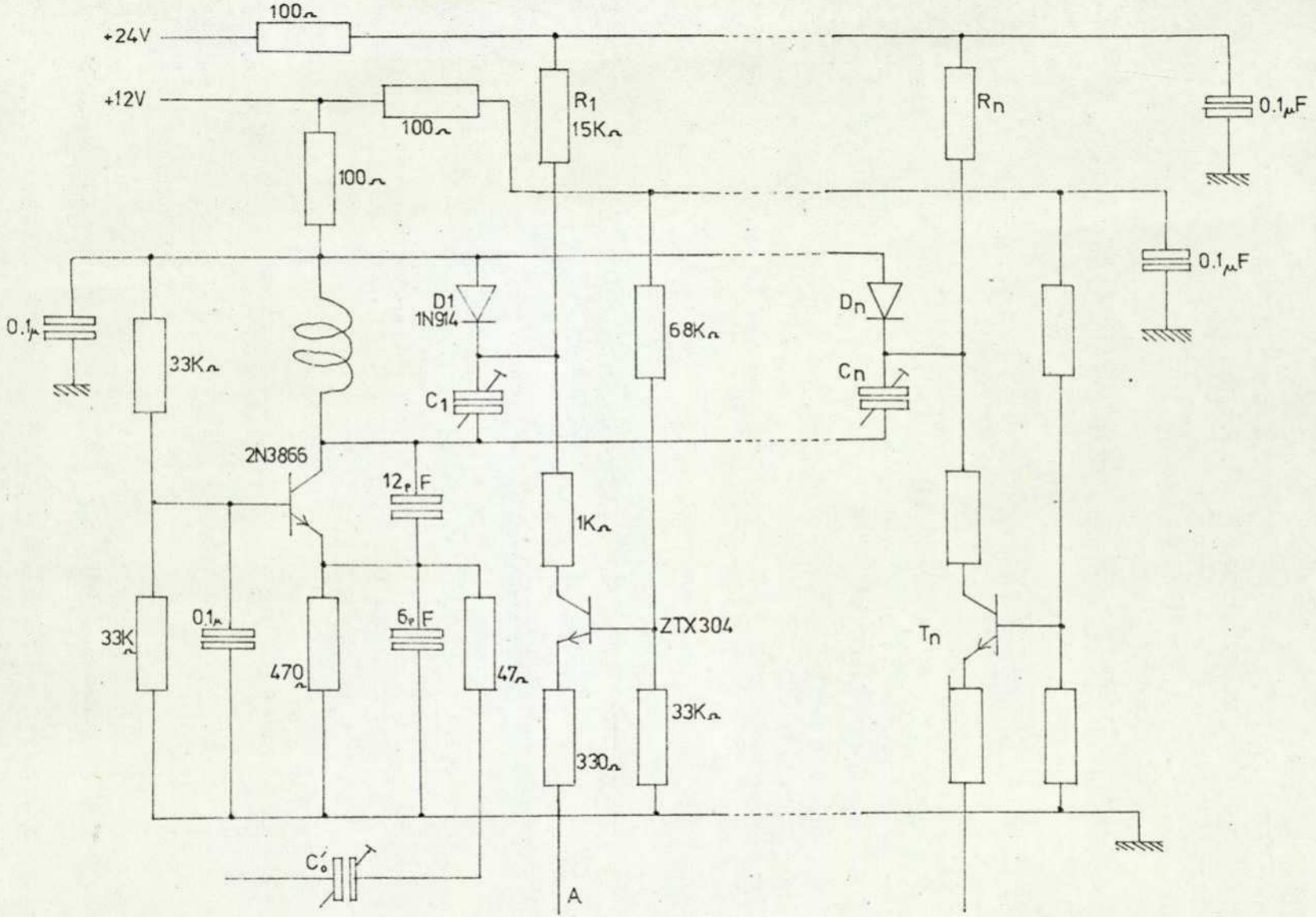

Fig. G.1. Circuit of r.f. stepped oscillator.

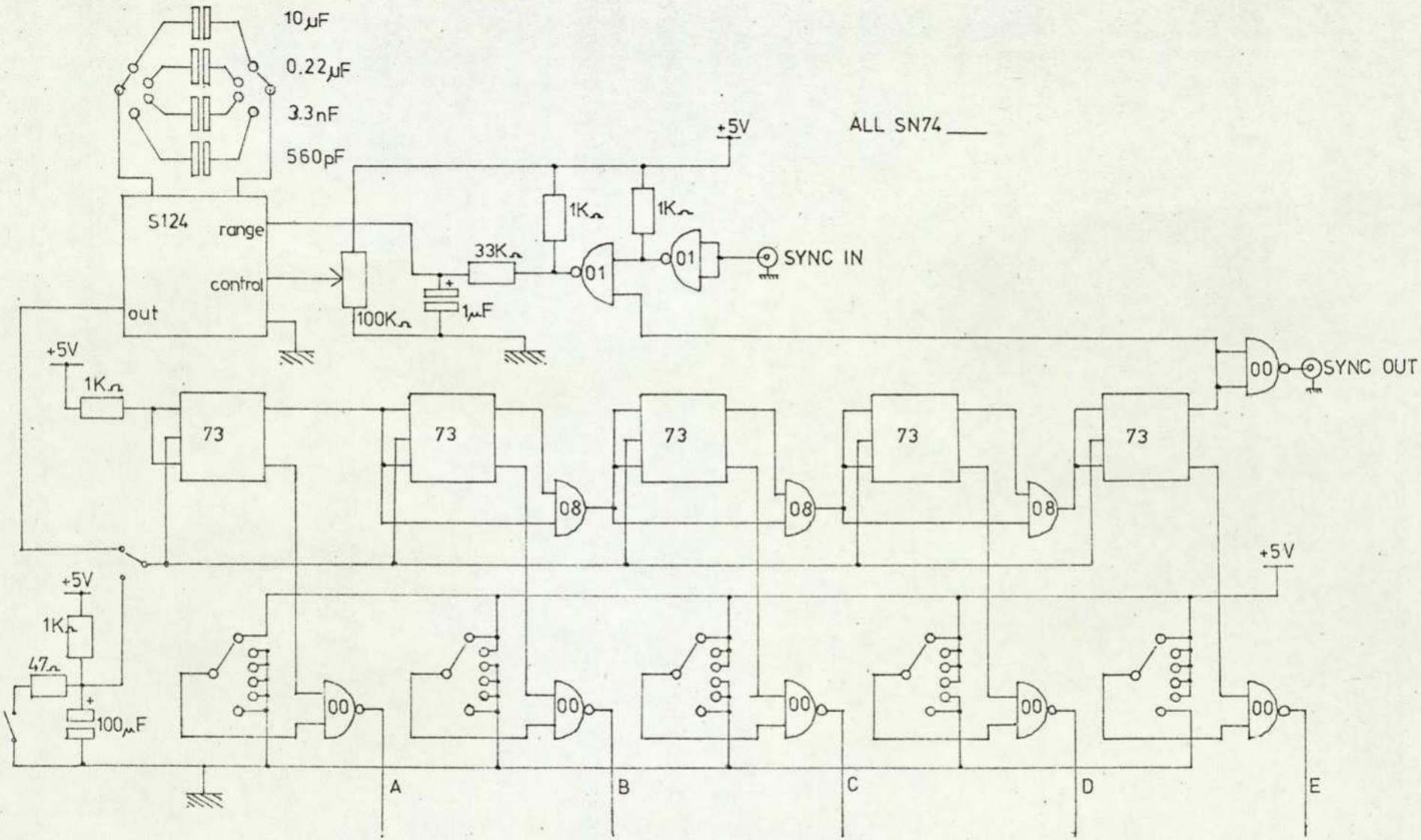

Fig. G.2. Ciruit of control logic for stepped oscillator.

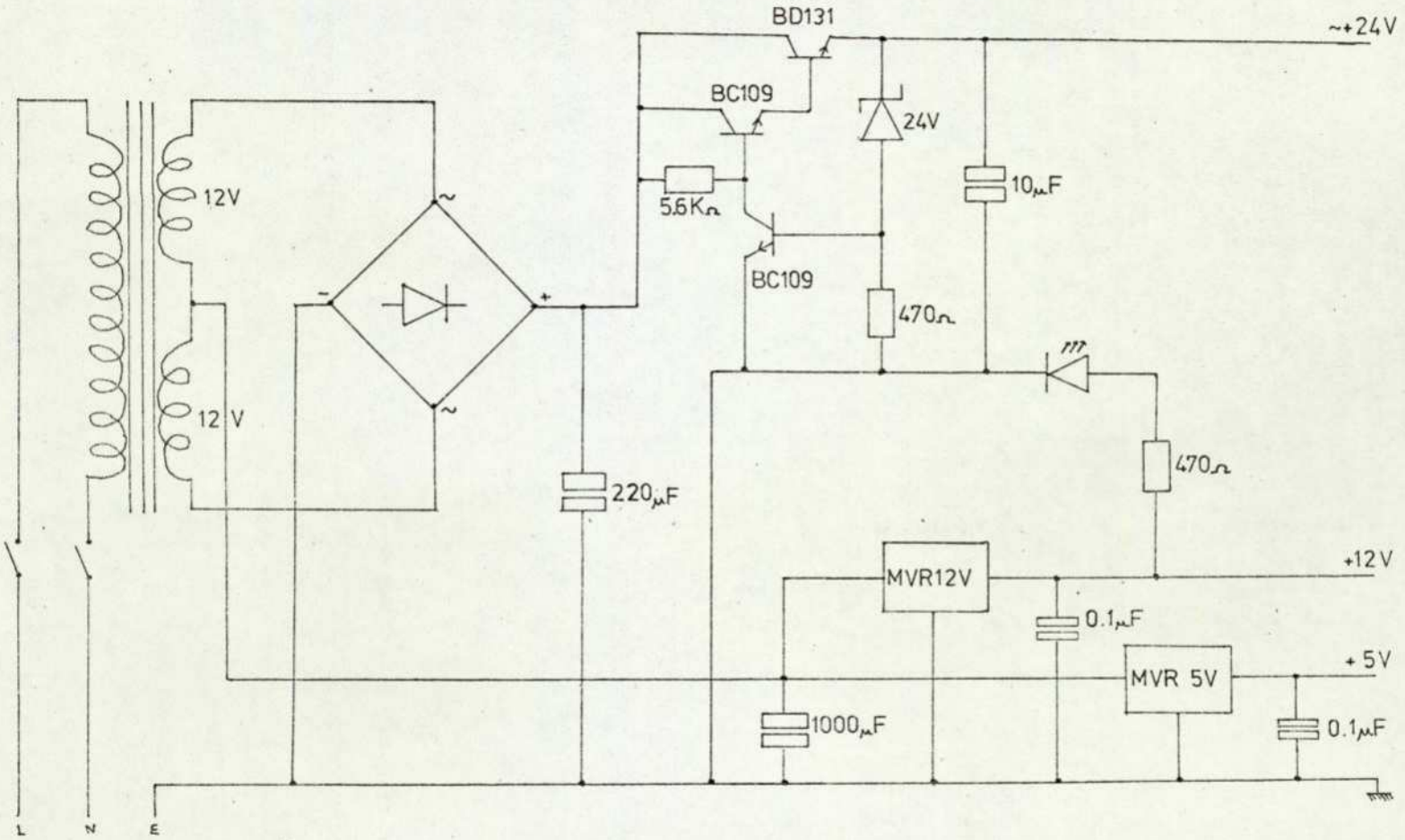

Fig. G.3. Power supply for the stepped frequency generators.

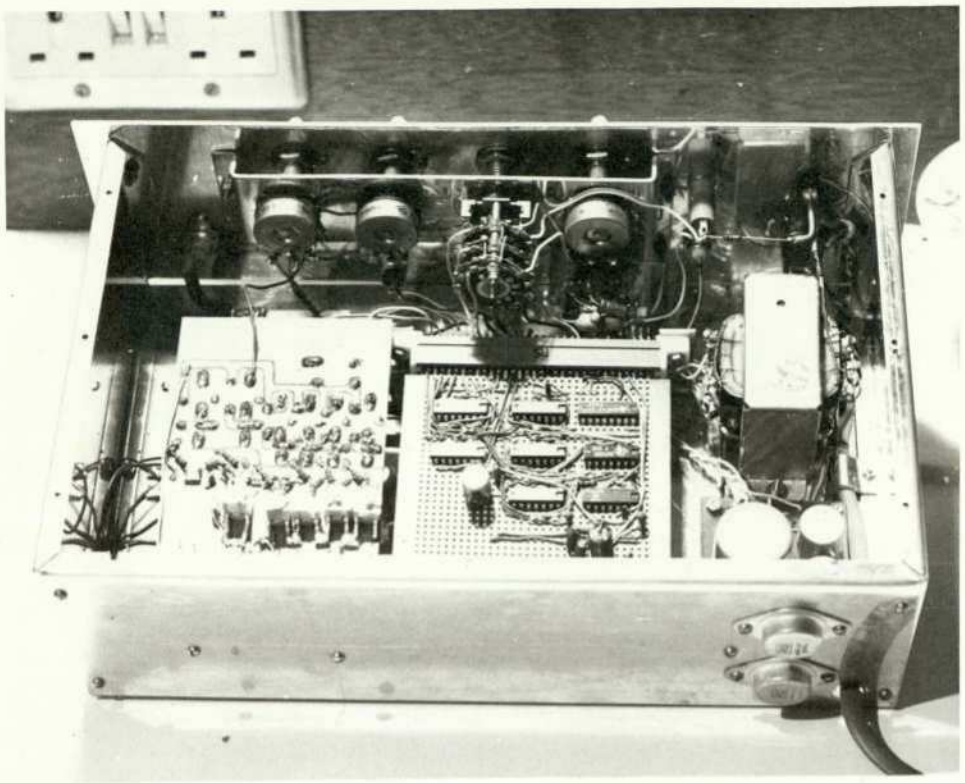

Plate G.1. One of the stepped frequency generators constructed.